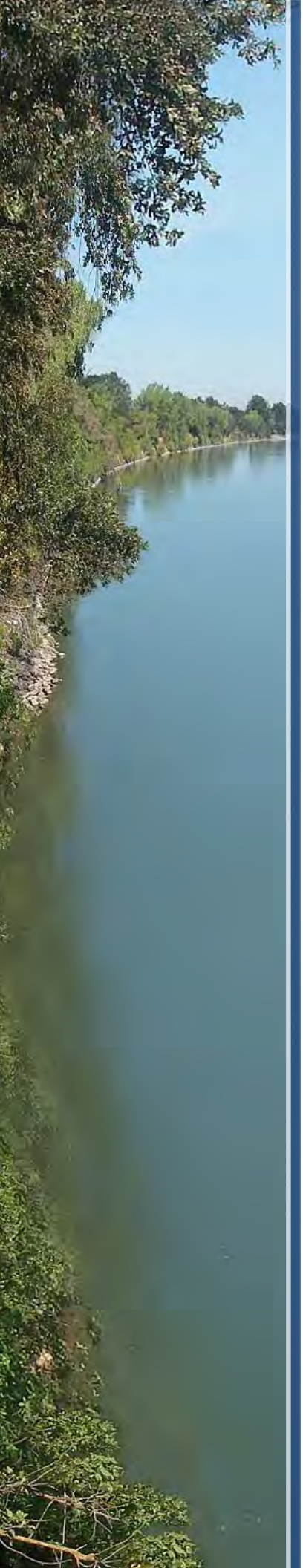

California Levee Vegetation Research Program

Influence of Tree Roots and Mammal Burrowing Activity on Levee Performance:
Volume 2. – Parallel Trench Wetting Front Test, North Levee of the American River at Cal Expo Sacramento, California

Michelle Shriro, Diego Cobos-Roa, Jonathan D. Bray, Nicholas Sitar

University of California, Berkeley, CA

John Lichter

Tree Associates, Winters, CA

Richard Evans

University of California, Davis, CA

Grant funding provided by:

The California Department of Water Resources (Contract No. 4600008761) and the Sacramento Area Flood Control Agency (Contract No. 984)

May 2014

Geotechnical Engineering
University of California, Berkeley
Report UCB GT 13-03 vol.2

Sponsoring/Advisory Agencies of the California Levee Vegetation Research Program

California Levee Vegetation Research Program

Influence of Tree Roots and Mammal Burrowing Activity on Levee Performance:
Volume 2. - Parallel Trench Wetting Front Test, North Levee of the American River at Cal Expo Sacramento, California

Michelle Shriro, Diego Cobos-Roa, Jonathan D. Bray, Nicholas Sitar

Department of Civil and Environmental Engineering
University of California, Berkeley, CA

John Lichter

Tree Associates, Winters, CA

Richard Evans

Department of Plant Sciences
University of California, Davis, CA

Grant funding provided by:

The California Department of Water Resources (Contract No. 4600008761) and the Sacramento Area Flood Control Agency (Contract No. 984)

May 2014

Geotechnical Engineering
University of California, Berkeley
Report UCB GT 13-03 vol. 2

SUMMARY

To examine the effects of live and decaying root systems on levee seepage and slope stability, we conducted two field tests to measure the effects of seepage in the vicinity of live and decaying tree root systems. This report summarizes the results of the first of these tests and involved the construction of parallel trenches in the vicinity of a eucalyptus stump located along the landside of the northern levee bordering the American River adjacent to the California Exposition and State Fair ('Cal Expo'). A live hackberry tree with healthy roots was present at the toe of the levee. A control set of parallel trenches was constructed away from the eucalyptus stump. During the test, the upslope trench was flooded and maintained at constant hydraulic head to induce slope-parallel seepage and the downslope trench was used to make observations and collect any intercepted seepage. Piezometers and tensiometers were installed to measure positive and negative pore water pressures within the zone of flow to describe the wetting and flow patterns as they evolved within the levee. Instrumentation was placed to specifically assess the influence of the stump and its decomposing root system. Live roots, mammal burrows, and other features added complexity to the system. In addition to instrumentation data, visual observations were recorded during the 6-day flow test. During the flow test, wetting front and water flow patterns appeared to be dominated by flow through a network of shallow mammal burrows. Physical observation of the saturation front, as seen from the lower wall, confirmed that the area below the stump was the last location to saturate during the wetting test. Ground-based tripod light detection and ranging (T-LiDAR) technology was used to complement traditional field logging techniques and for constructing a 3D model of the root system, burrows and stratigraphy. Preliminary computer simulations of the wetting front progression support the basic patterns observed in the field test.

ACKNOWLEDGEMENTS

This study was performed collaboratively as part of the California Levee Vegetation Research Program (CLVRP) and was sponsored by the local, state, and federal agencies of the California Levees Roundtable through grants from Sacramento Area Flood Control Agency (SAFCA Contract No. 984), and the California Department of Water Resources (DWR Contract No. 4600008761). A great deal of support was provided by these agencies during our studies. The authors wish to thank Mr. Peter Buck, Program Manager for the CLVRP, consultant Mr. Mick Klasson, Ms. Cassandra Musto and Mr. Roy Kroll of the DWR and Ms. Laura Kaplan of the Center for Collaborative Policy for their invaluable help. We would like to thank the entire CLVRP team for their support and assistance during this research.

The authors would like to acknowledge the local maintaining agencies and landowners that provided access and support to our team during field efforts. Special thanks go to Mr. Tim Kerr, Mr. Richard Marck and the staff of the American River Flood Control District, as well as Mr. Ron King and the staff of Cal Expo. Their patience, support, and contributions are greatly appreciated.

Kleinfelder Inc., URS Inc., U.S. Army Engineer Research and Development Center (ERDC) and Prof. Alison Berry of UC Davis shared field equipment with us during our studies. Field efforts were assisted by Mr. Roy Kroll of the DWR, graduate students Aine Steiner, Justin Hollenback and Titus Chen of UC Berkeley, and Jeffrey Wu and Adam Akkari of UC Davis. We thank each of them for their hard work and commitment to the project.

The Cal Expo root characterization effort incorporating Ground-Based Tripod Light Detection and Ranging (T-LiDAR) technology was performed as a joint effort between the UC Berkeley team, Dr. Gerald Bawden of the USGS, Prof. Richard Evans of UC Davis, Mr. John Lichter, consulting arborist, and with advising from Prof. Alison Berry and Mr. Shih-Ming Chung of UC Davis. All T-LiDAR work for the project was performed by Dr. Gerald Bawden with assistance from Mr. James Howle and Ms. Sandra Bond of the USGS.

We had the good fortune of being advised by a number of key individuals whose advice benefited our study greatly. We would like to thank the entire advisory panel of the CLVRP and in particular Professors Dirk Van Vuren and Alison Berry of UC Davis, Dr. Les Harder of HDR Inc., Mr. Doug Shields of the USDA, Prof. Donald Gray of University of Michigan, Prof. Chris Peterson of the University of Georgia, Mr. George Sills, Mr. Mike Inamine of the Sutter Butte Flood Control Agency, and Mr. George Qualley of the California Department of Water Resources. Mr. Erik Mikkelsen provided great insight on the use of fully grouted piezometers and instrumentation. Mr. James Warner advised our team on burrow grouting methods. In addition, we would like to thank ERDC for their collaboration and feedback on our work, especially Dr. Maureen Corcoran and Dr. Kyle McKay.

CONTENTS

SUMMARY ..... **I**

ACKNOWLEDGEMENTS ..... **II**

1 MOTIVATION FOR RESEARCH **9**

2 PROGRAM SUMMARY AND OBJECTIVE **11**

3 PARALLEL TRENCH WETTING FRONT TEST **12**

3.1 SITE SELECTION – CALIFORNIA EXPOSITION AND STATE FAIR (CAL EXPO) 12
3.2 CAL EXPO SITE DESCRIPTION 14
3.3 SUBSURFACE STRATIGRAPHY 22
3.4 TEST LAYOUT 25
3.5 SITE CONSTRUCTION 33
3.5.1 Trench Excavation 33
3.5.2 Preparation of Trenches for Flow Test 44
3.5.3 Instrument Installation 46
3.6 FLOW TEST 49
3.6.1 Levee Slope Face Seepage 50
3.6.2 Burrows at Instrument Lines B and C 56
3.6.3 Wall Surface Saturation Progression 63
3.6.4 Instrument Results 77
3.6.5 Water Volume Usage During Flow Test 81
3.7 POST-FLOW TEST SITE CHARACTERIZATION EFFORT 85
3.7.1 Written and Photographic Documentation of Stump Excavation 86
3.7.2 Post Flow Test Site Characterization – Analysis of Data 101
3.7.3 T-LiDAR Applied to Flow Test Characterization 104

4 DISCUSSION OF FINDINGS **112**

5 RESULTS IN THE CONTEXT OF PREVIOUS STUDIES **114**

6 CONCLUSIONS **116**

REFERENCES **117**

APPENDIX A: SOIL BORINGS AND INSTRUMENTATION LOGS **121**

APPENDIX B: LABORATORY TESTING **122**

APPENDIX C: REGIONAL SOIL DATA **123**

APPENDIX D: TRENCH LOGS **124**

APPENDIX E: INSTRUMENT DATA **125**

APPENDIX F: FIELD CHARACTERIZATION TEST LOGS **126**

LIST OF FIGURES

Figure 1-1. USACE Vegetation-Free Zone (Source: USACE ETL 1110-2-571). 9
Figure 2-1. Conceptual Sketch of Parallel Trench Wetting Front Test. 12
Figure 3-1. California Exposition and State Fair (Cal Expo) site. Source of base aerial imagery: Google Earth. 13
Figure 3-2. Aerial view of the site showing the scatter of onsite mammal burrows (undifferentiated) and those identified to be collapsed burrows of the California ground squirrel. Base photo source: Google Earth, September 19, 2010. 14
Figure 3-3. Photos of the study site at the Eucalyptus stump. 15
Figure 3-4. Plan view showing trench configuration and stump locations identified during construction. Base photo provided by Cal Expo, 1973. 16
Figure 3-5. Aerial view of Cal Expo and the north levee of the American River in 1968 during the construction of Cal Expo. Aerial image provided by Cal Expo. 17
Figure 3-6. 1973: Approximate alignment of planting plan with aerial photo of site. Aerial image provided by Cal Expo. 17
Figure 3-7. A view of the four trees on site as of 1973 with corresponding planting plan showing proposed planting for those trees. Aerial images provided by Cal Expo. .. 18
Figure 3-8. View of the site in 1973, 1979, 1983, and 1990. Aerial images provided by Cal Expo. 20
Figure 3-9. Aerial photo comparison of the site in 1994 and 1995. In 1994, a distinct shadow of the eucalyptus tree(s) is seen. In 1995, the shadow is absent. 20
Figure 3-10. Aerial view of the site in 1996, 1997, 1998, and 2010. Source: 1996-1998, Cal Expo; 2010, Google Earth. 21
Figure 3-11. Aerial image from 1998-1999. Source: American River Watershed Improvements project (USACE, 1999). 21
Figure 3-12. Statigraphic section between upper and lower trenches at the eucalyptus stump. 23
Figure 3-13. Stratigraphic section at control trenches, located just west of instrument Line C (see Figure 3-20). 24
Figure 3-14. Cross section between upper and lower trenches at eucalyptus stump showing concept of proposed wetting front flow test. 25
Figure 3-15. Site plan with coordinate grid showing the stump and trenches under study, and the location of hand auger borings HB1 and HB2. 26
Figure 3-16. T-LiDAR image looking east at the eucalyptus stump and root system. Base T-LiDAR Image provided by Gerald Bawden of the USGS. 27
Figure 3-17. Eucalyptus stump is shown A) close in, B) from the east end of the trenches looking west, C) from below the stump trench looking southeast, and D) from the west end of the stump trench looking east. 28
Figure 3-18. Plan view of field test layout. 29

Figure 3-19. Field test layout looking west (upper left), east (upper right), and south (bottom left). Lower right is a site overview looking east and showing the hackberry tree in relation to trench excavations. 30
Figure 3-20. Instrument layout plan showing the locations of piezometers and tensiometers. 31
Figure 3-21. Photographic instrument plan showing the locations of piezometers and tensiometers as well as the naming conventions..... 32
Figure 3-22. Instrument layout at Line A at the eucalyptus stump in photograph and cross section. Base T-LiDAR image provided by Gerald Bawden, USGS. 33
Figure 3-23. Construction equipment used during excavation. A) hand excavation with vacuum to remove spoils; B) a vacuum trailer; C) air knife used to excavate around live roots; D) 375 CFM compressor to run the air knife. 34
Figure 3-24. View of trenches, A) looking east at stump trench and; B) looking west at control trench. 34
Figure 3-25. View of upper trenches, A) looking west at stump trench and; B) looking east at control trench. 35
Figure 3-26. Upper stump and control trench plan view logs (Stations 117-162). 36
Figure 3-27. Lower stump and control trench plan view logs (Stations 117-161.5). 37
Figure 3-28. Lower control trench Stations 124-132. Spliced plan view photos (top) during excavation of lower control trench and log of analogous segment below... 38
Figure 3-29. Stump found on downhill side of control trench at Station 127 as shown on Figure 3-28. 38
Figure 3-30. Lower stump trench Stations 140.5-146 (increasing to left). Spliced plan view photos (top) during excavation of lower stump trench and log of analogous segment below. Excavation not shown to full depth. 39
Figure 3-31. View looking south of 4’ deep trench at Station 145. Upper left photos are a cluster of live and decomposing roots and a 1” diameter pipe. Bottom right is a larger view of the same trench segment. 39
Figure 3-32. A 1-foot by 1-foot square grid was constructed to aid in logging and documentation of observations during the flow test. Source: Cobos-Roa et al. 2012. 40
Figure 3-33. Field log of uphill trench wall of lower stump trench, Stations 144-155 with corresponding photos above. 41
Figure 3-34. Lower trench photos with A) burrows and decomposing roots, B) a decomposing root, C) live roots, and D) a squirrel burrow and a material change . 43
Figure 3-35. Ants encountered during trenching activities (left). Small holes (1/2 to ¼ inch) found in trench wall could be related to ant activity (right). 44
Figure 3-36. Worm activity was observed to be responsible for some of the small holes (<¼ inch diameter) encountered during trenching. 44
Figure 3-37. Trench preparation prior to commencement of flow. A) Upper trenches lined with plastic sheeting (uphill and base walls) and permeable fabric (downhill wall); B) shored lower trench lined with plastic sheeting and gravel (base); C) water truck moistens site to prevent cracking prior to flow test. 45

Figure 3-38. A) Upper gravel-filled trenches; B) Water delivery system; C) ¾" flow meter for monitoring flows into water storage tank; D) Mechanical float to maintain constant head in upper trenches; E) Control valves at tank..... 46
Figure 3-39. A typical tensiometer is shown including a mechanical gauge and pressure transducer. White silica sealing material is seen at the hole entrance..... 47
Figure 3-40. Silica flour migration pattern below the stump (red circle) following installation of tensiometers..... 48
Figure 3-41. Flow test timeline 49
Figure 3-42. View of instrument line C (left) looking west and instrument Lines A and B looking east (right) 9.25 hours into the flow test. Note isolated seeps (darker spots) and gravel bags (covering seeps) at the top of Line C and extending down Line B. 51
Figure 3-43. View of instrument Lines B and C looking south 19.5 hours into the flow test. Note wet zones in slope face (darker spots) and gravel bags (covering seeps). 51
Figure 3-44. View looking west from instrument Line A at stump at 55 hours into the flow test. Note the outline (red) of the growing wet zone observed at the levee slope face 52
Figure 3-45. Location of mammal burrows in relation to Instrument Lines A, B, and C. . 57
Figure 3-46. Water seepage at lower trench wall near gopher burrow at instrument Line B minutes after first water appeared on the levee slope face..... 58
Figure 3-47. Saturation patterns in lower wall face at 29.1 hours after inundation of the upper trench with water. The lower stump (top left) and control (top right) trench wall seepage patterns are documented by station with corresponding photos below..... 64
Figure 3-48. Saturation patterns in lower wall face at 29.4 hours after inundation. Note the appearance of seeps in permeable zones near the trench bottom. The lower stump (top left) and control (top right) trench wall seepage patterns are documented by station with corresponding photos below. 65
Figure 3-49. Saturation patterns in lower wall face at 29.9 hours after inundation. Note that seeps seem to be related to permeable material types. The lower stump (top left) and control (top right) trench wall seepage patterns are documented by station with corresponding photos below..... 66
Figure 3-50. Saturation patterns in lower wall face at 46.6 hours after inundation. Note the depression in the saturation pattern in the area of the decomposed root at Station 147. The lower stump (top left) and control (top right) trench wall seepage patterns are documented by station with corresponding photos below. 67
Figure 3-51. Saturation patterns in lower wall face at 51.7 hours after inundation. Note the wetting front continues to rise near the stump at Stations 145-150, though a depression is still visible indicating the stump is the last zone to saturate. The lower stump (top left) and control (top right) trench wall seepage patterns are documented by station with corresponding photos below. 68
Figure 3-52. Wide angle view of saturation patterns at 67.9 hours into the flow test. The area below the stump has begun to saturate. 69

Figure 3-53. Saturation patterns in the stump and control trenches at 140 hours into the flow test, just before the end of the test. Only small changes were observed in saturation patterns between 67.9 hours and 140 hours..... 70
Figure 3-54. Comparison after 51.7 hours of flow. The zone in front of the stump was the last to saturate. 71
Figure 3-55. View looking west at the uphill wall of the lower stump trench 50 hours into the flow test. Gopher burrow outlet locations at Stations 138.25 and 117 are identified on the diagram as well as approximate alignments of burrows. 72
Figure 3-56. Control trench gopher burrow advances the wetting front (left) tracing a pathway to the outlet location at Station 117 (right). The outlet flowed briefly. ... 72
Figure 3-57. The wetting front is advanced by gopher burrow at Station 138.25. Slope saturation patterns looking A) south; and B) east. Photo C traces zone of early saturation due to the gopher burrow at a time of 12.7 hours into the flow test 73
Figure 3-58. Squirrel burrow extending at least 18 inches into the uphill wall of the lower trench at A) the time of trench construction and B) 50 hours into the flow test. No free water flows until a seep upon saturation at 125 hours (See Table 3-2) 73
Figure 3-59. Progression of wetting at the decomposed root at Station 147.5. 74
Figure 3-60. Progression of wetting at decomposed roots showing no preference to flow through the root or the gapping or loose zones surrounding the roots. 74
Figure 3-61. During the flow test water is shown flowing through the gopher burrow and seeping out of permeable soils within the wall face, though no flow was observed through the adjacent live roots. 75
Figure 3-62. Live roots are shown during the flow test throughout the lower stump trench. At no time during the flow test were live roots observed to conduct water. 76
Figure 3-63. Typical tensiometer result plot..... 78
Figure 3-64. Tensiometer data for instrument Line A (at stump). 79
Figure 3-65. Tensiometer data for instrument Line B (7 ft from stump). 79
Figure 3-66. Tensiometer data for instrument Line C (23 ft from stump). 80
Figure 3-67. Pore pressures measured during flow test at instrument Lines A and C..... 81
Figure 3-68. Calculation of flow volumes into and out of trenches. Note that a significant fraction of the input water was lost to areas outside of the study zone. 82
Figure 3-69. Plot of cumulative water delivered to the upper trenches from the 2,500 gallon reservoir and water recycled from the lower stump trench to reservoir. 83
Figure 3-70. Cumulative gallons of water either delivered to the upper trench from the reservoir or recycled from the lower trench back to the reservoir. Curves are broken into segments with slopes representing the rate of flow. 84
Figure 3-71. Relative permeability of water and air as a function of degree of saturation during drainage (Freudlund and Rahardjo, 1993; originally from Brooks and Corey, 1964). Note: Diagram intended for the illustration of concepts only. Actual relative permeability is expected to vary by soil or rock type. 85
Figure 3-72. Excavation was completed around the stump in a series of vertical slices from Stations 138 to 153 as shown. 86

Figure 3-73. ARFCD grout plant and trailer combination is shown (left). To the right, burrows are plugged with burlap sacks using a rod leveraged against the ground in order to prevent loss of grout. 87
Figure 3-74. Mammal burrows at instrument Lines B and C following post-flow grouting and characterization efforts. 87
Figure 3-75. View of decomposing root encountered in the lower stump trench, Station 155. 88
Figure 3-76. Close in view of decomposing root at Station 155. No gap was observable around this friable and highly decomposed root. 88
Figure 3-77. View looking southeast at the trenches following excavation of the downhill wall of the lower stump trench. 89
Figure 3-78. View of the uphill wall of the lower stump trench between Stations 138 and 151 just prior to scanning with T-LiDAR. 89
Figure 3-79. View of air knife operation during post-flow test site characterization effort. 90
Figure 3-80. View of uphill wall of the lower stump trench as excavation of Slice 1 began. The root that was a conduit for silica slurry to the face of the lower wall during tensiometer installation is pictured. 90
Figure 3-81.View of upper wall in lower trench below the stump A) during the flow test, and B) following the completion of 'Slice 1' excavation. 91
Figure 3-82. Typical appearance of decomposing roots encountered. Bark was fragile and discontinuous in many places. Annular spaces are seen on larger roots. Photos by Richard Evans. 91
Figure 3-83. Examples of discontinuous annular space found in some decomposing roots. Many decomposing roots did not display this gap 92
Figure 3-84. Slice 1 wall surface 93
Figure 3-85. Hardened silica slurry associated with tensiometers T4A-36 (left) and T4A-60 (right) is discovered. Flow paths were observed showing that silica flowed through a burrow or void when a direct hydraulic connection was present. 94
Figure 3-86. Silica slurry freely flowed in burrows (as shown in A) and void spaces within roots (as shown in B) when a direct hydraulic connection was available (or present). 94
Figure 3-87. Bark fully decomposed with annular space between the woody core and bark, loosely filled with decomposed organic matter and soil (A and B). White silica slurry in Photos A and C are from a tensiometer intersecting loose organic soils and the silica slurry permeating the void space for a short distance. 95
Figure 3-88. Roots can leave a void where they become completely decomposed and surrounding soils and live roots have not yet in filled the void. The root in Photo D has likely been subjected to decomposition from biological activity. 95
Figure 3-89. Photos A through D are examples of sands in-filling void spaces present between the decaying roots woody center and the bark. In Photo B, from right to left we see the woody core, an infill sand layer, a layer of decomposing bark, a live root, and then the surrounding soil matrix 96

Figure 3-90. Live roots frequently observed growing within the decomposing organic matter of old root systems. 96
Figure 3-91. Final position of 'Slice 2' at the time of logging and before T-LiDAR scanning. Note presence of burrow networks between the root system in Photo B (indicated by vertically-oriented orange nylon strips). Photo C shows the newly revealed burrow casting at Station 138.25..... 97
Figure 3-92. View of stump excavation following removal of 'Slice 3' soils. Photo A is a view of the stump from the crest of the levee looking down into the upper trench. Photos B through D show the stump from varying angles. Photo D also shows T-LiDAR scanning in progress. 98
Figure 3-93. View root system of the decomposing stump looking north from the upper trench (top). Note migration of silica flour through a path directly traceable to a location where the installation of a tensiometer penetrated the root..... 99
Figure 3-94. View of the excavated eucalyptus stump looking A) southwest from the former location of the lower trench, B) north from the upper trench, C) south at the roots at base of stump, and D) west from between the upper and lower trenches as Richard Evans, UC Davis, inspects the roots system from the uphill side. 100
Figure 3-95. As-built site plan showing T-LiDAR scans of root system and burrow (provided by Gerald Bawden, USGS) at Station 138.25..... 101
Figure 3-96. The area of each root intersected was calculated and sorted by distance from the stump center. The chart shows the cumulative sum of root area from the center of the stump extending radially outward..... 103
Figure 3-97. Slice 1 comparison between T-LiDAR image (left) and photograph (right). Note reflectors in T-LiDAR image indicating burrows (vertically oriented) and decomposing roots (horizontally oriented). Source: Cobos-Roa et al. 2012. 104
Figure 3-98. T-LiDAR data is viewed in 3D at the UC Davis KeckCAVES. Point clouds are selected and isolated, separated, relocated, and rotated through this user-friendly 3D interface. Gerald Bawden of the USGS gives the UC Berkeley team a tour. Photos courtesy of Mick Klasson. 105
Figure 3-99. T-LiDAR images provided by Gerald Bawden of the USGS (top) looking south compared with photograph of root system (bottom) and burrow at Station 138.25. 106
Figure 3-100. T-LiDAR scan of root system and burrow at Station 138.25 (provided by Gerald Bawden of the USGS). View is from the top. Most roots are decomposing roots related to the eucalyptus stump, but live roots are present, particularly in the vicinity of the burrow..... 107
Figure 3-101. View of the decomposing eucalyptus root system from above as scanned with T-LiDAR. The image is used here to show the path of silica flow from the tensiometers and instrument positions within the root system. Photographs show silica flow through the root intersecting with tensiometer T1A-36 (upper right) and a south-facing frontal view of the stump and root system. T-LiDAR image courtesy of Gerald Bawden of the USGS. 108

Figure 3-102. A south-facing view of eucalyptus stump and root system (right) and the corresponding point cloud image (left) derived from combining data from a series of T-LiDAR scans. T-LiDAR image courtesy of Gerald Bawden of the USGS. 109
Figure 3-103. A west-facing view of the Eucalyptus stump and root system stitched together from a series of T-LiDAR scans (provided by Gerald Bawden, USGS)..... 110
Figure 3-104. A view of the Eucalyptus root system as a point cloud generated from T-LiDAR scans (left) and a vectorized plot of the root system to aid in modeling efforts. Base source: Gerald Bawden, USGS. 111
Figure 4-1. Simple conceptual models illustrating volumetric water content from initial state (yellow) to saturation (red). The predicted effects of various void spaces on saturation patterns as modeled using the software package SeepW..... 114

LIST OF TABLES

Table 3-1. Trench Dimensions and Coordinates 27
Table 3-2. Photographic Timeline of Slope Face Seepage 53
Table 3-3. Summary of observations at animal burrow at Station 138-140 (Line B) 59
Table 3-4. Summary of observations at gopher burrow, Station 117 (control trench).... 61
Table 3-5. Flow Rate Breakdown 84
Table 3-6. Burrow density at excavated stump and control trenches. 103

1 MOTIVATION FOR RESEARCH

The devastating flooding of New Orleans resulting from Hurricane Katrina brought to light the fragility of levee systems across the United States. The years following this disaster have brought a renewed focus on public safety and a closer look at policies, standards, and conditions of existing levee systems. In 2009, the United States Army Corps of Engineers (USACE) released the document "Guidelines for Landscape Planting and Vegetation Management at Levees, Floodwalls, Embankment Dams, and Appurtenant Structures" (ETL 1110-2-571). The guidelines show a vegetation-free zone across the levee surface and extending 15 feet from the toe of both the land and water sides (Figure 1-1). The vegetation-free zone is expanded where stability berms or other structures are present near the toe.

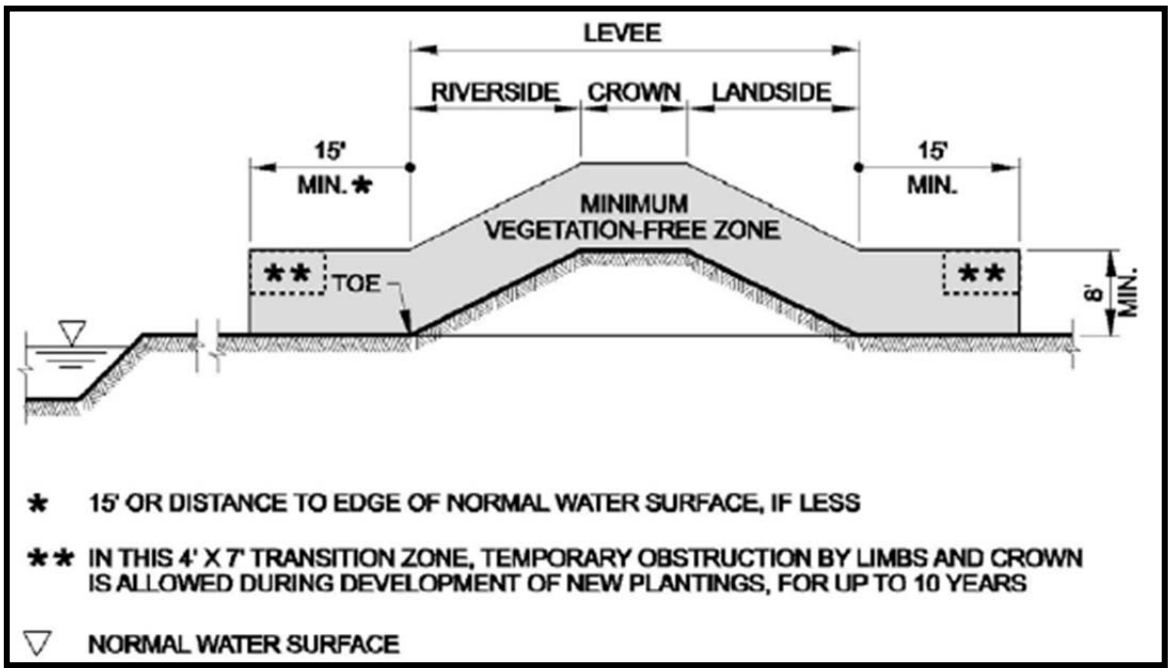

Figure 1-1. USACE Vegetation-Free Zone (Source: USACE ETL 1110-2-571).

Though consensus has not been reached with regard to the impact of woody vegetation on levee integrity (Corcoran et al., 2010), the presence of woody vegetation can introduce uncertainty in the reliability of levee performance. Trees and their roots have been suggested to possibly undermine the integrity of compacted earthen levees by providing enhanced and focused seepage through the levees. It is argued that tree roots could potentially provide paths that water could more easily flow through which could bring the full water pressure of the water retained by the levee to locations within the levee (Pierson, 1983). These high water pressures within the levee could produce piping and erosion of the levee materials, which could undermine levee integrity and stability (ASDSO, 2002). Further, windthrow of levee trees during large storms or hurricane events leading to concentrated flow through the levee or erosion and scour present additional

concerns (ASDSO, 2002). Maintenance and access for inspectors is another stated reason for USACE's policy on vegetation.

Alternately, live tree roots are believed to strengthen the levee and improve slope stability in many cases (e.g., Shields and Gray, 1992; Ziemer, 1981). It is not known whether the documented benefits of roots in terms of reinforcing earth slopes and strengthening the slopes may more than offset the potentially damaging effects of any localized regions of higher pore water pressure within the levee. The effects of roots of healthy woody vegetation on seepage patterns through levees are not well understood. Additionally, the removal of trees from levees may destabilize levees due to the decay of roots that remain after the trees are cut down (Ziemer, 1981). Decomposed and decayed roots could provide enhanced seepage that might degrade long-term levee performance.

The federal levee vegetation standard outlined in ETL 1110-2-571 (USACE, 2009) is designed to be applied broadly with a focus on public safety. California's levees were built close together, adjacent to the rivers as a means of flushing mining debris from the rising riverbeds (California Department of Water Resources, 2013). As a result of this unique history, critical riverine habitat shares space with structures providing flood protection (Harder et al., 2011). The USACE can opt to grant a variance to vegetation standards where locally appropriate (USACE, 2009). Acquiring such a variance can be a costly and lengthy process. Vegetation can affect levee performance in a variety of ways (Gray et al., 1991), however levee integrity has historically been compromised primarily by factors other than the presence of vegetation (e.g., overtopping, underseepage), or at times by the absence of vegetation (e.g., erosion). Based on a review of performance records related to California levees, a study by Punyamurthula and Millet (2012) found few records that indicated vegetation had an influence on levee performance and those that did were primarily related to visibility and access issues associated with levee operation and maintenance. With limited monetary resources available to California for flood protection, levee improvements that bring the greatest increases to public safety per dollar are desirable.

The above issues have spawned debate as to the hazards and benefits associated with vegetation on levees. The agencies of the California Roundtable for Central Valley Flood management (formerly the California Levees Roundtable) are conducting research that will determine the extent to which woody vegetation, such as trees, may affect the safety and integrity of levees in California's Central Valley.

These studies include:

1. A national research program implemented by the U.S. Army Engineer Research and Development Center (ERDC).
2. Parallel and complementary effort initiated in California referred to as the California Levee Vegetation Research Program (CLVRP).

ERDC and the CLVRP have been collaboratively coordinating their research efforts. As part of the CLVRP research effort, researchers from several universities along with expert consultants and advisors were brought together to investigate the effects of woody vegetation on levee performance. The overall objective of the CLVRP research effort is to gain the technical knowledge needed for the development of sound vegetation management policies in an effort to obtain the most flood risk reduction at the lowest environmental and monetary cost. The primary objective of this research effort by the UC Berkeley team is to examine the effects of live and decaying root systems on levee seepage and slope stability. The research is ongoing, and presented herein are the preliminary results of our first field study.

2 PROGRAM SUMMARY AND OBJECTIVE

As part of this overall research effort of the CLVRP, this study is focused on developing and understanding of the effects that live and decaying root systems have levee seepage and slope stability. Specifically, the objective of the UC Berkeley team's program is to investigate whether roots have an effect on levee seepage, the extent of that effect, and how the presence of roots may influence the overall stability of the levee. Two field tests have been designed and performed to evaluate the effects of decayed and decomposed tree roots on seepage through an earthen levee and the resulting potential for seepage-induced instability.

This second volume of the six volume series summarizes the results of our first field test. This initial effort involved constructing and executing a Parallel Trench Wetting Front Test. The concept of the test involves excavating small parallel trenches above and below the root system of a tree on a levee slope. The upslope trench is supplied with water and held at a constant hydraulic head, imposing a two-dimensional flow path from the upslope trench to the downslope trench. Instrumentation installed within the zone of flow captures positive and negative pore water pressures before, during, and after flow. A conceptual sketch of the first field test is provided as Figure 2-1.

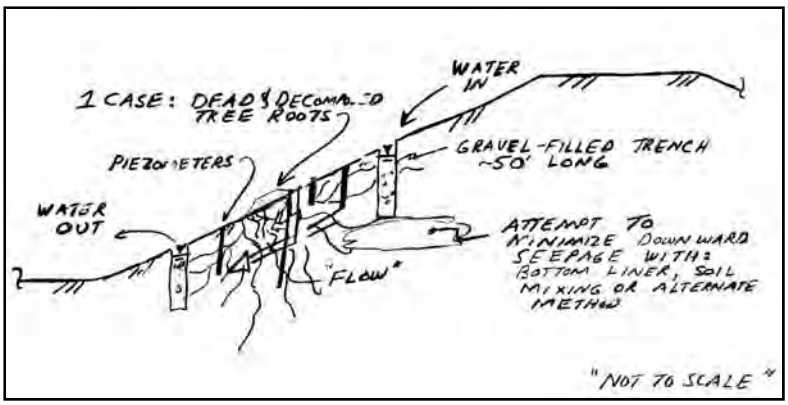

Figure 2-1. Conceptual Sketch of Parallel Trench Wetting Front Test.

3 PARALLEL TRENCH WETTING FRONT TEST

Conceptual sketches began to evolve into a design phase as site selection began. Each site viewed possessed unique qualities with its own set of advantages and disadvantages. The final was ultimately customized to adapt to the conditions of the most suitable site.

3.1 SITE SELECTION – CALIFORNIA EXPOSITION AND STATE FAIR (CAL EXPO)

Selection of an appropriate site to study was an important element of the field effort and involved the combined efforts of the UC Berkeley team, DWR and SAFCA to contact reclamation and flood control districts within areas known to maintain levees with vegetative cover. Individual districts provided information regarding possible stump sites and promising sites were viewed and evaluated for suitability.

The primary considerations in selecting a test site were soil conditions, age of stump, position of stump on slope, and proximity to 'control' conditions. Additionally, the reclamation districts needed to allow access to the levees for a large-scale excavation effort in the months just prior to flood season. A mid-slope stump was important in order to accomplish the test shown in Figure 2-1 and keep both upper and lower trenches within levee soils rather than foundation soils. Soils exhibiting no cohesion were determined to be undesirable for reasons of temporary stability during the flow test. In terms of stump age, we were seeking a stump that was likely to be undergoing significant decomposition, but without having achieved complete decomposition within the root system at the time of the study. Gray and Leiser (1982) provide a discussion of tensile resistance of roots with time after felling. They cite the work of Burroughs and Thomas (1977) where 75 percent of root tensile strength for a 1 cm root is lost over 4 years after felling of a Pacific Coast Douglas fir. The tensile resistance of this root was approximately a tenth of its fresh strength at 10 years after felling. A Rocky Mountain Douglas fir lost only 10 percent of fresh tensile strength in a 4 year period following felling and took about 10 years for the root strength to drop to 70 percent of fresh strength. Based on discussions

with the CLVRP advisory panel, including Professor Gray, a target age of stump was determined to be on the order of 5 to 10 years with an understanding that this may vary based on a number of factors including tree species and size. Other factors considered were tree species, observed animal activity, and proximity to other trees and stumps.

Based on the criteria presented above, we selected a site within the American River Flood Control District (ARFCD). The site is located along the landside of the northern levee bordering the American River adjacent to California Exposition and State Fair ('Cal Expo') and was selected due to the presence of the decaying eucalyptus stump shown on Figure 3-1. The stump was well positioned on the slope, appeared to be significantly decayed, and exhibited minimal signs of animal activity in the immediate vicinity of the stump. The northern levee of the American River in the vicinity of Cal Expo has a crest elevation approximately 16 feet above adjacent grades with a landside horizontal to vertical slope gradient of approximately 2 to 1.

Figure 3-1. California Exposition and State Fair (Cal Expo) site. Source of base aerial imagery: Google Earth.

3.2 CAL EXPO SITE DESCRIPTION

As previously discussed, the selected site is located along the landside of the northern levee bordering the American River. A site walkover was performed to evaluate site conditions from the surface. Professor Dirk Van Vuren of UC Davis served as the CLVRP team expert on burrowing mammals. Professor Van Vuren viewed the site with our team and burrow locations were flagged and categorized based on his experience. A total of 17 surface expressions of burrows were found within 20 feet of the test (to the east and west) on the landside slope face. Based on Professor Van Vuren's visual observations, the burrows consisted of abandoned and some collapsed burrows of the California ground squirrel and the pocket gopher (Figure 3-2).

Figure 3-2. Aerial view of the site showing the scatter of onsite mammal burrows (undifferentiated) and those identified to be collapsed burrows of the California ground squirrel. Base photo source: Google Earth, September 19, 2010.

The landside of the levee is inclined at approximately 2H:1V (horizontal:vertical). The eucalyptus stump selected for study was positioned approximately 6 feet from the crown and 10 feet from the toe of the levee, measured vertically (Figure 3-3).

A second stump was found just east of the study area adjacent to the lower trench. The stump was observed by Professor Alison Berry of UC Davis, and determined to be a eucalyptus stump. Trench construction revealed two additional stumps, both north (downslope) of the control trench that were not previously visible from the ground surface. Figure 3-4 shows the configuration of all stumps found within the

study area overlain onto a 1973 aerial photograph. A live hackberry tree with a 36 inch trunk diameter is located at the toe of the levee on an alignment 4 feet west of the stump as shown on Figure 3-2 through Figure 3-4. Aerial imagery shows the tree to have a canopy diameter of approximately 55 feet at the time of our study in 2010.

The history of trees and stumps within the study area was explored by examination of aerial photography. Cal Expo has an extensive library of photography and construction documents, including a planting plan showing trees proposed for planting on the levee at the time of construction of Cal Expo between 1967 and 1968. Cal Expo retains aerial photos flown on a nearly annual basis, typically during the state faire each year in late August. Many photos were not high enough quality in the study area to identify individual trees with certainty.

Figure 3-3. Photos of the study site at the Eucalyptus stump.

Figure 3-5 shows Cal Expo under construction in 1968 at which time trees has not yet been planted along the levee. A planting plan prepared by Lawrence Halprin and Associates and dated November 27, 1967 was provided by Cal Expo for our review. Figure 3-6 shows an approximately 1500 foot stretch of the planting plan aligned with an aerial photo taken in 1973. The plan shows many trees that do not exist in the 1973 photograph, while trees actually seen in the 1973 aerial photograph do not appear to have been planted in the precise locations proposed. Nevertheless, a mass planting took place and many more trees are present in 1973 than in 1968. According to Ron King, the head of grounds maintenance for Cal Expo, many of the initial trees planted at that time did not survive. This observation is

consistent with our review of planting plans as compared with aerial photography in the years following construction.

Figure 3-7 shows a close-up of the aerial photo from 1973 with the tree identified as the stump under study indicated. Four trees are shown within the study area and street lights are used to pinpoint the location of our Eucalyptus stump. The planting plan shows the two trees to the east are *Eucalyptus rostrata*, while the two trees to the west are *Pinus radiata*. The position of trees does not seem to correlate exactly with the plan. In general, the species of the trees onsite currently seem to match those planted and consist primarily of eucalyptus and pine. Based on a visual evaluation, CLVRP root architecture research expert, Professor Alison Berry of UC Davis identified the two stumps to the east as Eucalyptus. Stumps to the west were not evaluated for species as they were not visible from the surface, were highly decomposed and generally downslope of the study area. Additional stumps were found during trench construction and may have been remnants of the trees shown on Figure 3-7.

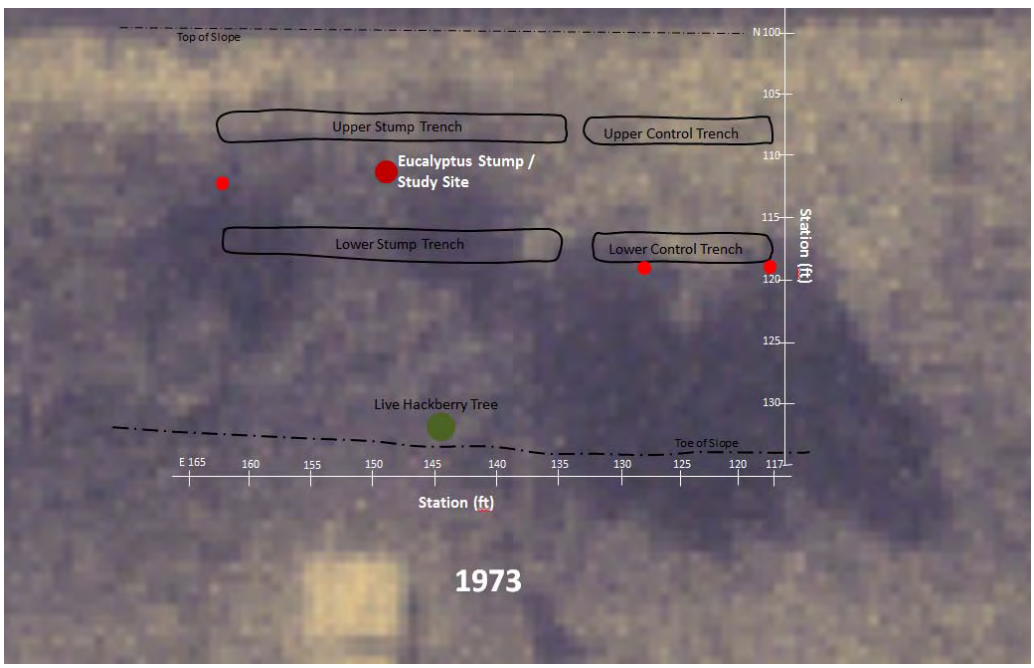

Figure 3-4. Plan view showing trench configuration and stump locations identified during construction. Base photo provided by Cal Expo, 1973.

Figure 3-5. Aerial view of Cal Expo and the north levee of the American River in 1968 during the construction of Cal Expo. Aerial image provided by Cal Expo.

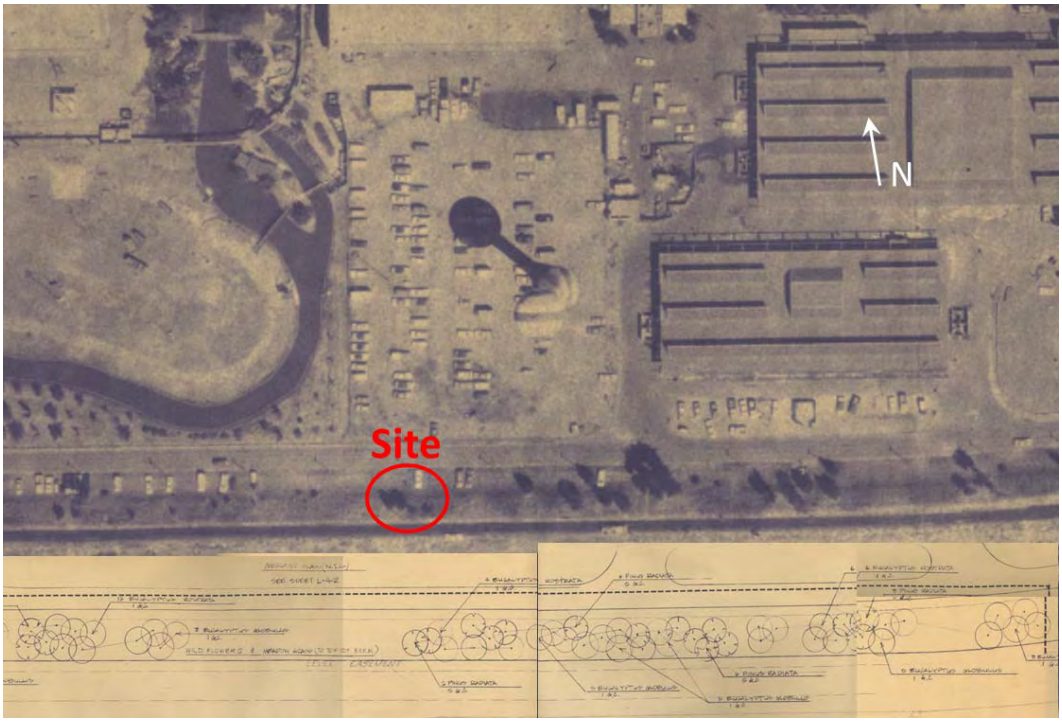

Figure 3-6. 1973: Approximate alignment of planting plan with aerial photo of site. Aerial image provided by Cal Expo.

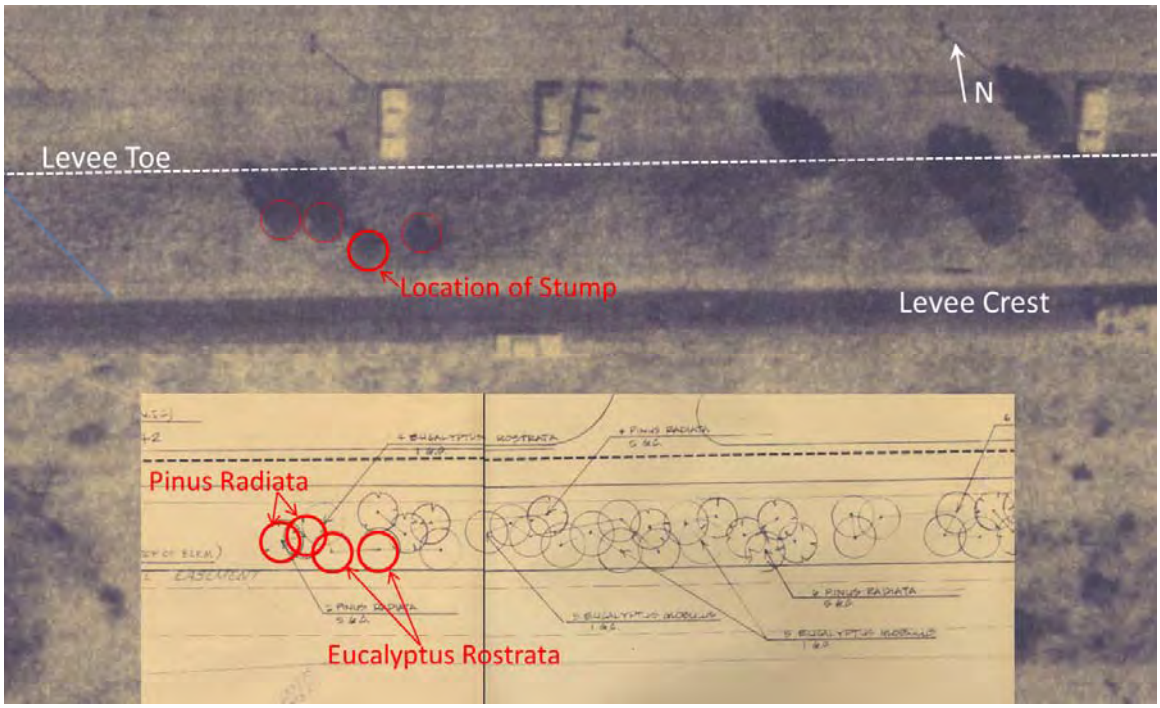

Figure 3-7. A view of the four trees on site as of 1973 with corresponding planting plan showing proposed planting for those trees. Aerial images provided by Cal Expo.

Based on our review, we estimate the Eucalyptus tree studied was cut between 1994 and 1998. Figure 3-8 shows the site in 1975, 1979, 1983, and 1990. In 1975, four trees can be seen at site. In 1979, a small shadow could be the hackberry tree. In 1983, both the hackberry and the eucalyptus trees are clearly visible. In 1990, it is clear that there is at least one tree with multiple main branches or possibly two trees upslope of the hackberry tree. In Figure 3-8 and Figure 3-9, the Eucalyptus tree(s) can be seen in 1990 and 1994 and appear to be two trees. The following year in 1995, the aerial photograph appears to have been taken at a similar time of day and the shadow of the Eucalyptus tree shown in 1994 is not present in 1995 (Figure 3-9). Trees may have been cut back or removed between 1994 and 1995.

Figure 3-10 shows the site in 1996, 1997, 1998, and 2010. The 2010 image shows the hackberry tree during our flow test. In 1996 and 1997, the shadow patterns, overlapping canopies, and poor image quality make it difficult to discern whether the Eucalyptus trees are present. In 1997, leaves of the hackberry are beginning to change color, while the uphill segment of the canopy appears a slightly different shade of green, possibly indicative of a tree that does not lose leaves in the winter, such as a Eucalyptus. Between 1997 and 1998, a number of trees, including those just west of our stump, were removed. The removal was likely part of the 1998-1999 American River Watershed Improvements project that involved construction of a slurry wall within the levee crown. The eucalyptus trees upslope of the Hackberry may have been removed between 1997 and 1998 in preparation for this work. The USACE's plans approved in April of 1999 (USACE, 1999) and prepared by the Sacramento District, Central Valley Section show the hackberry tree, the

eucalyptus tree(s) and other nearby trees to be present in the background aerial photograph (Figure 3-11). Also shown is the water pipeline found during trench excavation (N3-10 as shown on the plan) and further discussed in Appendix C. Many trees are noted as requiring removal for construction, but the eucalyptus is not specified, perhaps because it had already been removed.

A summary of information gained from our review of aerial photography follows:

- The eucalpytus stump under study was likely the remains of a tree removed in 1998 prior to the installation of the slurry wall along the north levee of the American River. It is also possible that the tree was aggressively cut back or removed between 1994 and 1995, making the stump 12 to 16 years old at the time of our study.
- The two trees west of the stump under study may be *Pinus radiata*, planted around 1968 and removed between 1983 and 1990.
- The eucalyptus west of the stump under study was planted during or shortly after 1968. This tree may have been removed in 1994 or 1998 with the stump being studied.
- The hackberry tree at the toe of slope was not planted and appears in the late 1970's and is clearly visible in a 1983 aerial photograph. The age at the time of study is estimated at 31 years. This is consistent with estimates by Professor Berry based on her visual evaluation.

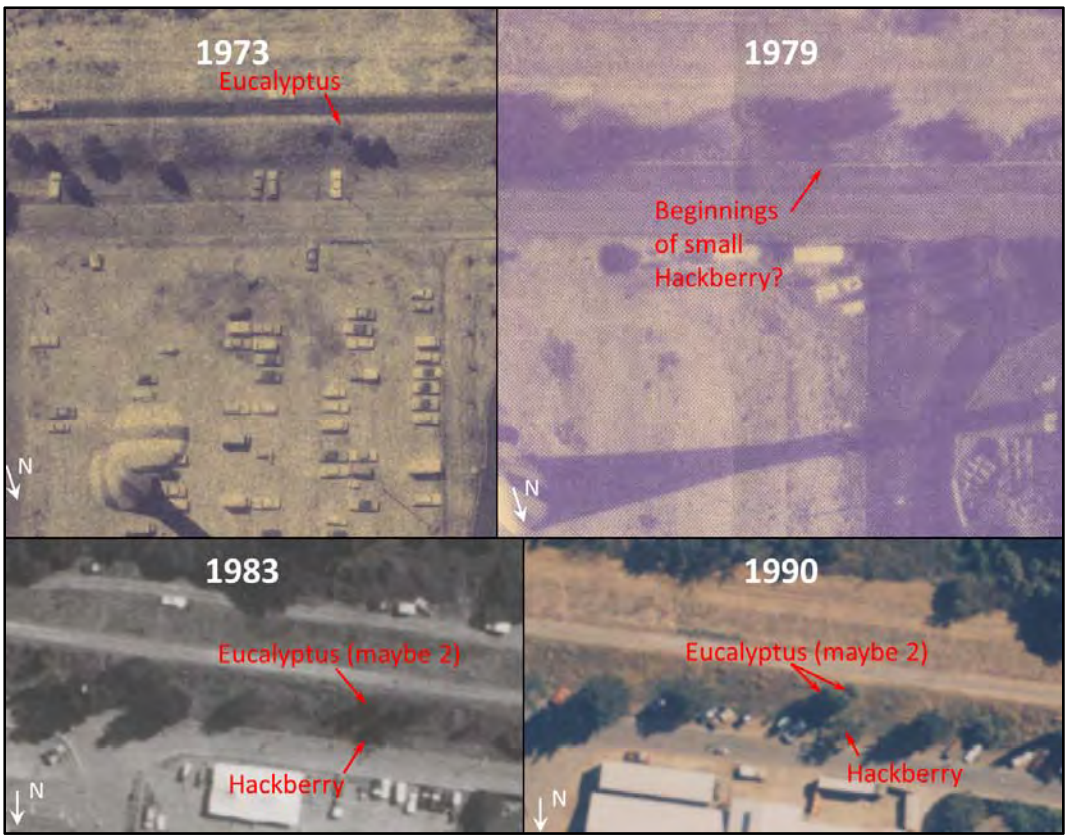

Figure 3-8. View of the site in 1973, 1979, 1983, and 1990. Aerial images provided by Cal Expo.

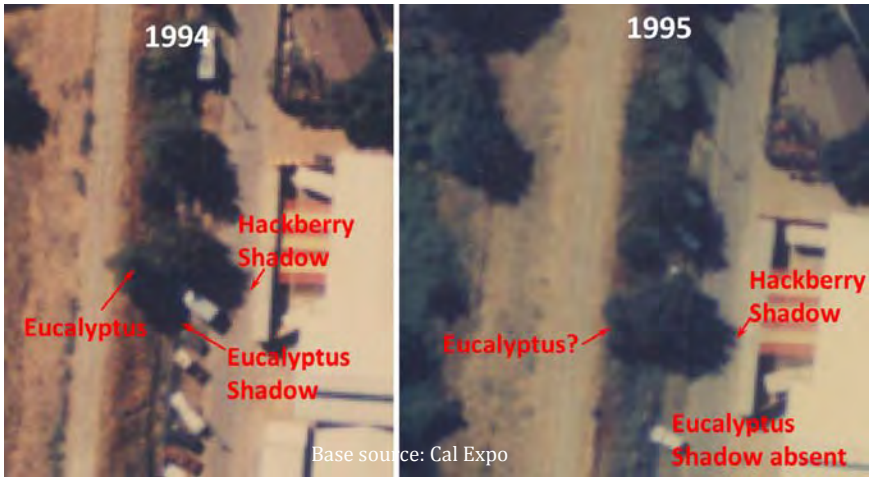

Figure 3-9. Aerial photo comparison of the site in 1994 and 1995. In 1994, a distinct shadow of the eucalyptus tree(s) is seen. In 1995, the shadow is absent.

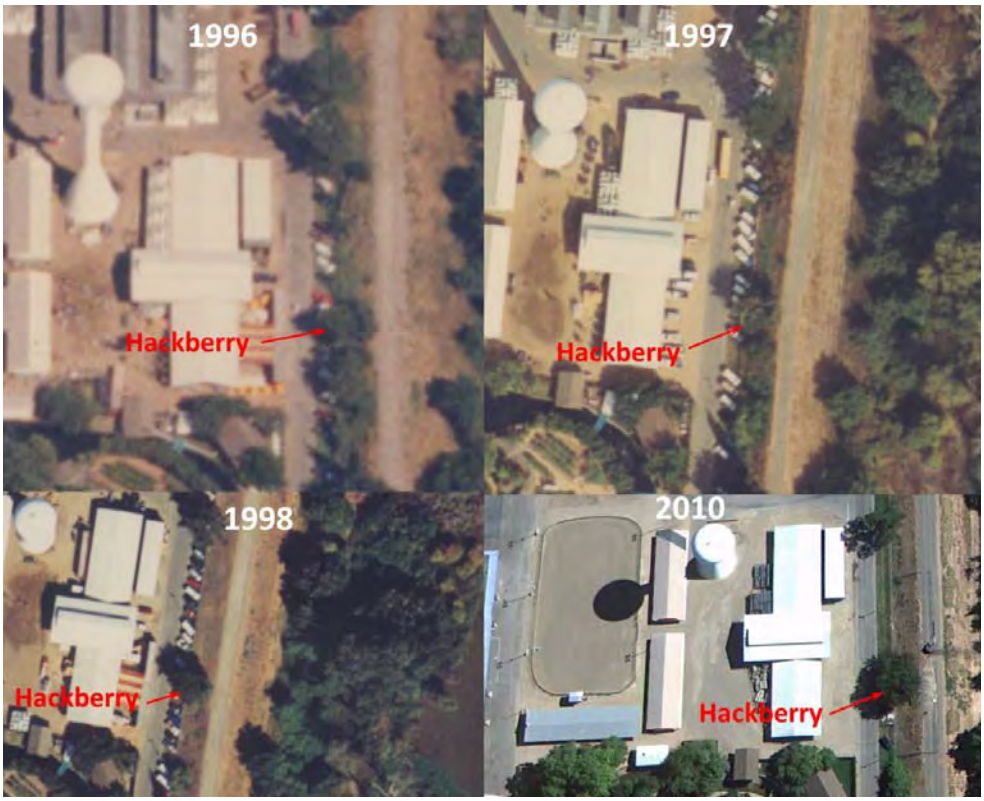

Figure 3-10. Aerial view of the site in 1996, 1997, 1998, and 2010. Source: 1996-1998, Cal Expo; 2010, Google Earth.

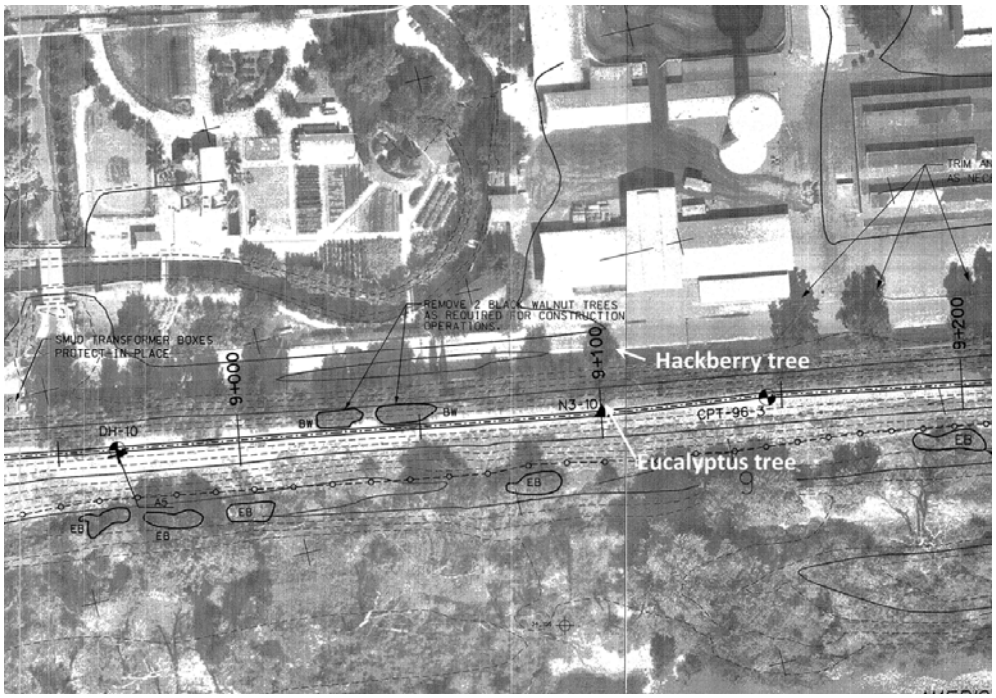

Figure 3-11. Aerial image from 1998-1999. Source: American River Watershed Improvements project (USACE, 1999).

3.3 SUBSURFACE STRATIGRAPHY

Soil conditions were an important factor in the selection of the site, in the implementation of the test, and in the interpretation of test results. The site soils were characterized using the Unified Soil Classification System (USCS) prior to and during test construction. Test borings and instrument holes were augered and conditions logged and summarized in Appendix A, with associated laboratory testing presented in Appendix B. We reviewed available regional and local soil information in the American River Common Features General Re-evaluation Report (URS, 2009), the American River Watershed Project Right (North) Bank Levee Strengthening plans dated April 1999 (USACE, 1999), and the American River Levee General Design dated June of 1956 (USACE, 1956). In Appendix C, we included relevant plans, soil boring logs, cross sections and excerpts.

During construction and after the flow test, trench walls and excavations were observed and observations were recorded onto field logs. These field logs are provided in Appendix D. Our post-flow characterization effort included excavation of the zone surrounding the stump with observations recorded through both traditional field logging and tripod-based light detection and ranging (T-LiDAR) imaging (Cobos-Roa et al., 2012). A cross section showing the stratigraphy in the area of the eucalytus stump under study is provided as Figure 3-12. T-LiDAR was used only in the area around the stump and root system. At the control section, a backhoe test pit was excavated at instrument Line C in order to view the and log the stratigraphy (Figure 3-13). Site soils consisted of interbedded silts, silty sands, sandy silts, and lean clay.

The site soils generally consisted of clayey and sandy silts and silty sands. Pockets and lenses of low fines content sands were observed during excavation and characterization efforts. Relatively horizontal layering was found within localized excavation areas. Based on our excavations, site soils consist of roughly continuous layering of heterogeneous blends of materials where pockets of homogeneity are encountered. Material 3 is comprised of materials 3a and 3b in a heterogeneous blend. Material 4, lean clay with zones of clayey silt, is found to be about 1 foot deeper in the control than in the stump section. Like all onsite materials, the layer is heterogeneous and contains pockets of sands and silts. Additional information is provided in Appendix D. In general, our findings are consistent with general levee profiles for the region by URS (showing layered silts and lean clays to the west of our study site and layered sandy silts and silty sands to the east) as well as available boring and Cone Penetration Test (CPT) data for the American River Watershed Project Right (North) Bank Levee Strengthening plans (USACE, 1999).

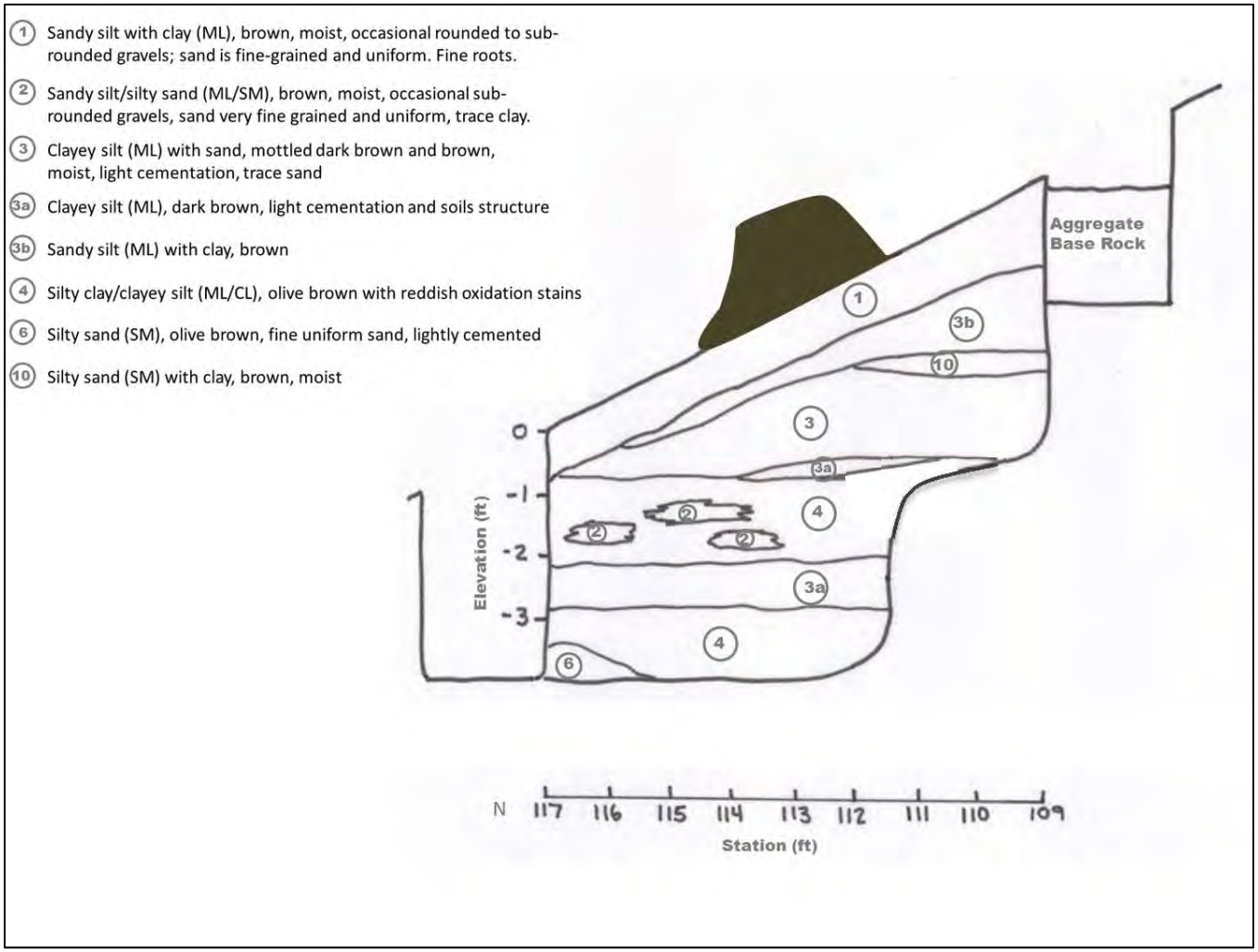

Figure 3-12. Statigraphic section between upper and lower trenches at the eucalyptus stump.

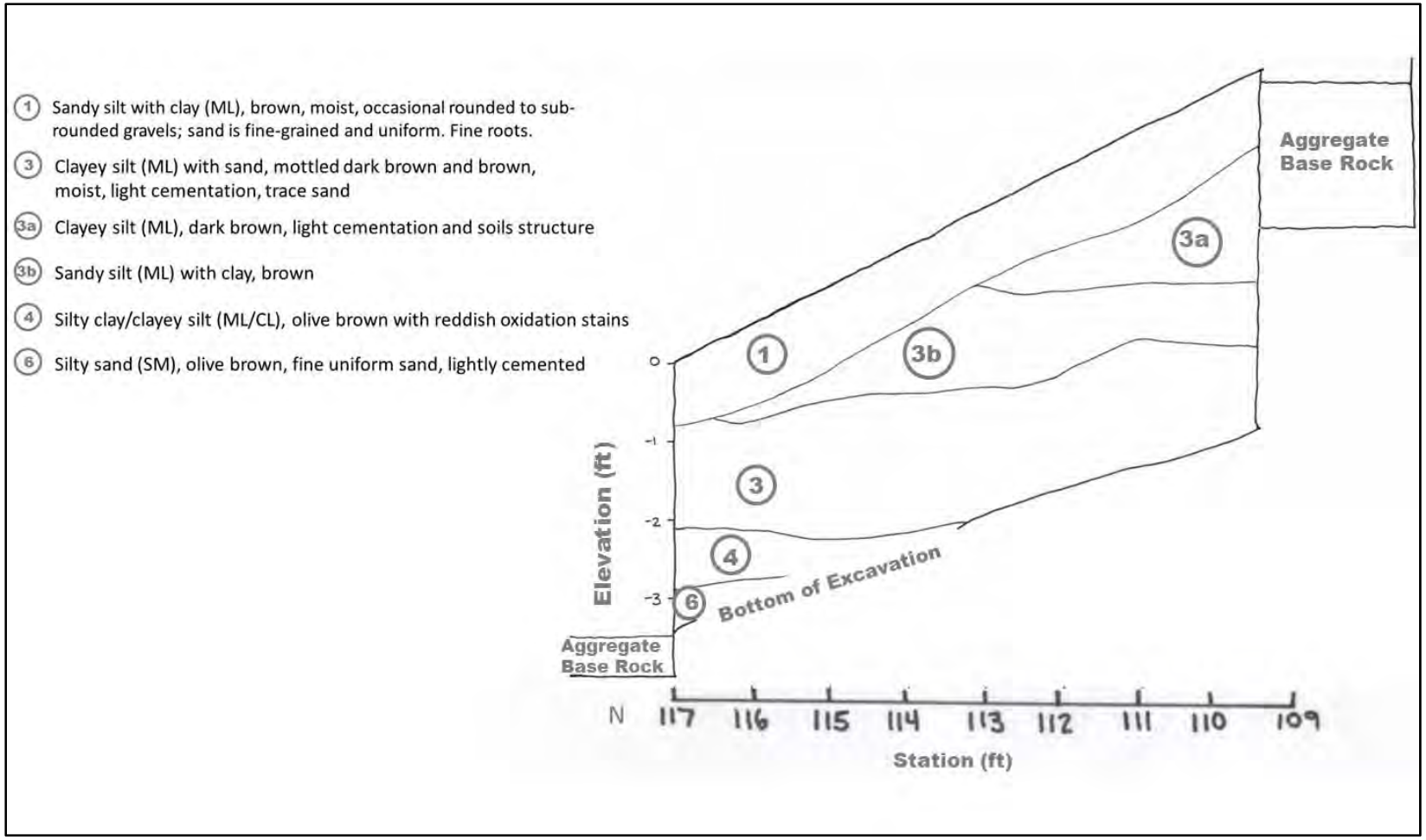

Figure 3-13. Stratigraphic section at control trenches, located just west of instrument Line C (see Figure 3-20).

3.4 TEST LAYOUT

As previously discussed, the flow test was designed to deliver water above the decomposing root system of the eucalyptus stump, inducing a wetting front and a flow net that could be monitored through observation and instrumentation. Water was delivered to an upper trench, constructed above the stump, and held at a constant head during the test (Figure 3-14 and Figure 3-15). A lower trench was constructed below the stump for viewing the exposed trench wall face and to capture seepage flowing downslope during the flow experiment. The walls of the trench were braced with shoring to prevent collapse. The uphill side and base of the upper trench as well as the base of the lower trench were lined with plastic sheeting to minimize water losses outside the study area. Stockpiled gravel was available to rapidly infill the lower trench in the event of instability prior to the equilibration of flow patterns.

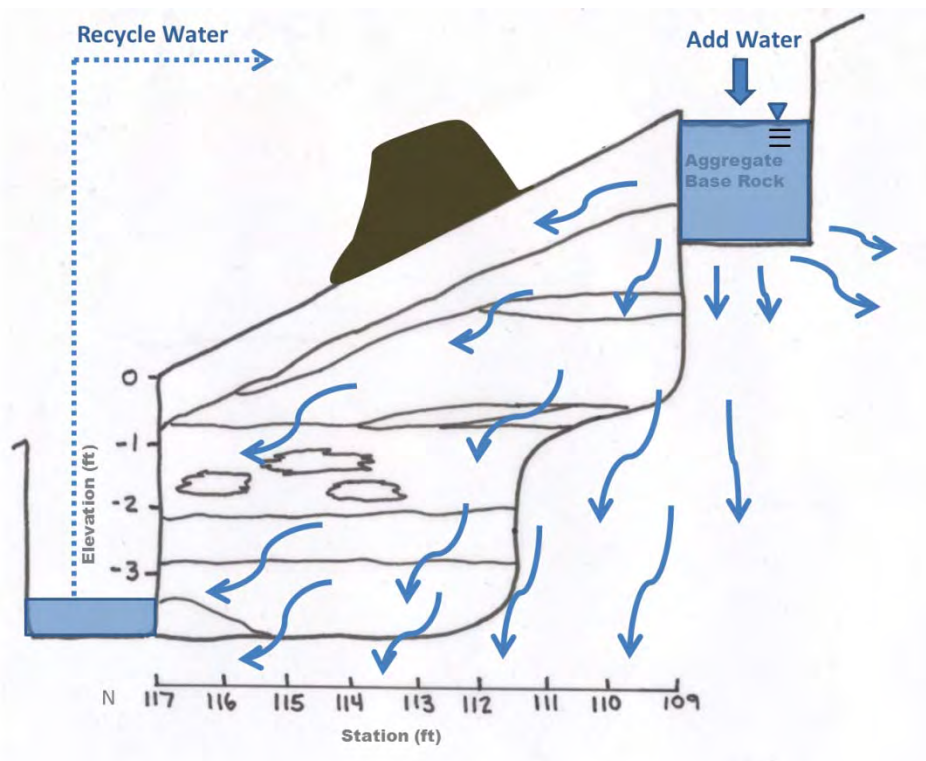

Figure 3-14. Cross section between upper and lower trenches at eucalyptus stump showing concept of proposed wetting front flow test.

Figure 3-15 shows the configuration of trenches constructed above and below the stump. An approximate 30-foot long zone around the stump was deemed the 'stump zone' and a 'stump trench' was constructed above and below this segment. The water delivery trench above the stump will be referred to as the 'Upper Stump Trench' while the viewing trench below the stump will be known as the 'Lower

Stump Trench'. As seen on the figure, the stump and control trenches were separated by a small gap in excavation in order to control water flow and volumes to the two trenches separately.

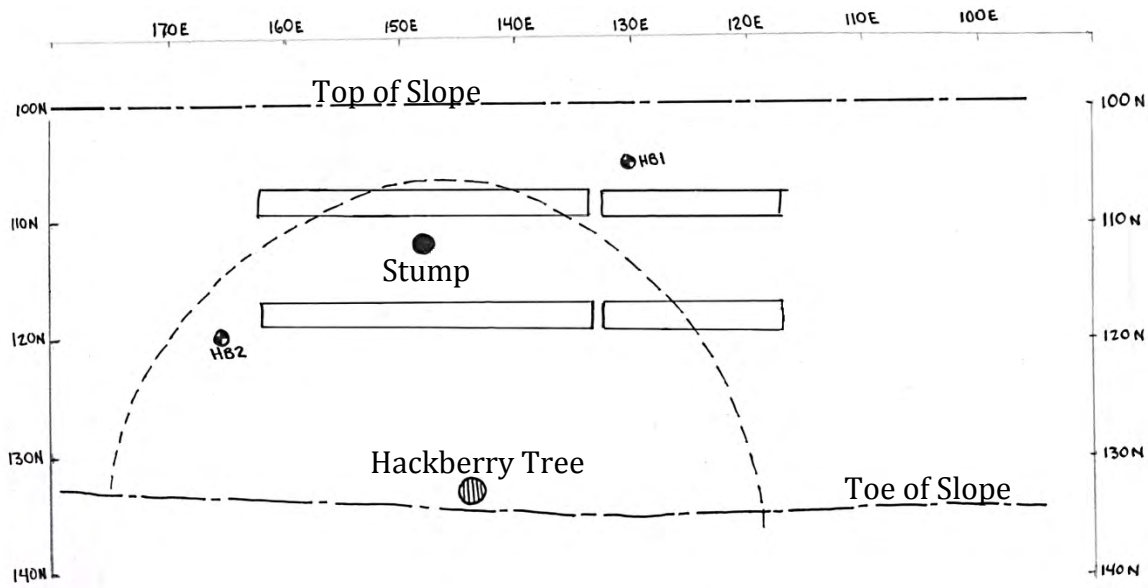

Figure 3-15. Site plan with coordinate grid showing the stump and trenches under study, and the location of hand auger borings HB1 and HB2.

A detailed site design began with development of a plan view layout consistent with observed conditions. Three levee cross sections were surveyed with increasing distance from the tree stump using handheld tools such as a compass, measuring tape, and hand level with collapsible survey stick. Based on the sections, a decision was made to align the trenches and coordinate system with the hinge point of the landside slope at the levee crest and lay out the site from that line. This decision minimized topographic differences between instrument lines. Figure 3-16 shows the site in cross section with the root system as scanned with T-LiDAR after the completion of the test. The T-LiDAR scan contains points throughout the study area and the thickness of the point cloud in cross section is a measure of the topographic variations across the site. The image shows that topographical variations between cross sections are on the order of 6 to 12 inches. Layout of the site was completed by establishing a grid of northings and eastings, beginning with an arbitrarily selected station number at north 100 ft and east 100 feet (N100, E100) and with increasing station numbers to the north and east. For the purposes of a practical coordinate system, north was defined as the downslope direction rather than true north (Figure 3-15). When not noted otherwise, station numbers used in this report are eastings (i.e. along the reference line parallel to the levee hinge).

The separation between upper and lower trenches was 10 feet on center, measured horizontally. Each trench was 2 feet wide, leaving an 8-foot wide mass of soil (measured horizontally) from the downhill wall of the upper trench to the uphill

wall of the lower trench. To the west of the stump trenches, a 15-foot long levee segment was identified as a 'control' area. Both an upper and lower trench were constructed spanning this zone. Measured trench dimensions and coordinates are shown on Table 3-1. In Figure 3-17, the stump is shown in relation to the upper and lower trenches. An as-built plan showing trenches, soil borings, stumps (those visible from the surface and those found during trench construction), the hackberry tree at the toe, surface expressions of burrows, as well as the top and toe of slope is provided in Figure 3-18.

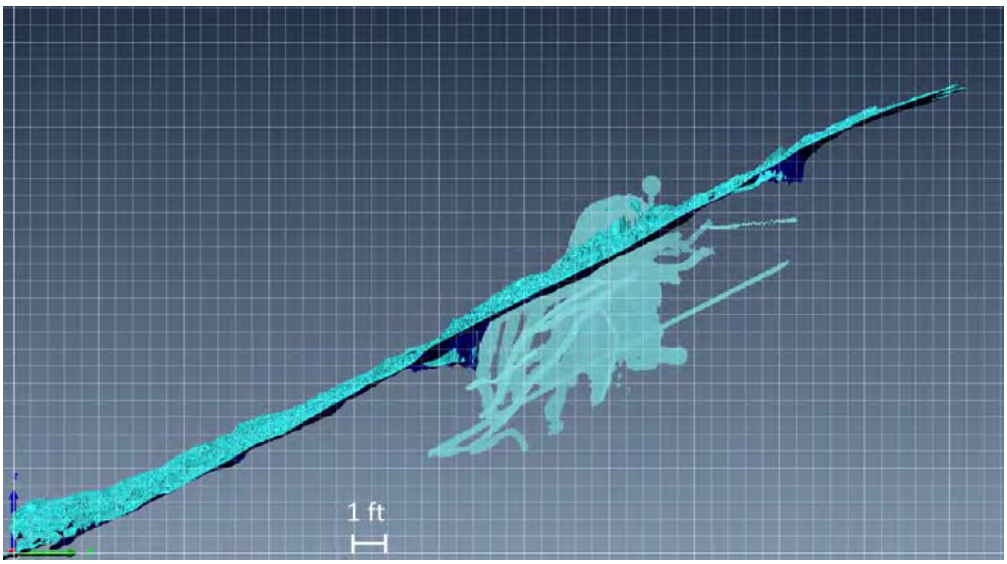

Figure 3-16. T-LiDAR image looking east at the eucalyptus stump and root system. Base T-LiDAR Image provided by Gerald Bawden of the USGS.

Table 3-1. Trench Dimensions and Coordinates

	Uphill Depth (ft)	Downhill Depth (ft)	Width (ft)	Length (ft)	Coordinates (ft)
Upper Control Trench	3	2	2	15.5	(N107.5, E132.5), (N109.5, E132.5), (N107.5, E117), (N109.5, E117)
Upper Stump Trench	3	2	2	28.5	(N107.5, E133.5), (N109.5, E133.5), (N107.5, E162), (N109.5, E162)
Lower Control Trench	4	3	2	15.5	(N117.25, E132.5), (N119.25, E132.5), (N117.5, E117), (B119.5, E117)
Lower Stump Trench	4	3	2	28.5	(N117.25, E133.5), (N119.25, E133.5), (N117, E162), (N119, E162),

Figure 3-17. Eucalyptus stump is shown A) close in, B) from the east end of the trenches looking west, C) from below the stump trench looking southeast, and D) from the west end of the stump trench looking east.

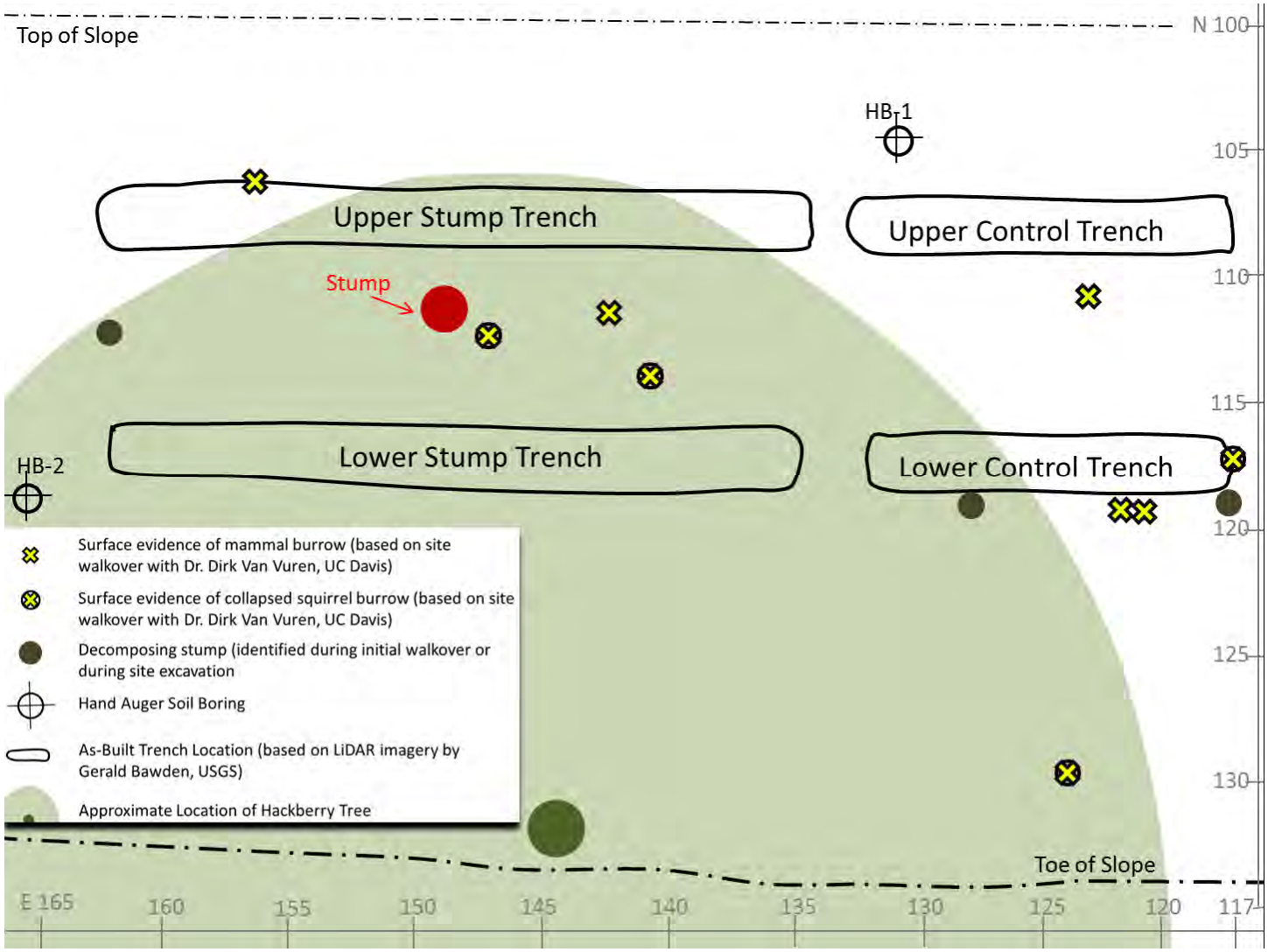

Figure 3-18. Plan view of field test layout.

Photos showing an overview of the overall site are shown on Figure 3-19. As can be seen in the photographs, the site design concept includes three instrument lines to monitor the progression of the wetting front and pore pressures at increasing distance from the stump center. Instrument Lines A, B, and C were placed a distance of 0, 7, and 23 feet west of the stump center, respectively (Figure 3-20).

Figure 3-19. Field test layout looking west (upper left), east (upper right), and south (bottom left). Lower right is a site overview looking east and showing the hackberry tree in relation to trench excavations.

Piezometers and tensiometers were installed to measure positive and negative pore water pressures, respectively, within the zone of flow to monitor the wetting and flow patterns with increasing distance from the decomposing root system. A complete instrument line consisted of 7 tensiometers with electronic transducers installed to depths of 18 to 60 inches as well as two vibrating wire piezometers installed to depths of 60 to 84 inches. Instrument Line A was located in the vicinity of the decomposing stump (Section A of Figure 3-20). Instrument Line C was located approximately 23 feet from the stump (Section C of Figure 3-20). Supplemental instrumentation consisting of 5 tensiometers were installed a distance of 7 feet from the stump, between Instrument Lines A and C. The supplemental line is referred to as Instrument Line B and was installed a distance of 7 feet from the stump at Section B as shown on Figure 3-20.

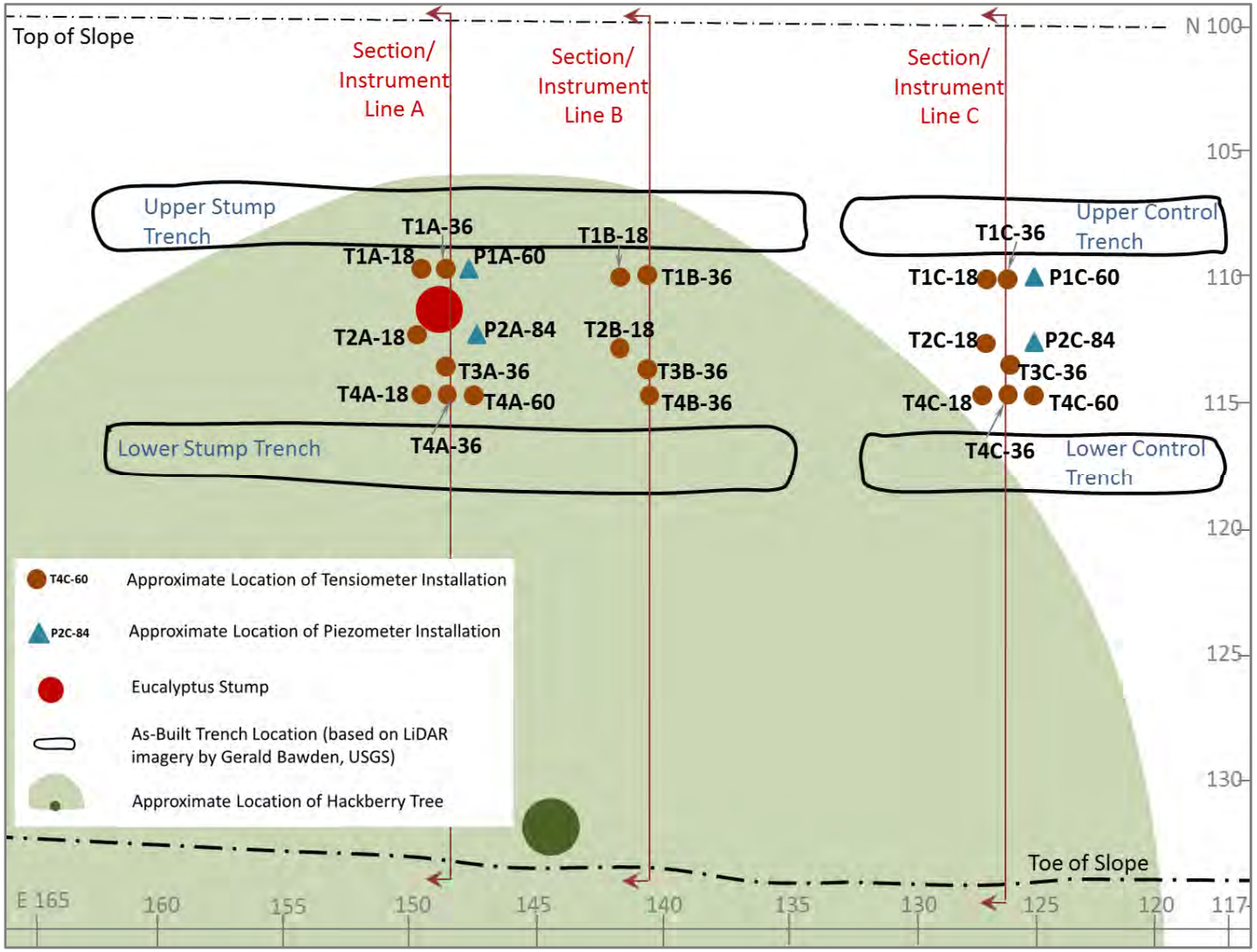

Figure 3-20. Instrument layout plan showing the locations of piezometers and tensiometers.

Transducers continuously recorded suction values during the flow test. Piezometers were read manually at varied intervals determined in the field based on the rate of change of the data. Figure 3-21 shows a typical instrument line as well as a photographic view of the three installed instrument lines. Tensiometer locations are named to reflect the type of instrument, the row number, the section number, and the depth in inches (i.e., T4A-18 is a tensiometer located in row 4 within Section A, and was installed to a depth of 18 inches below grade). The naming convention is illustrated in Figure 3-21. Figure 3-22 shows the layout of instrument Line A in cross section relative to the upper and lower trenches. Instrument Line C, within the control area, has an identical instrument layout.

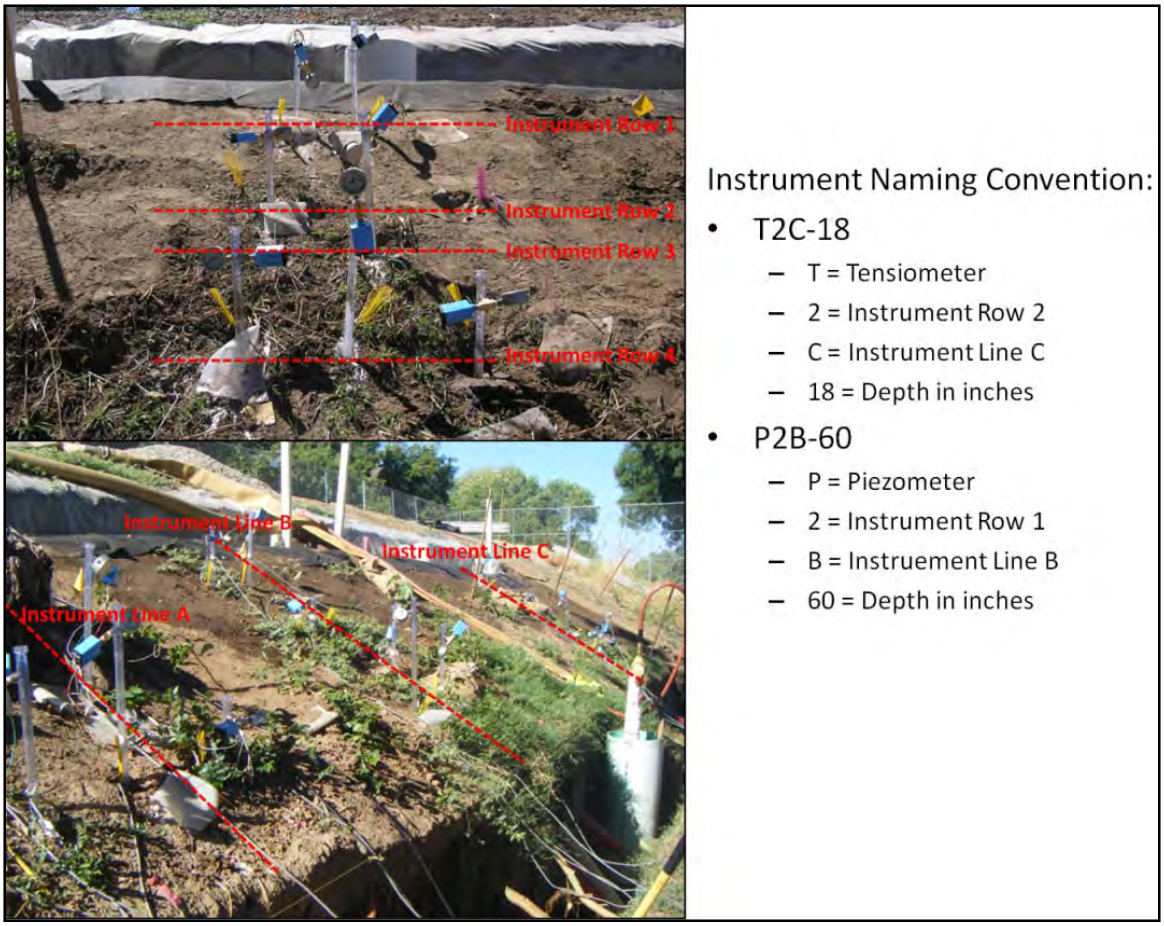

Figure 3-21. Photographic instrument plan showing the locations of piezometers and tensiometers as well as the naming conventions.

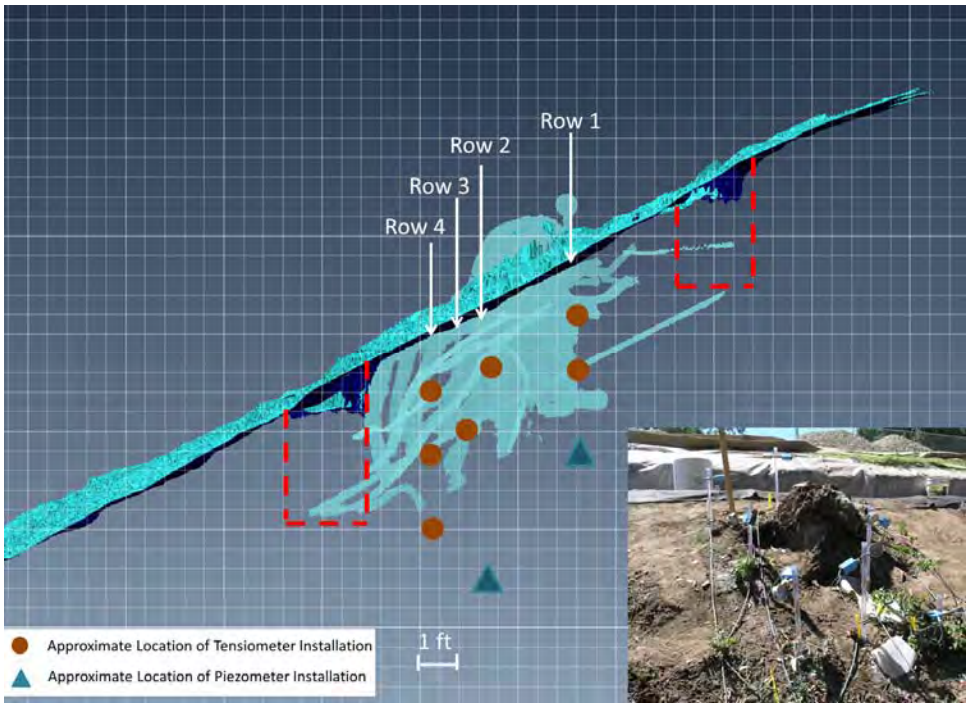

Figure 3-22. Instrument layout at Line A at the eucalyptus stump in photograph and cross section. Base T-LiDAR image provided by Gerald Bawden, USGS.

3.5 SITE CONSTRUCTION

3.5.1 Trench Excavation

Upper and lower trenches were constructed to depths of 3 and 4 feet, respectively, using primarily manual efforts to loosen soils (shovels, digging bars, and trowels) and a vacuum trailer to remove spoils (Figure 3-23). Where decomposing roots were found, manual excavation allowed them to be viewed photographed and appropriately characterized. Where live roots were encountered, an air knife operating with a compressor capable of compressing 375 cubic feet of air per minute (CFM) was used to excavate around roots. Most areas were excavated with a lower compressor setting in order to minimize disturbance to sidewalls and fragile areas where decomposing roots were suspected.

Live roots were sketched onto logs and photographed prior to being gently cut with hand tools to avoid disturbance in the vicinity of roots. Roots were more abundant in the stump trenches relative to the control trenches (Figure 3-24 and Figure 3-25).

Figure 3-23. Construction equipment used during excavation. A) hand excavation with vacuum to remove spoils; B) a vacuum trailer; C) air knife used to excavate around live roots; D) 375 CFM compressor to run the air knife.

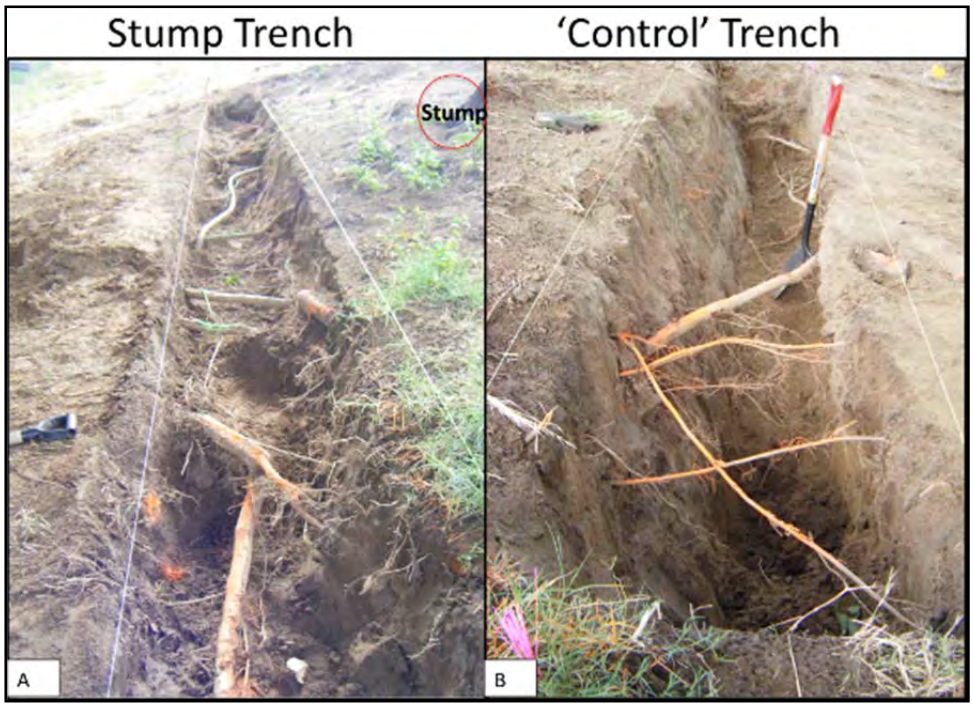

Figure 3-24. View of trenches, A) looking east at stump trench and; B) looking west at control trench.

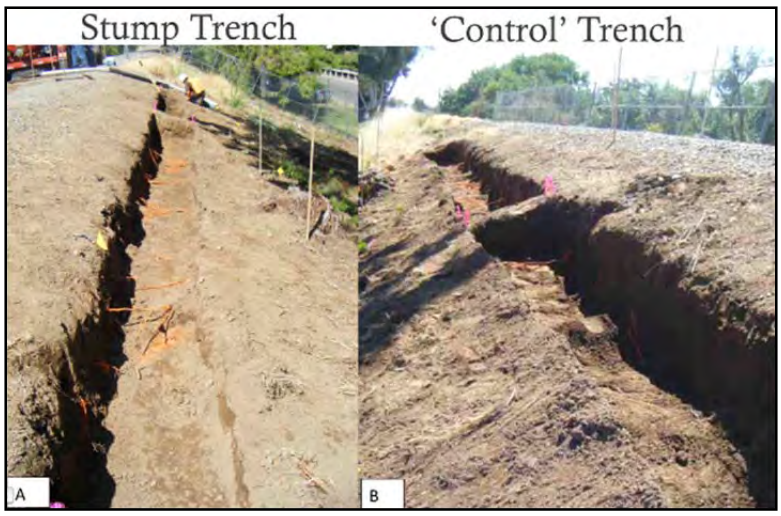

Figure 3-25. View of upper trenches, A) looking west at stump trench and; B) looking east at control trench.

String was stretched across the trenches in 1 foot increments to facilitate plan-view sketches and photographic documentation of the root system (Figure 3-26 and Figure 3-27). Not all roots in the logs are visible in the photograph as shallow roots were removed as needed to achieve depth. Appendix D provides a complete set of similar plan view site logs and spliced photography. Roots are shown to be more abundant in the lower trenches than the upper. The lower trenches are closer to the live hackberry at the toe, which is the source of the live roots. Decomposing roots also appear to be more abundant in the downhill direction than the uphill direction.

Decomposing roots were found in the upper and lower trenches in the vicinity of the eucalyptus stump. Additional decomposing roots were found outside of the study area at the periphery of the excavations. Figure 3-28 and Figure 3-29 show an example of a segment of the control trench where a stump was uncovered on the downhill side during excavation. As discussed in Section 3.2, this may have been an original tree planted during Cal Expo construction in 1968 that was seen in aerial photographs to have disappeared between 1983 and 1990. The stump would have been decaying for 20 to 27 years at the time of our study there was no significant trace of a root system found to be associated with this stump within the trench.

Figure 3-30 provides another example of field logs correlated to photographic documentation of the roots encountered. When roots prevented excavation, they were carefully logged and cut prior to proceeding with additional excavation and documentation efforts. Figure 3-31 shows the same section of trench excavated to full depth. The photo shows roots and a metal pipe that are not visible in the photographs of Figure 3-30.

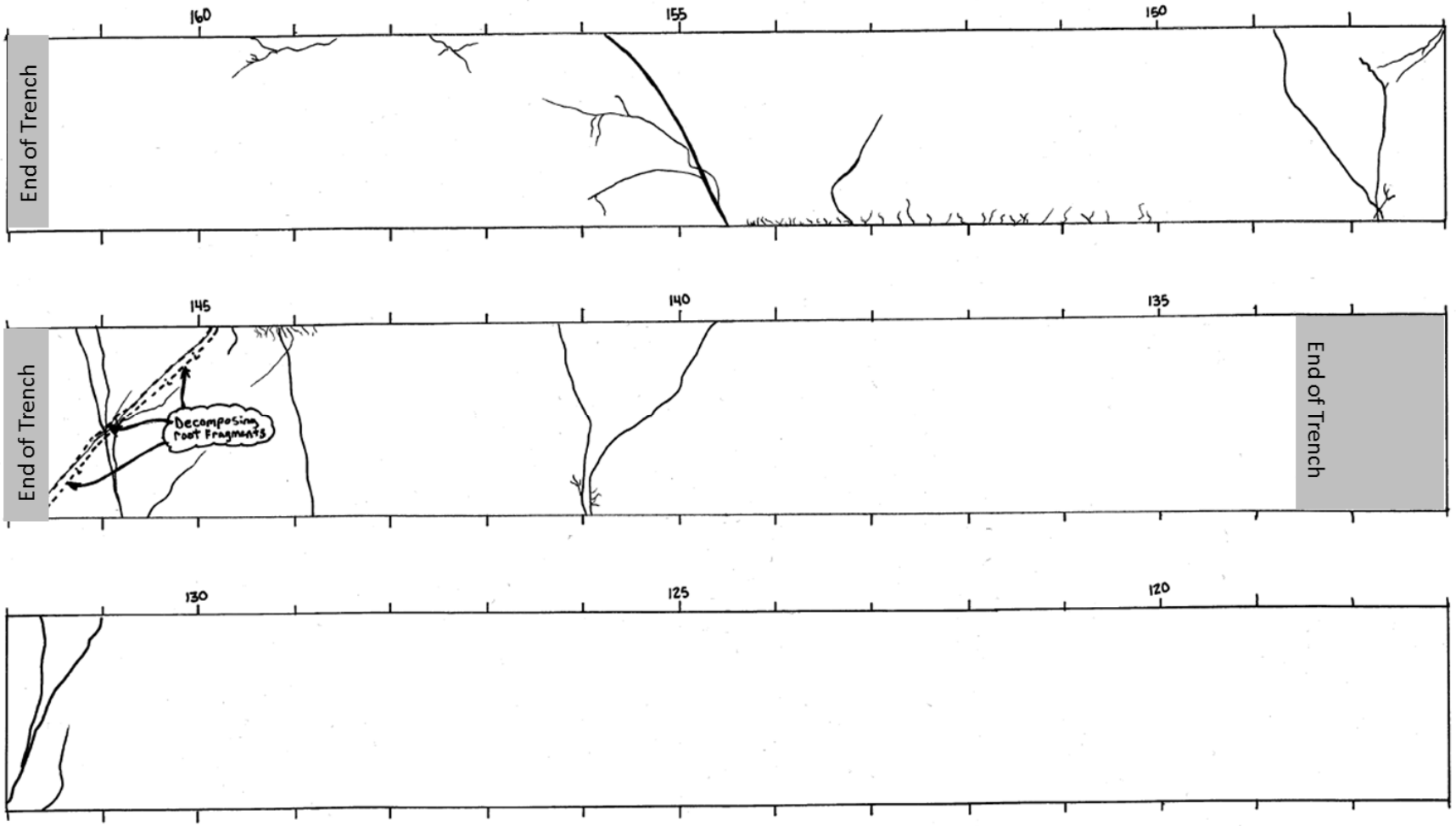

Figure 3-26. Upper stump and control trench plan view logs (Stations 117-162).

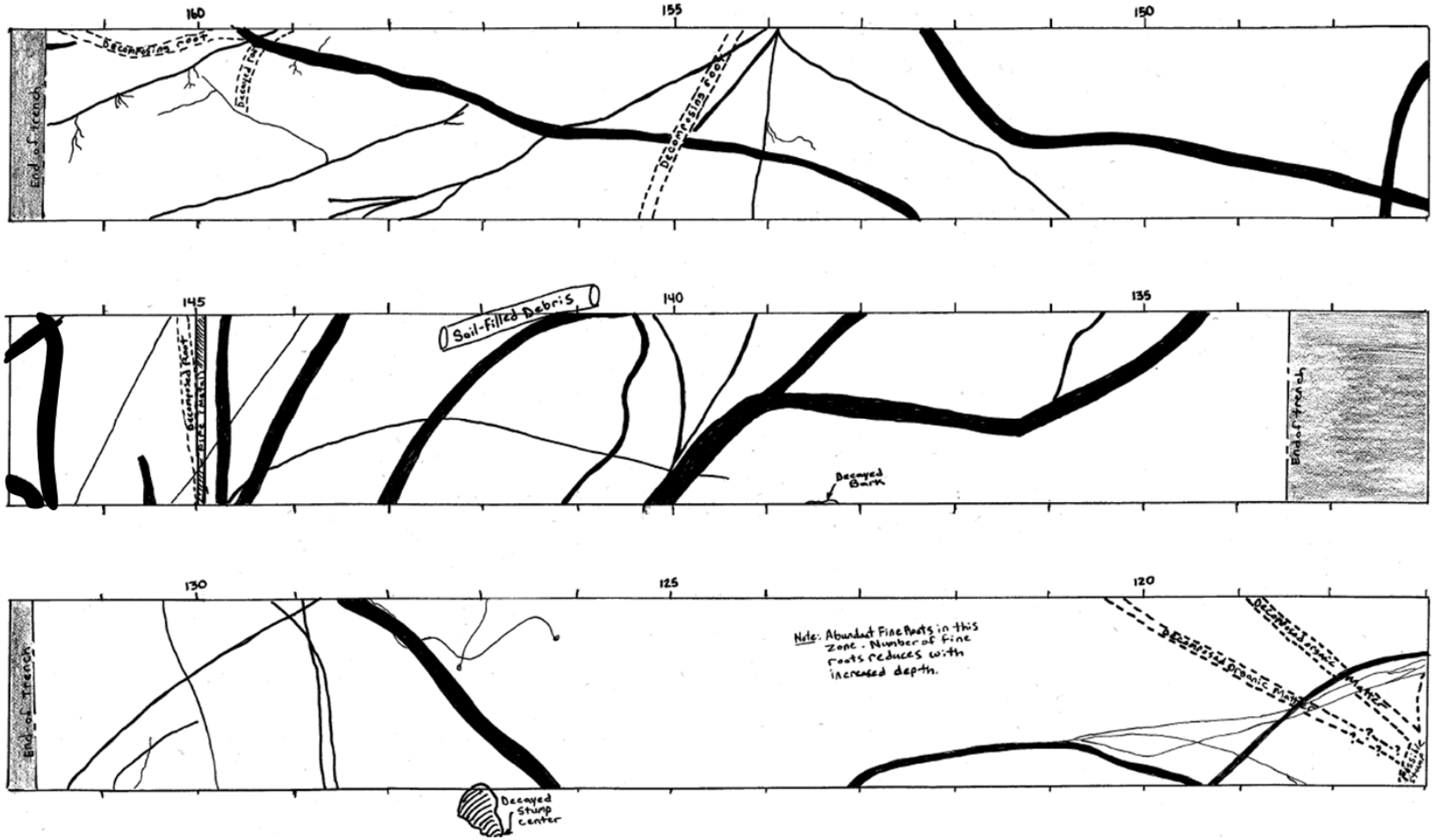

Figure 3-27. Lower stump and control trench plan view logs (Stations 117-161.5).

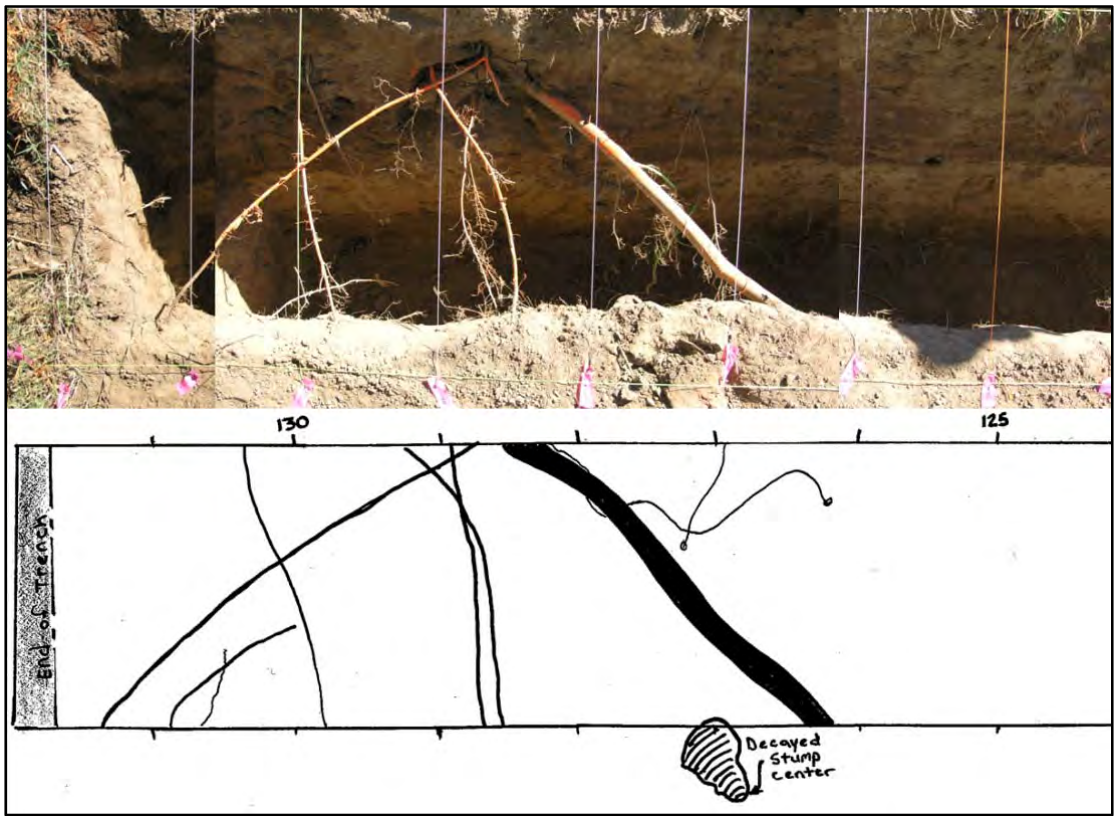

Figure 3-28. Lower control trench Stations 124-132. Spliced plan view photos (top) during excavation of lower control trench and log of analogous segment below.

Figure 3-29. Stump found on downhill side of control trench at Station 127 as shown on Figure 3-28.

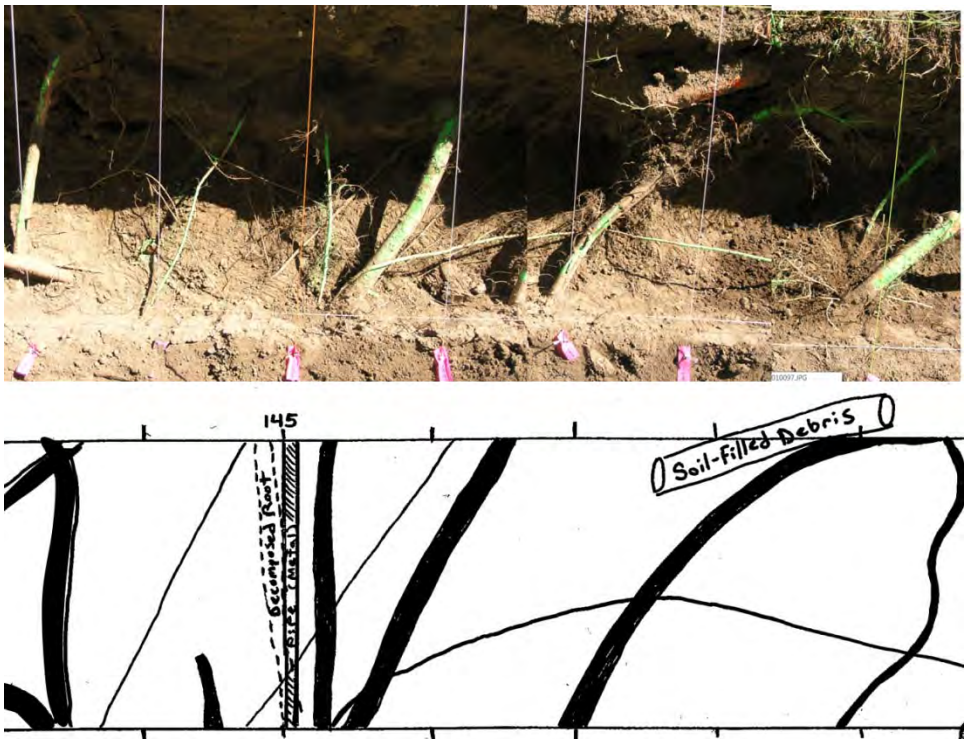

Figure 3-30. Lower stump trench Stations 140.5-146 (increasing to left). Spliced plan view photos (top) during excavation of lower stump trench and log of analogous segment below. Excavation not shown to full depth.

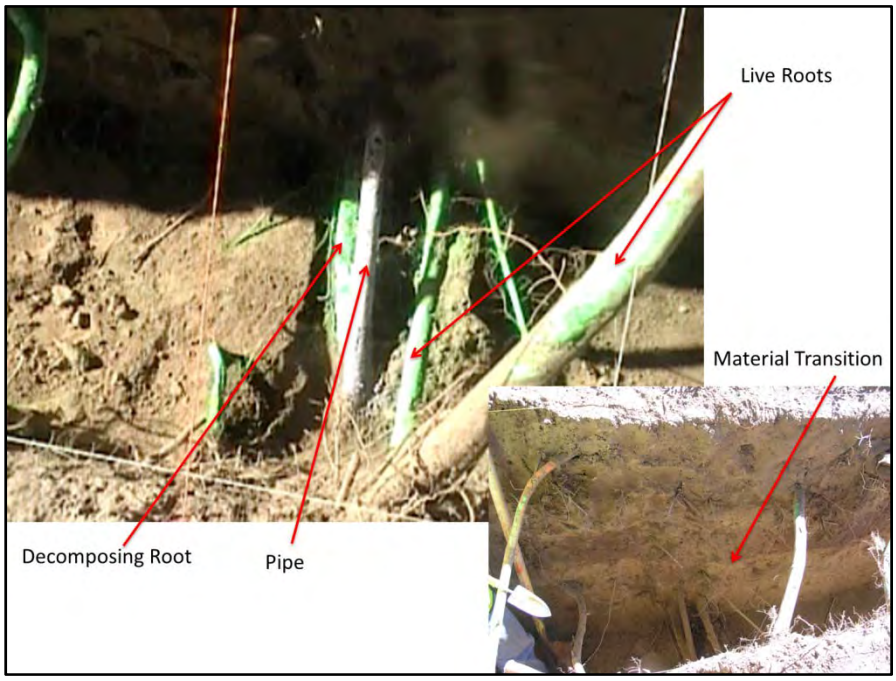

Figure 3-31. View looking south of 4' deep trench at Station 145. Upper left photos are a cluster of live and decomposing roots and a 1" diameter pipe. Bottom right is a larger view of the same trench segment.

Upon completion of trench excavation and plan view documentation, roots were cut flush with the wall face, a grid with 1-foot contours was placed over the uphill wall face in order to facilitate documentation (Figure 3-32). Figure 3-33 shows a typical wall face field log including decomposing and live roots, animal burrows, and the metal pipe shown on Figure 3-30 and Figure 3-31 above. Complete trench wall logs are provided in Appendix D along with the plan view logs previously discussed.

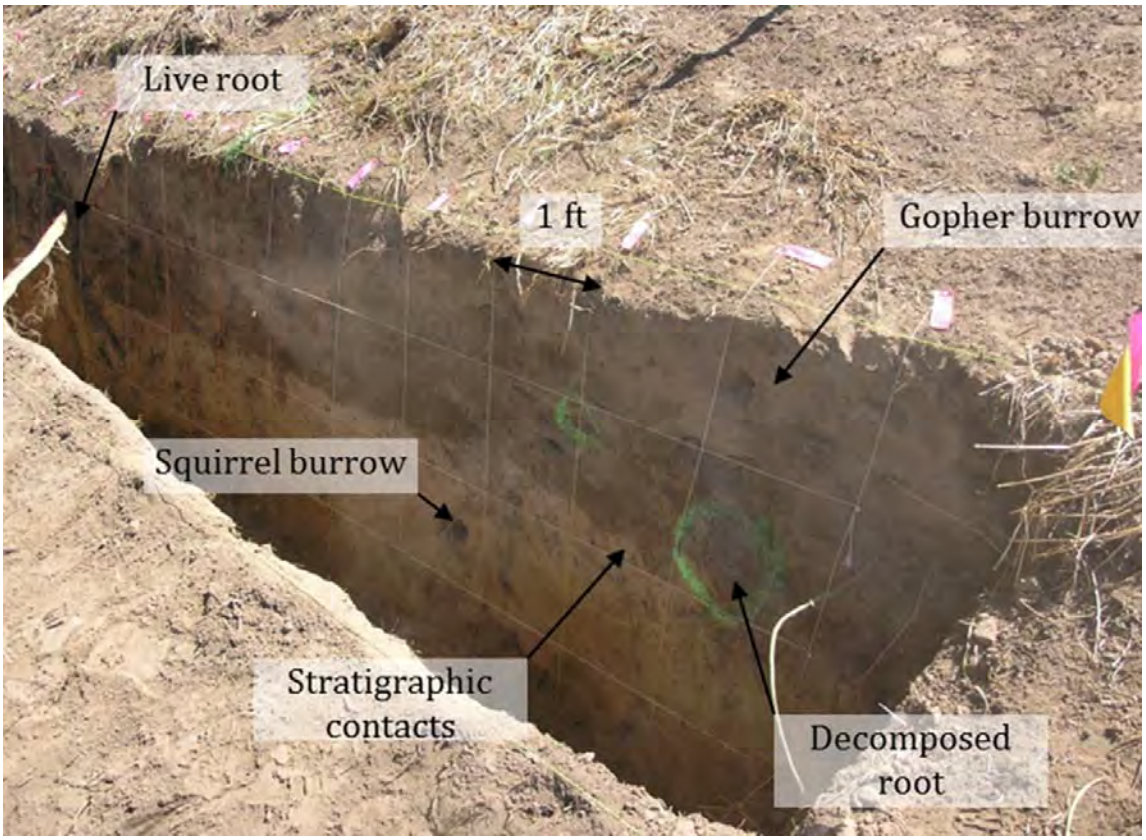

Figure 3-32. A 1-foot by 1-foot square grid was constructed to aid in logging and documentation of observations during the flow test. Source: Cobos-Roa et al. 2012.

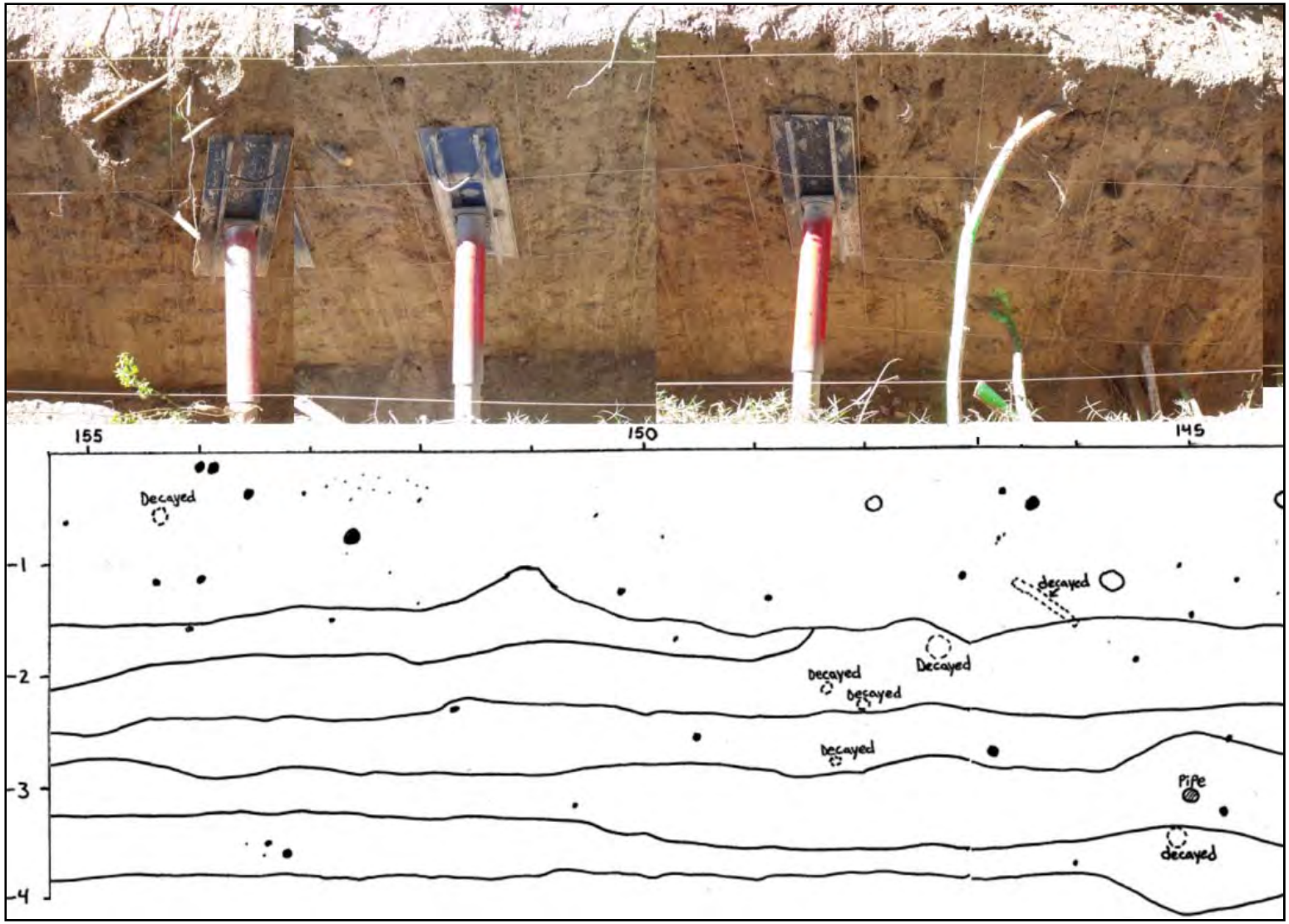

Figure 3-33. Field log of uphill trench wall of lower stump trench, Stations 144-155 with corresponding photos above.

During trench construction, consideration was given to grouting burrows onsite prior to the flow test. Field logs of the lower trench wall revealed 15 burrows in the uphill wall, while the downhill wall of the uphill trench did not reveal any burrows. As previously discussed and shown on Figure 3-2 and Figure 3-18, surface expressions of mammal burrows were observed across the site. The holes were viewed by a member of the CLVRP team, Dr. Dirk Van Vuren, a burrowing mammal expert from UC Davis. All of the locations were considered either abandoned ground squirrel burrows, which were partially collapsed and had not been in use for some time, or burrows of the pocket gopher.

Pocket gophers burrow day and night, using the burrow as a protective residence, a base for foraging, for feeding on roots encountered and to pull vegetation into the tunnel for food (Reichman et al., 1982). They may kick soil behind them as they dig, push soil to the surface, or backfill old tunnels as they make new excavations (Reichman and Smith, 1990). Holes are not much larger than the animal and are relatively horizontal and paralleling the ground surface (Reichman and Smith, 1990). Based on field discussions with Dr. Van Vuren, the work of Reichman et al (1982), and Reichman and Smith (1990), the pocket gopher leaves behind a shallow network of holes (1 to 2 inches in diameter), often slightly oval shaped, and partially filled with loose soil. On this basis, most holes in the trench walls were identified to be gopher burrows.

California ground squirrels make use of burrows for essential protection from predators, in inclement weather, for refuge at night, or for rearing offspring (Van Vuren and Ordeñana, 2012). These burrows have the potential to penetrate the width of a levee depending on burrow age and soil conditions, or could partially enter from both sides and full penetrate the levee (Van Vuren and Ordeñana, 2012). In the lower trench wall, Dr. Van Vuren was able to identifiy California ground squirrel burrows by their diameter (3 to 4 inches as opposed to 1 to 2 inches for the pocket gopher), as well as having a round, well-traveled appearance.

Of the fifteen (15) burrows logged in the lower trench wall, two (2) were considered squirrel burrows and thirteen (13) were identified as gopher burrows. One squirrel burrow extended back 10 inches into the uphill wall of the lower trench and the other 18 inches. A firm end was felt in these holes. The gopher burrows were small and exhibited many curves, making an accurate assessment of depth difficult. In generating field logs of the upper wall of the lower trench, numerous irregular features were documented, including:

- 1.5 to 2-inch holes (likely pocket gopher) in the shallow zones extending back a distance of a few inches to a little over a foot (Figure 3-34 A).
- Two holes of approximately 4 inches in diameter (believed to be ground squirrel burrows) extending back a distance of 10 and 18 inches from the upper wall of the lower trench.
- Live roots as shown on Figure 3-34C and in Sections 3.5.1 and 3.7.

- Decayed roots (of various levels of decomposition and some with small holes bored in them) as shown on Figure 3-34A and B and in Sections 3.5.1 and 3.7.
- A 1.5 inch diameter metal pipe at a depth of nearly 4 feet in the lower trench (pipe points downhill at approximately 11 degrees from horizontal) as shown previously in Figure 3-31.
- Small holes of ½ to ¼ inch in diameter. Based on observations with Dr. VanVuren, we believe the holes may be related to ant activity at the site (Figure 3-35). During excavation, worms were also seen creating and traveling through small holes in the trench walls as shown on Figure 3-36.
- Differing material types ranging from loose sandy silts and discontinuous pockets of clean sand to clayey silts and occasional lean clays.

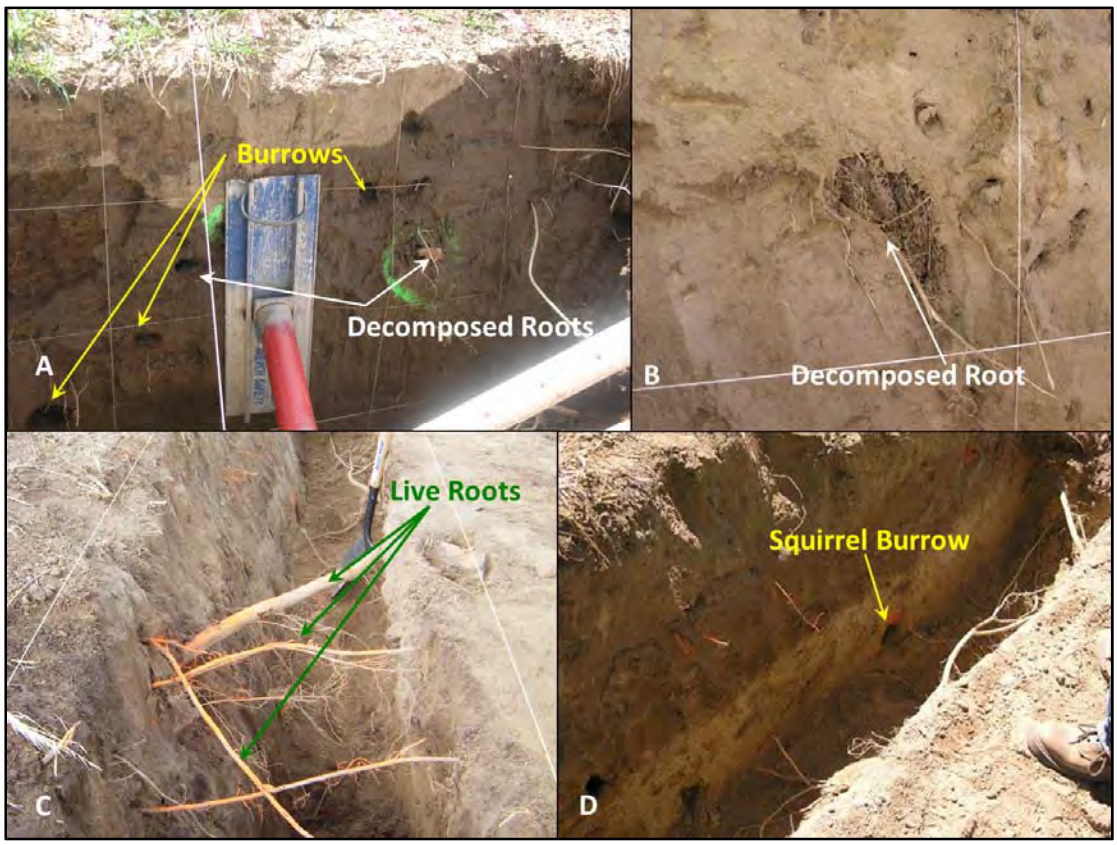

Figure 3-34. Lower trench photos with A) burrows and decomposing roots, B) a decomposing root, C) live roots, and D) a squirrel burrow and a material change.

With a range of irregular features present and no clear or unobstructed input locations to provide a natural place for grouting, we elected not to grout. During Dr. Van Vuren's visit, we explored several locations along the northern levee of the American River and found that gopher and ground squirrel activity would be difficult to avoid altogether. At the time of trench logging, no one hole appeared to act as a through pathway for seepage, or "pipe" from the top trench to the bottom

trench. Accordingly, we decided to view the relative influence of the live and decaying root systems in a real levee system rather than fill visible holes when uncertain which would become preferred pathways.

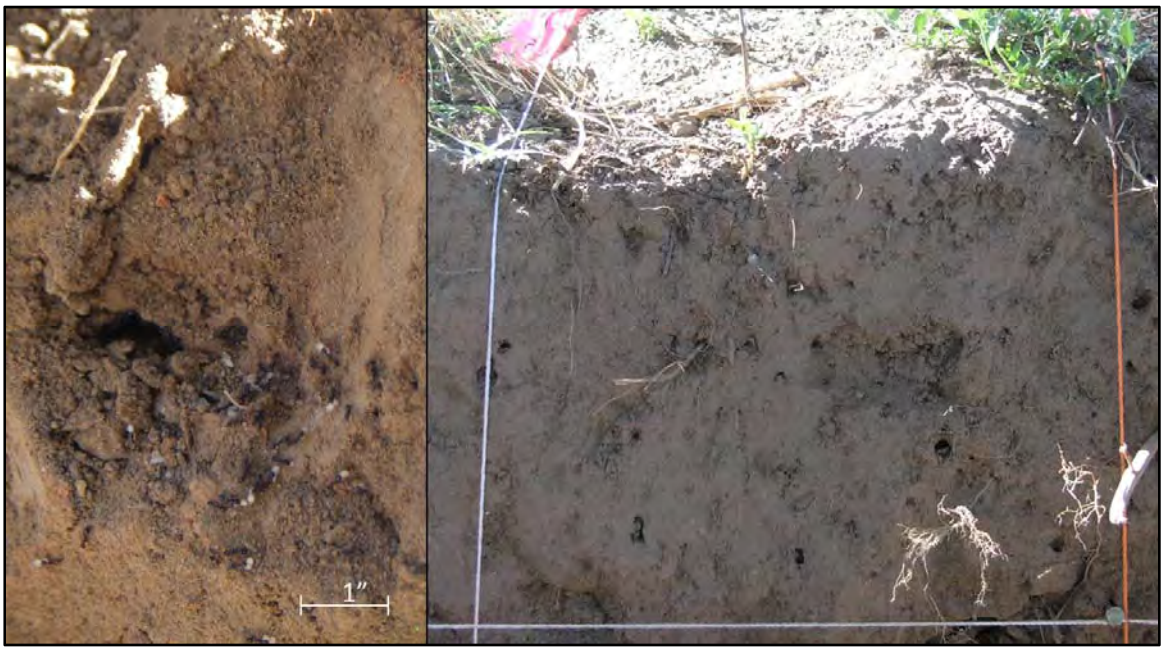

Figure 3-35. Ants encountered during trenching activities (left). Small holes (1/2 to ¼ inch) found in trench wall could be related to ant activity (right).

Figure 3-36. Worm activity was observed to be responsible for some of the small holes (<¼ inch diameter) encountered during trenching.

3.5.2 Preparation of Trenches for Flow Test

Upon completion of trench excavation, the upper trench was lined with a plastic membrane along the upslope wall, base, and sides to minimize flow of water to areas outside of the study area. The upper trenches were then filled with ¾ inch of clean crushed rock to maintain stability throughout the test. Lower trenches were

lined with plastic sheeting along the base and a thin layer of rock was placed to hold the sheeting in place. The upslope wall was left open for viewing during the test (Figure 3-37). An effort was made to place hydraulic shoring such that key features observed in the wall during the logging phase were not obscured from view.

Figure 3-37A shows the 1 foot wide band of soil that separated the 'control' and 'stump' trenches. The band of soil was not expected to fully prevent flow between the zones. The upper trench was separated to allow the flexibility of inflow into the two trenches separately in the event that one or the other needed to be shut off due to unforeseen conditions. The lower trench was separated so that outflow volumes from water entering the two trenches could be separately tracked. In photo B, the lower trenches are shown shored for stability with hydraulic vertical shores placed at intervals of 2 to 5 feet across the lower trench, taking care not to obscure visible irregularities such as decaying or live roots or mammal burrows. Slopes and trench walls were periodically moistened to aid in air knife excavation and prevent cracking prior to the flow test as shown on photo C.

Figure 3-37. Trench preparation prior to commencement of flow. A) Upper trenches lined with plastic sheeting (uphill and base walls) and permeable fabric (downhill wall); B) shored lower trench lined with plastic sheeting and gravel (base); C) water truck moistens site to prevent cracking prior to flow test.

Once trench excavations were complete, the water delivery and pumping systems were installed to deliver water into the upper trench. A 2500-gallon polyethylene tank was placed on the levee crown and filled prior to commencement of the test. Figure 3-38 shows the water delivery and recycling system installed at the site.

Water was delivered into the upper trenches via a 15-inch well casing connected to a perforated pipe embedded in the gravel-filled upper trench. The pipes acted as a water delivery manifold rapidly distributing the water throughout the upper trenches (Figure 3-38A). Perforated riser pipes at the trench ends provided points along the trench to confirm water levels. Fire hoses were used to deliver water (Figure 3-38B and D) into a 15-inch diameter perforated pipe through a mechanical float valve (Figure 3-38D). The float valve is shown mounted into the well casing and used to maintain a constant head in the upper trenches during the flow test. The water tank was refilled throughout the test and the level of water in the tank as well as flow volumes of water into the tank were measured and used to approximate the amount of water delivered into the upper trenches with time. Water collected from the lower trenches was recycled into the delivery tank. All flows into the tank were tracked using ¾ inch flow meters (Figure 3-38C).

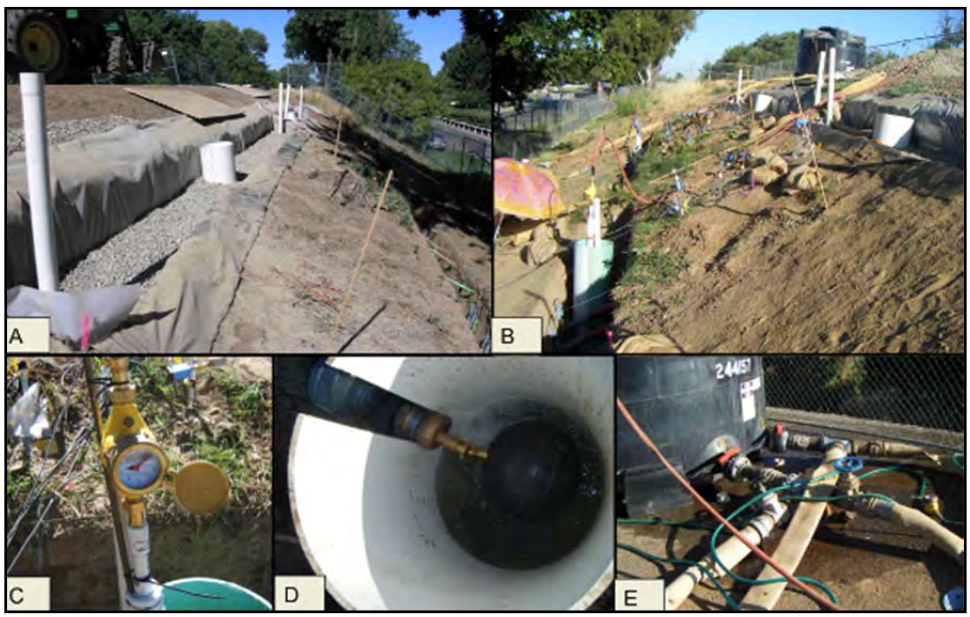

Figure 3-38. A) Upper gravel-filled trenches; B) Water delivery system; C) ¾" flow meter for monitoring flows into water storage tank; D) Mechanical float to maintain constant head in upper trenches; E) Control valves at tank

3.5.3 Instrument Installation

Tensiometers were obtained from Soil Moisture, Inc. and equipped with a mechanical pressure gauge and a pressure transducer with maximum suction capacity of 100 kpa (Figure 3-39). Tensiometers of 24, 48 and 60 inches were installed to depths of 18, 36, and 60 inches, respectively. All instruments were installed in accordance with the manufacturer's specifications. Holes were advanced with a gauge auger (provided by the manufacturer) with a diameter slightly larger than the instrument diameter of ¾ inch. The instrument holes were logged for soil conditions prior to installation.

Figure 3-39. A typical tensiometer is shown including a mechanical gauge and pressure transducer. White silica sealing material is seen at the hole entrance.

Tensiometers were pre-assembled and saturated prior to installation. All connections were cleaned, and the gauge and transducer ensemble were connected to the tensiometer, taking care to properly achieve a seal on each connection. The porous tips were pre-saturated and brought to the site in de-aired water. In a lab, the porous stones that communicate with the soil were pre-saturated in a vacuum with de-aired water and connected to the tensiometer onsite just prior to installation. De-aired water was brought into each instrument through a suction pump attached at the top. Once the tensiometer was filled, the suction pump was used, along with tapping action, to remove trapped pockets of air from the gauge and transducer connections.

With all seals checked and no observed leaks, a silica slurry was mixed to create a seal between the soil and the tensiometer. This step is optional according to the manufacturer if the hole is snug to the tensiometer, but proved helpful in our soil conditions. A seal was established between the porous ceramic tip of each tensiometer and the surrounding soil using a slurry of water and silica flour with silt-sized particles (Figure 3-29). The tensiometer then communicates with the surrounding soil by allowing water in the instrument to flow into the surrounding soils until the tension in the instrument matches the tension in the surrounding soils. The suction created by the column of water in the instrument is subtracted from recorded suction values. Water is periodically refilled by opening the

instrument, losing tension, refilling, closing the instrument, and allowing time for re-establishment of tension.

During installation of instrument Line A in the vicinity of the Eucalyptus stump, 6 of 6 tensiometers encountered decomposing roots in the auger holes, 3 instruments encountered live roots, and 2 instrument tips were placed partially within decomposing roots. While augering holes for tensiometer installation at Line C, two holes encountered live roots. See Figure 3-20 for instrument locations. A detailed summary follows:

- T4A-18 and T4A-36 encountered live roots at their tip
- T1A-18, T3A-36, T4A-18, T4A-36, T4A-60, P2A-84 encountered decomposing roots during augering
- P1A-60, T4A-36, P2A-84, T4C-18, P2C-84 encountered live roots during installation

Instruments installed within row 4 of instrument Line A (below the Eucalyptus stump) were among those encountering decomposing roots during installation (T4A-18, 36, and 60). The tensiometers were located approximately 16 inches from the uphill wall face of the lower trench (measured horizontally). Within 1 hour of installation, silica slurry was observed trickling out of two exposures of one of the decomposing roots. Photos were taken and observations were recorded (Figure 3-40). Excavation of the root system at the end of the flow test revealed a number of locations where silica slurry flowed for distances of a few inches to approximately 5 feet along a decomposing root within a cavity observed between the decaying bark and the inner woody core (*xylem*) of the root.

Figure 3-40. Silica flour migration pattern below the stump (red circle) following installation of tensiometers.

3.6 FLOW TEST

Following instrument installation, instruments were monitored for several days with stable readings prior to the beginning of the flow test. On September 7, 2010 at 11:57 am, the valve from the 2500 gallon polyethylene water storage tank located at the crown of the levee was opened and water was channeled via gravity flow into the upper trenches via the input hoses connected to mechanical float valves located at two input sites at the approximate centers of the upper stump and control trenches (Figure 3-38). The flow test ran for approximately 6 days after which the trench was allowed to drain and monitoring continued as measured soil suction values began to increase with the drying of site soils. A detailed timeline showing the duration of each phase of testing as well as key observations is presented as Figure 3-41.

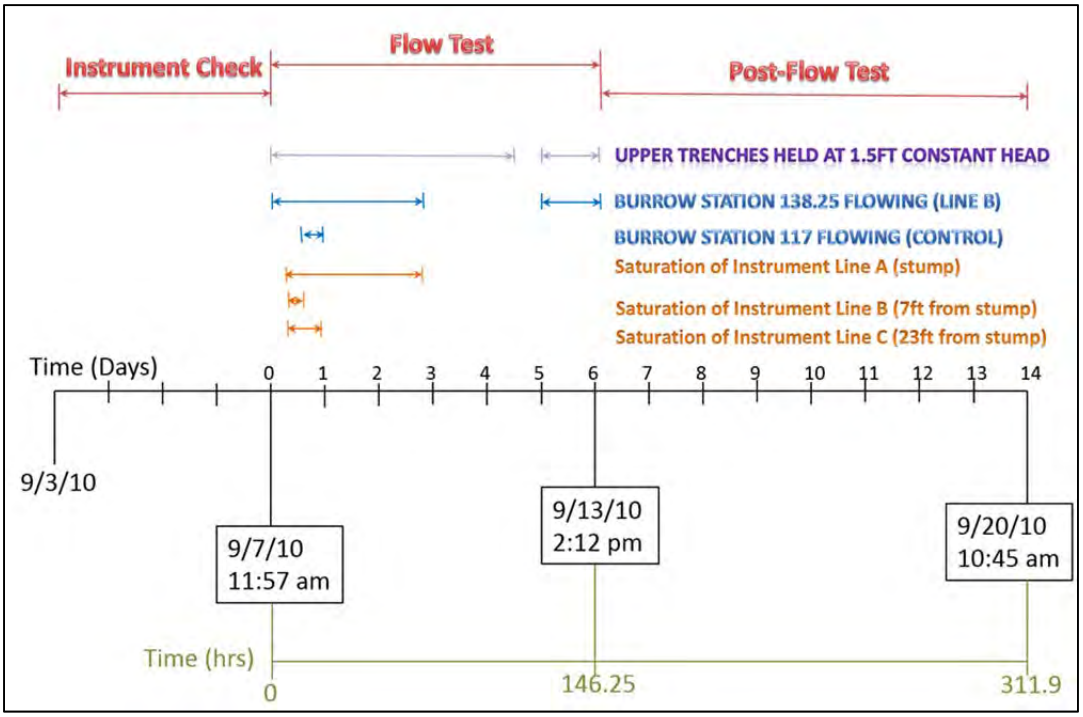

Figure 3-41. Flow test timeline.

The upper trench was approximately 2 feet deep on the downhill side. The constant head height in the upper trench was set to 1.5 feet above the base to avoid overflow or failure of the trench wall. A constant head was held for 4 days after which a nighttime malfunction caused the water to temporarily stop flowing. On the morning of September 12, water in the trenches was brought back up to a constant 1.5 feet above the trench base and held for the remainder of the flow test. When water in the lower trench reached 5 inches in depth, a pump recycled the water into the storage tank. Visual observations and measurements of soil suction and pore pressure between the trenches were recorded during the 6 day flow test.

Upon the commencement of water flow into the upper trench, early observations in the first 24 hours were primarily surficial seeps along the face of the levee slope between the two trenches, and flow from animal burrows. When surficial seeps were first observed, the location and time of seep was noted in field logs and then photographed. If the seep was rapid or threatened to erode the slope surface, it was slowed through use of a gravel bag placed over the seep.

On days 2 and 3 of the flow test, we saw seepage locations expanding and saturating the slope face and by day 3 we saw a reduction and then stoppage of flow from the gopher burrows. On days 2 through 4, our observations gradually shifted from the saturation and seepage patterns of the slope face to the arrival of the wetting front in the uphill wall face of the lower trench. The wetting front began to slowly move up the trench wall from the bottom up. The uphill face of the trench wall saw the wetting front climbing faster than the lower trench wall, indicating that the water was not purely a result of capillary action from the standing water that had accumulated in the base of the lower trench (from gopher burrow flows). This capillary action from the standing water in the trench masked any arrival of the wetting front in the lower 1 foot of the wall trench on day 1. By day 2, however, wetting patterns began to climb above the wet zone at the base of the trench and patterns were recorded.

Photographic timelines are provided below detailing levee slope face seepage and wetting patterns, the seepage observed related to two gopher burrows that played prominent roles in the flow test, and the wetting front patterns observed on the wall faces of the lower trenches.

3.6.1 Levee Slope Face Seepage

Seeps along the levee slope face between the upper and lower trench were the first sign of water movement between the two trenches and began happening within 30 minutes of turning on the water to the upper trench. The stump trench reached the pre-determined constant head of 1.5 feet of water in the upper trench at 12:22pm after the water had been turned on at 11:57am. Water was observed seeping out of the slope face at 12:21pm (Time=0.45 hrs) at Station 140. A gravel bag was placed over the seep within a few minutes of the initial seep and within seconds water began flowing from the lower wall face through a gopher burrow at Station 138.25. This burrow will be discussed in detail in Section 3.6.2. Figure 3-42 through Figure 3-44 follow the slope seepage patterns at instrument Lines B and C at 9.25 hours, 19.5 hours, and 55 hours into the flow test, respectively. A detailed timeline of slope face seepage is provided below in Table 3-2.

Figure 3-42. View of instrument line C (left) looking west and instrument Lines A and B looking east (right) 9.25 hours into the flow test. Note isolated seeps (darker spots) and gravel bags (covering seeps) at the top of Line C and extending down Line B.

Figure 3-43. View of instrument Lines B and C looking south 19.5 hours into the flow test. Note wet zones in slope face (darker spots) and gravel bags (covering seeps).

Figure 3-44. View looking west from instrument Line A at stump at 55 hours into the flow test. Note the outline (red) of the growing wet zone observed at the levee slope face.

Table 3-2. Photographic Timeline of Slope Face Seepage.

Time (hrs)	Observation	Photo or Illustration
0	Water flow begins	
0.45	Sta. 140 (Instrument Line B) at 2.3 feet upslope of lower wall face, water seeping out of slope near T4B-36, P2B-24, and T3B-36; water began pouring down the face of the lower wall threatening to erode; gravel bag was placed over each seep	
0.60	Seep at Sta. 123, 125, 127 (Instrument Line C – Control). Gravel bags were placed	
0.73	Seep Sta. 116 (west of control and 7" uphill of lower trench)	

0.9	Seep at Sta. 135, 1.8 ft down from upper trench	
1.4	New seeps between old seeps at instrument rows 1 and 2 at Stations 121, 122, 125 (Instrument Line C). Instrument rows increase from top trench to bottom trench.	No photo available.
2.3	Sta. 120-122 seeps observed between upper trench and instrument row 2 (just west of seeps at Instrument Line C)	
3.7	Sta. 120-128 existing seeps expanding in size while adjacent new small seeps form between gravel bags	

5.2	Sta. 141 a 7” diameter seep southeast of tensiometer T3B-36	
10.3	Seep at Sta. 117 at western limit of lower trench and extending down the western end wall of the trench as it grows	
15.7	Sta. 117 to 125; Seeps growing larger and pipe placed at area of rapid flow to prevent erosion	
19.8	Moisture seeping from eastern-most leg of equipment table below lower trench (outside of study area)	No photo
23.6	New seep at Sta. 127 at 1 ft above tensiometer T4C-18	No photo
54.4	New seep near Sta. 131	

54.4	Seep near upper trench at Sta. 155 and greater	
67.6	Pattern of small seeps observed about 10 feet west of western limit of control trench, following a line of gopher burrows visible from surface	

As shown in Table 3-2, burrow patterns were found to have a major influence on slope face seepage patterns and flows throughout the test. For this reason, burrows influencing flow patterns are discussed in detail in Section 3.6.2.

3.6.2 Burrows at Instrument Lines B and C

During the flow test, wetting front and water flow patterns appeared to be dominated by flow through a network of shallow gopher burrows in the vicinity of instrument Lines B (7 feet west of the stump) and C (in the control trench). Figure 3-45 shows the alignment of the burrows. The burrow pathways were grouted, excavated, and mapped after the flow test. The burrow at Line B extended all the way from the upper water delivery trench down to the lower stump trench. The burrow at instrument Line C began at the upper control trench but did not appear to continue all the way to the lower control trench. Both burrows connected to the upper trench and neither was detected prior to the flow test, despite careful documentation. Figure 3-45 shows the excavated burrow alignments.

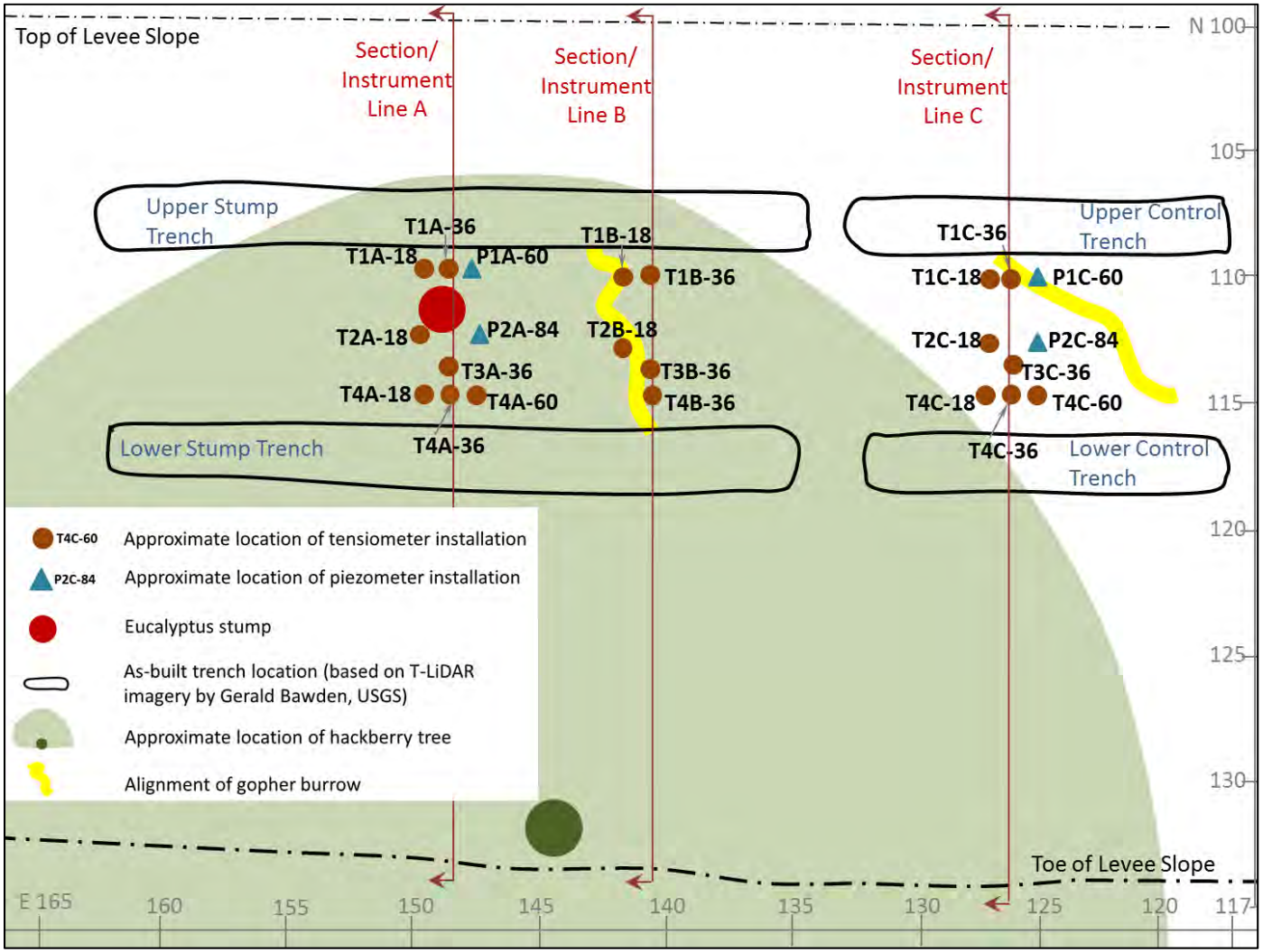

Figure 3-45. Location of mammal burrows in relation to Instrument Lines A, B, and C.

The gopher burrow at Line B produced water at the lower trench approximately 30 minutes following the beginning of water flow to the upper trench, about the time needed to fill the trench. Flow began as a small seep at the levee surface and proceeded to flow through a gopher burrow at the face of the lower wall upon placement of a gravel bag at the location of the initial seep (Figure 3-46). Table 3-3 provides a detailed account of observations associated with the flow of water through the gopher burrow at instrument Line B, Station 138-140. Table 3-4 provides a similar account for a gopher burrow encountered near instrument Line C that extended down toward the western corner of the control trench. Based on post-test grouting of the burrow adjacent to instrument Line C, the hole did not connect directly to the lower trench. A preferred flow pathway appears to have been established via another gopher burrow at the western extent of the lower control trench. It is possible that the gopher burrow networks once connected and a collapsed or plugged segment did not allow the grout to fill the full extent of the burrow. Instrument test results presented later in this report will detail the arrival of the wetting front in the vicinity of these burrows compared to the vicinity of the eucalyptus stump.

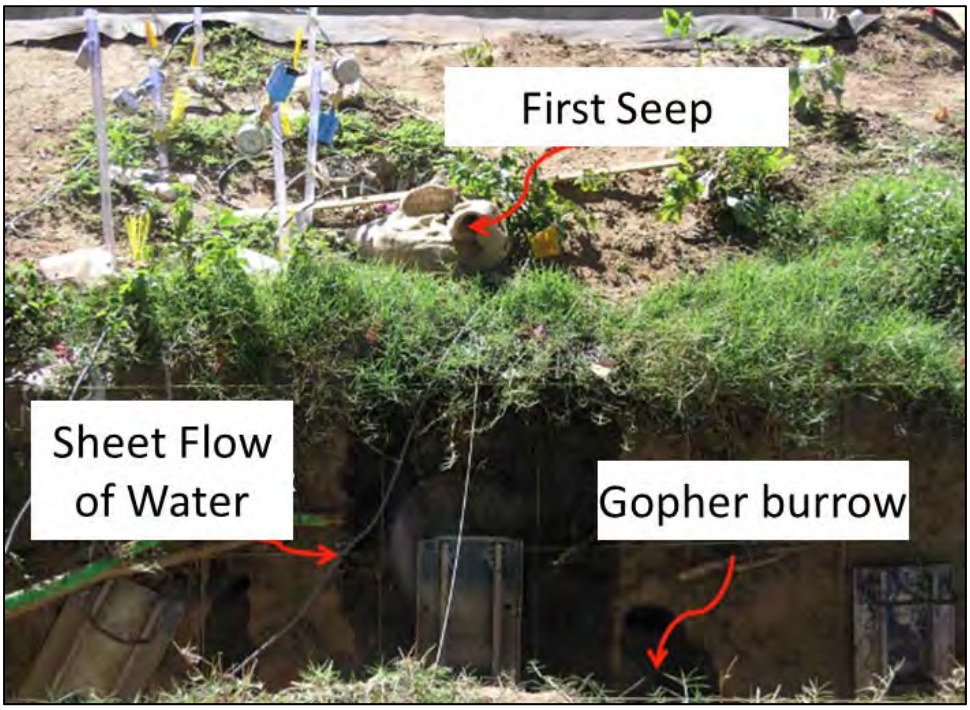

Figure 3-46. Water seepage at lower trench wall near gopher burrow at instrument Line B minutes after first water appeared on the levee slope face.

Table 3-3. Summary of observations at animal burrow at Station 138-140 (Line B).

Time (hrs)	Observation	Photo or Illustration (if available)
0	Begin water flow.	No photo
0.45	Water seeping out of slope face at tensiometers T4B-36, P2B-24, T3B-36.	
0.52	Gravel bag placed on slope seep.	Figure 3-46
0.53	Water burst from gopher burrow at Sta 138-139 and Sta 141 (both about 1.2 feet down from top of wall). Station 138-139 produced the majority of free water.	
1.2	Measured 4.3 inches standing water in lower stump trench due entirely to water flow through gopher burrow at Sta 138-139.	No photo
4.7	Water level in lower stump trench at Sta 138 is 0.65 ft above bottom.	

5.85	Water seeping out of saturated zone east of gopher hole at Sta 138-139.	
55.1	Flow through gopher hole at Sta 138-139 slowing rapidly between 53.1 (rate = 2 gal/min) and 55.1 hrs (rate = 1.7 gal/min).	
67.1	Flow has stopped and all that remains is moisture seeping through as seen in the photo to the right. This observation was made early in the morning and no observations were made between the last recorded observation at time = 55.1 hours.	
97.6	Left site for the night; tank full and upper trenches at constant head 1.5 ft above trench bottom.	No photo
118.4	Arrived onsite in the morning (Sept. 12) to find the tank empty and upper trenches below 0.5 ft.	No photo
122.1	Tank full and upper trenches back to constant head. Gopher burrow at Sta 138.25 begins to flow water.	See photo at 125.9 hours

125.9	Water seeping out of wall face near burrows at Station 138.25. Much of the walls appear to be saturated.	

Table 3-4. Summary of observations at gopher burrow, Station 117 (control trench).

Time (hrs)	Observation	Photo or Illustration (if available)
0	Begin water flow	
0.73	Seep Sta. 116 (west of control and 7" uphill of lower trench). Original seep location is under the gravel bag in the photo below (time =10.27 hrs).	See photo at time = 10.27 hours.
10.27	Seep observed at the western end of the control trench at Sta. 117	

10.52	Water burst through trench wall at Sta. 117 and began to flow through gopher burrow (< 2” in dia). Some decomposed root fragments came out of the hole, likely from old stump and root system. Water begins ponding in control trench.	
22.6	Water stops flowing through gopher burrow. Seep continues to produce moisture and water wicks up the lower trench walls adjacent from the standing water in the base.	
28.4	No water observed free flowing through gopher burrow but saturation zone continues to expand around zone of seep.	
97.6-122.1	Left site with full water tank and trenches at 97.6 hours. Trenches nearly empty by 118.4 hrs and re-filled by 122.1.	No photo

125	Small seep seen producing a trickle of water at squirrel burrow in control trench (Sta. 121.5). Photo to the right is of the squirrel burrow	

3.6.3 Wall Surface Saturation Progression

As previously discussed, on the first day of the flow test, observations primarily consisted of surficial slope seeps and flow into the lower trenches via conduits identified as gopher burrows. In these initial hours, saturation patterns in the lower trenches were mostly related to capillary action of water moving up the trench walls from the standing water in the base delivered by the flowing burrows. On days 2 and 3 of the flow test, saturation patterns began to emerge on the uphill wall of the lower trenches.

Figure 3-47 through Figure 3-51 show sketches of wetting front patterns in the uphill wall of the lower trench beginning at 29.1 hours from the time of initial inundation of the upper trench to 51.7 hours from inundation. Sketches were made to support observations during this time window as changes in site conditions were occurring rapidly. Figure 3-52 and Figure 3-53 show photographs of the site (both stump and control trenches) at 67.9 hours and 140 hours, respectively. Some visual changes can be detected between photos at 67.9 hours and 140 hours (the end of the test), but the site had essentially achieved a steady state by 67.9 hours into the flow test. These figures show only minor changes in the arrival of the wetting front at the uphill wall of the lower trench.

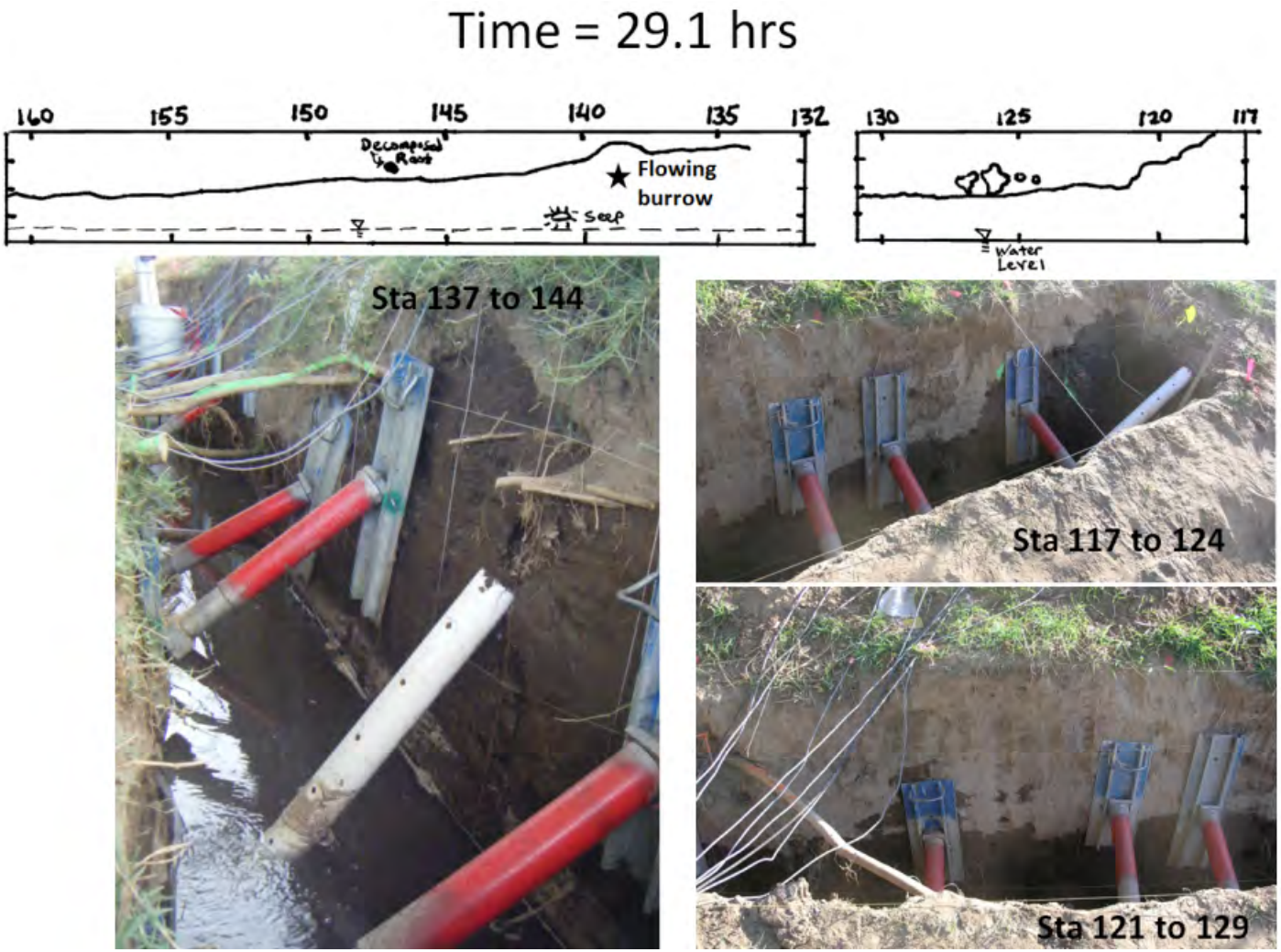

Figure 3-47. Saturation patterns in lower wall face at 29.1 hours after inundation of the upper trench with water. The lower stump (top left) and control (top right) trench wall seepage patterns are documented by station with corresponding photos below.

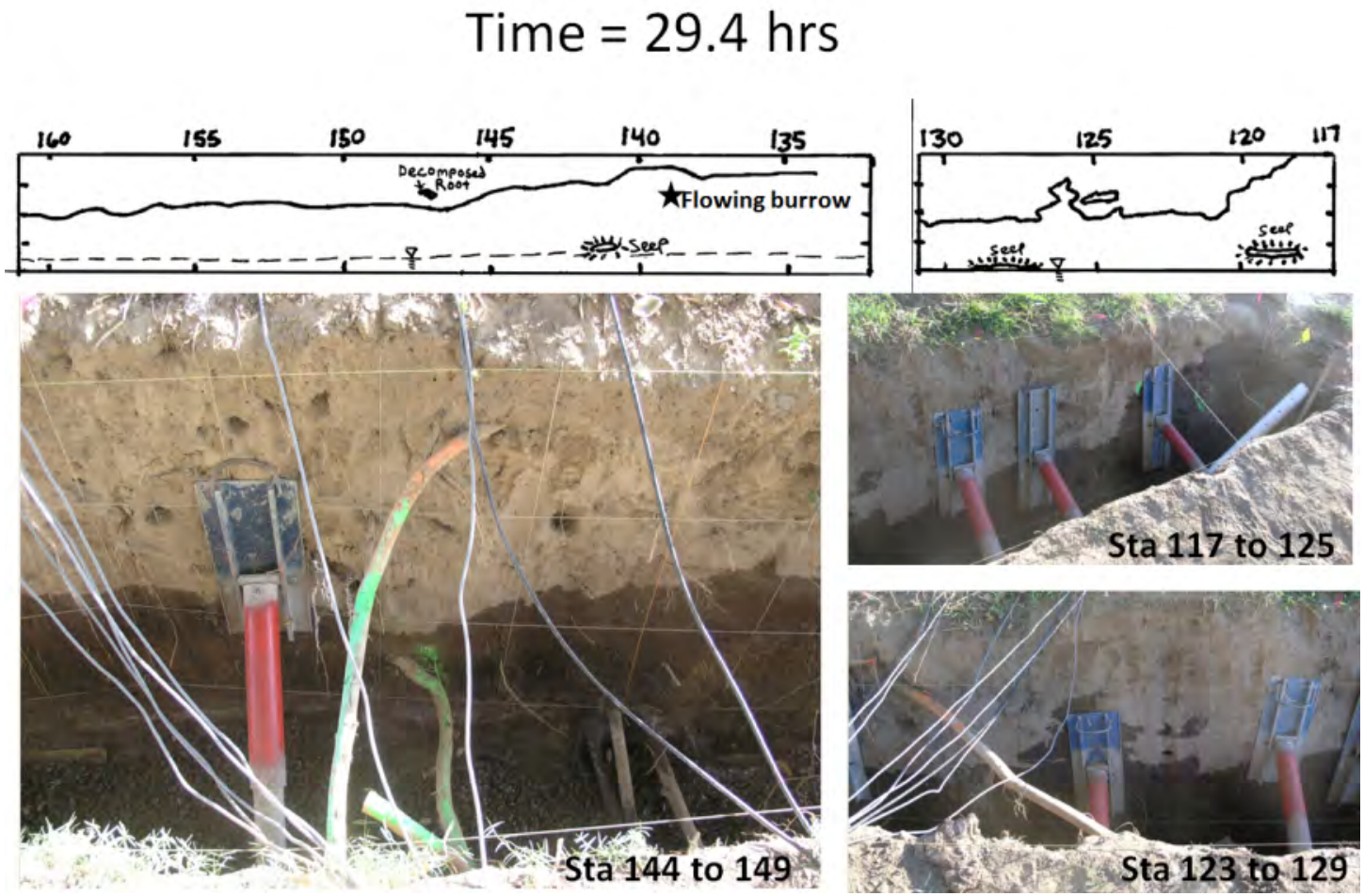

Figure 3-48. Saturation patterns in lower wall face at 29.4 hours after inundation. Note the appearance of seeps in permeable zones near the trench bottom. The lower stump (top left) and control (top right) trench wall seepage patterns are documented by station with corresponding photos below.

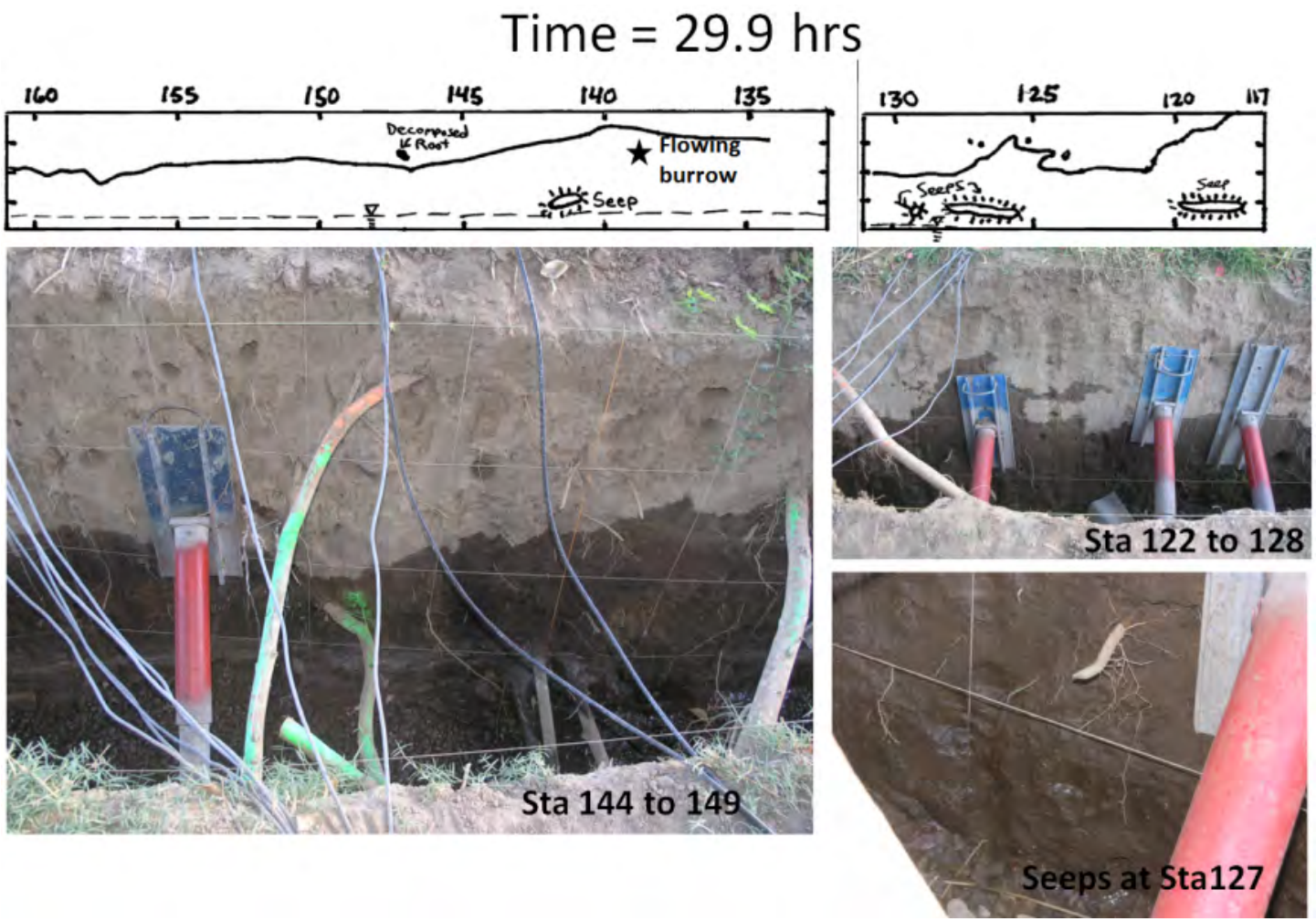

Figure 3-49. Saturation patterns in lower wall face at 29.9 hours after inundation. Note that seeps seem to be related to permeable material types. The lower stump (top left) and control (top right) trench wall seepage patterns are documented by station with corresponding photos below.

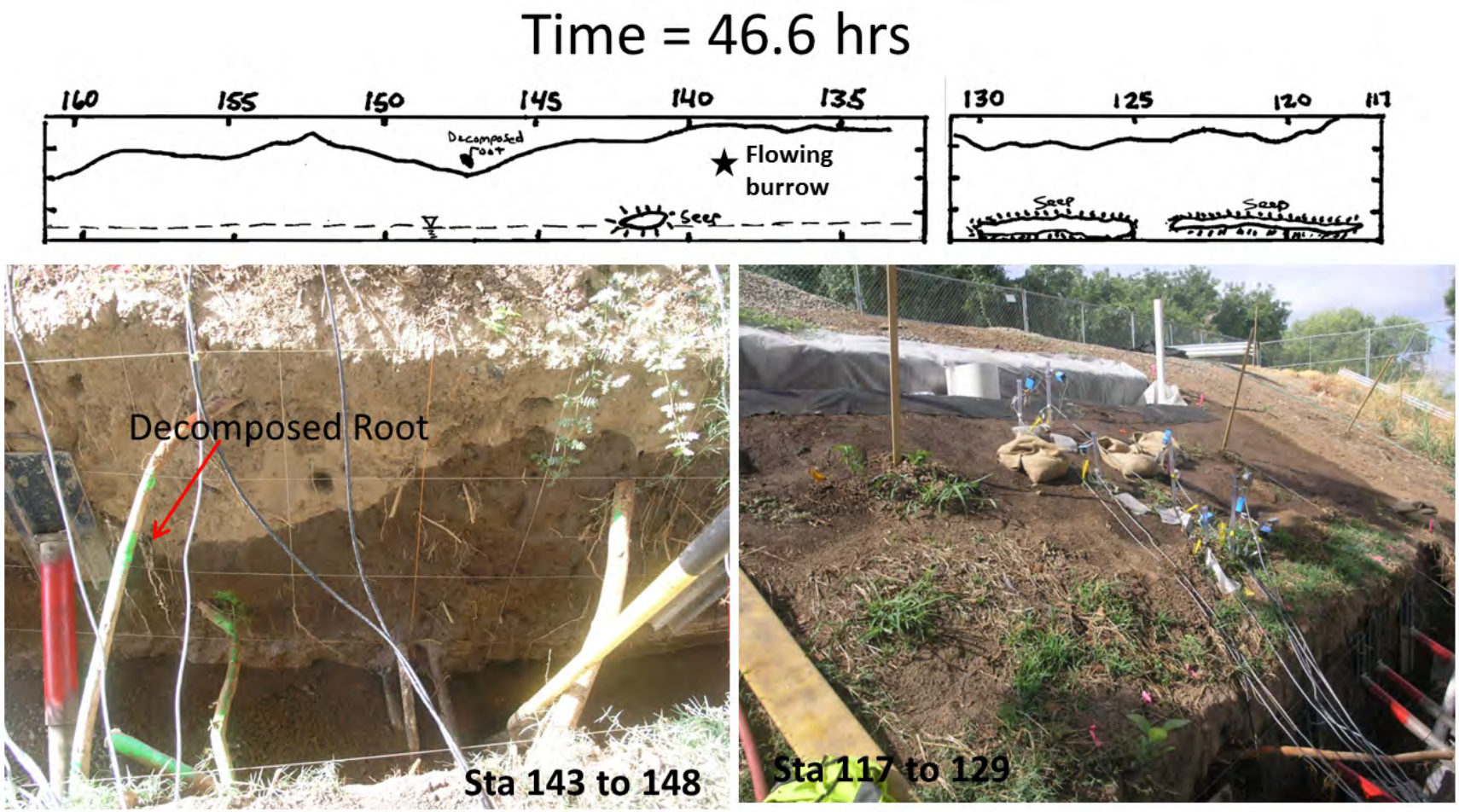

Figure 3-50. Saturation patterns in lower wall face at 46.6 hours after inundation. Note the depression in the saturation pattern in the area of the decomposed root at Station 147. The lower stump (top left) and control (top right) trench wall seepage patterns are documented by station with corresponding photos below.

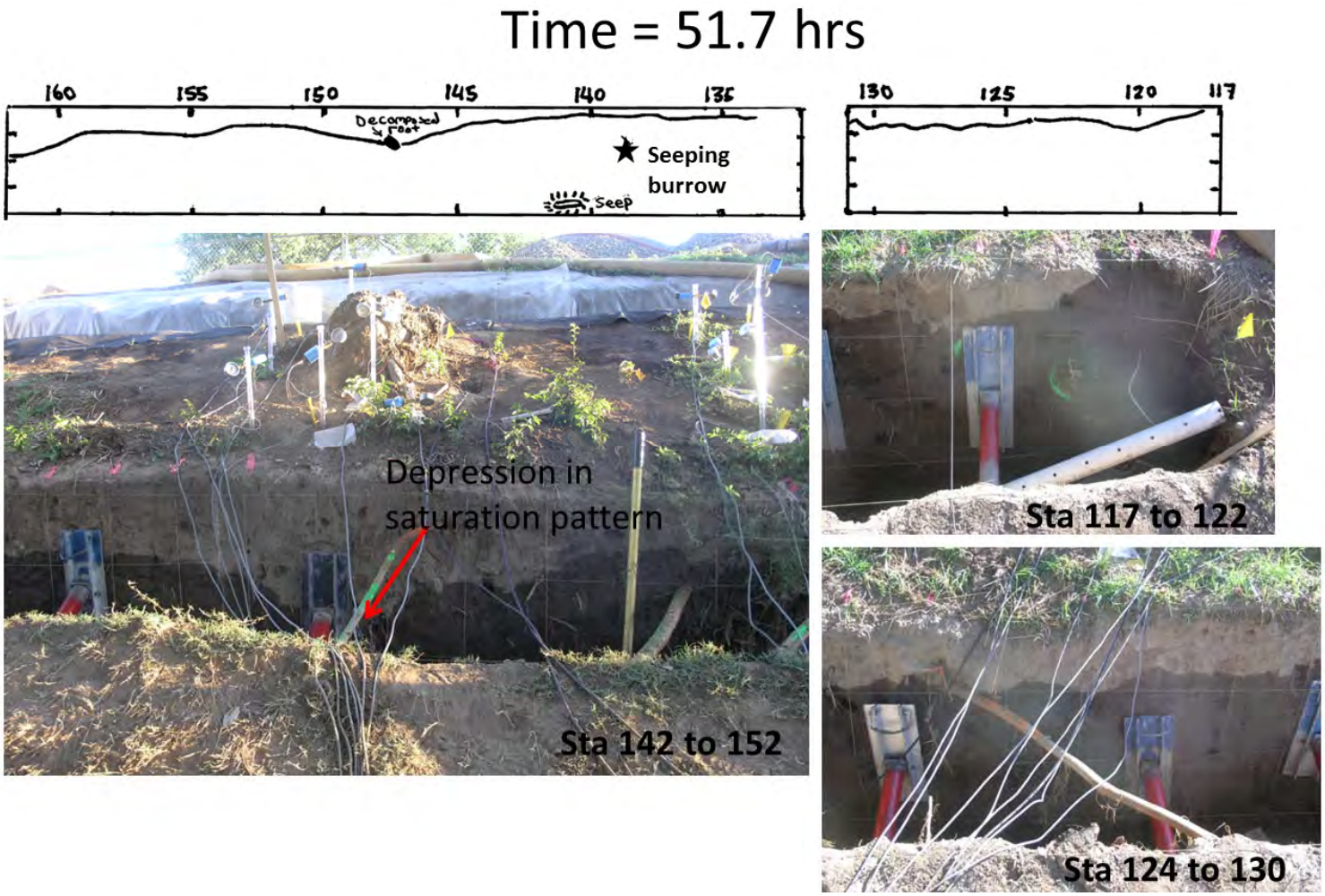

Figure 3-51. Saturation patterns in lower wall face at 51.7 hours after inundation. Note the wetting front continues to rise near the stump at Stations 145-150, though a depression is still visible indicating the stump is the last zone to saturate. The lower stump (top left) and control (top right) trench wall seepage patterns are documented by station with corresponding photos below.

Figure 3-52. Wide angle view of saturation patterns at 67.9 hours into the flow test. The area below the stump has begun to saturate.

Figure 3-53. Saturation patterns in the stump and control trenches at 140 hours into the flow test, just before the end of the test. Only small changes were observed in saturation patterns between 67.9 hours and 140 hours.

Figure 3-54 shows a direct comparison between the stump and control trenches showing a delayed wetting front in the vicinity of the decaying stump. Possible reasons include a reduced permeability in soils surrounding the stump, a physical obstacle to saturation and flow is created by the stump and root system, or the water is being redirected beneath the test through permeable layers or anomalies. Adding further complexity, the saturation of instrument Lines B and C are influenced by the presence of animal burrows, making a direct comparison between the instrument results and observations increasingly complex. Observations were made with regard to factors which may be influencing the pattern of the wetting front.

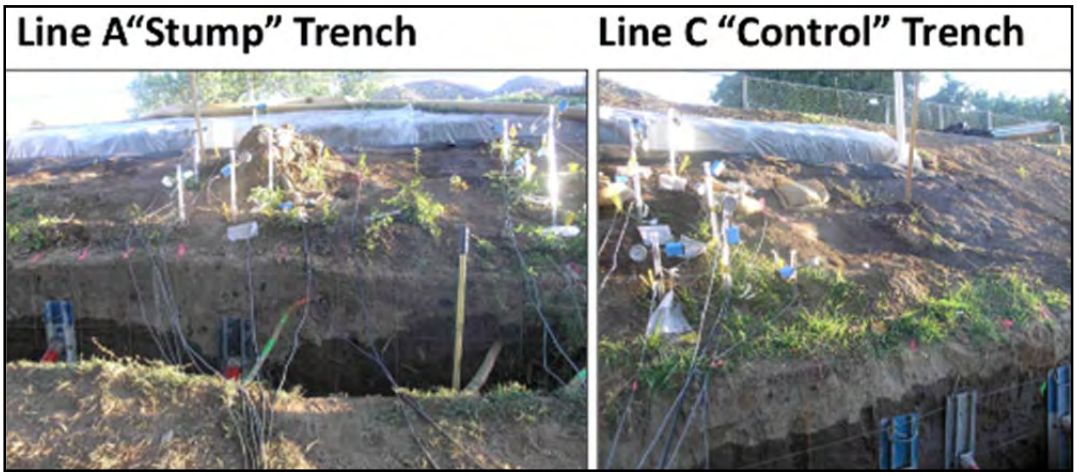

Figure 3-54. Comparison after 51.7 hours of flow. The zone in front of the stump was the last to saturate.

Figure 3-55 combines approximate gopher burrow alignments, outlet locations and wetting front patterns at 50 hours into the flow test to better understand the effect of these burrows on the wetting front at the lower trench. During a post-flow test site characterization effort, the gopher burrow at Line C was found to not connect directly to the lower trench, while the gopher burrow at Line B connected directly to both the upper and lower trenches. The influence of these gopher burrow patterns on the wetting front at the lower wall is shown in Figure 3-56 and Figure 3-57. Gopher burrows that did not connect directly with the upper trench, also did not conduct water preferentially (Figure 3-58) – at least not until saturation was achieved in surrounding soils. As shown in Table 3-3 at a time of 125 hours, the squirrel burrow shown in Figure 3-58 did eventually produce water once the surrounding walls had saturated. The small metal water pipe encountered during trench excavation at Station 145 was found to extend beyond our study area on each end and did not conduct visible free water along the zone of backfill (consisting of gravel within a fine-grained soil matrix). The pipe can be seen on Figure 3-48, Figure 3-49, and Figure 3-50 at times 29.4, 29.9, and 46.6 hours into the flow test, respectively.

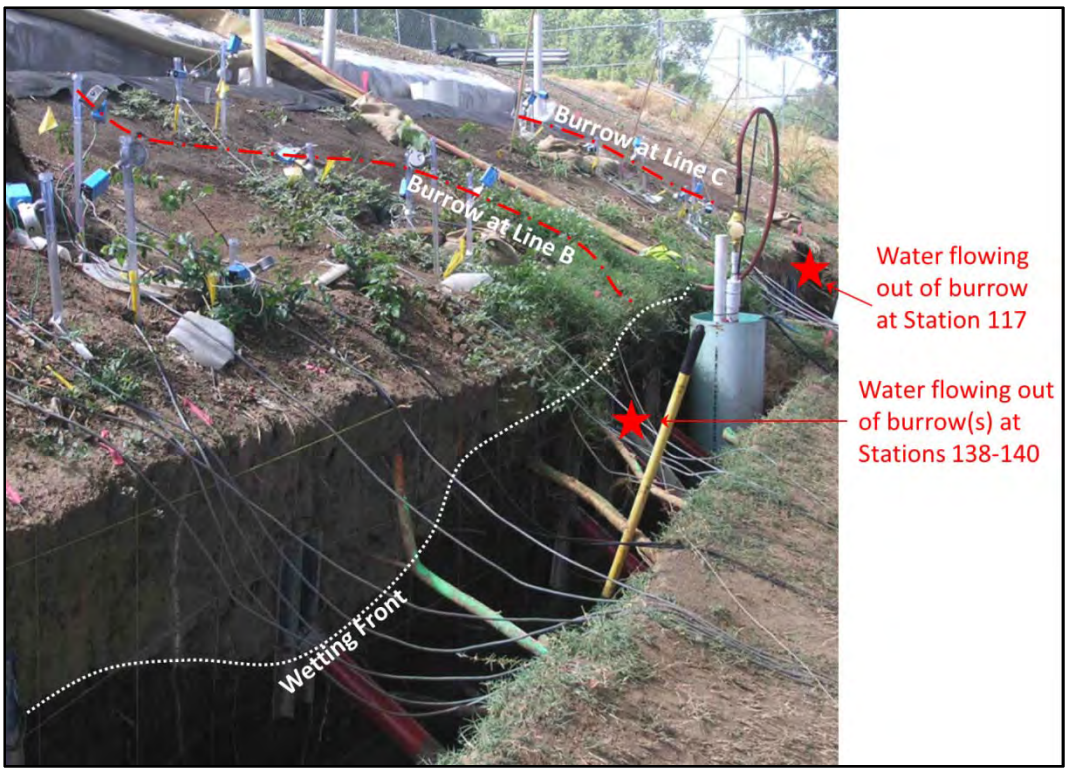

Figure 3-55. View looking west at the uphill wall of the lower stump trench 50 hours into the flow test. Gopher burrow outlet locations at Stations 138.25 and 117 are identified on the diagram as well as approximate alignments of burrows.

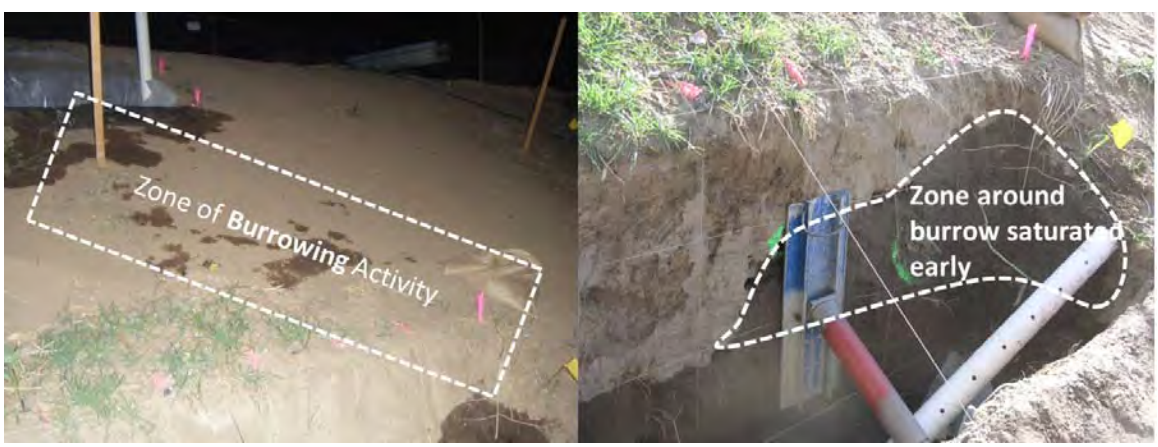

Figure 3-56. Control trench gopher burrow advances the wetting front (left) tracing a pathway to the outlet location at Station 117 (right). The outlet flowed briefly.

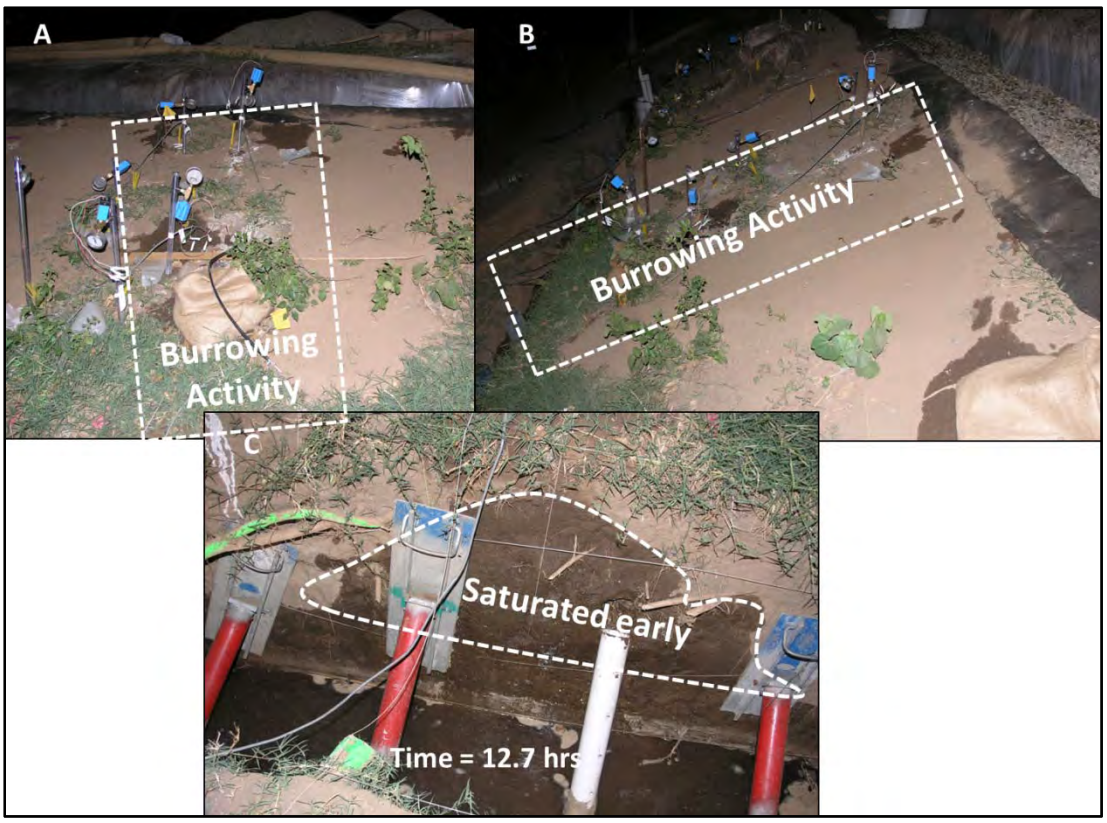

Figure 3-57. The wetting front is advanced by gopher burrow at Station 138.25. Slope saturation patterns looking A) south; and B) east. Photo C traces zone of early saturation due to the gopher burrow at a time of 12.7 hours into the flow test.

Figure 3-58. Squirrel burrow extending at least 18 inches into the uphill wall of the lower trench at A) the time of trench construction and B) 50 hours into the flow test. No free water flows until a seep upon saturation at 125 hours (See Table 3-2).

Neither live roots nor decomposing roots were observed to conduct water preferentially during the flow test. Figure 3-59 and Figure 3-60 show how the wetting front progressed in the vicinity of the decomposing roots. In particular, the

root shown on Figure 3-59 was initially observed to conduct silica slurry during the installation of tensiometers. Preferential flow of water was not observed through the annular space between the bark and the woody core of the root during the flow test, despite an intermittent annular space which was found and explored in the post flow test site characterization effort. As previously discussed, the area of the stump was the last zone to saturate.

Figure 3-59. Progression of wetting at the decomposed root at Station 147.5.

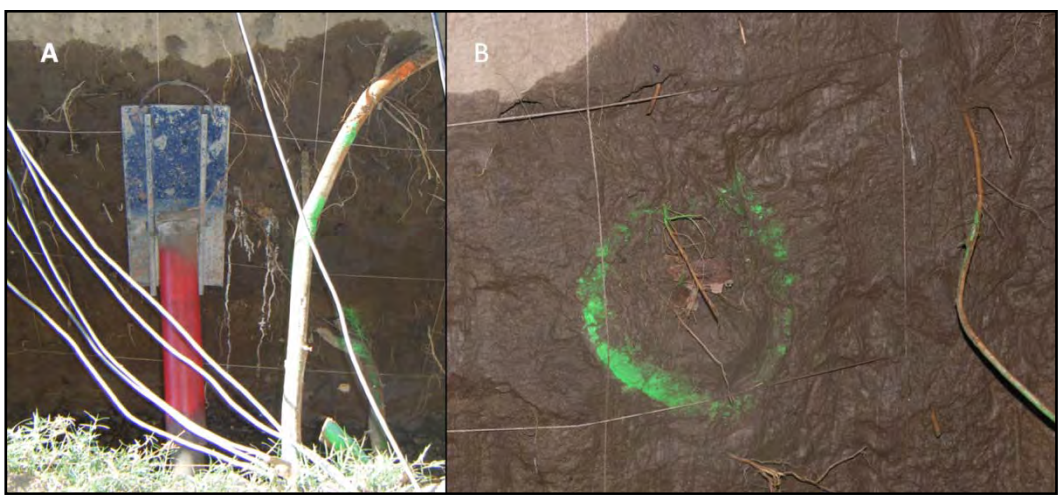

Figure 3-60. Progression of wetting at decomposed roots showing no preference to flow through the root or the gapping or loose zones surrounding the roots.

No impact on flow or wetting front patterns were observed to be connected with live roots. No voids or annular spaces were observed in connection with the live roots extending radially from the hackberry tree located at the toe of the levee. Figure 3-61 shows water preferentially flowing through the gopher burrow at Station 138.25 while no flow is observed through nearby live roots. Even as the wetting front arrived, observations of numerous live roots during the duration of

the flow test show no preference for water to flow through or around these live root systems (Figure 3-62).

Figure 3-61. During the flow test water is shown flowing through the gopher burrow and seeping out of permeable soils within the wall face, though no flow was observed through the adjacent live roots.

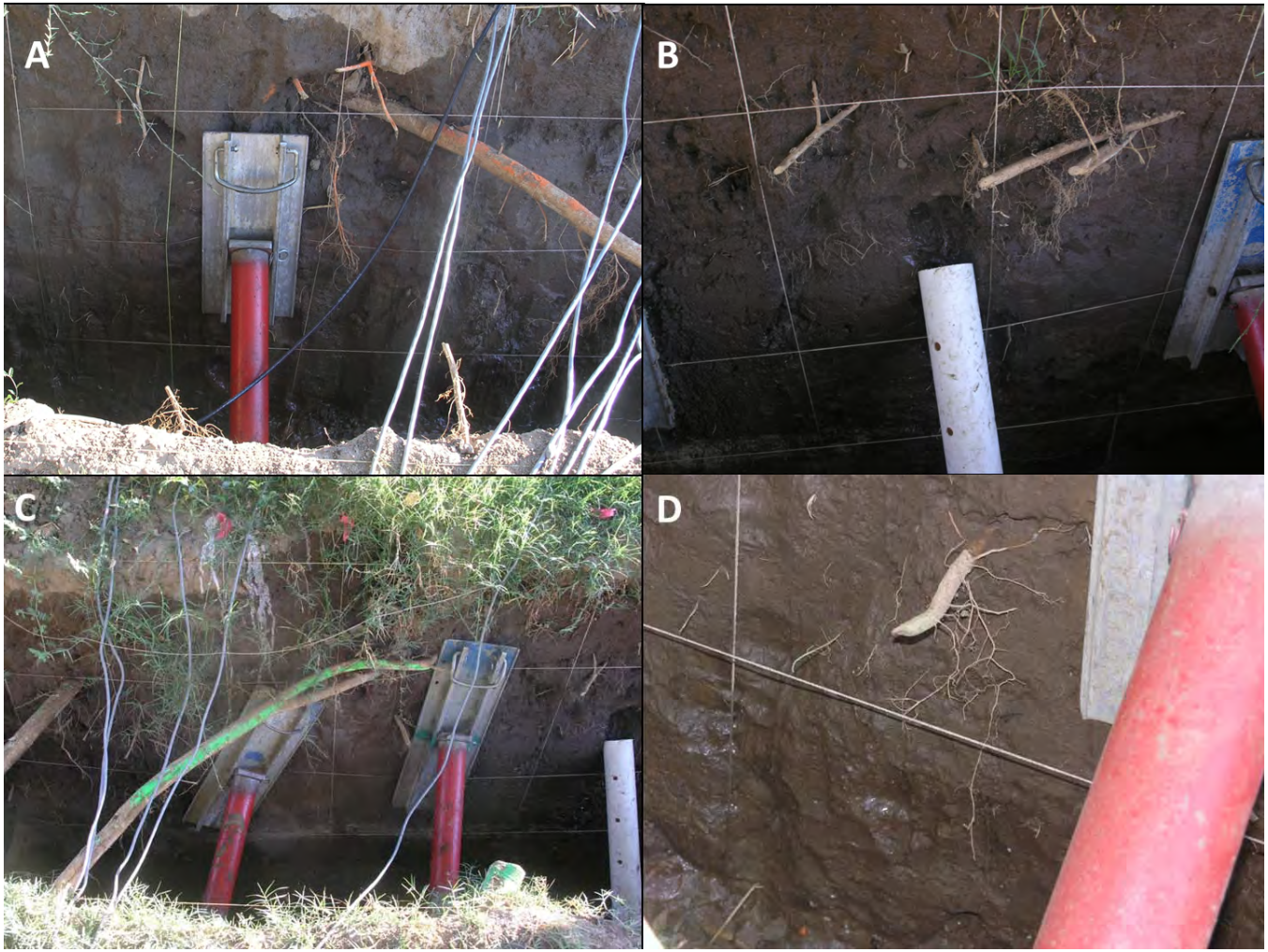

Figure 3-62. Live roots are shown during the flow test throughout the lower stump trench. At no time during the flow test were live roots observed to conduct water.

3.6.4 Instrument Results

Tensiometers and piezometers measured negative and positive pore water pressures before, during, and after the flow test. Complete results of all instruments including a discussion of instruments used and their calibration are presented in Appendix E. The results recorded by each tensiometer during the first four days of the flow test are summarized by instrument line and presented below. This time interval was selected because the wetting front had reached each instrument by this time. All piezometer data is presented together on a single plot.

Tensiometers were installed one week prior to the flow test and were connected to a continuously reading datalogger for several days prior to the inundation of the upper trenches to establish baseline values in the instruments and to check functionality. Initial moisture contents of surficial soils are presented in Appendix B and results of initial testing is presented in Appendix E. These moisture contents resulted in observed initial suction values of approximately 8 to 60 kPa. Suction values are discussed at length in Volume 5 of this report covering 2D and 3D seepage modeling. In this volume, results of tensiometer data is used for determining the time to arrival of the wetting front at each location based on relative changes in suction values.

Typical tensiometer results showing values of soil suction measured with time are shown on Figure 3-63. An initial drop in suction and recovery is seen during refilling of the instruments with water. Stable values drop suddenly indicating the time corresponding to the arrival of the wetting front at the instrument tip. The drop in suction values beginning at 30 hours indicates the arrival of the wetting front.

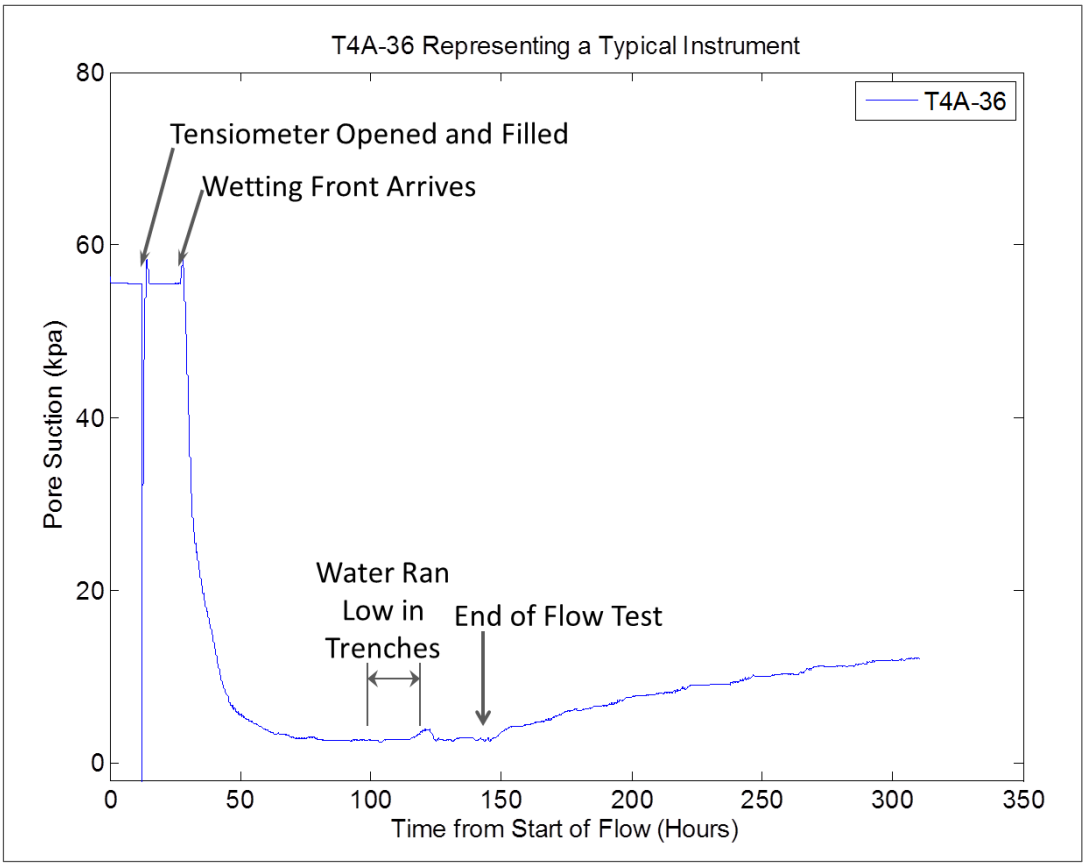

Figure 3-63. Typical tensiometer result plot.

The saturation front in the vicinity of instrument Line A was observed to progress more slowly than in instrument Lines B and C. In particular, Line A instruments in the area below the stump showed the arrival of the wetting front at approximately 70 hours after the start of the test. In contrast, analogous instruments of Lines B and C recorded no suction approximately 10 and 20 hours, respectively, from the start of the test, indicating rapid saturation in comparison to Line A. Physical observation of the saturation front, as seen from the lower wall, confirmed the area below the stump was the last location to saturate during the wetting test.

Figure 3-64 through Figure 3-66 show tensiometer data by instrument line. Figures showing comparisons of similarly positioned instruments across the various instrument lines are provided in Appendix E. As discussed previously, gopher burrows at Lines B and C appear to have accelerated the progression of the wetting front and the stump at Line A appears to have retarded the progression of the wetting front. Tensiometer T4A-60 (Line A) was observed to saturate more quickly than surrounding shallower instruments. This is likely due to free water present in the base of the lower stump trench flowing through the gopher burrow at Station 138.25. Tensiometers T2B-18 (Line B) and T2C-18 (Line C) were very proximal to the path of the gopher burrow which likely acted as a water conduit with patterns extending radially from the burrow. This accelerated the arrival of the wetting front

at these tensiometers. The relative effects of these competing influences will be evaluated in future seepage modeling.

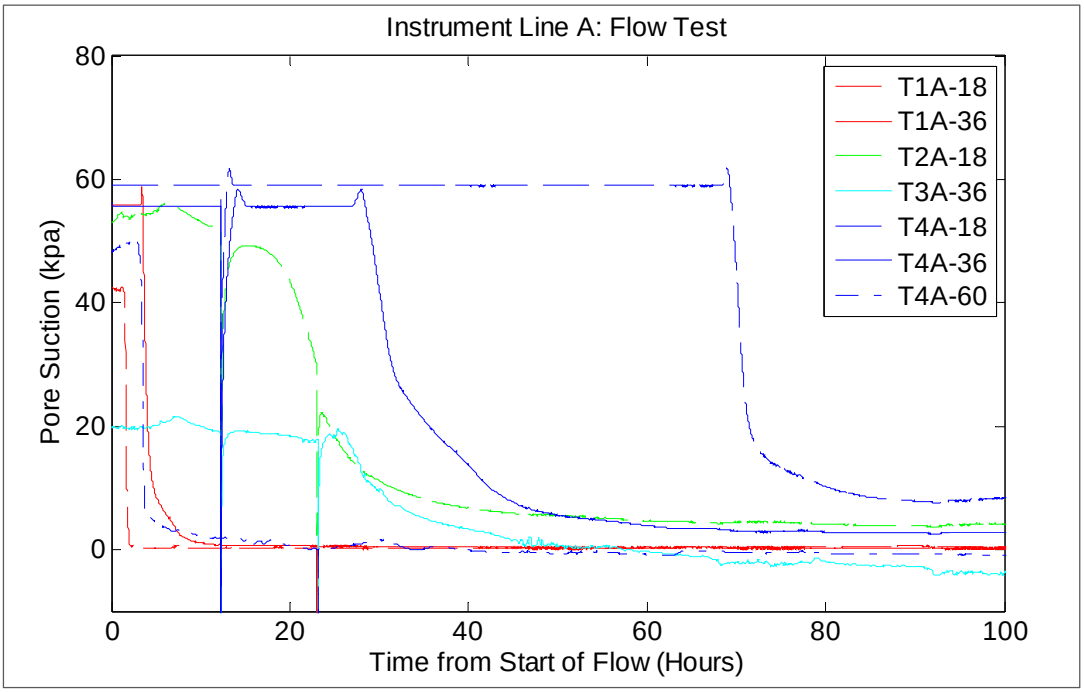

Figure 3-64. Tensiometer data for instrument Line A (at stump).

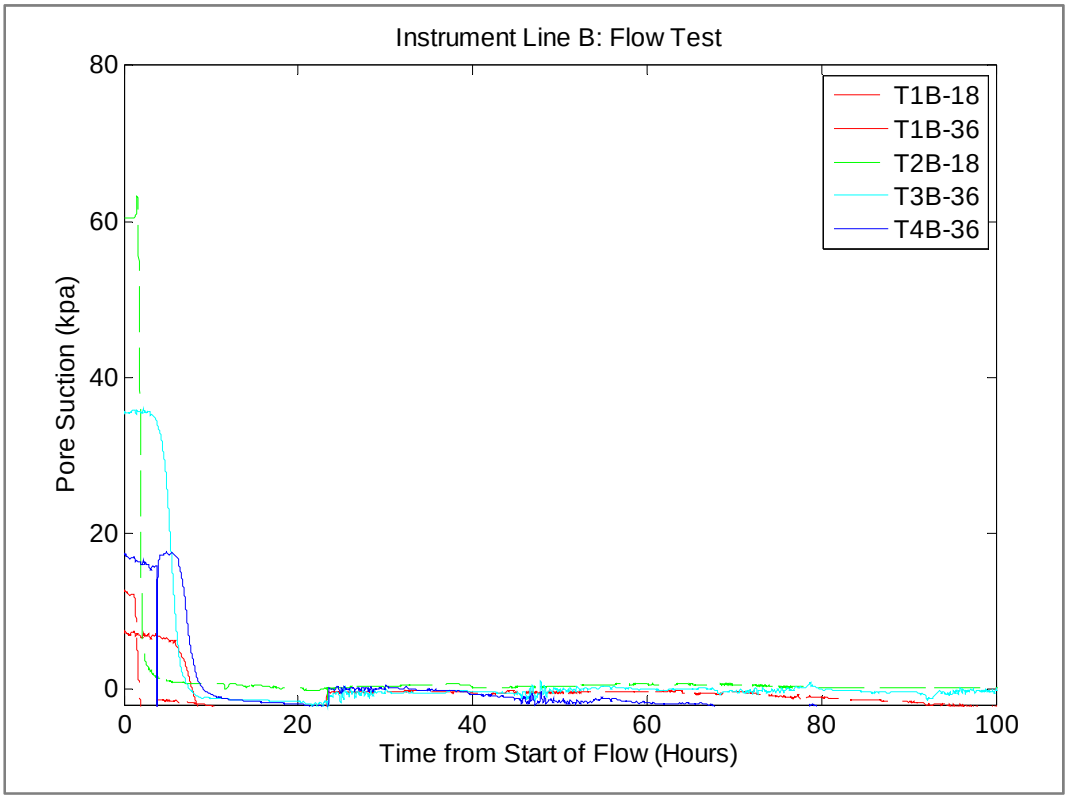

Figure 3-65. Tensiometer data for instrument Line B (7 ft from stump).

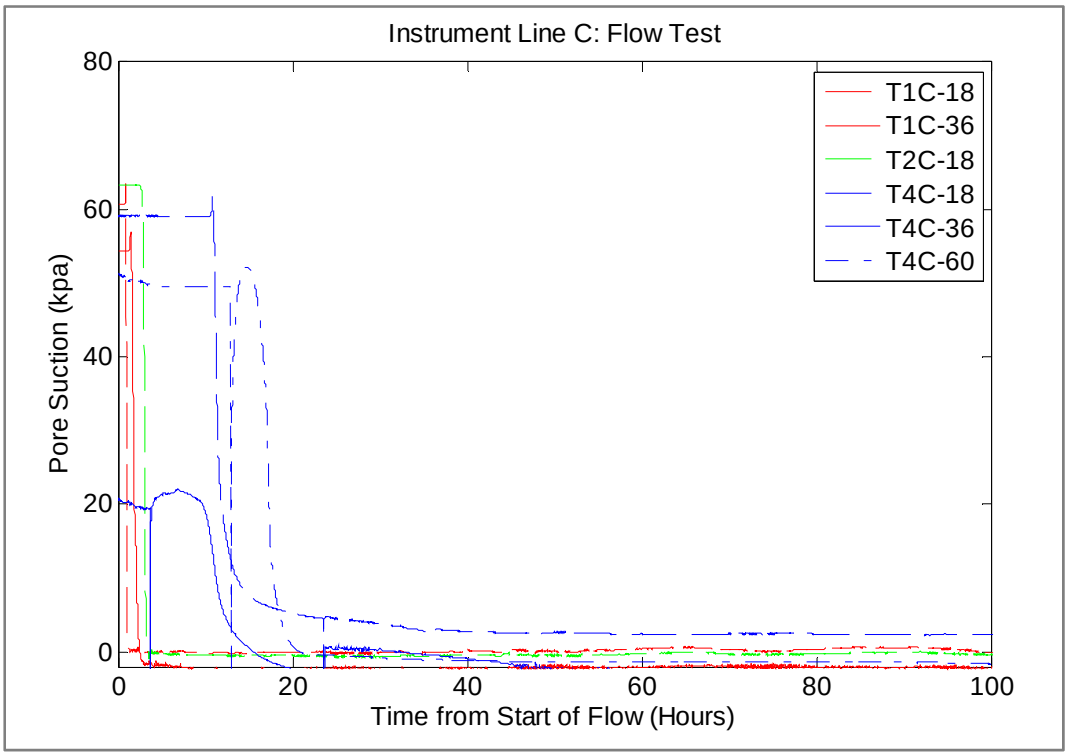

Figure 3-66. Tensiometer data for instrument Line C (23 ft from stump).

Piezometers were installed into 4-inch diameter auger holes and grouted in place with a mix of Portland cement and bentonite in accordance with the specifications of the manufacturer (Slope Indicator). Due to initially unsaturated conditions and the likelihood of low measured pressures throughout the flow test area, the Slope Indicator 10 psi Low Pressure Vibrating Wire model was selected. The constant head in the trench was held a maximum of 9 feet above the porous stone of the deepest piezometer (84 inches from surface grade, installed at mid-slope) resulting in a maximum possible pressure of 3.9 psi. The 10 psi low-pressure instrument was the most sensitive available for this application. The instruments were pre-saturated in a water bath and grouted into the hole upside down in order to minimize loss of saturation in its porous element due to the unsaturated conditions.

Based on piezometer data, saturation of the instruments was achieved within 1 to 2 days of flow. Pore pressures of less than 10 kPa (1.45 psi) developed following saturation (Figure 3-67) for 3 of the 4 instruments. High initial and final pressures in Piezometer P2A-84 did not fit with physical observations and available data. The piezometer was not able to be recovered for laboratory calibration testing and therefore data from this instrument was excluded from our analysis.

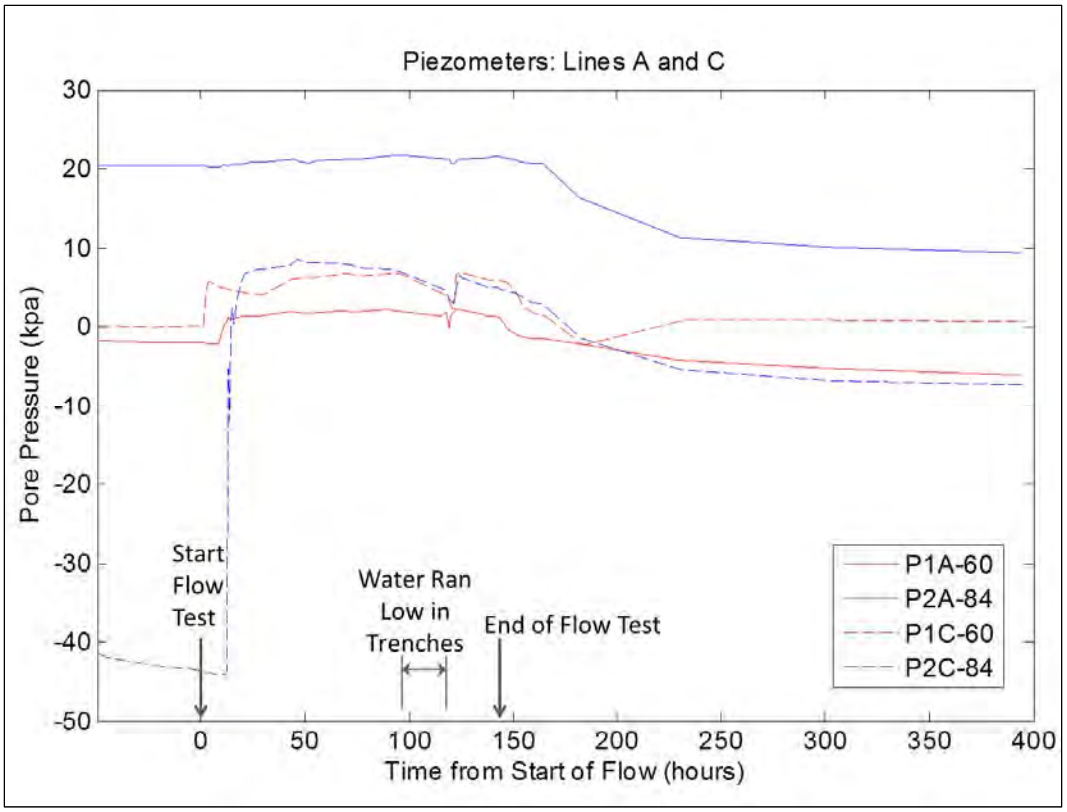

Figure 3-67. Pore pressures measured during flow test at instrument Lines A and C.

3.6.5 Water Volume Usage During Flow Test

During the 6-day flow test, approximately 45,000 gallons of water were released by gravity into the upper trenches. Two flow meters were installed in total on the two lines supplying water from a nearby source into the 2500 gallon reservoir. Two additional flow meters were installed at the two electric pumps controlled by float valves. The pumps were set up to recycle water back into the reservoir and volumes were recorded for each. Initially, one pump was placed in the stump trench and one in the control trench. Once the gopher burrow at Station 117 stopped flowing in the lower control trench on Day 2, the pump in the lower control trench was relocated into the lower stump trench to help control large flows coming through the gopher burrow at Station 138.25. All flow meters were read at regular intervals and at the same time. The water level in the reservoir was also measured at this time and we estimated and recorded the volume of water flowing by gravity into the upper trenches. Inflow volumes for water flowing into the trenches are therefore combined volumes.

The volume of water that flowed from the gopher burrow at Station 117 was not enough to actvate the control trench pump and the burrow stopped flowing before the water in this trench was ever pumped. The total volume of water pumped from the lower stump trench during the flow test was approximately 19,000 gallons,

virtually all of which flowed through the gopher burrow at Station 138.25. The volume that flowed through this burrow was underestimated by the amount lost to the surrounding soil of the lower trench. Figure 3-68 shows the balance of water during the flow test. Approximately 23,000 gallons of water were lost outside of the study section based on the assumption that the soil in the zone of study (assumed unit weight 120 pcf and 17 to 22% moisture content) would take approximately 2,300 to 3,700 gallons to achieve saturation (calculation based on 3,000 gallons for Figure 3-68).

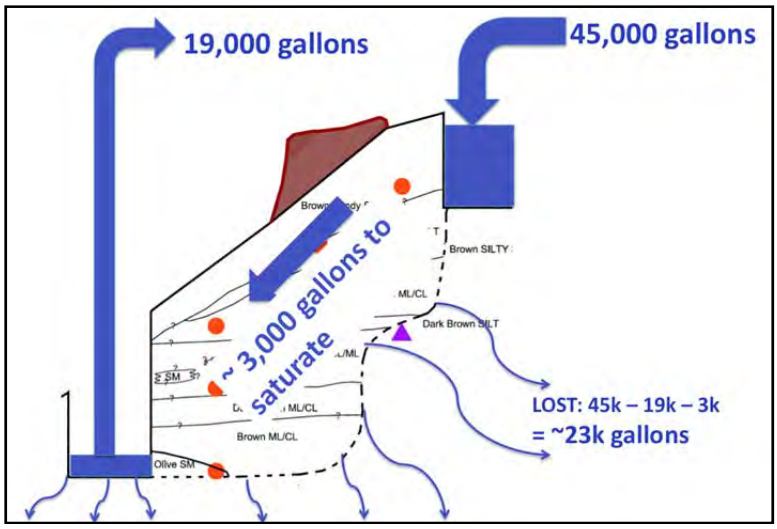

Figure 3-68. Calculation of flow volumes into and out of trenches. Note that a significant fraction of the input water was lost to areas outside of the study zone.

Figure 3-69 shows the cumulative volume of water delivered to the upper trenches and cumulative water recycled/pumped from the lower stump trench as a function of time during the flow test. Note the slope of the water delivery curve changes over the course of the test.

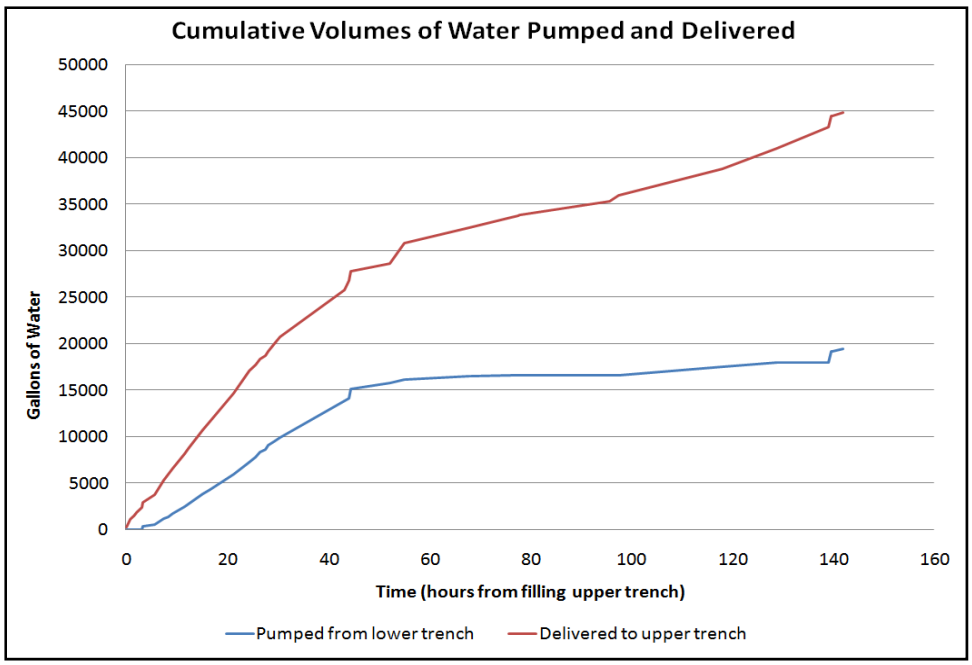

Figure 3-69. Plot of cumulative water delivered to the upper trenches from the 2,500 gallon reservoir and water recycled from the lower stump trench to reservoir.

Figure 3-70 breaks the curve into segments and the slope of each segment is calculated with a linear regression. The slope of each segment is the rate of water flow over that time period. Table 3-5 provides a summary of flow rates along with a reminder of key observations relevant within each interval.

During field observations, at approximately 55 hours, we observed a rapid decline in the rate of flow from the gopher burrow in the lower stump trench at Station 138.25. It appears that flow began slowing at 30 hours, though the decline in flow rate became apparent after a time of 55 hours. The recycle rate refers to the number of gallons of water pumped from the lower stump trench into the 2500 gallon reservoir over a period of 1 hour. Virtually all of this water was delivered to the lower trench via the gopher burrow at Station 138.25. This rate underestimates the actual rate of flow through the burrow. Water lost through the lower trench due to standing water percolating into surrounding soils arrived through the burrow and was lost outside of the study area prior to being recycled into the reservoir. In the first 30 hours of the flow test, a minimum of 367 gph flowed through the burrow, while 321 gph was saturating soils between the trenches, or was lost outside of the study zone.

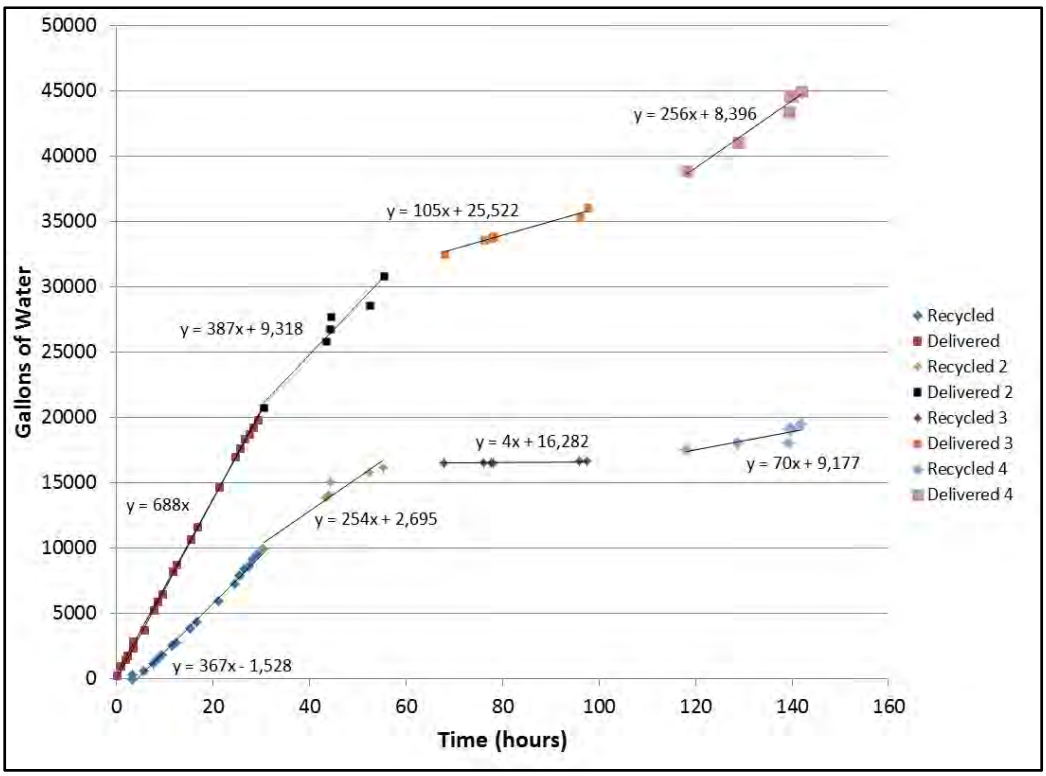

Figure 3-70. Cumulative gallons of water either delivered to the upper trench from the reservoir or recycled from the lower trench back to the reservoir. Curves are broken into segments with slopes representing the rate of flow.

Table 3-5. Flow Rate Breakdown.

Time (hrs)	Delivery Rate (gal/hr)	Recycle Rate (gal/hr)	Water Loss Rate to Soils (gal/hr)	Notes
0 to 30	688	367	321	Burrows flowing Sta. 138.25, Sta. 117
30 to 55	387	254	140	Burrow flowing Sta. 138.25
55 to 67	-	-	-	Burrow Sta.138.25 flow slowing; no data
67 to 97	105	4	101	Burrow Sta. 138.25 stopped flowing
97 to 118	-	-	-	Water tank ran dry; trenches ran low
118 to 142	256	70	186	Burrow Sta. 138.25 began flowing again

Between hours 30 and 55, the rate of recycled water pump, which flowed through the gopher burrow at Station 138.25 decreased from 367 to 254 gph. The loss rate for water declined from 321 to 140 gph. Between 55 and 97 hours into the flow test, burrow flow slowed and then stopped and the loss rate for water dropped to 101 gph. When the reservoir ran out of water at 97 hours and was refilled at 118 hours, the burrow at Station 138.25 began to flow again, but resulting in only 70 gph,available for recycle while the loss rate of water to surrounding soil was 186 gph.

Two burrows were observed to stop flowing over the course of the test. A reduction in macropore flow is expected as losses to surrounding soils rise with increased saturation of surrounding soils (Figure 3-71). This is consistent with observations by Beven and Germann (1982), who note that the rate of input into the hole must exceed losses to the surrounding soils and continuity must be maintained for the macropores to preferentially flow water. Collapse, siltation, or plugging may also have occurred over the course of the flow test. The gopher burrows may have been partially backfilled with loose soils, aiding in siltation or plugging of the burrows during the flow test. The overall reduction in water losses from the beginning of the flow test to the end is indicative of the reduction in flow through macropores as hydraulic conductivity of soil is expected to rise with increased degree of saturation (Figure 3-71), increasing rather than decreasing the flow rates.

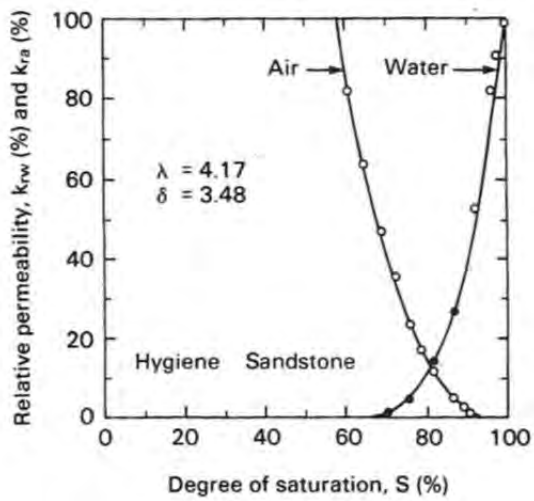

Figure 3-71. Relative permeability of water and air as a function of degree of saturation during drainage (Freudlund and Rahardjo, 1993; originally from Brooks and Corey, 1964). Note: Diagram intended for the illustration of concepts only. Actual relative permeability is expected to vary by soil or rock type.

3.7 POST-FLOW TEST SITE CHARACTERIZATION EFFORT

After completion of the flow test, the site was allowed to dry for two weeks prior to the characterization phase that began on October 1, 2010. The work was overseen by the UC Berkeley team, and excavation work was logged by Professor Richard Evans of UC Davis and John Lichter of Tree Associates, Consulting Arborists. The effort incorporated Ground-Based Tripod Light Detection and Ranging (T-LiDAR) technology in order to capture the root architecture. The T-LiDAR imaging (performed by Gerald Bawden of the USGS) was also adapted for use in capturing the soil stratigraphy and mammal burrow locations (Cobos-Roa et al., 2012).

3.7.1 Written and Photographic Documentation of Stump Excavation

Soil surrounding the eucalyptus stump was excavated in vertical slices extending back from the upslope side of the lower stump trench wall face as shown on Figure 3-72. When the last segment of soil was removed and the stump was removed to view the roots beneath. Segments of approximately 1.5 to 2 feet in thickness (measured into the trench wall) were removed with an air knife (connected to a compressor as described earlier). In the vicinity of delicate, decomposing roots, hand excavation was necessary to observe and document the *in-situ* condition. Areas of decomposing roots were carefully hand excavated, logged, photographed, and shot with T-LiDAR. Original logs prepared by Richard Evans and John Lichter are provided in Appendix F. The mammal burrow at Instrument Lines B and C were grouted, uncovered, photographed, and shot with T-LiDAR.

Figure 3-72. Excavation was completed around the stump in a series of vertical slices from Stations 138 to 153 as shown.

Grouting of burrows was performed by the American River Flood Control District (ARFCD) using a Chemgrout plant and trailer equipped with a moyno pump for grout delivery. Jim Warner, PE was retained as a grout expert to consult with our team on the grouting approach. At his recommendation, a grout mix was prepared with 10 percent bentonite and blended to a consistency that maximized thickness while remaining flowable. The mix was placed under low pressure (less than 10 psi) and injected slowly with enough pressure to move the grout to maximize filling of the hole while minimizing upheaval of the shallow surface soils covering the burrow. Burlap gravel sacks were positioned near the burrow outlet and were used to plug the burrows when grout began to flow from the lower trench wall (Figure 3-73).

Figure 3-73. ARFCD grout plant and trailer combination is shown (left). To the right, burrows are plugged with burlap sacks using a rod leveraged against the ground in order to prevent loss of grout.

The mammal burrow in Lines B and C were grouted and the soil covering them was excavated to expose the alignment extending from the upper trench. Figure 3-74 shows the exposed mammal burrows at Lines B and C.

Figure 3-74. Mammal burrows at instrument Lines B and C following post-flow grouting and characterization efforts.

Excavation began by removing the downslope wall of the lower stump trench for access and in doing so gently following the remains of a decomposing root extending downslope of the lower trench from Station 155 (Figure 3-75). Careful excavation around the root revealed no gap between it and the soil. The root was sufficiently decomposed such that a distinction could not be made between bark and woody center. Figure 3-76 shows a sandy silt soil matrix directly against the root.

Figure 3-75. View of decomposing root encountered in the lower stump trench, Station 155.

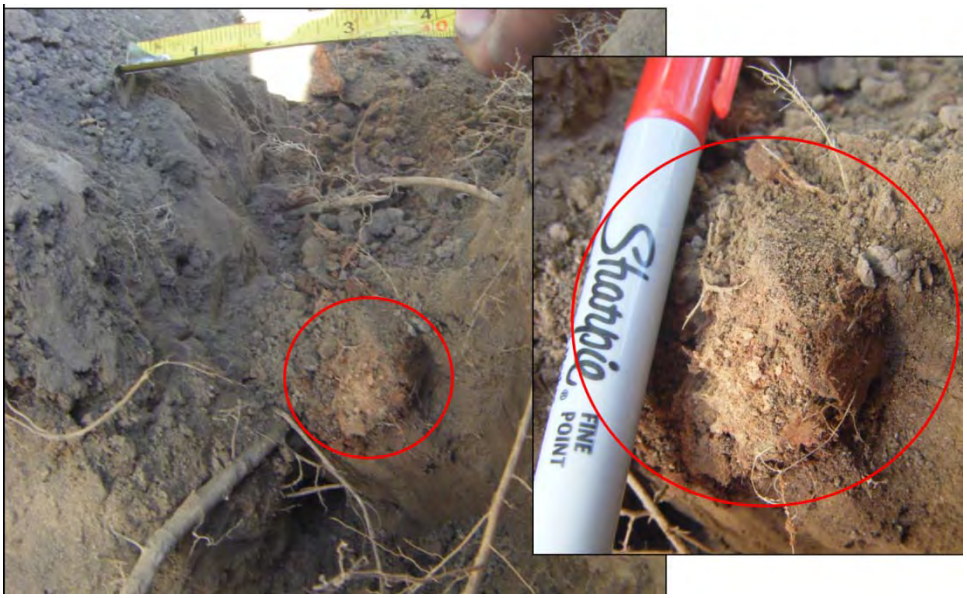

Figure 3-76. Close in view of decomposing root at Station 155. No gap was observable around this friable and highly decomposed root.

Figure 3-77 shows the final excavation of the upper wall of the lower trench, revealing the uphill wall to be scanned with T-LiDAR. Though field logs of this wall had already been generated, the wall was labeled with a consistent system for consistency and for the purposes of collecting T-LiDAR data (Figure 3-78). Visible live and decomposing roots as well as burrows were given labels and a reflective strip affixed proximally to aid in location of features that were difficult to isolate with T-LiDAR data.

Figure 3-77. View looking southeast at the trenches following excavation of the downhill wall of the lower stump trench.

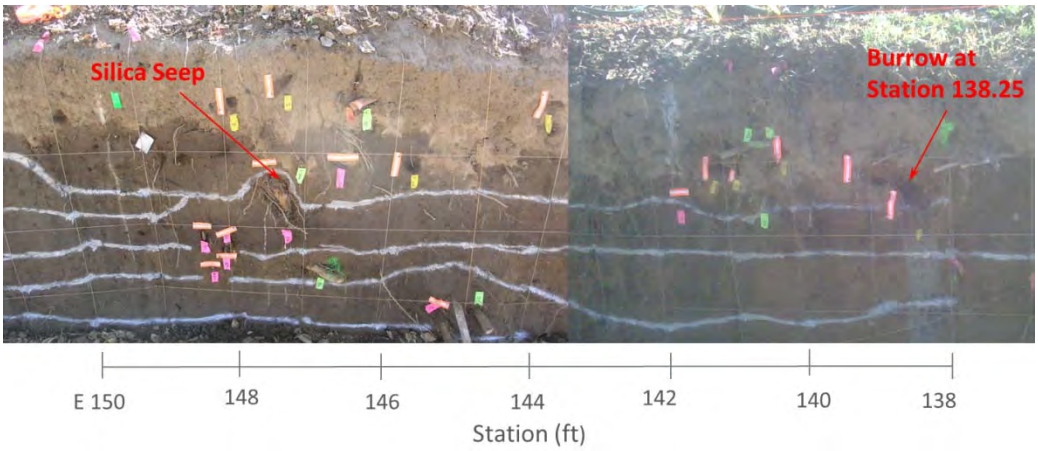

Figure 3-78. View of the uphill wall of the lower stump trench between Stations 138 and 151 just prior to scanning with T-LiDAR.

Excavation of the first slice began with removal of overburden and soils surrounding the stump using the air knife (Figure 3-79). As excavation proceeded, a prominent root emerged between tensiometers T4A-36 and T4A-60 (Figure 3-80). The excavation revealed this root to be the conduit for the silica seen flowing through a decomposing root at Station 147 during installation of tensiometers in the 4th row of Line A. Figure 3-81 shows the location of that root relative to the approximate installation position of tensiometers T4A-36 and T4A-60 and the seep location. The figure also shows the completed the first slice –'Slice 1' - excavation wall with roots exposed in the vicinity of the observed seep as compared with the initial lower trench wall. The silica slurry had traveled down the back of the root

and a small volume turned to the west following the bend in the root. The silica traveled a tortuous path of approximately 5 feet in total length. Another prominent root was revealed to the east and silica staining was also found on this root likely originating from its connection with Tensiometer T4A-18. Typical decomposing roots encountered are shown on Figure 3-82. Examples of annular spaces were most common in larger roots, likely because these spaces were larger and more noticeable. Figure 3-83 shows some examples of annular spaces and hollowed roots.

Figure 3-79. View of air knife operation during post-flow test site characterization effort.

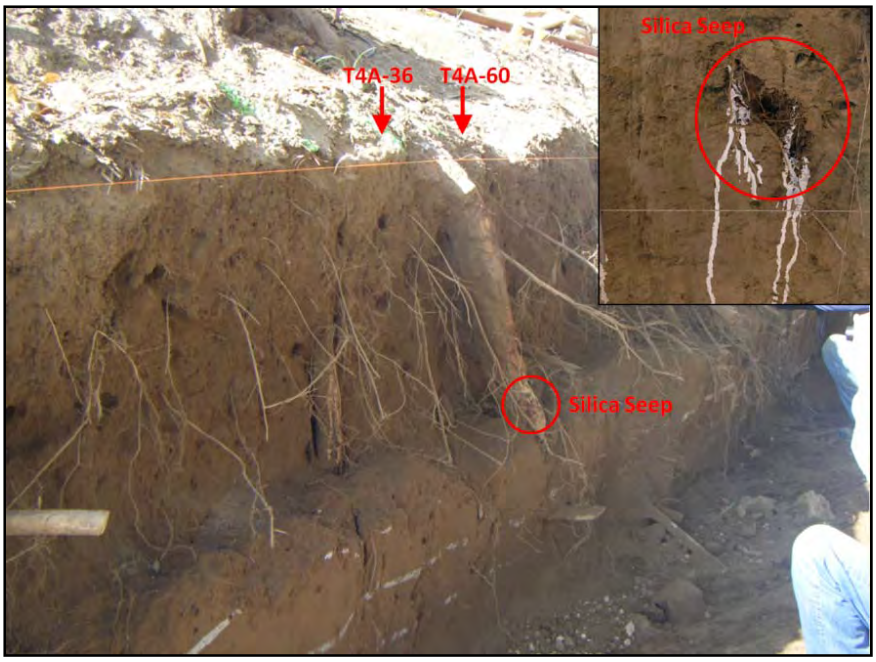

Figure 3-80. View of uphill wall of the lower stump trench as excavation of Slice 1 began. The root that was a conduit for silica slurry to the face of the lower wall during tensiometer installation is pictured.

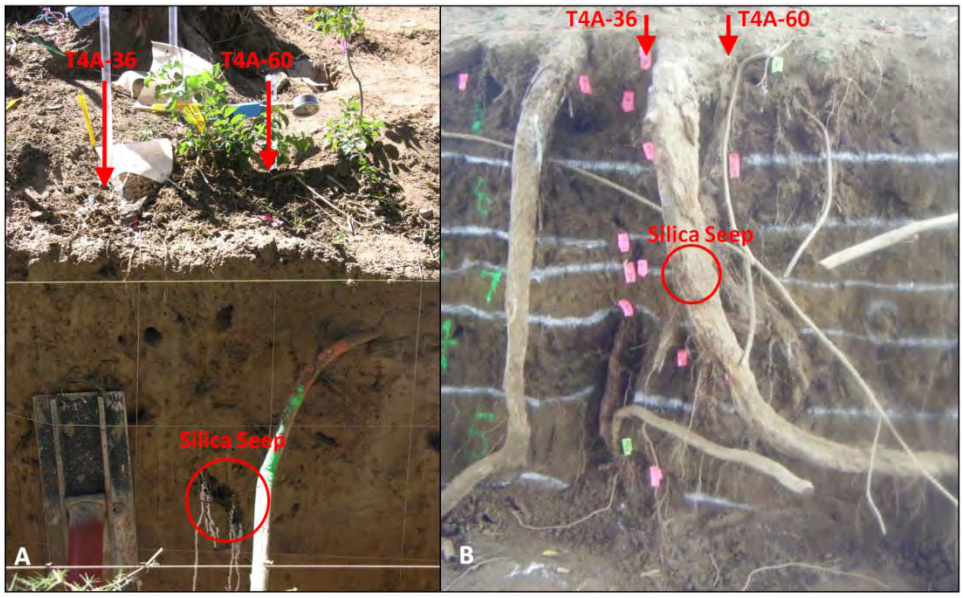

Figure 3-81.View of upper wall in lower trench below the stump A) during the flow test, and B) following the completion of 'Slice 1' excavation.

Figure 3-82. Typical appearance of decomposing roots encountered. Bark was fragile and discontinuous in many places. Annular spaces are seen on larger roots. Photos by Dr. Richard Evans.

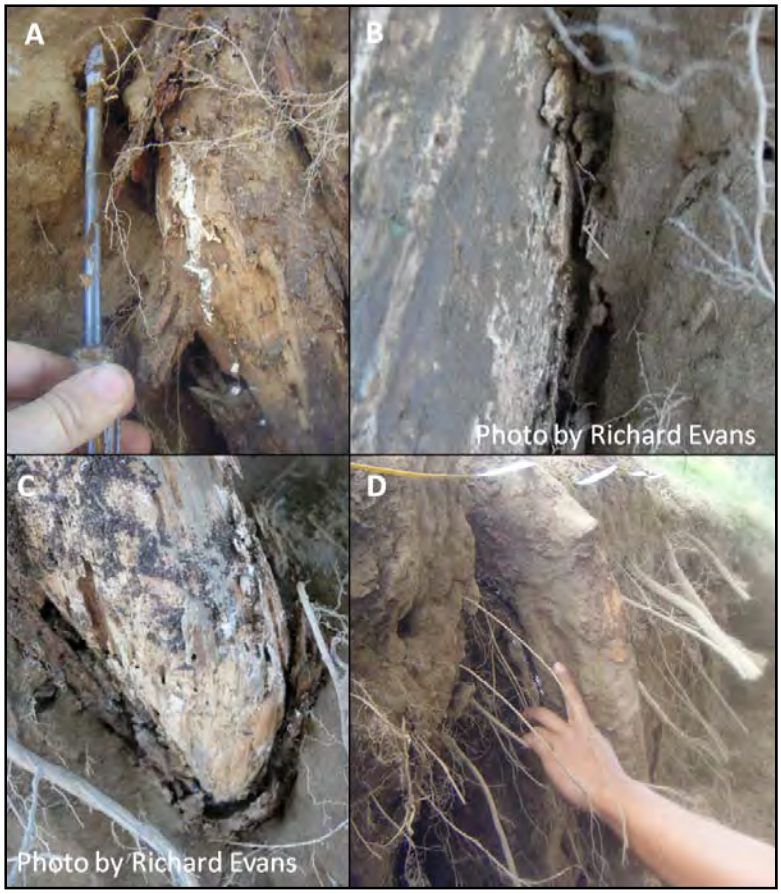

Figure 3-83. Examples of discontinuous annular space found in some decomposing roots. Many decomposing roots did not display this gap

Figure 3-84 provides an overview of findings from the excavation of 'Slice 1'. Live roots smaller than about ½ inch in diameter were cut as they interfere with T-LiDAR data collection. Figure 3-84B shows the excavation team exposing the decomposing root system through manual excavation. In Figure 3-84C, the burrow can be seen prior to removal of overburden soils. Portions of the burrow could not be grouted as seen in the photograph.

Excavation of 'Slice 2' proceeded, revealing the entry points of the silica (used in sealing tensiometers into the ground) into the decaying roots. Each instance of silica observed within the annular spaces around decaying roots were traced to a tensiometer instrument. The silica slurry generally did not flow far absent a direct connection to a void space. Figure 3-85 shows that though both T4A-36 and T4A-60 were installed on either side of a prominent decomposing root, it was tensiometer T4A-60 that was the conduit (or source) for silica that flowed that flowed out the lower trench wall face. Likewise, T4A-18 was found to connect directly to another prominent root and flow of silica was observed through annular spaces associated with this root also.

Figure 3-84. Slice 1 wall surface.

Throughout excavation, examples were uncovered of silica slurry flowing in animal burrows, in burrows within the woody core of the root (Figure 3-86), and even for short distances into loose soils (Figure 3-86A and C). With the exception of mammal burrows, the annular spaces were generally not sufficiently continuous to permit liquid silica slurry to flow far or to conduct large volumes. In general, the decomposition process of a root was found to be heterogeneous and segments where a clear gap was visible were followed by segments where the bark (Figure 3-87) or even the entire root (Figure 3-88) were so decomposed that all that remained was a hole with a loose fill of organic matter and soil. Depending on the stage of decomposition, voids may fill with surrounding soils and decomposed organic matter. Figure 3-89 illustrates examples of decaying roots exhibiting a space between the woody center and the bark and where sand has infilled the annular space of these root sections.

In addition to sand infilling/occupying these gaps, live roots were present at the site from the nearby hackberry tree located at the levee toe. Live roots observed did not conduct fluid or function as a preferred seepage pathway during our flow test or during instrument installation. Annular spaces were not observed between the bark and the woody core of these roots or between the soil and the root. Live root growth within the decomposing roots was very common (Figure 3-90). At times, the live root networks around the decomposing roots held root fragments together as a single unit. Live roots seemed to occupy the void spaces and thrive in the mixture of decomposed organic matter and soil. Small live roots were growing 'opportunistically' through bark and the woody cores of decomposing roots.

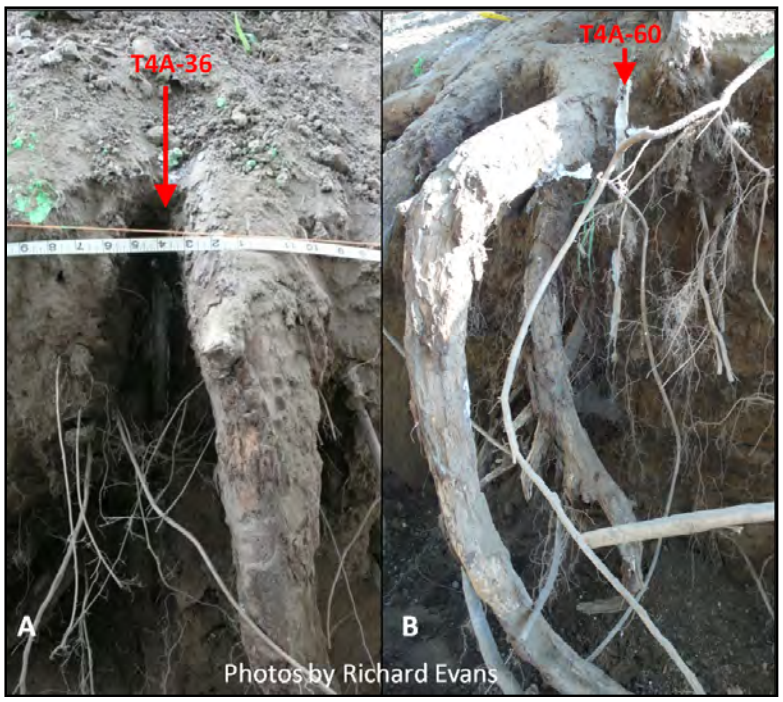

Figure 3-85. Hardened silica slurry associated with tensiometers T4A-36 (left) and T4A-60 (right) is discovered. Flow paths were observed showing that silica flowed through a burrow or void when a direct hydraulic connection was present.

Figure 3-86. Silica slurry freely flowed in burrows (as shown in A) and void spaces within roots (as shown in B) when a direct hydraulic connection was available (or present).

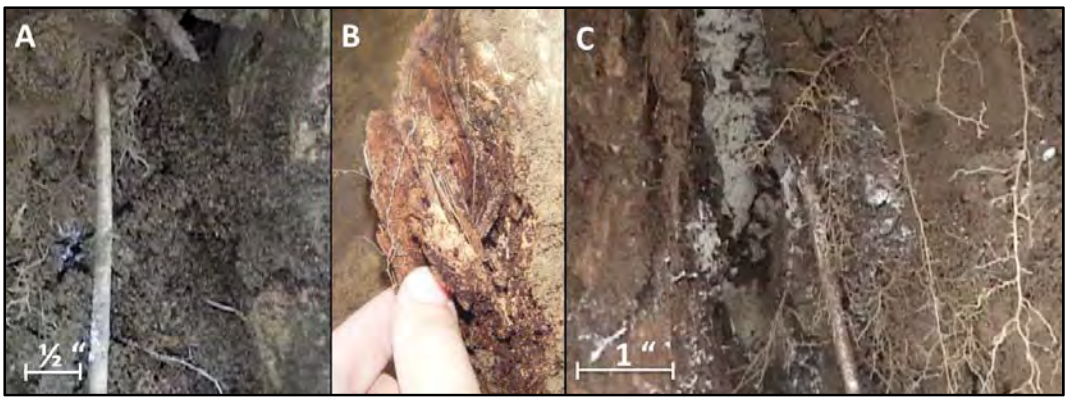

Figure 3-87. Bark fully decomposed with annular space between the woody core and bark, loosely filled with decomposed organic matter and soil (A and B). White silica slurry in Photos A and C are from a tensiometer intersecting loose organic soils and the silica slurry permeating the void space for a short distance.

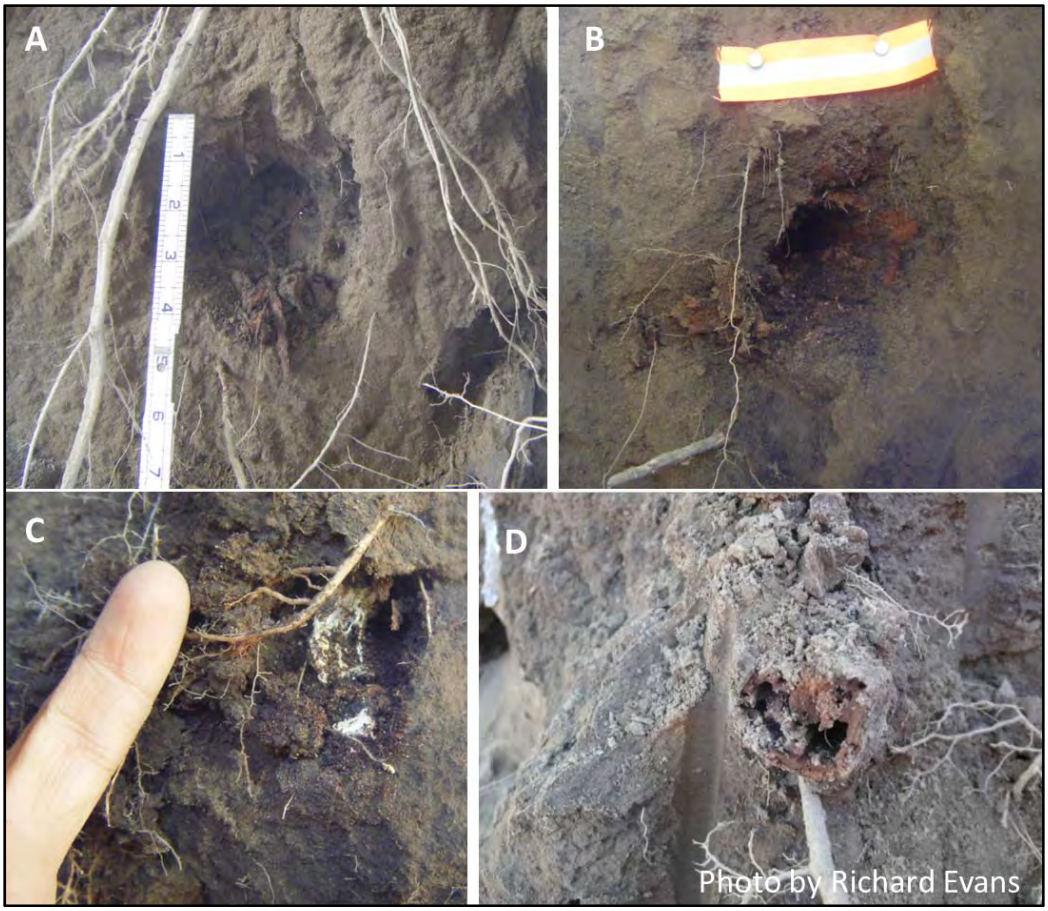

Figure 3-88. Roots can leave a void where they become completely decomposed and surrounding soils and live roots have not yet in filled the void. The root in Photo D has likely been subjected to decomposition from biological activity.

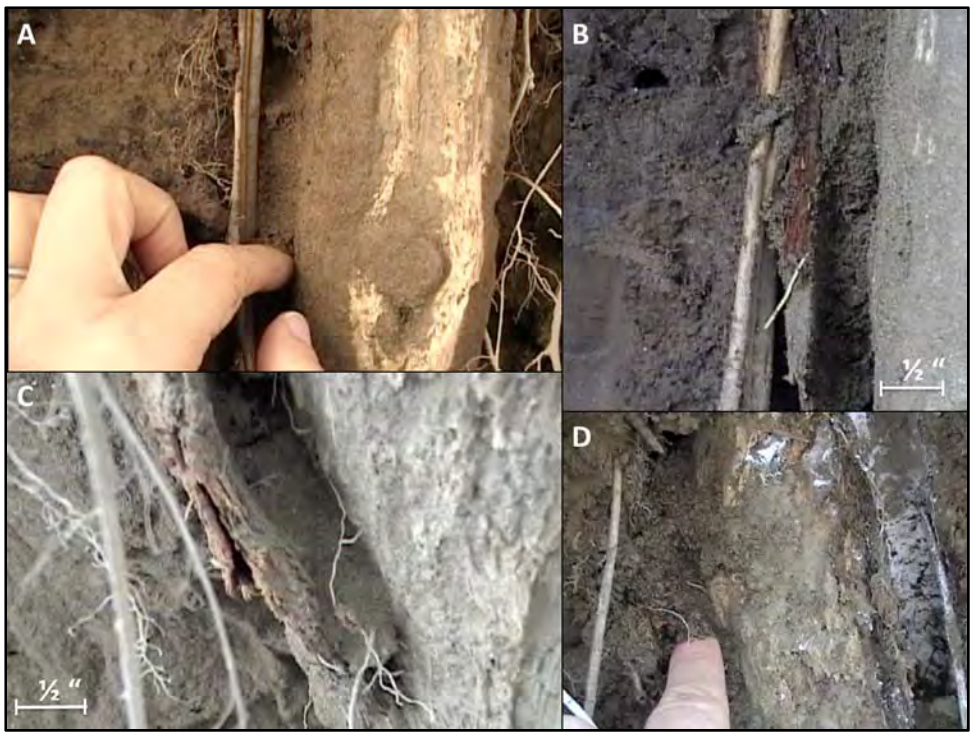

Figure 3-89. Photos A through D are examples of sands in-filling void spaces present between the decaying roots woody center and the bark. In Photo B, from right to left we see the woody core, an infill sand layer, a layer of decomposing bark, a live root, and then the surrounding soil matrix

Figure 3-90. Live roots frequently observed growing within the decomposing organic matter of old root systems.

Figure 3-91 illustrates the final wall face following excavation of Slice 2. At this time, the gopher burrow (grouted) at Station 138.25 has been revealed and the root

architecture of the stump has begun to take shape. Burrows were present in the vicinity of the stump, though animal burrows were present in large numbers throughout the site and did not seem to be more common at the stump than in other areas of the site, as discussed in a subsequent section. Once uncovered, the gopher burrow casting at Station 138.25 was cleaned and undermined slightly in several places to capture its dimension with a T-LiDAR scan. The casting was painted orange for photographs.

Figure 3-91. Final position of 'Slice 2' at the time of logging and before T-LiDAR scanning. Note presence of burrow networks between the root system in Photo B (indicated by vertically-oriented orange nylon strips). Photo C shows the newly revealed burrow casting at Station 138.25.

Slice 3 more fully revealed the architecture of the stump. As excavation proceeded, creating a 'wall log' became challenging as the wall became increasingly thin and formed the support soils beneath the stump. For the last slice, logs were generated on the sides of the stump. Below the stump soils were strategically left in place in order to make a final T-LiDAR image before the stump was undermined and removed. A segment of soil was left behind (Figure 3-92A) and below the stump, supports rods added, and additional soils were removed just prior to the final T-

LiDAR scan. Figure 3-92 shows the final slice from multiple angles. Figure 3-92D shows the final wall face of Slice 3 and provides a perspective of the proximity of the stump and root system to the burrow (cast painted orange) that allowed over 19,000 gallons to pass from the upper to lower stump trench during the 6 day flow test.

Figure 3-92. View of stump excavation following removal of 'Slice 3' soils. Photo A is a view of the stump from the crest of the levee looking down into the upper trench. Photos B through D show the stump from varying angles. Photo D also shows T-LiDAR scanning in progress.

Once the final logs and T-LiDAR scanning were complete, additional excavation was performed behind the stump and then beneath the stump to reveal and photograph more of the root system. The excavation effort behind the stump revealed few roots extending into the levee uphill of the stump (Figure 3-93 and Figure 3-94). Figure 3-93 shows another example of a root that had been pierced by a tensiometer on the uphill side of the stump. This root had begun to decompose inside the woody core of the root. When a tensiometer installation pierced this friable root, the silica slurry used to seal the instrument into the hole filled voids traceable to the tensiometer (Figure 3-93).

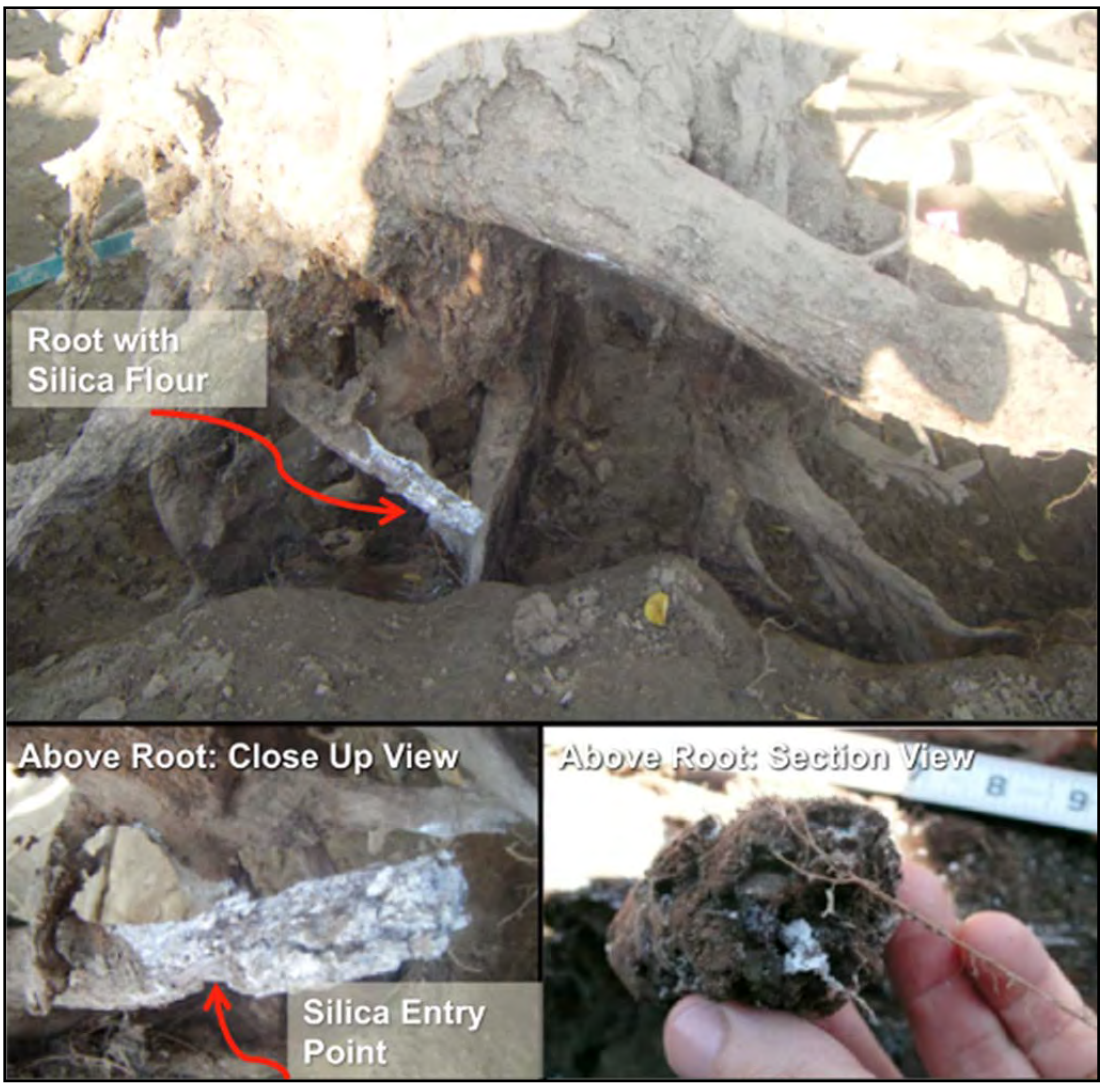

Figure 3-93. View root system of the decomposing stump looking north from the upper trench (top). Note migration of silica flour through a path directly traceable to a location where the installation of a tensiometer penetrated the root.

Figure 3-94. View of the excavated eucalyptus stump looking A) southwest from the former location of the lower trench, B) north from the upper trench, C) south at the roots at base of stump, and D) west from between the upper and lower trenches as Richard Evans, UC Davis, inspects the roots system from the uphill side.

In summary, careful excavation around the decomposing elements of the root system of the eucalyptus stump led to a number of observations as follows:

- Discontinuous annular spaces found within some decomposing roots between bark and woody core.
- Bark that was completely decomposed with an intact woody core.
- Entire roots completely decomposed.
- Void spaces loosely filled with sand.
- No annular spaces or voids observed associated with decomposing root.
- Decomposing roots exhibit small, discontinuous voids and holes throughout, likely a result of biological activity.
- Live roots opportunistically growing around and through decomposing root systems.
- Silica slurry/flour flowed into burrows and voids in roots, but only where a direct hydraulic connection existed with the silica source.
- Stratigraphic layering of soils were found to be essentially horizontal.

3.7.2 Post Flow Test Site Characterization – Analysis of Data

The site excavation phase revealed qualitative data that was used to better understand the state of decomposition of the root system as well as the discernible root architecture. Qualitative data in the section are analyzed to gain insights to stability and seepage implications of a complex, decomposing root system at a snapshot in time.

As previously discussed, the site characterization effort consisted of excavation around the decaying stump in a series of slices/soil segments. Root conditions were photographed and logged at 4 wall faces as shown on Figure 3-72. Detailed logs were created through a collaborative effort of our team with Professor Richard Evans of UC Davis and John Lichter, consulting arborist with Tree Associates. The logs are provided in Appendix F and are examined herein.

The soil 'slices' were placed in the coordinate system developed for the site (Figure 3-95) and radial distances from the stump center were calculated for each of the decomposing roots logged in each slice. The data was merged into a single database and categorized by root size, radial distance from stump, degree of weathering and presence or absence of void spaces creating a potential hydraulic conduit through the root.

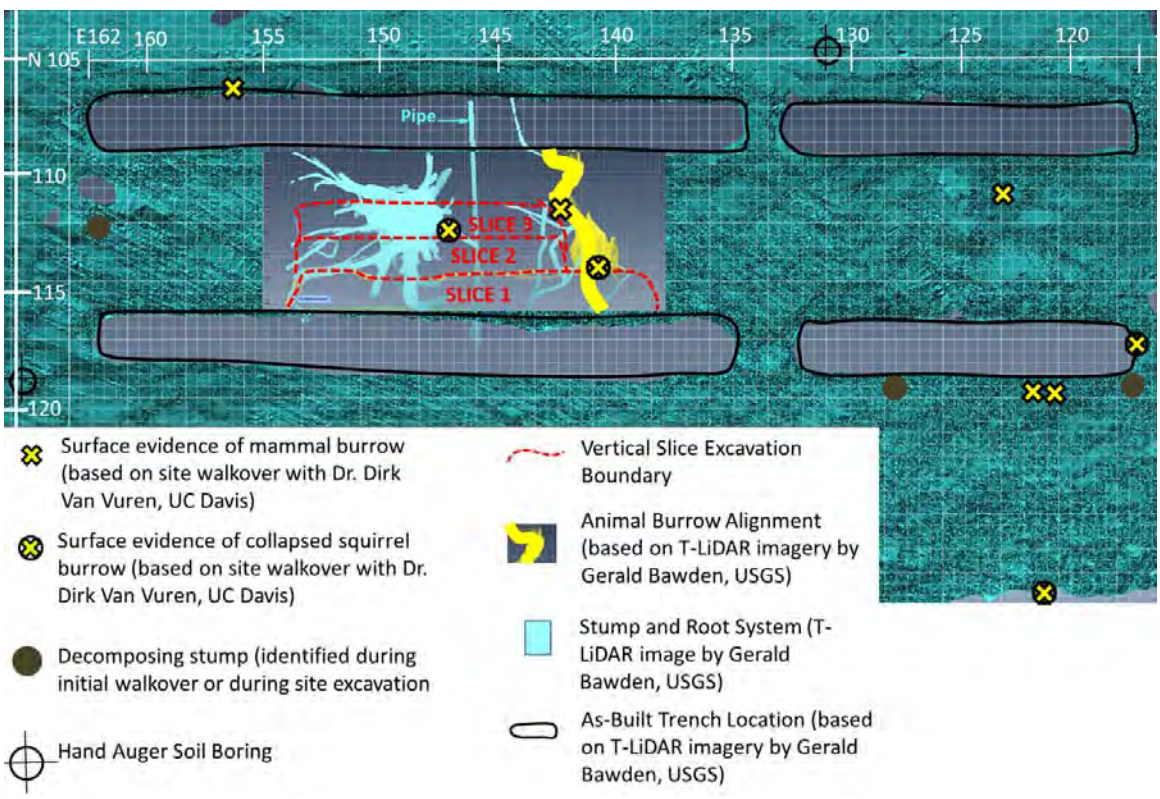

Figure 3-95. As-built site plan showing T-LiDAR scans of root system and burrow (provided by Gerald Bawden, USGS) at Station 138.25.

Annular spaces or voids, as shown on Figure 3-83, were observed in some form in approximately 39% of the roots intersected. This included roots hollowed or cored in sections by biological activity as well as spaces between the woody root center (xylem) and the bark, or the bark and the soil. In general, annular spaces were not noted in roots smaller than 1 inch in diameter. These spaces can be difficult to positively identify for smaller roots. Annular spaces were noted to be absent in 24% of the roots intersected. while for 37% the presence or absence of these spaces was not clear and therefore not noted.

Root size was found to be an important factor in degree of decomposition. An estimated 22% of roots 2 inches in diameter and smaller were described as very or completely decomposed, while 18% of roots in this range were described as 'intact'. In the category of roots larger than 2 inches in diameter, 8% were described as very or completely decomposed while 25% of roots in this range were described as 'intact'. In general, smaller roots displayed a greater degree of weathering than larger ones. These observations are consistent with the findings of Gray and Leiser (1982).

Our final analysis examined total root area with distance from the center stump. Total root area is calculated for each root based on diameter and an assumption that the root is circular. The area of all roots intersected within a given radius is summed and plotted with increasing radius from the stump center. The total intersected area of root as a ratio with total intersected area is a commonly used measure of root density within a soil (Bischetti et al., 2005; Shields and Gray, 1992).

Root area was calculated for all roots within a given radius and the areas were summed and plotted. Roots were then segregated into three size categories:

1. Roots with a diameter larger than 2 inches
2. Roots with a diameter larger than 1 inch
3. Roots with a diameter larger than ½ inch

Figure 3-96 provides a plot of the total root area with distance for each size category. It should be noted that roots smaller than about ¼ inch were not logged. Removal of all roots down to ½ inch in diameter would require excavation of up to twelve (12) feet in diameter around this Eucalyptus stump. Removal to a radius of eight (8) feet is estimated to remove 98% of root matter, while a removal radius of five (5) feet would result in a 92% removal of root matter. These estimates assume an excavation depth of six (6) feet.

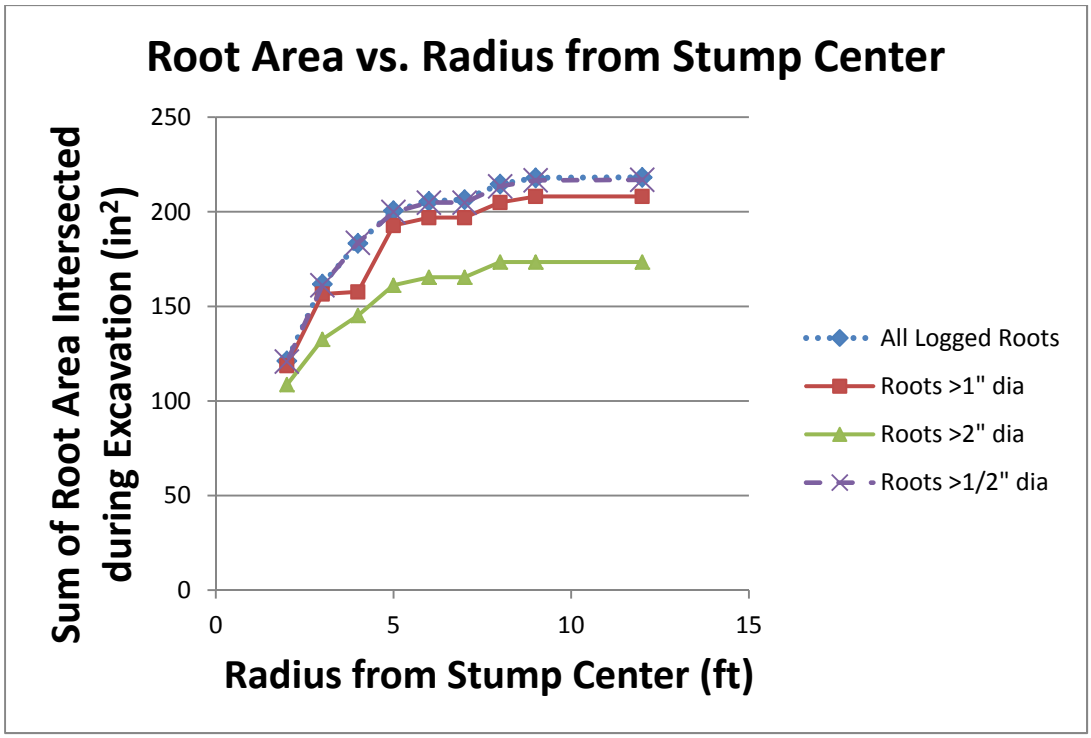

Figure 3-96. The area of each root intersected was calculated and sorted by distance from the stump center. The chart shows the cumulative sum of root area from the center of the stump extending radially outward

In addition to decomposing roots, the flow test site characterization effort documented burrows encountered during excavation. Burrows were counted for each soil segment, or 'slice', excavated and compared to the number of burrows recorded along the uphill wall of the lower control trench. A summary of results is provided as Table 3-6.

Table 3-6. Burrow density at excavated stump and control trenches.

	Station (ft)	Number of Burrows	Wall Area (ft^2)	Burrow Density ($burrows/ft^2$)	Average Burrow Density ($burrows/ft^2$)
Control Trench	117-131.5	6	58	0.10	0.10
Stump Trench, uphill wall of lower trench	138-153	8	60	0.13	0.10
Stump Trench, 'Slice 1'	138-153	5	60	0.08	
Stump Trench, 'Slice 2'	138-153	6	60	0.10	
Stump Trench, 'Slice 3'	143-153	3	40	0.08	

Five burrows were initially identified along the control trench, while an additional burrow appeared during the flow test at Station 117, bringing the total count to 6 burrows in 15 feet stretch as shown on Table 3-6. Based on average burrow

densities, it was concluded that burrowing occurred onsite at a similar rate adjacent to and away from the stump.

3.7.3 T-LiDAR Applied to Flow Test Characterization

T-LiDAR scans were taken to generate a three-dimensional model of the pre-test site condition, excavation walls and flow test site, and throughout excavation efforts to expose the root system. Reflective targets were placed next to roots and burrows (Figure 3-97) and metallic paint was used to highlight the different stratigraphic contacts, thus allowing the T-LiDAR to capture these features given the reflectance contrast between the reflective strips, metallic paint and moist soil (Cobos-Roa et al., 2012).

Figure 3-97 shows a comparison between a T-LiDAR image and a photograph of the site at the same time, following removal of the first segment of soil - 'Slice 1'. Stratigraphic contacts, live and decomposing roots, and reflective targets are visible in the T-LiDAR image. The points gathered can be digitally processed into 3D images of the entire root system. In addition the technology facilitates taking measurements or making calculations that would be difficult to capture using other methods. Data can be managed in a 3D environment in the KeckCAVES at University of California Davis shown on Figure 3-98. Personnel from the USGS-Sacramento Western Remote Sensing and Visualization Center and the UC Davis KeckCAVES were able to use the center's facilities to isolate decomposing roots, burrows, and geologic layers so that they may be viewed separately.

Figure 3-97. Slice 1 comparison between T-LiDAR image (left) and photograph (right). Note reflectors in T-LiDAR image indicating burrows (vertically oriented) and decomposing roots (horizontally oriented). Source: Cobos-Roa et al. 2012.

Figure 3-98. T-LiDAR data is viewed in 3D at the UC Davis KeckCAVES. Point clouds are selected and isolated, separated, relocated, and rotated through this user-friendly 3D interface. Gerald Bawden of the USGS gives the UC Berkeley team a tour. Photos courtesy of Mick Klasson.

Figure 3-99 provides a view of the completed excavation looking south with a corresponding T-LiDAR scan and a view where the live and decomposing root systems, pipe, and burrow are isolated for easier interpretation. Figure 3-100 is useful to visually understand the extent (in plan-view) of the decomposed root system. Fully decomposed roots are not included in this image. Scans were viewed in the KeckCAVE as a means of enhancing field documentation, sketches, and measurements. In Figure 3-101, the root system of the stump is isolated and this plan view image is useful in illustrating the path of silica flow during installation of tensiometers. Figure 3-102 and Figure 3-103 are additional T-LiDAR images generated from different vantage points to illustrate the different geometric characteristics of the root system. The T-LiDAR image in Figure 3-104 shows a view of the stump looking west as compared with a vectorized version of the root system generated from the data.

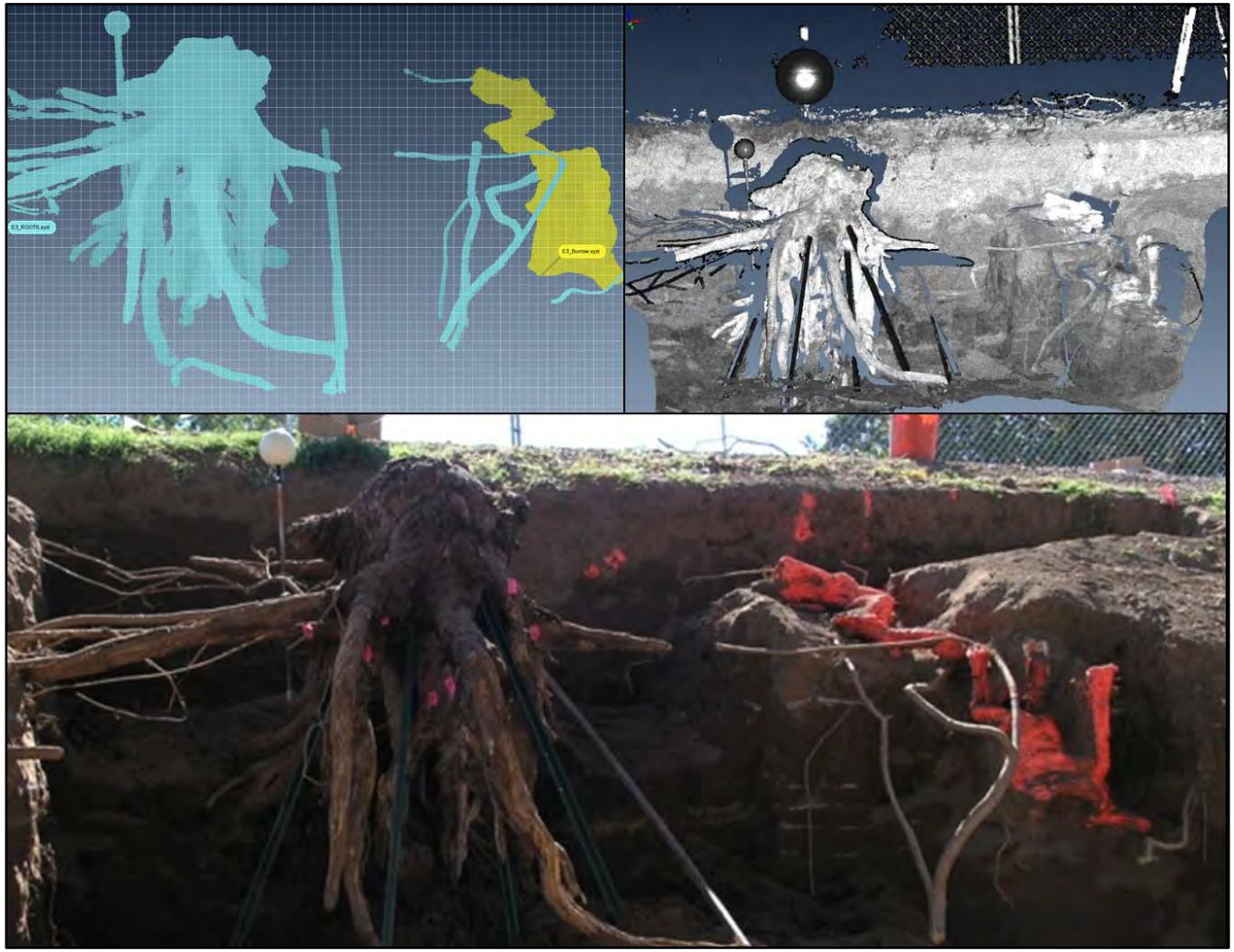

Figure 3-99. T-LiDAR images provided by Gerald Bawden of the USGS (top) looking south compared with photograph of root system (bottom) and burrow at Station 138.25.

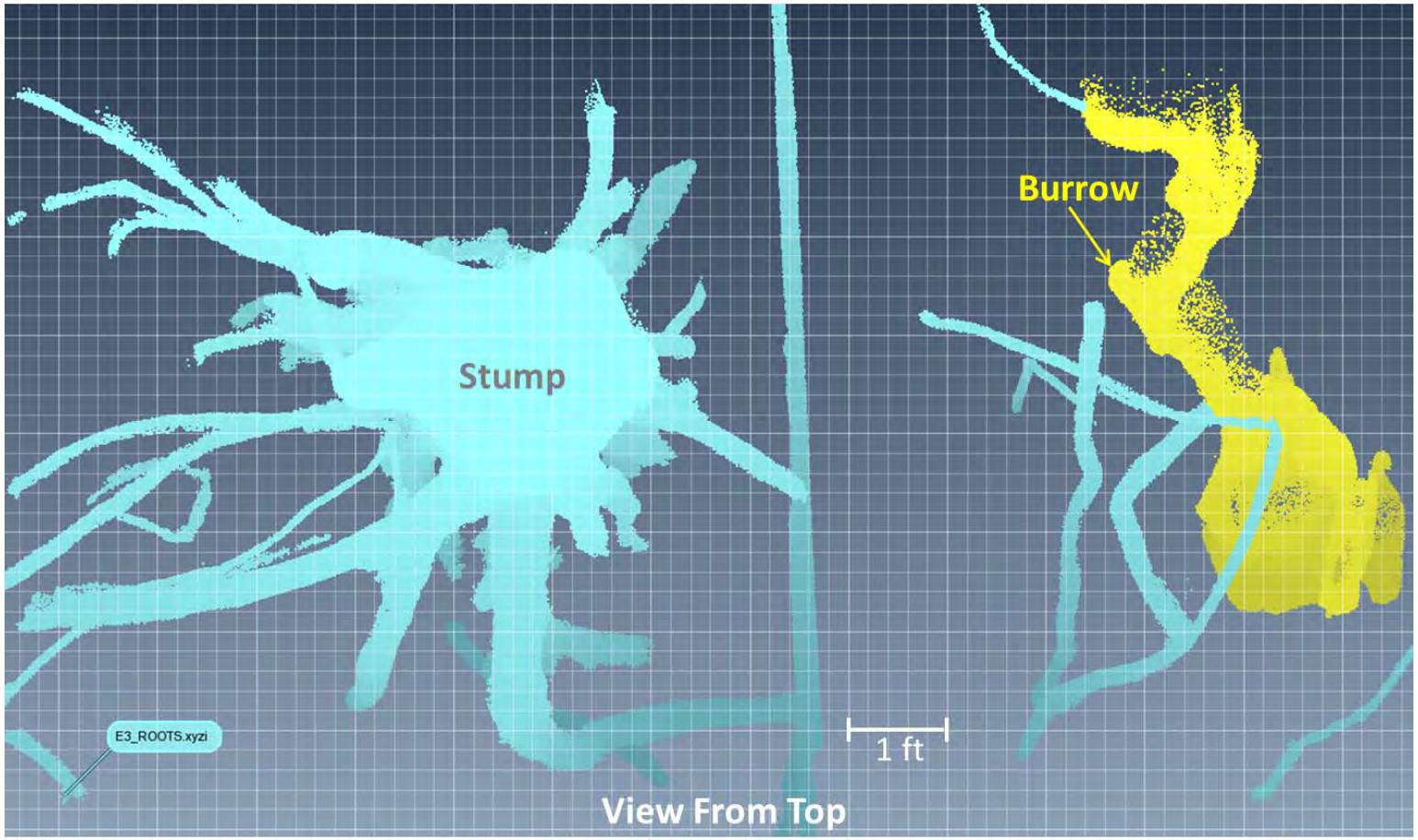

Figure 3-100. T-LiDAR scan of root system and burrow at Station 138.25 (provided by Gerald Bawden of the USGS). View is from the top. Most roots are decomposing roots related to the eucalyptus stump, but live roots are present, particularly in the vicinity of the burrow.

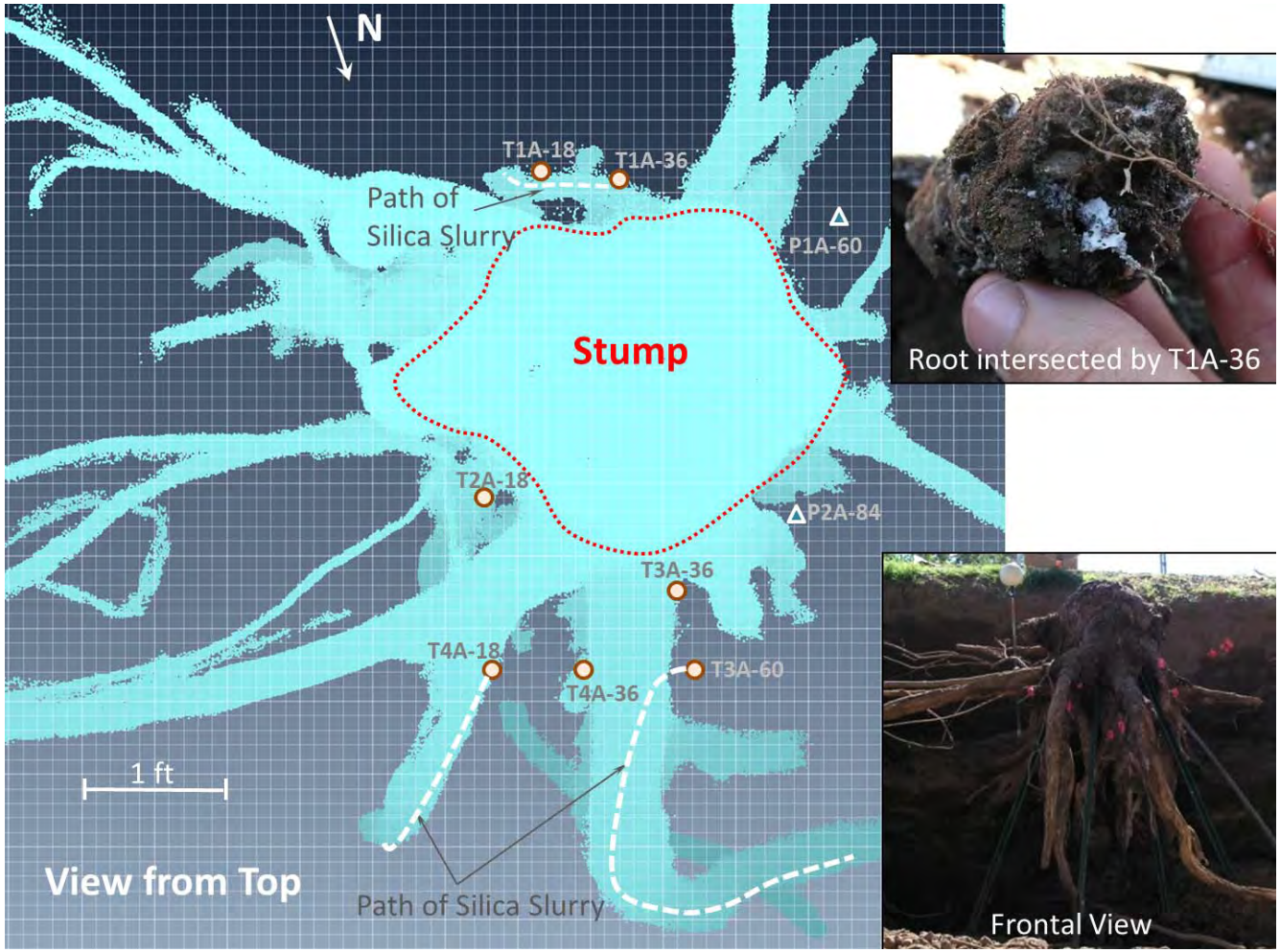

Figure 3-101. View of the decomposing eucalyptus root system from above as scanned with T-LiDAR. The image is used here to show the path of silica flow from the tensiometers and instrument positions within the root system. Photographs show silica flow through the root intersecting with tensiometer T1A-36 (upper right) and a south-facing frontal view of the stump and root system. T-LiDAR image courtesy of Gerald Bawden of the USGS.

Figure 3-102. A south-facing view of eucalyptus stump and root system (right) and the corresponding point cloud image (left) derived from combining data from a series of T-LiDAR scans. T-LiDAR image courtesy of Gerald Bawden of the USGS.

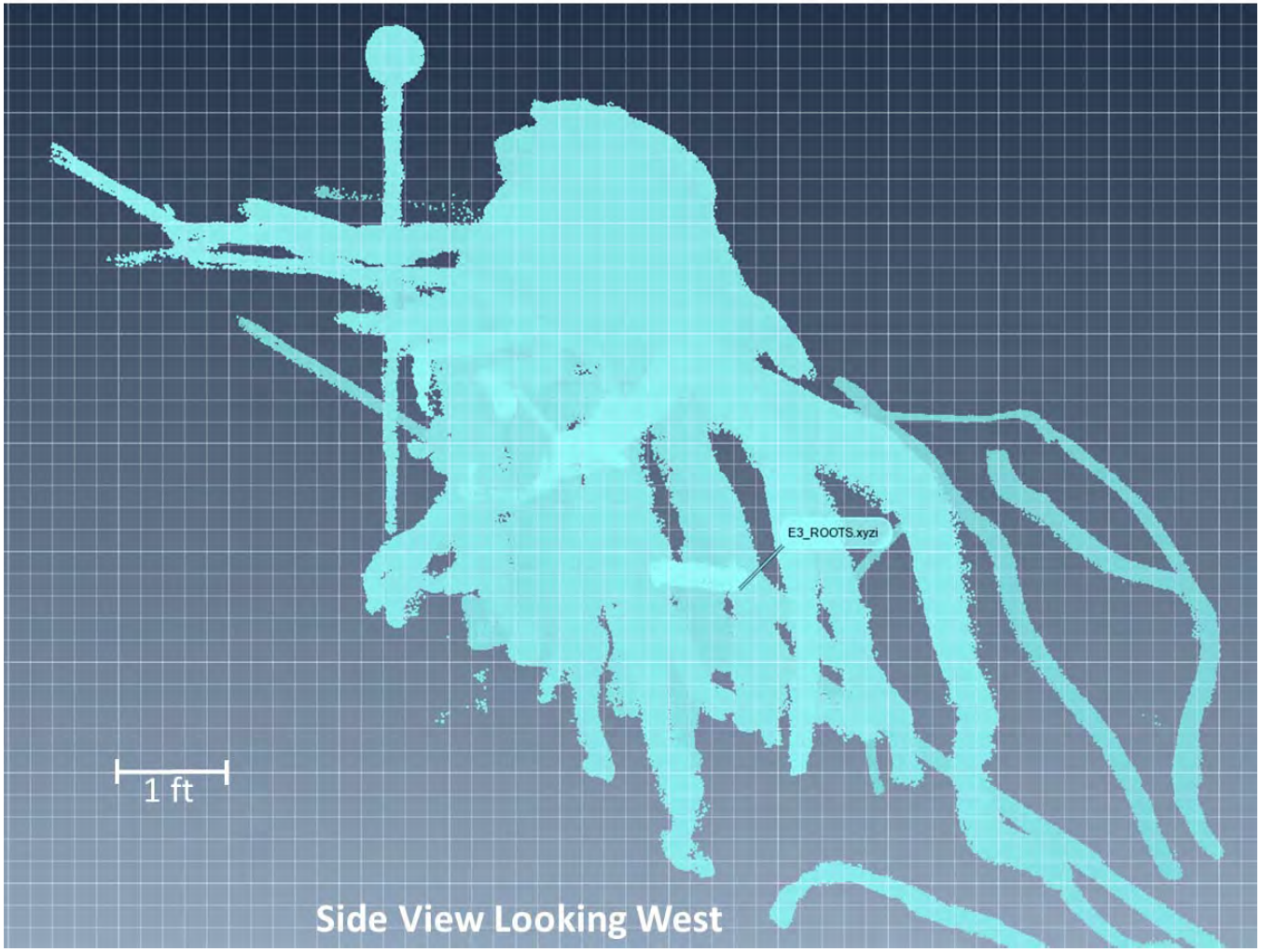

Figure 3-103. A west-facing view of the Eucalyptus stump and root system stitched together from a series of T-LiDAR scans (provided by Gerald Bawden, USGS).

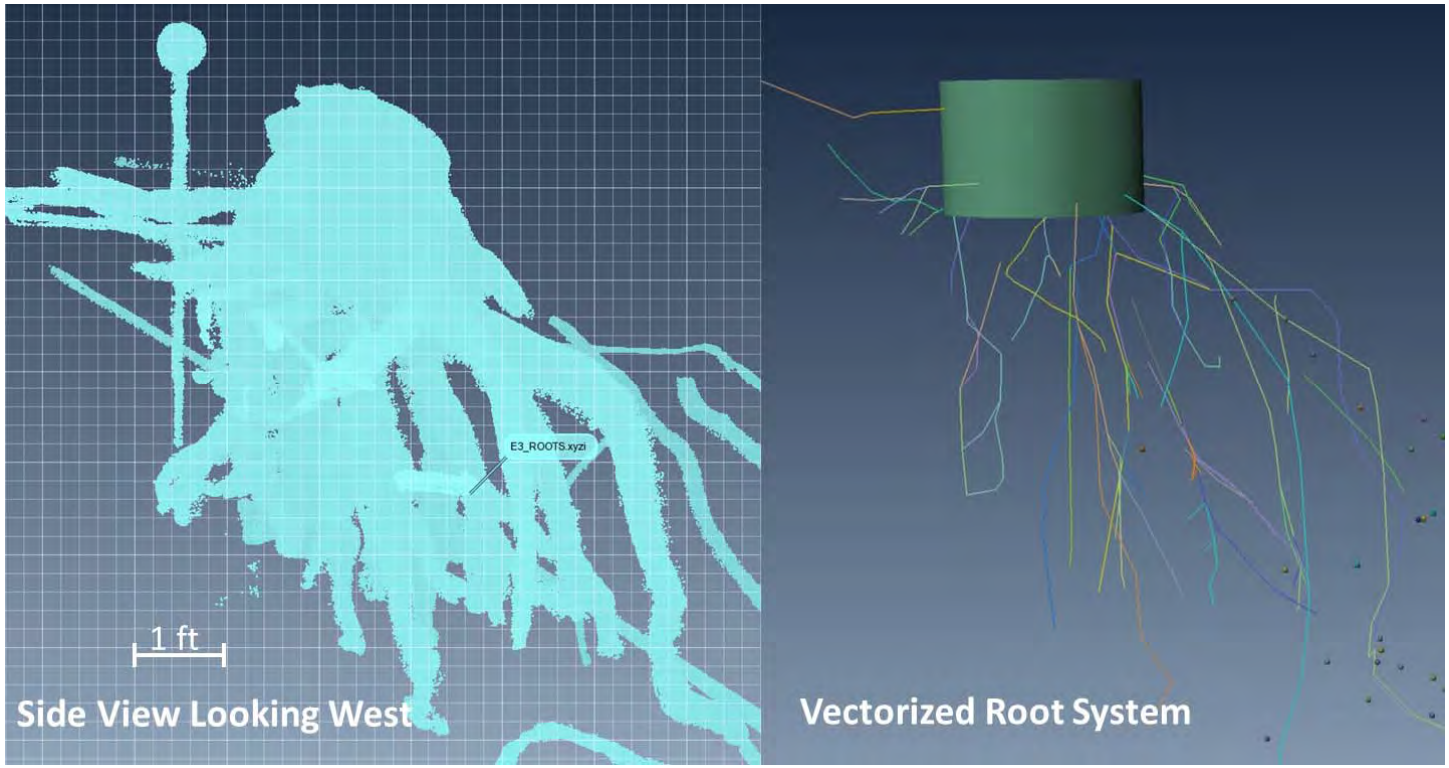

Figure 3-104. A view of the Eucalyptus root system as a point cloud generated from T-LiDAR scans (left) and a vectorized plot of the root system to aid in modeling efforts. Base source: Gerald Bawden, USGS.

4 DISCUSSION OF FINDINGS

The parallel trench wetting front test subjected the levee site to an imposed flow of water over a period of 6 days during which time positive and negative pore pressures were monitored within the study area. As noted, the test site was generally composed of silty soils and the test was focused around a decomposing eucalyptus stump and root system. The tree was cut sometime between 1994 and 1998 and the stump left decomposing for 12 to 16 years prior to the field test. Decomposing roots, excavated following the flow test, displayed varying degrees of decomposition with voids or annular spaces in 39 percent of roots intersected by the excavation. Annular spaces were continuous over short distances, and many were partially or loosely filled with organic matter. Some roots had voids partially filled with organic matter and soil. Live roots growing from a hackberry tree located at the toe of the levee, mammal burrows, ant and worm holes, and a water pipeline added complexity to the system and the study. Small live roots were observed to be concentrated in the voids around and within decomposing roots. The field test benefited from the complexity of this site as these diverse conditions represent the reality of a levee system.

Tensiometer installation revealed the sealant materials (a silica slurry) could flow through a gap between the bark and woody core of a decomposing root at the lower trench wall face downhill from the stump. Silica slurry was found in several other roots as well as in loose soil pockets and cracks, but only where the tensiometer hole made a direct hydraulic connection with the void space.

Beven and Germann (1982) assert that for a macropore to flow, the supply of water must be in excess of the lateral losses to the surrounding matrix and the macropore must be sufficiently connective to transport the water downslope. Absent a direct hydraulic connection, pore suction would prevent flow from smaller pores into larger macropores or voids. However, eventual saturation of smaller pores allows flow into larger pores as pore suction is eliminated and pore pressure is generated, driving flows. As full saturation is achieved in the surrounding matrix, however, lateral losses are increased and supply must keep pace for flow to continue. Further, continuity of void space is also necessary for flow. We observed that where voids are shallow, seeps can form at the slope surface. Burrow networks, including gopher burrows (which are often partially backfilled as gophers excavate new tunnels) were found to be sufficiently continuous to flow once water enters the macropore/burrow. In this case, water entered the macropore through a direct hydraulic connection to the water source. During the flow test, these influences dominated flow and wetting patterns.

The presence of two gopher burrow greatly impacted flow patterns during the test and both were hydraulically connected to the water source. Initially, the burrow at

instrument Line C resulted in observed seeps at the levee slope face. For a window of about 12 hours, water supply was sufficient and the burrow was sufficiently connective to allow for slow flows emerging through the upper wall of the lower control trench at Station 117. After that time, flow stopped, possibly due to collapse of the hole or saturation patterns causing the lateral losses of water through the walls of the burrow to exceed inflow. Similarly, rapid flow was initially observed through the gopher burrow at Station 138.25. Flow eventually slowed, then stopped. Though burrows dominated flow patterns and brought seepage to the slope surface, preferential flow through macropores diminished with time and with saturation of the surrounding soil matrix. Flow eventually stopped in the burrows.

The two (2) ground squirrel burrows encountered did not exhibit a direct hydraulic connection with the water source (the upper control trench). Flow can, however, concentrate into a macropore but is limited by the rate of water delivery from surrounding soils. At approximately 125 hours into the flow test, a small amount of water was seen seeping from the ground squirrel burrow at Station 121.5 of the lower control trench.

To illustrate these concepts of flow in unsaturated soils, a series of conceptual simulations were performed. Void spaces were modeled within the finite element mesh. When voids were connected to the upper trench, the same hydraulic heads applied along the surface of the trench were applied to the boundary nodes, to simulate the direct connection between these openings and the water filling the trench. Figure 4-1 shows 5 simulations representing: A) No void; B) Void connected to source trench only; C) Void connected to source trench and lower trench; D) Void connected to neither source nor lower trench; and E) Void connected only to lower trench.

Simulations B and C illustrate modified flow patterns due to their direct connection to a hydraulic source. The gopher burrow at Station 138.25 that flowed over 19,000 gallons of water over 6 days is most similar to Simulation C. Simulation B most closely represents our observations of the gopher burrow extending from instrument Line C toward the western corner of the control trench. It did not make a direct connection to the lower trench, except for a brief window (10 to 22 hours into the flow test) as discussed in Table 3-4, and was found to be plugged along its length (i.e., upon grouting we observed that grout did not reach the lower trench). In this case, wetting patterns on the slope were altered but free flow was not observed. In Simulations D and E, large pore suction prevents filling of the void spaces until saturation is achieved and suction values have dropped. Consistent with Simulations D and E, mammal burrows (a combination of gopher and ground squirrel) that did not form a connection with the upper trench were found to be relatively unaffected by flow and wetting patterns until saturation was achieved. As observed with the ground squirrel burrow at Station 121.5, eventually, the wetting front reached the hole and water began to concentrate within the burrow, limited by the flow delivered by the permeability of surrounding soils. Exit gradients and soil erodibility must be evaluated in these cases to determine the impact on levee integrity. In the

studied case, soils were sufficiently fine-grained and observed seepage upon saturation of the levee did not impact levee performance.

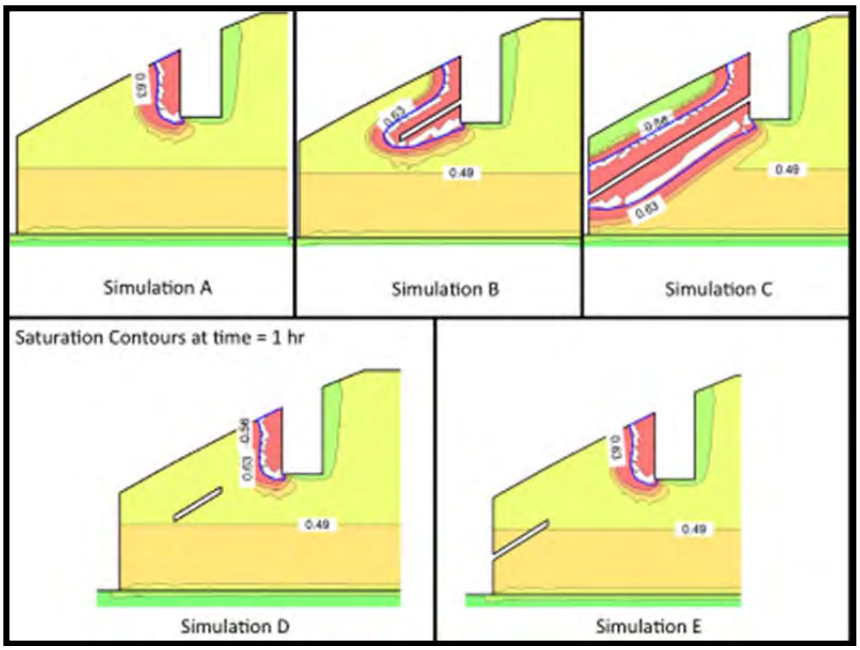

Figure 4-1. Simple conceptual models illustrating volumetric water content from initial state (yellow) to saturation (red). The predicted effects of various void spaces on saturation patterns as modeled using the software package SeepW.

Similarly, excavation of the root system revealed intermittent annular spaces or voids in about 39 percent of decomposing roots intersected during the site characterization effort. These voids were found to be discontinuous, at times loosely filled with decomposed bark or sand, or simply not present in segments of the root. Flow was not observed through these known voids during the flow test, though flow of silica slurry was observed when a direct hydraulic connection was made by intersection of a root with a tensiometer installation. The 6 day flow test, however, did not result in visible flow through the voids. A direct hydraulic connection did not exist between the upper and lower trenches and the system of voids associated with the decomposing root system lacked sufficient inflow of water and continuity of void spaces to flow water. The soil segment between the stump and the uphill wall face of the lower trench was the last to saturate, despite the presence of voids associated with decaying roots in that segment.

5 RESULTS IN THE CONTEXT OF PREVIOUS STUDIES

A better understanding of our findings can be gained by viewing our results in the context of similar studies. In 1971, Aubertin performed field and laboratory scale seepage testing on forest soils within Tuscarawas County, Ohio. Trees primarily consisted of white oak, beach, and hickory. Field scale testing occurred at two sites -

a sandy loam and silt loam site – where simulated rainfall was introduced to an undisturbed soil surface just above an observation pit. Water was observed to flow through many root channels (the term 'channels' was used to describe macropores remaining following the decomposition of roots) and burrows, though the author noted soils immediately around the root channels were very low permeability, proposing a theory that vertical macropores (possibly from earthworms) may have influence the introduction of water into macropores associated with root channels or burrows. Macropores observed by Aubertin (1971) were primarily shallow with the number and diameter of open channels decreasing at depths greater than 12 inches. Mitchell et al. (1995), discusses how, in expansive soil conditions, smaller macropores such as those associated with earthworms tended to close as soils swelled under saturation. Beven and Germann (1982) suggest that undisturbed forest environments are more conducive to the preservation of macropores than sites experiencing more intensive land use. According to Whipkey (1965), leaf litter covers the forest surface and acts to maintain permeability in forest soils.

Aubertin (1971) observed lower flow through channels in a sandy loam site as compared to a silt loam and found that 'channels' tended to fill with soils at the sandy loam site. Similarly, an abundance of root channels were discovered in a coarse textured test site studied by Gaiser (1952), though most were found to be loosely filled with soil. Beven and Germann (1982) conclude that channels tend to persist in soils with clay contents greater than 30 percent, but could be destroyed by the in-washing from one large rainstorm. Similarly, in an agricultural context, Green and Askew (1965) found that macroporosity had a significant influence on hydraulic conductivity where soils had clay content greater than 40 percent. Our study consisted of lean clays, various silts, and silty sands where annular spaces around some decomposing roots were discontinuous and loosely filled with sands while others were not filled.

Beven and Germann (1982) assert that the volume of water entering the pore must exceed the volume lost laterally for flow to occur. In a study by De Vries and Chow (1978), disturbance of a surface layer, where macropores were initially open to the atmosphere, resulted in a shift of flow to the soil matrix over the macropores. Similarly, Beasley (1976) found that for channels to flow, the channel needed to be open to the environment and offer a depression as a means for water to gather and be channeled into the macropore. Aubertin (1971) demonstrated, through dye testing, the need for a direct hydraulic connection to a water source for through flow and for advancement of a wetting front through a pore. Channels without a direct hydraulic connection did not flow as indicated by an absence of dye. Similarly, our field study found that a direct hydraulic connection to a water source facilitated advancement of the wetting front through a network of gopher burrows.

Barley (1954) asserts that roots decrease permeability of the soils around roots by compacting them as they grow. According to Aubertin (1971), this compaction can result in a decreased permeability of soils directly around root channels. Barley (1954) also found that decaying roots can increase overall soil permeability but this

depends on which of the opposing processes of growth and decay tend to dominate based on seasons and conditions. Where live roots continue to grow, studies have shown that these roots tend to grow preferentially within the organic matter and void spaces of decomposing roots, often filling those voids (Parker and Van Lear, 1995; McKee, 2001). Similarly, live roots of a nearby hackberry tree were observed growing preferentially within the decaying root system of the eucalyptus stump that was excavated.

The fraction of water flowing through a macropore network is expected to be reduced as the soils surrounding the macropore become saturated and later losses to the soil matrix are increased (Beven and Germann, 1982). This behavior was observed in our study as flow rates decreased with time and burrow flow either slowed or stopped as the soil matrix approached saturation.

6 CONCLUSIONS

A network of macropores created by mammal burrowing activity dominated early wetting front and flow patterns at the research site. Macropores require inflows into a pore that exceed lateral losses through the walls of the pore for flow to occur. In this study, a direct connection to a water source was needed in unsaturated conditions, and where this direct connection was continuous into the observation trench, rapid initial flow was observed, diminishing in volume with saturation of the matrix soils. For surficial seeps, gravel bags were effective as a means of initially controlling rapid flows, backing water up in the burrow until increased saturation of matrix soils allowed for increased lateral loss of water to the matrix soils and therefore reduced concentrated flows through burrow networks. Decaying roots created sufficiently continuous channels for the flow of a silica slurry (used in instrument installation) over short distances when the instrument hole intersected the void and created a direct hydraulic connection. These same roots were not sufficiently continuous to flow water from the upper trench to the lower trench through the levee soils. The presence of the stump impeded the rate of the wetting of the soil in the zone of decomposing roots. These concepts will be further explored in the summary of our centerline trench wetting front and seepage test (Volume 3) and in the context of 2D and 3D seepage modeling presented in Volume 5.

REFERENCES

Association of State Dam Safety Officials (ASDSO) (2002) A Technical Manual on the Effects of Tree and Woody Vegetation Root Penetrations on the Safety of Earthen Dams, December 2002.

Aubertin, G. M. (1971). *Nature and extent of macropores in forest soils and their influence on subsurface water movement* (Vol. 192). Northeastern Forest Experiment Station.

Barley, K. P. (1962). The effects of mechanical stress on the growth of roots. *Journal of Experimental Botany*, *13*(1), 95-110.

Beasley, R. S. (1976). Contribution of subsurface flow from the upper slopes of forested watersheds to channel flow. *Soil Science Society of America Journal*, *40*(6), 955-957.

Beven, K., & Germann, P. (1982). Macropores and water flow in soils. *Water resources research*, *18*(5), 1311-1325.

Bischetti, G. B., Chiaradia, E. A., Simonato, T., Speziali, B., Vitali, B., Vullo, P., & Zocco, A. (2005). Root strength and root area ratio of forest species in Lombardy (Northern Italy). *Plant and soil*, *278*(1-2), 11-22.

Burroughs, E. R., & Thomas, B. R. (1977). *Declining root strength in Douglas-fir after felling as a factor in slope stability*. Intermountain Forest and Range Experiment Station, Forest Service, US Department of Agriculture.

Cobos-Roa, D., Shriro, M., Sitar, N., Bray, J., Bawden, G., Lichter, J. and Evans, R. (2012). "3-D Stratigraphy and Root Geometry from Trench and Ground-Based LiDAR Mapping", paper presented at *GeoCongress: the State of the Art and Practice in Geotechnical Engineering*, Oakland, CA, 25-29 March. New York, NY: Currin Associates, Inc., pp. 3031-3040.

Cobos-Roa, D. (2013, in press). *The Role of Transient Conditions on Levee Performance*. Ph.D.. University of California, Berkeley.

Corcoran, M. K., Gray, D. H., Biedenharn, D. S., Little, C. D., Leech, J. R., Pinkard, F., ... & Lee, L. T. (2010). *Literature Review-Vegetation on Levees* (No. ERDC-SR-10-2). Engineer Research and Development Center Vicksburg MS Geotechnical and Structures Lab.

De Vries, J., & Chow, T. L. (1978). Hydrologic behavior of a forested mountain soil in coastal British Columbia. *Water Resources Research*, *14*(5), 935-942.

Federal Emergency Management Agency (FEMA) (2005) Technical Manual for Dam Owners, Impacts of Plants on Earthen Dams, FEMA 534, Sept 2005.

Gaiser, R. N. (1952). Root channels and roots in forest soils. *Soil Science Society of America Journal*, *16*(1), 62-65.

Gray, D. H., & Sotir, R. B. (1996). *Biotechnical and soil bioengineering slope stabilization: a practical guide for erosion control*. Wiley-Interscience.

Gray, D. H., & Leiser, A. T. (1982). *Biotechnical slope protection and erosion control*. Van Nostrand Reinhold Company Inc.

Gray, D., et al. (1991). *The Effects of Vegetation on the Structural Integrity of Sandy Levees (Technical Report REMR-EI-5)*. Repair, Evaluation, Maintenance, and Rehabilitation Research Program. [report] Vicksburg, Mississippi: United States Army Corps of Engineers Waterways Experiment Station.

Green, R. D., & Askew, G. P. (1965). Observations on the biological development of macropores in soils of Romney Marsh. *Journal of Soil Science*, *16*(2), 342-344.

Harder, Jr., Leslie F.; Kroll, Roy, Claassen, Vic; Buck, Peter E. F.; and Berry, Alison M. (2010), *"Investigation of tree Root Penetration into a Levee Soil-Cement-Bentonite Slurry cutoff Wall,"* Proceedings of the Annual Conference of the Association of State Dam Safety Officials, Seattle, Washington, September 19-23, 2010.

Lawrence Halprin and Associates (1967). *Planting Plan*. General Area Landscape Architecture, Levee Area 11, 12, 13, 14. [report] Sacramento, CA: California Exposition and State Fair, Sheet L-45.

McKee, K. L. (2001). Root proliferation in decaying roots and old root channels: a nutrient conservation mechanism in oligotrophic mangrove forests. *Journal of Ecology*, *89*(5), 876-887.

Mckenna, G. (1995). Grouted-in Installation of Piezometers in Boreholes. *Geotechnical Journal 32*, pp.355-363.

Mikkelsen, P. (2002). Cement-Bentonite Grout Backfill for Borehole Instruments. *Geotechnical News*, Iss. December 2002.

Mikkelsen, P., and Green, E. (2003). "Piezometers in Fully-Grouted Boreholes", paper presented at *International Symposium on Geomechanics*, Oslo, Norway, September.

Mitchell, A. R., Ellsworth, T. R., & Meek, B. D. (1995). Effect of root systems on preferential flow in swelling soil. *Communications in Soil Science & Plant Analysis*, *26*(15-16), 2655-2666.

Parker, M. M., & Van Lear, D. H. (1996). Soil heterogeneity and root distribution of mature loblolly pine stands in piedmont soils. *Soil Science Society of America Journal*, *60*(6), 1920-1925.

Pierson, T. C. (1983). Soil pipes and slope stability. *Quarterly Journal of Engineering Geology and Hydrogeology*, *16*(1), 1-11.

Punyamurthula, S., and Millet, R. (2012). "Forensics and Performance of California Levees with Vegetation", paper presented at *Levee Vegetation Research Symposium 2012*, Sacramento, CA, August 28-30. Sacramento: California Levee Vegetation Research Program.

Reichman, O., Whitham, T., and G. A. Ruffner (1982). Adaptive geometry of burrow spacing in two pocket gopher populations. *Ecology*, 63 pp.687-695.

Reichman, O. J., & Smith, S. C. (1990). Burrows and burrowing behavior by mammals. *Current mammalogy*, *2*, 197-244.

Reid, M. E. (1997). Slope instability caused by small variations in hydraulic conductivity. *Journal of Geotechnical and Geoenvironmental Engineering*, *123*(8), 717-725.

Shields, F. D., & Gray, D. H. (1992). Effects of Woody Vegetation on Sandy Levee Integrity. *JAWRA Journal of the American Water Resources Association*, *28*(5), 917-931.

Shriro, M. (2013, in press). *California Earthen Levee Stability Considerations*. Ph.D.. University of California, Berkeley.

Shriro, M. Cobos-Roa, D. Bray, J., Sitar, N. Lichter, J. Evans, R. Kroll, R. (2011)." Study of Levee Seepage and Slope Stability in Relation to Roots". *Association of State Dam Safety Official 2011 Conference Papers*.

United States Army Corps of Engineers (USACE), Sacramento District (1956). *Design Memorandum No.1, American River Levee General Design*. American River Project. Sacramento, CA.

United States Army Corps of Engineers (USACE), Sacramento District (1999). *American River Watershed Project (Common Features), Right (North) Bank Levee Strengthening*. American River, California.

United States Army Corps of Engineers (USACE) (2007), "*Treatment of Vegetation within Local Flood-Damage-Reduction Systems*," Draft Final White Paper, April 20, 2007.

United States Army Corps of Engineers (USACE) (2009). *Guidelines for Landscape Planting and Vegetation Management at Levees, Floodwalls, Embankment Dams, and Appurtenant Structures, ETL 1110-2-571*.

URS (2009). *General Reevaluation Report*. American River Common Features . Sacramento County, California: U.S. Army Corps of Engineers Sacramento District, Contract Number W91238-08-D-0001, Delivery Order CM04.

California Department of Water Resources (DWR) (2013). *Levee Repair - History of Levees*. [online] Retrieved from: http://www.water.ca.gov/levees/history/ [Accessed: 12 May 2013].

Van Vuren, D., and Ordeñana, M. (2012). *Burrow Dimensions of Ground Squirrels, with Special Reference to the California Ground Squirrel* . [report] California Levee Vegetation Research Program.

Ziemer, R. R. (1981). Roots and the stability of forested slopes. *Erosion and Sediment Transport in Pacific Rim Steeplands, IAHS Publ*, (132).

APPENDIX A: SOIL BORINGS AND INSTRUMENTATION LOGS

Appendix A

Prior to site selection, available soil boring logs and geotechnical information were reviewed (see Appendix C) and two hand-auger soil borings to a depth of 9 feet were performed at the locations shown on Figure A-1. The logs are presented as Figures A-2 and A-3.

During installation of piezometers and tensiometers at the site, instrument holes were logged. Logs are presented on pages A-5 through A-10. Instruments P4B-84 and T4A-18 are shown on Figure A-1 and soil logs are provided for these locations, though the instruments failed to function in the field and are therefore not shown on other figures or data sheets.

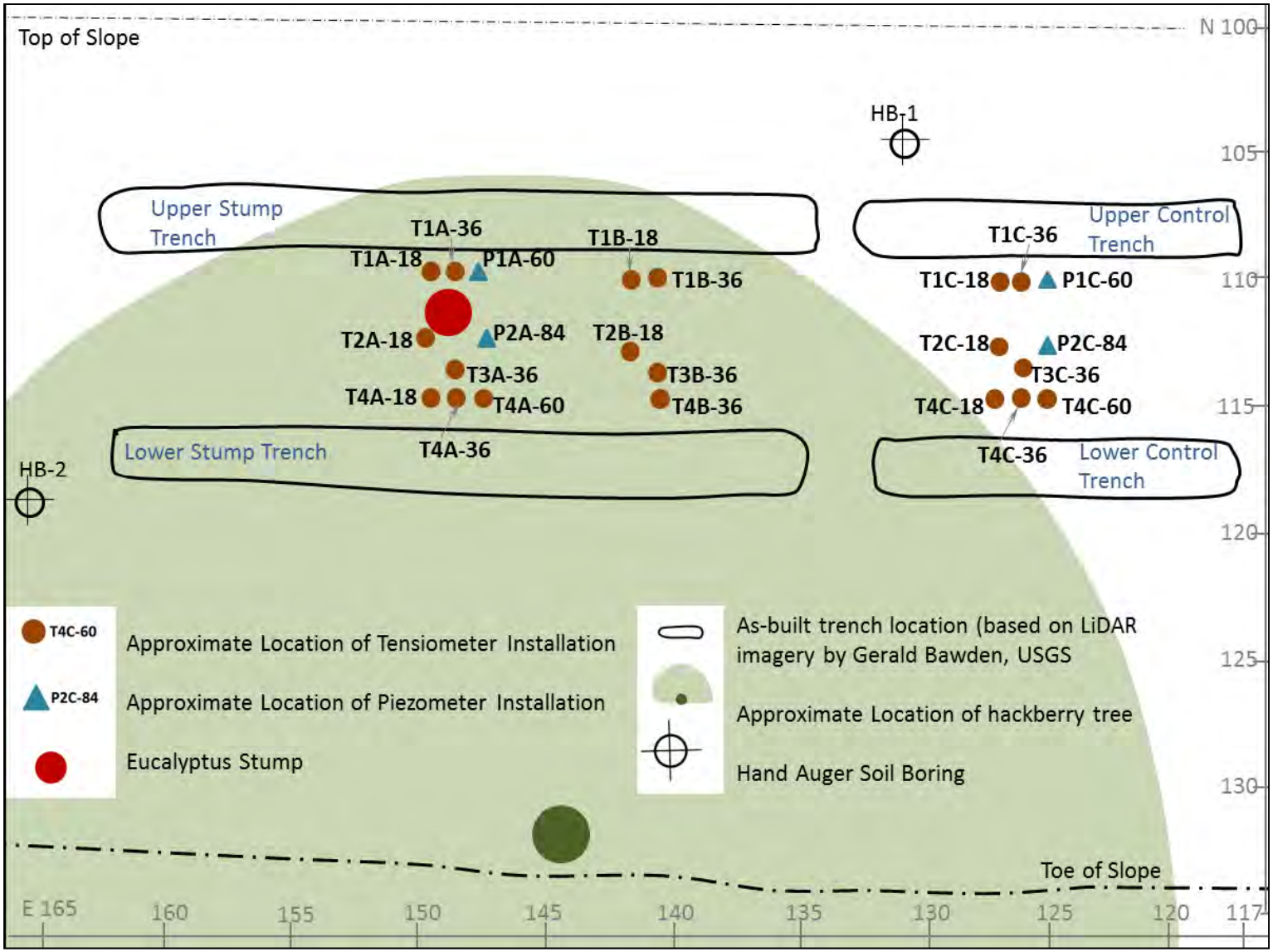

Figure A-1. Site plan showing locations of hand auger soil borings and logged instrument holes

BORING LOCATION: N38.58953, W121.43249	**PROJECT NUMBER** SAFCA-CALEXPO	**BORING NUMBER** EX-HB1	6/24/2010
		SHEET 1 **OF** 2	

SOIL BORING LOG

PROJECT	Cal Expo Field Investigation	**DRILLED BY**	J. Hollenback
ELEVATION	Levee Crest	**LOGGED BY**	M. Shriro
DRILLING METHOD AND EQUIPMENT	Hand Auger (4" Dia)	**REVIEWED BY**	D.Cobos-Roa
WATER LEVELS	n/a	**START** 8:30am	**FINISH** 10:00am

STANDARD PENETRATION TEST RESULTS 6-6-6" (N)	SAMPLE Number	SAMPLE BAG SAMPLE Depth	SAMPLE RECOVERY	LITHOLOGY	DEPTH BELOW SURFACE (ft)	SOIL DESCRIPTION (SOIL NAME, USCS GROUP SYMBOL, COLOR, MOISTURE CONTENT, RELATIVE DENSITY OR CONSISTENCY, SOIL STRUCTURE, MINERALOGY)	COMMENTS (DEPTH OF CASING, DRILLING RATE, DRILLING FLUID LOSS, TESTS AND INSTRUMENTATION, ETC...)
					0.0	Clayey Silt (ML), brown, moist, stiff, fine sand (FILL)	
		1/2' - 1'			0.5		
					1.0		
					1.5		increased clay content at 1.5'
					2.0		
					2.5		
		3 1/4' - 3 1/2'			3.0		
					3.5	Silt (ML), brown with trace clay and fine sand (FILL)	
					4.0		
		4 1/2' - 5'			4.5		increased clay content at 4.5'
					5.0		
					5.5		
					6.0		
		6 1/2' - 6 3/4'			6.5		
					7.0	Silty Fine Sand (SM),brown, moist with trace rootlets thinly interbedded with SILT (ML), brown mottled with yellow brown, with clay and fine sand (FILL)	fine roots at 6 3/4 feet below grade
		7 1/2 - 7 3/4			7.5		
					8.0		
		8 1/4' -8 1/2'			8.5		
					9.0	Bottom of Boring at 9 feet; No Groundwater Encountered	

Notes:
FP - 5-inch Fixed Piston Sampler
VS - Field Vane Shear Test
BS - Bag Sample
Soil type transition
Water Table (not encountered during drilling)

Figure A-2. Boring log for hand-auger boring 1 (HB1). For location, see Figure A-1.

BORING LOCATION: N38.58959, W121.43233	PROJECT NUMBER SAFCA-CALEXPO	BORING NUMBER EX-HB2	6/24/2010
		SHEET 2 OF 2	

SOIL BORING LOG

PROJECT	Cal Expo Field Investigation	DRILLED BY	J. Hollenback
ELEVATION	~10feet down from crest	LOGGED BY	M. Shriro
DRILLING METHOD AND EQUIPMENT	Hand Auger (4" Dia)	REVIEWED BY	D.Cobos-Roa
WATER LEVELS	n/a	START 9:00am	FINISH 12:00pm

STANDARD PENETRATION TEST RESULTS 6-6-6" (N)	SAMPLE Number	SAMPLE BAG SAMPLE Depth	SAMPLE RECOVERY	LITHOLOGY	DEPTH BELOW SURFACE (ft)	SOIL DESCRIPTION: SOIL NAME, USCS GROUP SYMBOL, COLOR, MOISTURE CONTENT, RELATIVE DENSITY OR CONSISTENCY, SOIL STRUCTURE, MINERALOGY	COMMENTS: DEPTH OF CASING, DRILLING RATE, DRILLING FLUID LOSS, TESTS AND INSTRUMENTATION, ETC...
					0.0	Silt (ML), brown with trace clay and fine sand (FILL)	
					0.5		
		1' - 1 1/2'			1.0		
		1 1/2' - 1 3/4'			1.5		
		2' - 2 1/2'			2.0	CLAYEY SILT (ML), olive brown, moist, trace fine sand, trace fine rootlets, increased soil structure (FILL)	
		2 1/2' - 2 3/4'			2.5		
					3.0	SANDY SILT (ML) gradually grading to Silty Sand (SP), moist, olive brown, very fine sand, trace fine rootlets (FILL)	
		3 1/2' - 3 3/4'			3.5		
					4.0		
		4 3/4' - 5 1/4'			4.5		
					5.0		
					5.5		
		6' - 6 1/2'			6.0		
					6.5		
					7.0	SAND (SP), yellow brown, moist, sand is clean and fine grained	
		7 1/4' - 7 1/2'			7.5		
					8.0		
		8 1/4' -8 1/2'			8.5	SILTY CLAY (CL), olive brown, moist	
					9.0	Bottom of Boring at 9 feet; No Groundwater Encountered	

Notes:
FP - 5-inch Fixed Piston Sampler
VS - Field Vane Shear Test
BS - Bag Sample
Soil type transition
Water Table (not encountered during drilling)

Figure A-3. Boring log for hand-auger boring 2 (HB2). For location, see Figure A-1.

Instrument Logs

T1A-18; Coordinates = (150.3, 111)

0 – 19.5” Sandy Silt (ML) to silty sand (SM), trace clay, brown, moist. Decomposed root at 10”.

Bottom of hole at 19.5”

T1A-36; Coordinates = (148.5, 111)

0 – 12” Sandy Silt (ML) to silty sand (SM), brown, moist.

12”-37.5” Clayey silt (ML), brown, moist.

Bottom of hole at 37.5”

P1A-60; Coordinates = (147, 111)

0 – 14” Silty sand (SM) to sandy silt (ML), trace clay, brown, moist, live roots between 6”-12”.

14”-19” Sandy silt (ML) with clay, brown, moist.

19”-45” Silty sand (ML) with clay, brown, moist, higher clay content inclusions.

Harder drilling and roots (live) encountered at 3’. Lower clay content at 3.25 ft.

45”-60” Sandy silt (ML), brown, moist; r

roots less than ¼” diameter at 4’.

Decreasing clay content to cleaner sand at 4 ¼ and siltier at the base.

Bottom of hole at 60”

T2A-18; Coordinates = (148.75, 113.25)

0 – 9” Sandy Silt (ML) to silty sand (SM), trace clay, brown, moist. Loose zone between 6”-12”.

9”-19.5” Clayey silt (ML), brown, moist.

Bottom of hole at 19.5”

P2A-84; Coordinates = (146.3, 113.25)

0 – 48” Silty sand (SM), trace clay, moist, brown, decayed root at 6” with pieces visible to 1.5 ft.
Small pieces of gravel and ¼” diameter live root at 2’.
Small clay pockets with silty sand matrix and live root of 5/8” diameter at 36”.

48”-52” Sandy silt (ML) with trace clay, moist, brown.

52”-68” Silty sand (SM), light brown, moist, fine root, lightly cemented.

68”-78” Clayey silt (ML) with trace sand, brown, moist.

78”-81” Silty clay (CL), brown, moist.

81”-84” Silty sand (SM), trace clay, light brown, moist, decreasing silt toward base.

Bottom of hole at 84”

T3A-36; Coordinates = (147.7, 114.15)

0 – 6” Decayed root

6”-23” Sandy silt (ML) to silty sand (SM), brown, moist

23”-37.5” Clayey silt (ML), brown, moist.

Bottom of hole at 37.5”

T3A-18; Coordinates = (149.5, 115.75)

0 – 12” Silty sand (SM), trace clay, moist, brown; decomposed organic matter at 6”-12”.

12”-19.5” Sandy silt with clay (ML), moist, brown.

Bottom of hole at 19.5”

T4A-36; Coordinates = (148.5, 115.75)

0 – 19” Sandy silt (ML) with trace clay and decomposed organic matter in upper 6”, brown, moist.

19”-25” Sandy silt with clay (ML), moist, dark brown.

25”-30” Silty sand (SM) with trace clay, light brown, moist, lightly cemented.

30”-37” Sandy silt (ML),brown, moist, fine roots at 30-37” with decomposed organic matter at 35” that damaged gauge auger.

Bottom of hole at 37”

T4A-60; Coordinates = (147.25, 115.75)

0 – 12” Sandy silt (ML) with clay, brown, moist, pyritic specs in sand fraction.

12”-18” Clayey silt with sand (ML), brown, moist.

18”-36” Silty sand (SM), light brown, moist, pyritic sands.

36”-60” Clayey silt (ML), moist, brown, with very fine sand.

Bottom of hole at 60”

T1B-18; Coordinates = (142, 111)

0 – 19.5” Sandy silt (ML) with clay, brown, moist.

Bottom of hole at 19.5”

T1B-36; Coordinates = (141, 111)

0 – 6” Sand (SP) with clay, brown, moist, fine sand.

6”-12” Silty sand (SM) with clay, moist, brown, very fine sand.

12”-24” Sandy silt to silty sand (ML/SM), light brown, moist, very loose between 18” and 24”. Auger dropped from 18” to 24” with single blow. Possible burrow.

24”-36” Silty sand (SM) with clay, brown, moist, very fine sand.

36” – 37.5 Sandy silt (ML) with clay, brown, moist.

Bottom of hole at 37.5”

P2B-84; Coordinates = (140, 113.25)

0 – 16” Silty sand to sandy silt (SM/ML) with trace clay, brown, moist.

16”-42” Silty sand (SM) with trace clay, brown, moist, grades to almost no clay.

42”-60” Sandy silt (ML) with clay, brown, moist.

60”-66” Silty sand (SM), brown, moist, fine sand.

66”-75” Sandy silt (ML) with clay, brown, moist.

75”-78” Sand (SP), brown, moist, fine grained.

78”-84” Silty clay (CL), brown, moist.

Bottom of hole at 84”

T2B-18; Coordinates = (141, 113.25)

0 – 19.5” Silty sand with clay (SM), brown, moist, fine sand.

Bottom of hole at 19.5”

T3B-36; Coordinates = (141, 114.2)

0 – 6” Silty sand (SM), brown, dry, fine sand.

6”-18” Silty sand with clay (SM), brown, moist.

18”-30” Sandy silt to silty sand (ML/SM), brown, moist

30”-37.5” Silty sand (SM), brown, moist, fine sand.

Bottom of hole at 37.5”

T4B-18; Coordinates = (142, 115.25)

0 – 19.5” Sandy silt (ML), brown, moist.

Bottom of hole at 19.5”

T4B-36; Coordinates = (141, 115.2)

0 – 24” Sandy silt (ML) with trace clay, brown.

Increasing clay content with depth.

24”-37.5” Silty sand (SM) with clay, brown, moist, fine sand.

Bottom of hole at 37.5”

T1C-18; Coordinates = (126.5, 111)

0 – 6” Silty sand (SM) with trace clay, brown, moist, some fine gravel.

6”-19.5” Silty sand (SM) with clay, moist, brown, sand very fine grained

Bottom of hole at 19.5”

T1C-36; Coordinates = (125.5, 111)

0 – 12” Silty sand with clay (SM), brown, moist.

12”-37.5” Silty sand to sandy silt (SM/ML), moist, brown.

Bottom of hole at 37.5”

P1C-60; Coordinates = (124.5, 111)

0 – 12” Silty sand (SM), moist, fine roots

12”-30” Sandy silt with clay (ML), brown, moist, live 5/8” diameter root at 24”.

30”-42” Silty sand with trace clay (SM), brown, moist, very fine sand, root at 36” (3/8” dia).
3/8” diameter live root at 36”.
3/8” diameter live root at 42”.

42”-60” Silty sand (SM), brown, moist, very fine sand, fine live roots.
Clay content low near top of layer and increasing at 4.5’.

Bottom of hole at 60”

T2C-18; Coordinates = (126.5, 113.25)

0 – 6” Silty sand (SM), brown, moist.

6”-19.5” Sandy silt (ML), brown, moist.

Bottom of hole at 19.5”

P2C-84; Coordinates = (124, 113.25)

0 – 12” Silty sand (SM) with trace clay, brown, moist.

12”-18” Sandy silt with clay (ML), brown, moist.

18”-30” Clayey silt (ML), brown, moist.

30”-36” Clayey sand (SM) with silt, brown, moist, very fine sand.

36”-54” Silty sand with clay (SM) brown, moist, very fine sand, some fine roots.

54”-66” Silty sand (SM), moist, light brown, lightly cemented, very fine sand.

66”-72” Sand (SP), moist, light brown, very fined grained with pockets of dark brown silty clay (CL)

72”-78” Silty sand with clay (SM), brown, moist

78”-90” Silty Clay (CL), brown, moist. Live root (1/4” diameter) at 7.5 ft.

Bottom of hole at 90”

T3C-36; Coordinates = (125.5, 114.2)

0 – 12” Silty sand (SM), brown, moist, fine sand.

12”-37.5” Sandy silt (ML), brown, moist, increased clay content with depth.

Bottom of hole at 37.5”

T4C-18; Coordinates = (126.5, 115.75)

0 – 19.5” Silty sand (SM), brown, moist, fine roots, higher silt content with depth.

Bottom of hole at 19.5”

T4C-36; Coordinates = (125.5,115.75)

0 – 6” Silty sand (SM), brown, moist, fine sand.

6”-30” Sandy silt (ML), brown, moist.

30”-37.5” Clayey silt (ML) with sand, olive brown, moist.

Bottom of hole at 37.5”

T4C-60; Coordinates = (124.5, 115.75)

0 – 18” Silty sand (SM), brown, moist, fine sand.

18”-30” Sandy silt (ML), brown, moist.

30”-42” Sand with silt (SM), light brown, moist, fine, uniform

42”-48” Sandy silt with clay (ML), moist, light brown with reddish stains

48”-60” Clayey silt (ML) with sand, moist, brown

Bottom of hole at 60”

APPENDIX B: LABORATORY TESTING

Appendix B

B-1 GRAIN SIZE ANALYSES

B-1-1 CAL EXPO TEST, MATERIAL 1

SIEVE ANALYSIS DATA SHEET

					Wet Sieve?	Yes
Date:	11-Nov-10				Over sieve #:	200
Performed by:	DCR				Total dry mass (g)	302.9
					Tare wt. (g)	110.9
Soil:	1		**Sample + tare**		Total dry + tare (g)	413.8
Depth:			**tare**		Coarse + tare (g)	191.26
Sample:	10/11 - #1		sample		Coarse (g)	80.36

US Sieve No	Opening (mm)	Sieve weight (g)	Sieve + Soil (g)	Soil (g)	% Ret. (each)	%Ret (cumulative)	%Finer
max	**7.5**			0	0.00	0	100
4	**4.7**	607.7	607.7	0	0.00	0.00	100.00
10	**2**	482.5	482.5	0	0.00	0.00	100.00
16	**1.18**	479.4	481.9	2.5	0.83	0.83	99.17
30	**0.59**	451.9	455.2	3.3	1.09	1.91	98.09
40	**0.425**	376	378.9	2.9	0.96	2.87	97.13
60	**0.25**	350.3	355.7	5.4	1.78	4.66	95.34
100	**0.147**	341.7	358.7	17	5.61	10.27	89.73
200	**0.075**	333.3	381	47.7	15.75	26.02	73.98
PAN/(#200wash)	**0**	396	398.6	2.6	74.33		

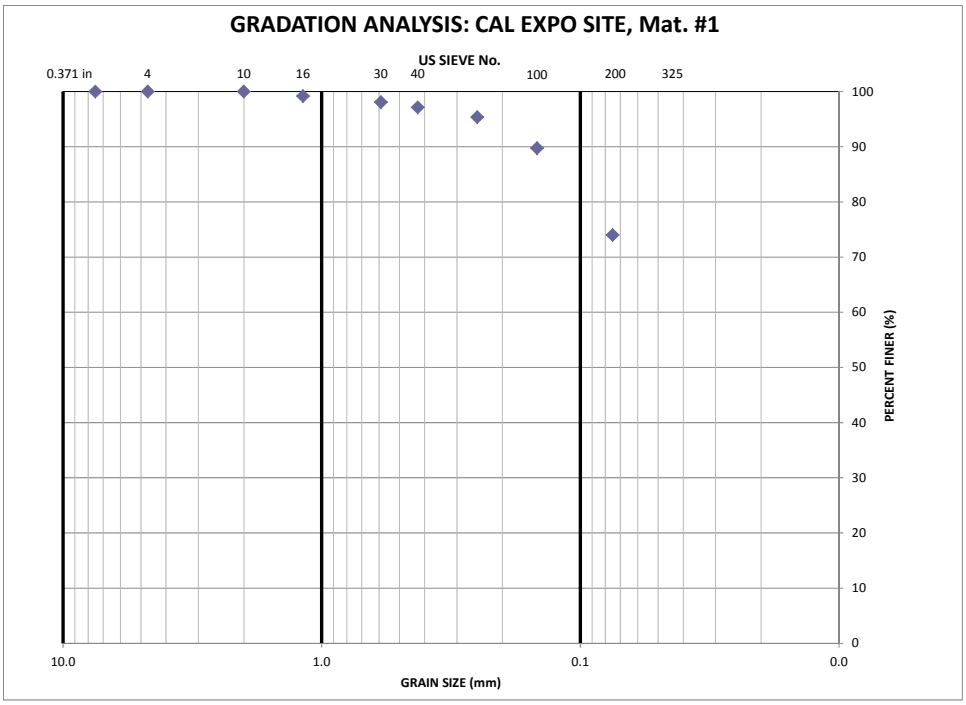

B-1-2 CAL EXPO TEST, MATERIAL 1 (second test)

SIEVE ANALYSIS DATA SHEET

					Wet Sieve?	Yes
Date:	20-Oct-10				Over sieve #:	200
Performed by:	DCR				Total dry mass (g)	366.74
					Tare wt. (g)	8.3
Soil:	1		**Sample + tare**		Total dry + tare (g)	375.04
Depth:			**tare**		Coarse + tare (g)	123.63
Sample:	10/20 - #1		sample		Coarse (g)	115.33

US Sieve No	Opening (mm)	Sieve weight (g)	Sieve + Soil (g)	Soil (g)	% Ret. (each)	%Ret (cumulative)	%Finer
max	**7.5**			0	0.00	0	100
4	**4.7**	607.7	607.7	0	0.00	0.00	100.00
10	**2**	482.6	482.6	0	0.00	0.00	100.00
16	**1.18**	479.8	485.9	6.1	1.66	1.66	98.34
30	**0.59**	452	453.8	1.8	0.49	2.15	97.85
40	**0.425**	376.2	377.3	1.1	0.30	2.45	97.55
60	**0.25**	350.3	354.3	4	1.09	3.54	96.46
100	**0.147**	342.5	377.5	35	9.54	13.09	86.91
200	**0.075**	333.4	396.8	63.4	17.29	30.38	69.62
PAN/(#200wash)	**0**	395.7	400	4.3	69.73		

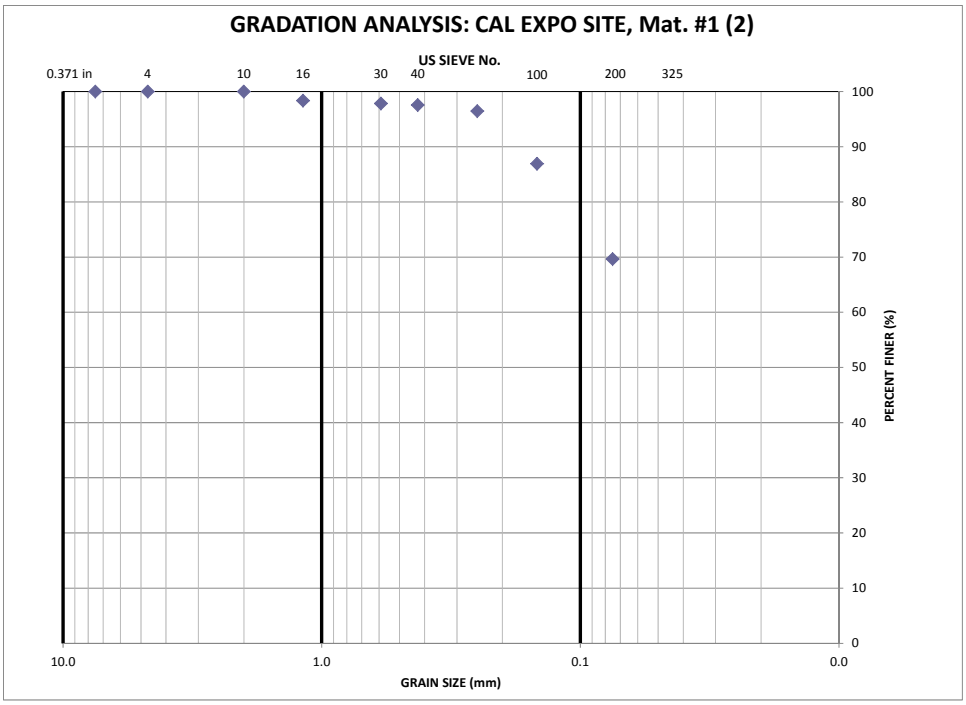

B-1-3 CAL EXPO TEST, MATERIAL 3

			SIEVE ANALYSIS DATA SHEET				
					Wet Sieve?	Yes	
Date:	11-Nov-10				Over sieve #:	200	
Performed by:	DCR				Total dry mass (g)	283.3	
					Tare wt. (g)	8.1	
Soil:	3		**Sample + tare**		Total dry + tare (g)	291.4	
Depth:			**tare**		Coarse + tare (g)	114.19	
Sample:	10/11 - #3		sample		Coarse (g)	106.09	
US Sieve No	**Opening (mm)**	**Sieve weight (g)**	**Sieve + Soil (g)**	**Soil (g)**	**% Ret. (each)**	**%Ret (cumulative)**	**%Finer**
max	**7.5**			0	0.00	0	100
4	**4.7**	607.7	607.7	0	0.00	0.00	100.00
10	**2**	482.6	482.6	0	0.00	0.00	100.00
16	**1.18**	479.8	480.2	0.4	0.14	0.14	99.86
30	**0.59**	452	453.2	1.2	0.42	0.56	99.44
40	**0.425**	376.2	377	0.8	0.28	0.85	99.15
60	**0.25**	350.3	356.3	6	2.12	2.97	97.03
100	**0.147**	342.5	379.3	36.8	12.99	15.95	84.05
200	**0.075**	333.4	393.2	59.8	21.11	37.06	62.94
PAN/(#200wash)	**0**	395.7	397.2	1.5	63.08		

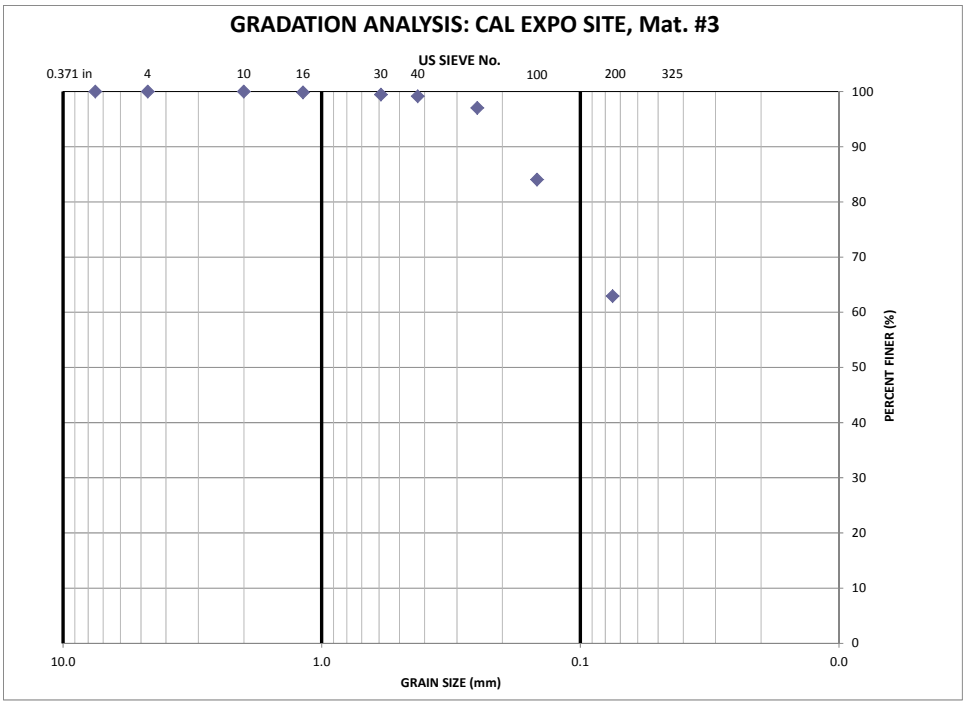

B-1-4 CAL EXPO TEST, MATERIAL 3 (second test)

SIEVE ANALYSIS DATA SHEET

					Wet Sieve?	Yes
Date:	20-Oct-10				Over sieve #:	200
Performed by:	DCR				Total dry mass (g)	343.23
					Tare wt. (g)	8.3
Soil:	3		**Sample + tare**		Total dry + tare (g)	351.53
Depth:			**tare**		Coarse + tare (g)	68.19
Sample:	10/20 - #3		sample		Coarse (g)	59.89

US Sieve No	Opening (mm)	Sieve weight (g)	Sieve + Soil (g)	Soil (g)	% Ret. (each)	%Ret (cumulative)	%Finer
max	**7.5**			0	0.00	0	100
4	**4.7**	607.7	607.7	0	0.00	0.00	100.00
10	**2**	482.6	482.6	0	0.00	0.00	100.00
16	**1.18**	479.8	480	0.2	0.06	0.06	99.94
30	**0.59**	452	453	1	0.29	0.35	99.65
40	**0.425**	376.2	404	27.8	8.10	8.45	91.55
60	**0.25**	350.3	354.4	4.1	1.19	9.64	90.36
100	**0.147**	342.5	358.1	15.6	4.55	14.19	85.81
200	**0.075**	333.4	370.2	36.8	10.72	24.91	75.09
PAN/(#200wash)	**0**	395.7	397.8	2.1	83.16		

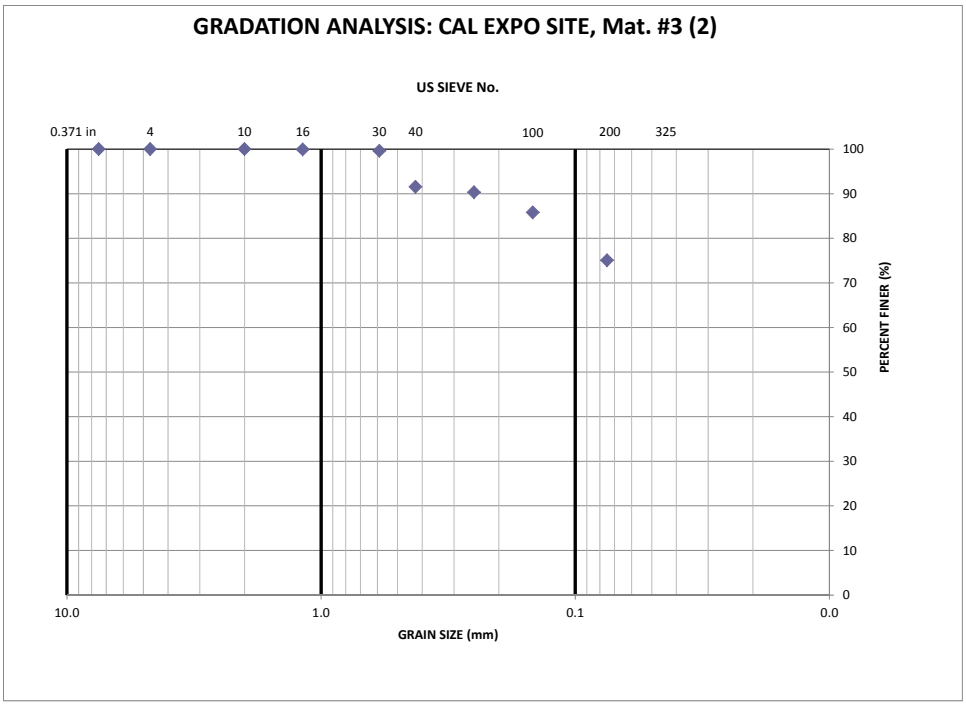

B-1-5 CAL EXPO TEST, MATERIAL 3a

		SIEVE ANALYSIS DATA SHEET					
					Wet Sieve?	Yes	
Date:	20-Oct-10				Over sieve #:	200	
Performed by:	DCR				Total dry mass (g)	338.36	
					Tare wt. (g)	8.3	
Soil:	3a		**Sample + tare**		Total dry + tare (g)	346.66	
Depth:			**tare**		Coarse + tare (g)	49.42	
Sample:	10/20 - #3a		sample		Coarse (g)	41.12	

US Sieve No	Opening (mm)	Sieve weight (g)	Sieve + Soil (g)	Soil (g)	% Ret. (each)	%Ret (cumulative)	%Finer
max	**7.5**			0	0.00	0	100
4	**4.7**	607.7	607.7	0	0.00	0.00	100.00
10	**2**	482.6	482.6	0	0.00	0.00	100.00
16	**1.18**	479.8	480.1	0.3	0.09	0.09	99.91
30	**0.59**	452	453.5	1.5	0.44	0.53	99.47
40	**0.425**	376.2	376.6	0.4	0.12	0.65	99.35
60	**0.25**	350.3	352	1.7	0.50	1.15	98.85
100	**0.147**	342.5	351.9	9.4	2.78	3.93	96.07
200	**0.075**	333.4	360.9	27.5	8.13	12.06	87.94
PAN/(#200wash)	**0**	395.7	397	1.3	88.23		

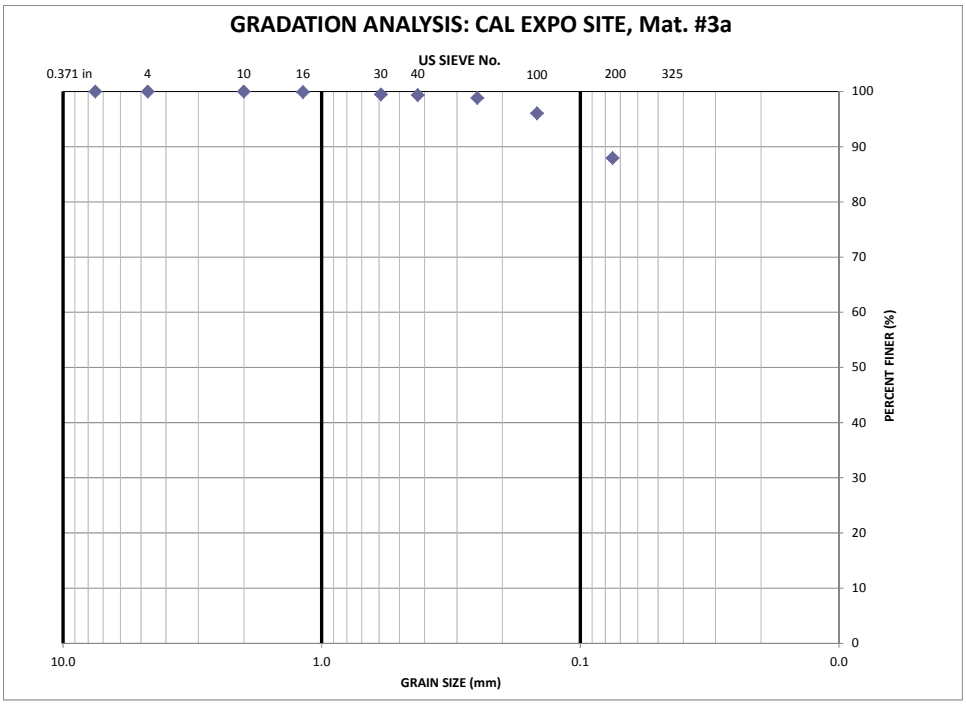

B-1-6 CAL EXPO TEST, MATERIAL 3b

		SIEVE ANALYSIS DATA SHEET					
					Wet Sieve?	Yes	
Date:	11-Nov-10				Over sieve #:	200	
Performed by:	DCR				Total dry mass (g)	409.47	
					Tare wt. (g)	8.3	
Soil:	3b		**Sample + tare**		Total dry + tare (g)	417.77	
Depth:			**tare**		Coarse + tare (g)	137.7	
Sample:	10/11 - #3b		sample		Coarse (g)	129.4	
US Sieve No	**Opening (mm)**	**Sieve weight (g)**	**Sieve + Soil (g)**	**Soil (g)**	**% Ret. (each)**	**%Ret (cumulative)**	**%Finer**
max	**7.5**			0	0.00	0	100
4	**4.7**	607.7	607.7	0	0.00	0.00	100.00
10	**2**	482.6	482.6	0	0.00	0.00	100.00
16	**1.18**	479.8	479.9	0.1	0.02	0.02	99.98
30	**0.59**	452	452.5	0.5	0.12	0.15	99.85
40	**0.425**	376.2	376.6	0.4	0.10	0.24	99.76
60	**0.25**	350.3	355.7	5.4	1.32	1.56	98.44
100	**0.147**	342.5	394.8	52.3	12.77	14.34	85.66
200	**0.075**	333.4	402	68.6	16.75	31.09	68.91
PAN/(#200wash)	**0**	395.7	398.6	2.9	69.11		

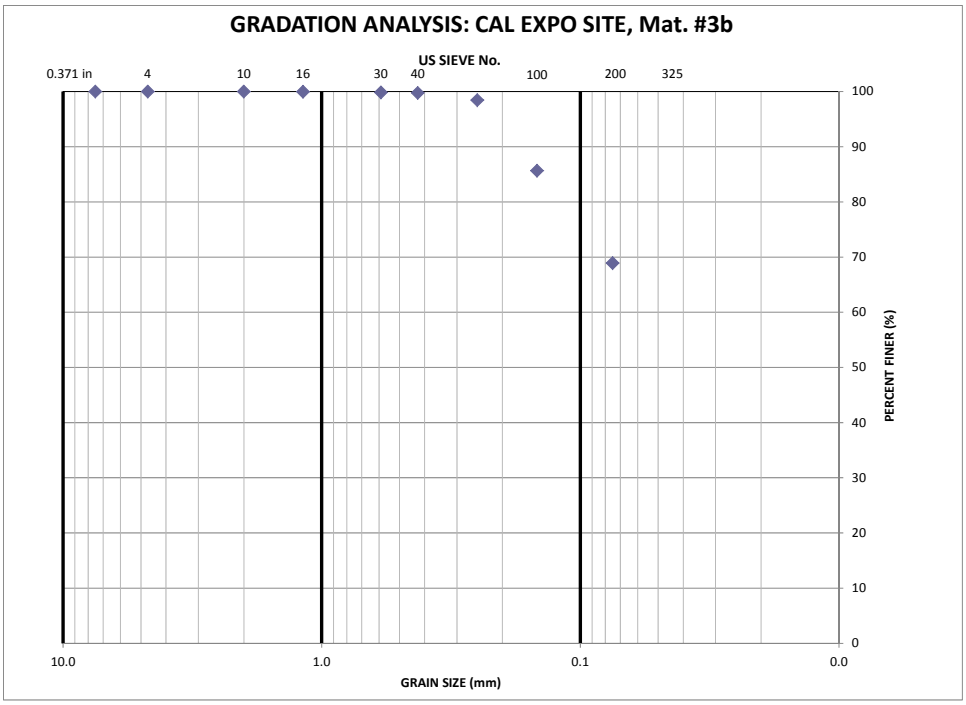

B-1-7 CAL EXPO TEST, MATERIAL 4

		SIEVE ANALYSIS DATA SHEET					
					Wet Sieve?	Yes	
Date:	11-Nov-10				Over sieve #:	200	
Performed by:	DCR				Total dry mass (g)	246.33	
					Tare wt. (g)	8.2	
Soil:	4		**Sample + tare**		Total dry + tare (g)	254.53	
Depth:			**tare**		Coarse + tare (g)	54.84	
Sample:	10/11 -#4		sample		Coarse (g)	46.64	
US Sieve No	**Opening (mm)**	**Sieve weight (g)**	**Sieve + Soil (g)**	**Soil (g)**	**% Ret. (each)**	**%Ret (cumulative)**	**%Finer**
max	**7.5**			0	0.00	0	100
4	**4.7**	607.9	607.9	0	0.00	0.00	100.00
10	**2**	482.6	482.6	0	0.00	0.00	100.00
16	**1.18**	479.8	479.9	0.1	0.04	0.04	99.96
30	**0.59**	452	452.5	0.5	0.20	0.24	99.76
40	**0.425**	376.2	376.5	0.3	0.12	0.37	99.63
60	**0.25**	350.4	352.5	2.1	0.85	1.22	98.78
100	**0.147**	342.6	356.3	13.7	5.56	6.78	93.22
200	**0.075**	333.4	362.9	29.5	11.98	18.76	81.24
PAN/(#200wash)	**0**	395.7	395.8	0.1	81.11		

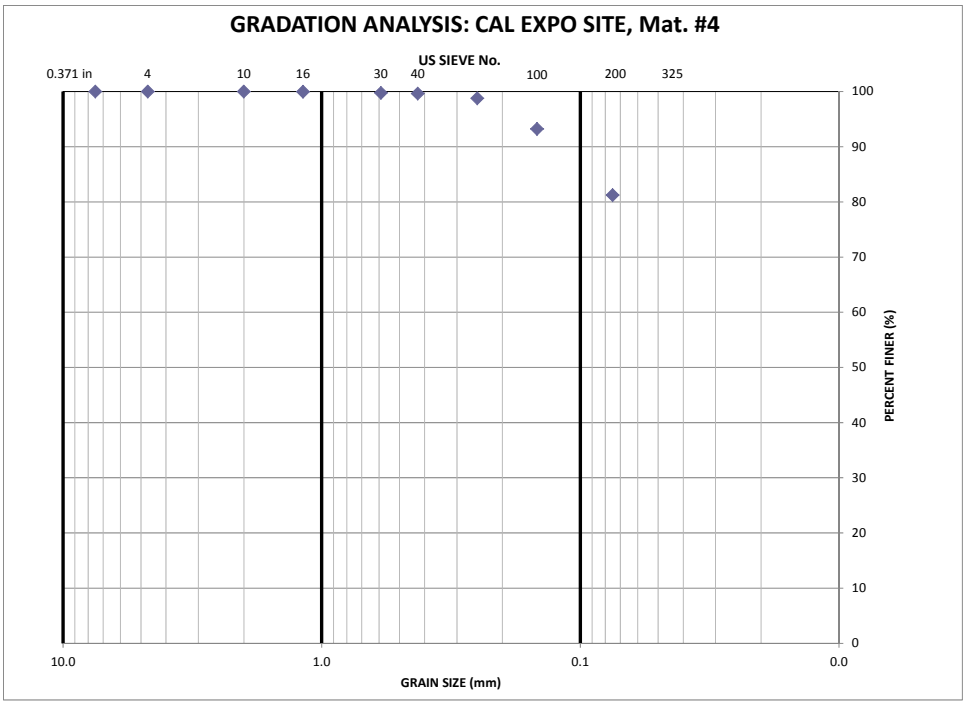
GRADATION ANALYSIS: CAL EXPO SITE, Mat. #4
US SIEVE No.
0.371 in
4
10
16
30
40
100
200
325
100
90
80
70
60
50
40
30
20
10
0
PERCENT FINER (%)
10.0
1.0
0.1
0.0
GRAIN SIZE (mm)

B-1-8 CAL EXPO TEST, MATERIAL 4 (second test)

		SIEVE ANALYSIS DATA SHEET					
					Wet Sieve?	Yes	
Date:	11-Nov-10				Over sieve #:	200	
Performed by:	DCR				Total dry mass (g)	389.21	
					Tare wt. (g)	6.6	
Soil:	3		**Sample + tare**		Total dry + tare (g)	395.81	
Depth:			**tare**		Coarse + tare (g)	101.44	
Sample:	10/11 - #3		sample		Coarse (g)	94.84	

US Sieve No	Opening (mm)	Sieve weight (g)	Sieve + Soil (g)	Soil (g)	% Ret. (each)	%Ret (cumulative)	%Finer
max	**7.5**			0	0.00	0	100
4	**4.7**	607.7	607.7	0	0.00	0.00	100.00
10	**2**	482.6	482.6	0	0.00	0.00	100.00
16	**1.18**	479.8	479.8	0	0.00	0.00	100.00
30	**0.59**	452	453.7	1.7	0.44	0.44	99.56
40	**0.425**	376.2	377.2	1	0.26	0.69	99.31
60	**0.25**	350.3	354.6	4.3	1.10	1.80	98.20
100	**0.147**	342.5	374.5	32	8.22	10.02	89.98
200	**0.075**	333.4	386.3	52.9	13.59	23.61	76.39
PAN/(#200wash)	**0**	395.7	399.2	3.5	76.53		

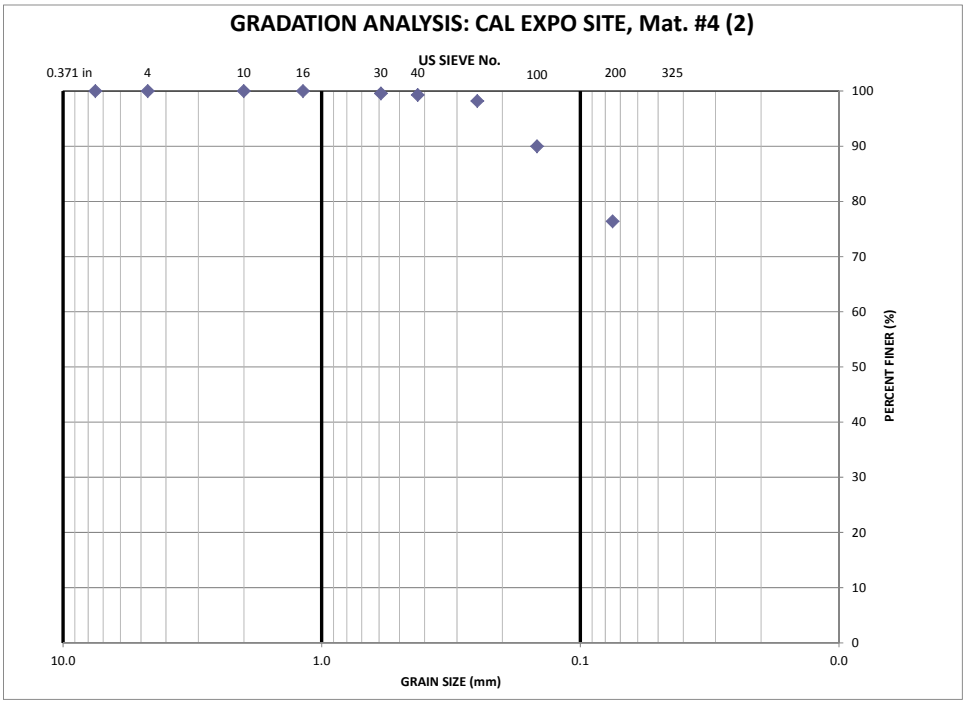

B-1-9 CAL EXPO TEST, MATERIAL 5

		SIEVE ANALYSIS DATA SHEET					
					Wet Sieve?	Yes	
Date:	11-Nov-10				Over sieve #:	200	
Performed by:	DCR				Total dry mass (g)	223.35	
					Tare wt. (g)	8.2	
Soil:	5		**Sample + tare**		Total dry + tare (g)	231.55	
Depth:			**tare**		Coarse + tare (g)	141.83	
Sample:	10/11 - #5		sample		Coarse (g)	133.63	

US Sieve No	Opening (mm)	Sieve weight (g)	Sieve + Soil (g)	Soil (g)	% Ret. (each)	%Ret (cumulative)	%Finer
max	**7.5**			0	0.00	0	100
4	**4.7**	607.7	607.7	0	0.00	0.00	100.00
10	**2**	482.6	482.6	0	0.00	0.00	100.00
16	**1.18**	480	480	0	0.00	0.00	100.00
30	**0.59**	452	452.3	0.3	0.13	0.13	99.87
40	**0.425**	376.2	376.4	0.2	0.09	0.22	99.78
60	**0.25**	350.4	352.9	2.5	1.12	1.34	98.66
100	**0.147**	342.2	365.5	23.3	10.43	11.78	88.22
200	**0.075**	333.5	437.2	103.7	46.43	58.20	41.80
PAN/(#200wash)	**0**	395.8	396.6	0.8	40.53		

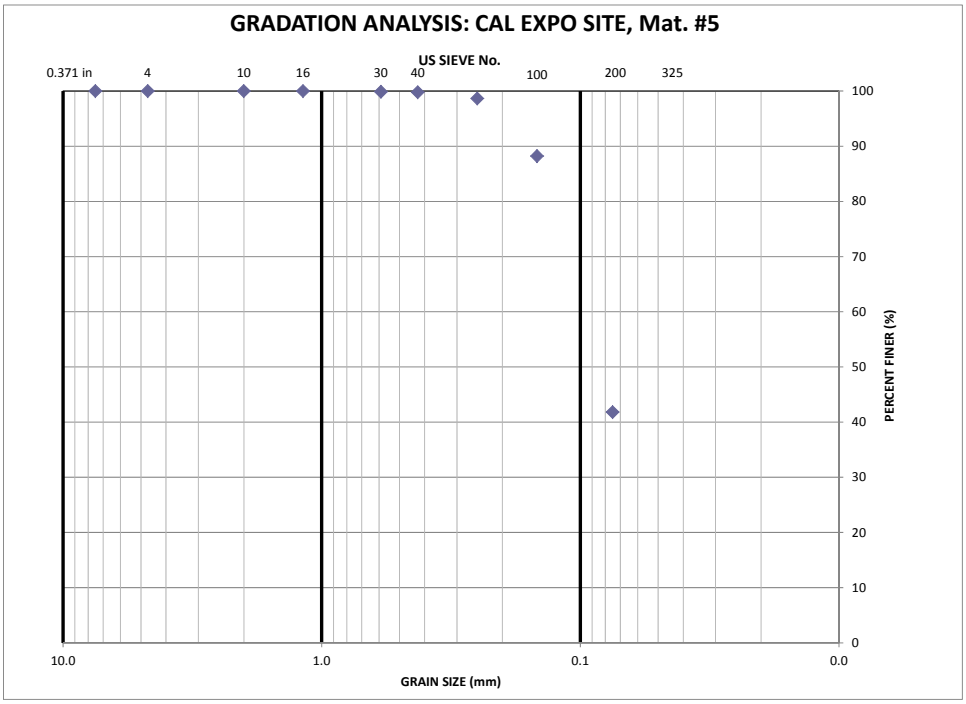

B-1-10 CAL EXPO TEST, MATERIAL 6

SIEVE ANALYSIS DATA SHEET

				Wet Sieve?	Yes
Date:	11-Nov-10			Over sieve #:	200
Performed by:	DCR			Total dry mass (g)	277.24
				Tare wt. (g)	8.3
Soil:	6		Sample + tare	Total dry + tare (g)	285.54
Depth:			tare	Coarse + tare (g)	94.35
Sample:	10/11 - #6		sample	Coarse (g)	86.05

US Sieve No	Opening (mm)	Sieve weight (g)	Sieve + Soil (g)	Soil (g)	% Ret. (each)	%Ret (cumulative)	%Finer
max	7.5			0	0.00	0	100
4	4.7	607.7	607.7	0	0.00	0.00	100.00
10	2	482.6	482.6	0	0.00	0.00	100.00
16	1.18	479.8	479.8	0	0.00	0.00	100.00
30	0.59	452	452.5	0.5	0.18	0.18	99.82
40	0.425	376.2	376.4	0.2	0.07	0.25	99.75
60	0.25	350.3	351.9	1.6	0.58	0.83	99.17
100	0.147	342.5	361.9	19.4	7.00	7.83	92.17
200	0.075	333.4	394.3	60.9	21.97	29.79	70.21
PAN/(#200wash)	0	395.7	399.9	4.2	70.48		

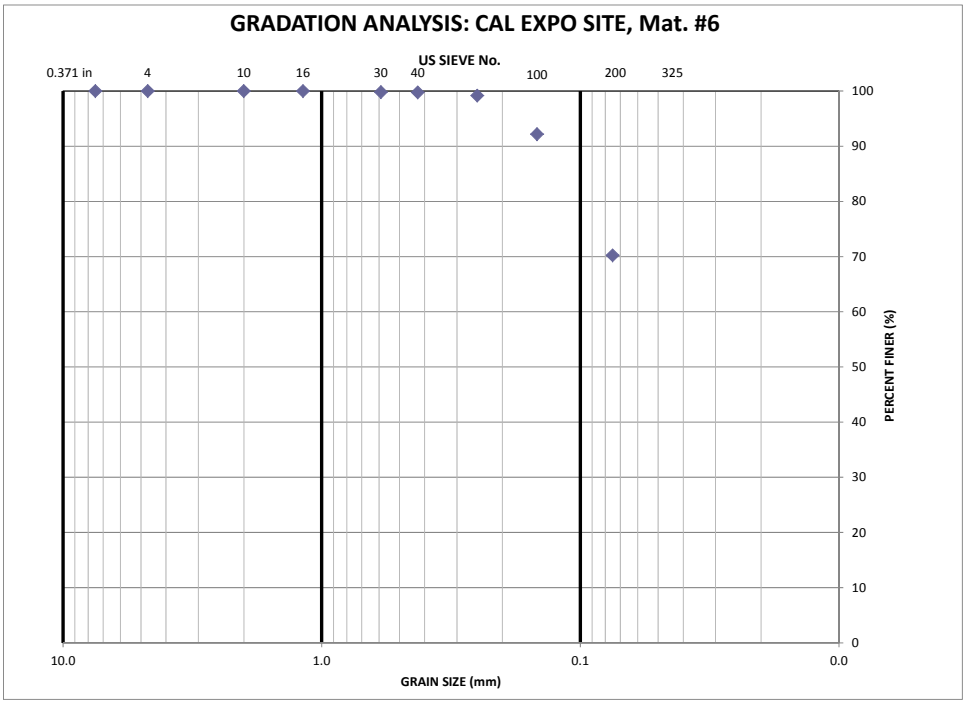

B-1-11 CAL EXPO TEST, MATERIAL 7

		SIEVE ANALYSIS DATA SHEET					
					Wet Sieve?	Yes	
Date:	11-Nov-10				Over sieve #:	200	
Performed by:	DCR				Total dry mass (g)	260.6	
					Tare wt. (g)	64	
Soil:	7		**Sample + tare**		Total dry + tare (g)	324.6	
Depth:			**tare**		Coarse + tare (g)	170.09	
Sample:	10/11 - #7		sample		Coarse (g)	106.09	

US Sieve No	Opening (mm)	Sieve weight (g)	Sieve + Soil (g)	Soil (g)	% Ret. (each)	%Ret (cumulative)	%Finer
max	**7.5**			0	0.00	0	100
4	**4.7**	607.7	607.7	0	0.00	0.00	100.00
10	**2**	482.7	482.7	0	0.00	0.00	100.00
16	**1.18**	479.9	480.1	0.2	0.08	0.08	99.92
30	**0.59**	452	452.6	0.6	0.23	0.31	99.69
40	**0.425**	376.2	376.5	0.3	0.12	0.42	99.58
60	**0.25**	350.4	351.1	0.7	0.27	0.69	99.31
100	**0.147**	342.3	349.5	7.2	2.76	3.45	96.55
200	**0.075**	333.3	412.6	79.3	30.43	33.88	66.12
PAN/(#200wash)	**0**	395.8	399.5	3.7	60.71		

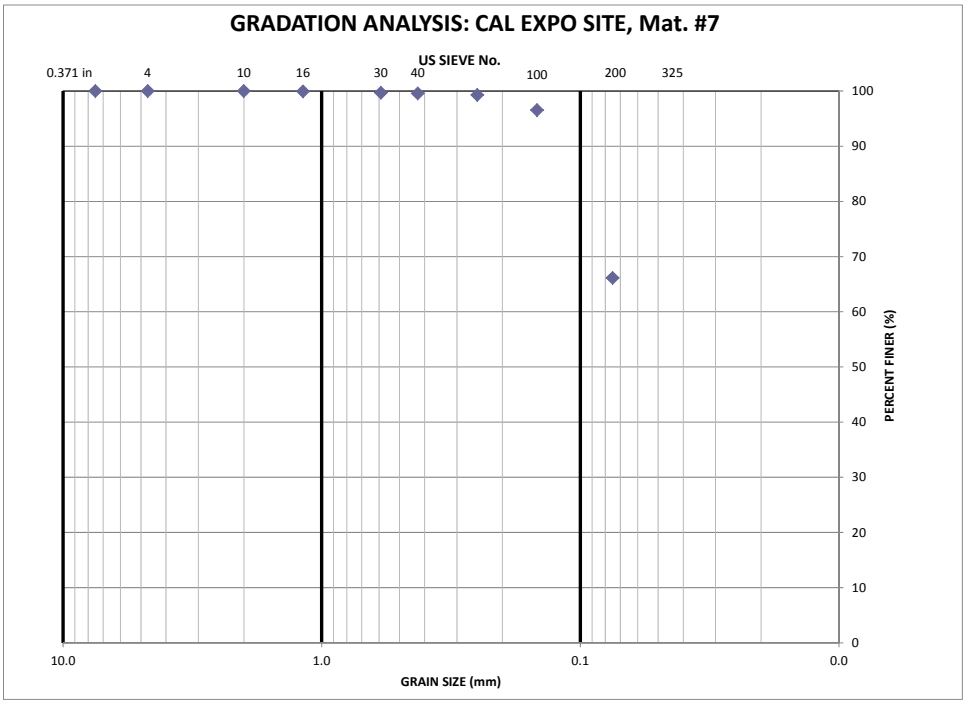

B-1-12 CAL EXPO TEST, MATERIAL 8

SIEVE ANALYSIS DATA SHEET

		Wet Sieve?	Yes
Date:	11-Nov-10	Over sieve #:	200
Performed by:	DCR	Total dry mass (g)	267.2
		Tare wt. (g)	8.1
Soil:	8	Total dry + tare (g)	275.3
Depth:		Coarse + tare (g)	98.18
Sample:	10/11 -#8	Coarse (g)	90.08

US Sieve No	Opening (mm)	Sieve weight (g)	Sieve + Soil (g)	Soil (g)	% Ret. (each)	%Ret (cumulative)	%Finer
max	**7.5**			0	0.00	0	100
4	**4.7**	607.7	607.9	0.2	0.07	0.07	99.93
10	**2**	482.6	482.6	0	0.00	0.07	99.93
16	**1.18**	479.8	479.9	0.1	0.04	0.11	99.89
30	**0.59**	452	453.2	1.2	0.45	0.56	99.44
40	**0.425**	376.2	376.7	0.5	0.19	0.75	99.25
60	**0.25**	350.3	353.8	3.5	1.31	2.06	97.94
100	**0.147**	342.5	377.9	35.4	13.25	15.31	84.69
200	**0.075**	333.4	382	48.6	18.19	33.50	66.50
PAN/(#200wash)	**0**	395.7	397.1	1.4	66.81		

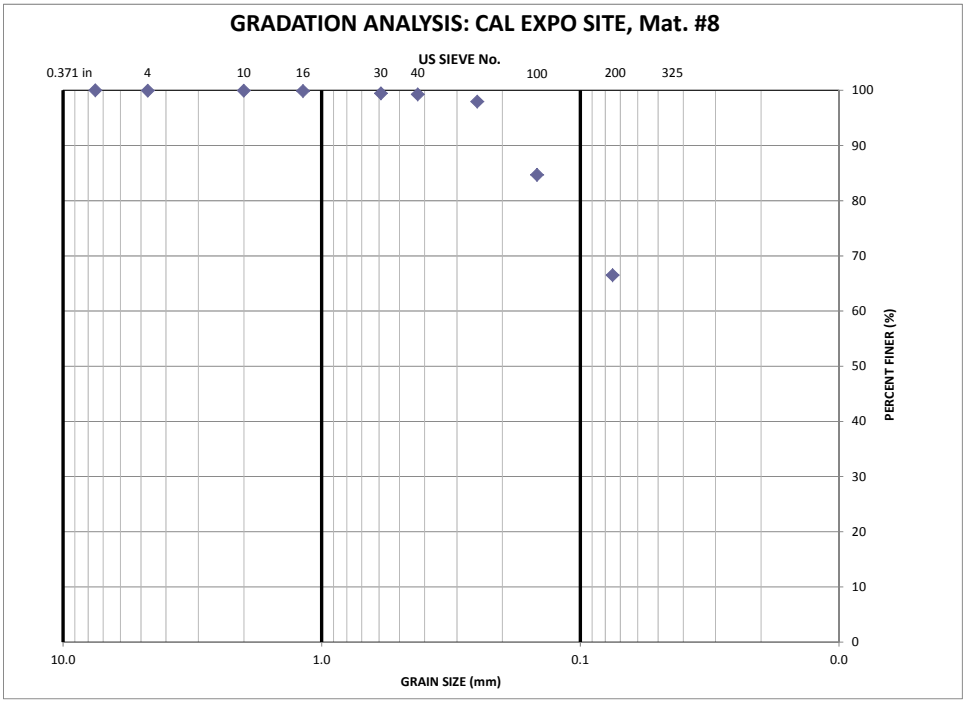

B-1-13 CAL EXPO TEST, MATERIAL 9

		SIEVE ANALYSIS DATA SHEET					
					Wet Sieve?	Yes	
Date:	11-Nov-10				Over sieve #:	200	
Performed by:	DCR				Total dry mass (g)	239.63	
					Tare wt. (g)	8.1	
Soil:	9		**Sample + tare**		Total dry + tare (g)	247.73	
Depth:			**tare**		Coarse + tare (g)	94.78	
Sample:	10/11 -#9		sample		Coarse (g)	86.68	
US Sieve No	**Opening (mm)**	**Sieve weight (g)**	**Sieve + Soil (g)**	**Soil (g)**	**% Ret. (each)**	**%Ret (cumulative)**	**%Finer**
max	**7.5**			0	0.00	0	100
4	**4.7**	607.9	607.9	0	0.00	0.00	100.00
10	**2**	482.6	482.6	0	0.00	0.00	100.00
16	**1.18**	479.8	479.9	0.1	0.04	0.04	99.96
30	**0.59**	451.9	453.1	1.2	0.50	0.54	99.46
40	**0.425**	376.1	376.5	0.4	0.17	0.71	99.29
60	**0.25**	350.3	351.6	1.3	0.54	1.25	98.75
100	**0.147**	342.7	367.6	24.9	10.39	11.64	88.36
200	**0.075**	333.4	390.7	57.3	23.91	35.55	64.45
PAN/(#200wash)	**0**	395.7	397.4	1.7	64.54		

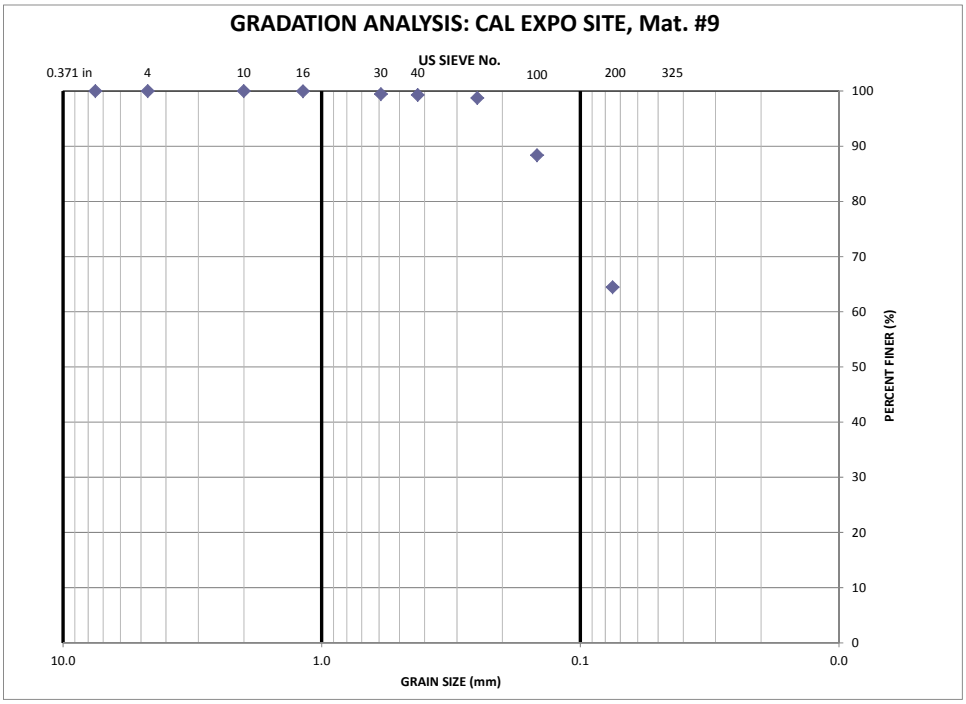

B-1-14 CAL EXPO TEST, MATERIAL 10

		SIEVE ANALYSIS DATA SHEET					
					Wet Sieve?	Yes	
Date:	11-Nov-10				Over sieve #:	200	
Performed by:	DCR				Total dry mass (g)	250.36	
					Tare wt. (g)	8.1	
Soil:	10		**Sample + tare**		Total dry + tare (g)	258.46	
Depth:			**tare**		Coarse + tare (g)	81.79	
Sample:	10/11 -#10		sample		Coarse (g)	73.69	

US Sieve No	Opening (mm)	Sieve weight (g)	Sieve + Soil (g)	Soil (g)	% Ret. (each)	%Ret (cumulative)	%Finer
max	**7.5**			0	0.00	0	100
4	**4.7**	607.9	607.9	0	0.00	0.00	100.00
10	**2**	482.6	482.6	0	0.00	0.00	100.00
16	**1.18**	479.8	479.8	0	0.00	0.00	100.00
30	**0.59**	451.9	452.4	0.5	0.20	0.20	99.80
40	**0.425**	376.1	376.4	0.3	0.12	0.32	99.68
60	**0.25**	350.3	351	0.7	0.28	0.60	99.40
100	**0.147**	342.6	359.1	16.5	6.59	7.19	92.81
200	**0.075**	333.4	388.2	54.8	21.89	29.08	70.92
PAN/(#200wash)	**0**	395.7	396.8	1.1	71.01		

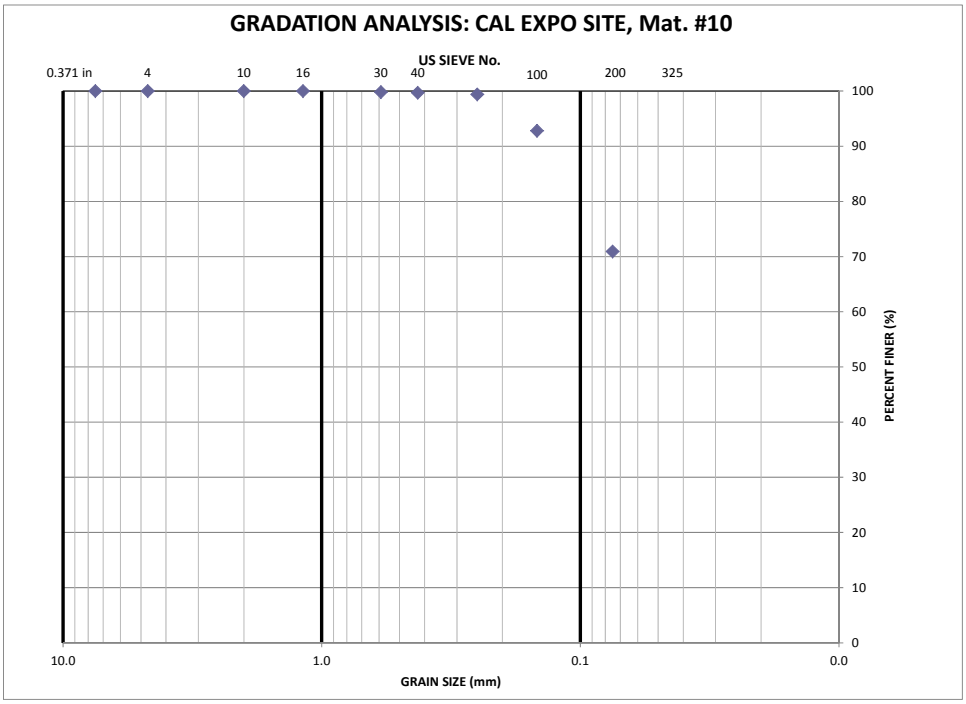

B-1-15 CAL EXPO TEST, MATERIAL 'Sand Lens'

SIEVE ANALYSIS DATA SHEET

					Wet Sieve?	Yes
Date:	11-Nov-10				Over sieve #:	200
Performed by:	DCR				Total dry mass (g)	298.6
					Tare wt. (g)	8
Soil:	Sand lens		**Sample + tare**		Total dry + tare (g)	306.6
Depth:			**tare**		Coarse + tare (g)	206.74
Sample:	10/11 -sand lens		sample		Coarse (g)	198.74

US Sieve No	Opening (mm)	Sieve weight (g)	Sieve + Soil (g)	Soil (g)	% Ret. (each)	%Ret (cumulative)	%Finer
max	**7.5**			0	0.00	0	100
4	**4.7**	607.7	607.9	0.2	0.07	0.07	99.93
10	**2**	482.6	482.6	0	0.00	0.07	99.93
16	**1.18**	479.8	479.9	0.1	0.03	0.10	99.90
30	**0.59**	452	452.2	0.2	0.07	0.17	99.83
40	**0.425**	376.2	376.3	0.1	0.03	0.20	99.80
60	**0.25**	350.3	351.9	1.6	0.54	0.74	99.26
100	**0.147**	342.5	399	56.5	18.92	19.66	80.34
200	**0.075**	333.4	463.8	130.4	43.67	63.33	36.67
PAN/(#200wash)	**0**	395.7	405.8	10.1	36.83		

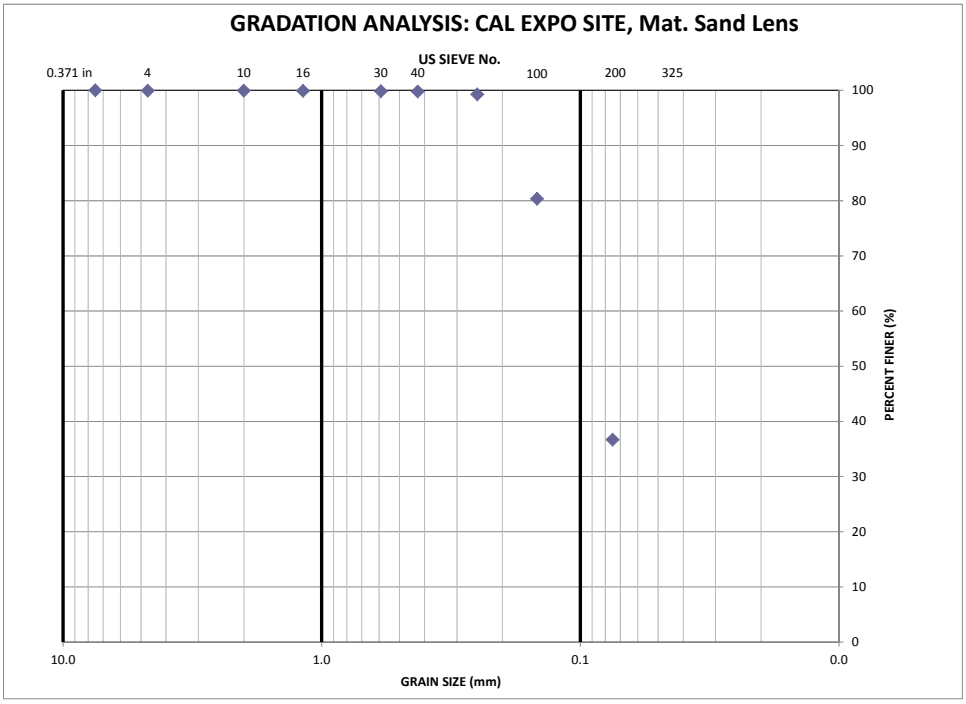

B-2 WATER CONTENT ESTIMATION

B-2-1 CAL EXPO TEST

WATER CONTENT DETERMINATION													
Soil name/description:	Cal Expo Levee Material												
Performed by:	Diego Cobos												
Density of Water	62.4	pcf											
Assumed soil density	90	pcf											
	1	**2**	**3**	**4**	**5**	**6**	**7**	**8**	**9**	**10**	**11**	**12**	**13**
Water Content													
Boring #	EX HB-1_1	EX HB-1_1	EX HB-1_1	EX HB-1_1	EX HB-1_1	EX HB-1_1	EX HB-1_2	EX HB-1_2	EX HB-1_2	EX HB-1_2	EX HB-1_2	EX HB-1_2	EX HB-1_2
Depth (ft)	0.5	3.25	4.5	6.5	7.5	8.25	1	2	3.5	4.75	6	7.25	8.25
Tare #	75	177	350	294	207	206	472	101	403	362	17	22	115
Tare mass (g)	39.56	63.93	64.25	63.6	64.08	64.1	64.08	64.26	64.5	64.59	64.31	64.41	64.15
Tare + moist soil (g)	107.63	170.61	189.11	167.74	192.85	211.08	126.25	154.88	170.98	145.91	149.25	134.53	176.57
Tare + dry soil (g)	97.43	154.67	167.34	149.36	165.22	178.52	115.75	135.79	158.19	129.33	137.84	127.92	152.4
Mass of water (g)	10.2	15.94	21.77	18.38	27.63	32.56	10.5	19.09	12.79	16.58	11.41	6.61	24.17
Mass of dry soil (g)	57.87	90.74	103.09	85.76	101.14	114.42	51.67	71.53	93.69	64.74	73.53	63.51	88.25
Gravimetric Water content, w %	17.63	17.57	21.12	21.43	27.32	28.46	20.32	26.69	13.65	25.61	15.52	10.41	27.39
Volumetric Water content, θ %	25.42	25.34	30.46	30.91	39.40	41.04	29.31	38.49	19.69	36.94	22.38	15.01	39.50

APPENDIX C: REGIONAL SOIL DATA

Appendix C

The study site bordering the California Exposition and State Fair (Cal Expo) is located at approximately USACE Levee Mile 0.75, Unit 3 within the American River Flood Control District (ARFCD) or approximately California DWR Station 3130 of the American River North Levee. URS completed a study in 2009 documenting regional soil and stability conditions for the area known as the American River Common Features, of which our study site is a part. The study is called "American River Common Features General Re-evaluation Report", or the 'ARCF GRR', dated March 24, 2009.

The report provides a detailed summary and analysis of geotechnical data within the study area. Levee reaches are identified and analyzed for seepage and stability in a number of scenarios with representative levee cross sections. The closest levee section to the east and west of our study site were identified and the available relevant data summarized herein.

Figure C-1 provides a site plan excerpted from the ARCF GRR and modified to show the Cal Expo site as well as the levee cross sections identified as most relevant to our study. Figures C-2 through C-5 show the cross sections of soil stratigraphy closest to the site as well as graphically represented soil borings. Tables C-1 through C-5 provide a summary of available index testing and soil strength assumptions for levee cross sections east and west of the study site.

In 1999, a set of design drawings for the American River Watershed project show proposed levee improvements including construction of a slurry wall in the locations shown on Figure C-6. Drawings include a topographic map showing soil borings and cone penetration tests and utilities in the area of the site (Figure C-7). The site is shown to be at Station 9+100 based on the stationing shown on the plans and the 1-inch diameter metal pipe encountered during construction of our field test appears on the plans. The eucalyptus tree appears to be intact in the aerial photograph on the plan, however the plans do not specify removal of the tree for construction of the slurry wall, while other trees nearby are slated for removal. The aerial photo used may not have been up to date and the tree may have already been removed at the time of the plan. Based on the aerial photo review discussed in Section 3.2 of Volume 1A of this report, the tree appears to have been removed prior to 1998. Figure C-8 shows the closest soil boring log, DH-10, as shown on Figure C-7. Figure C-9 shows a profile view of the stratigraphy with overlain borings. This is the only information available for CPT 96-3 (closest to our site). Figure C-10 shows a close in view of the graphical logs of Boring DH-10 and CPT 96-3 as well as the legend for interpretation of the graphical log. Figure C-11 shows cross sections of the levee geometry in the vicinity of our study site. Figure C-12 provides details with regard to the history and ownership of the water pipe encountered during our excavation. The water pipe was relocated into its current position as part of the construction of the slurry wall.

In 1956, the American River Levee General Design (USACE, 1956) provides some site history and shows that the levee site was likely not raised in order to comply with Corps standards in 1956. The report

shows that the levee was already at design elevation at the location of our test site (Figures C-13 through C-14). Records for construction of the original levee were not located.

F3 EXISTING CONDITIONS GEOTECHNICAL REPORT
For American River Common Features

AMERICAN RIVER COMMON FEATURES
GENERAL REEVALUATION REPORT
SACRAMENTO COUNTY, CALIFORNIA

Contract No.:	W91238-08-D-0001
Delivery Order:	CM04

US Army Corps
of Engineers
Sacramento District

PREPARED BY URS **24 MARCH 2009**

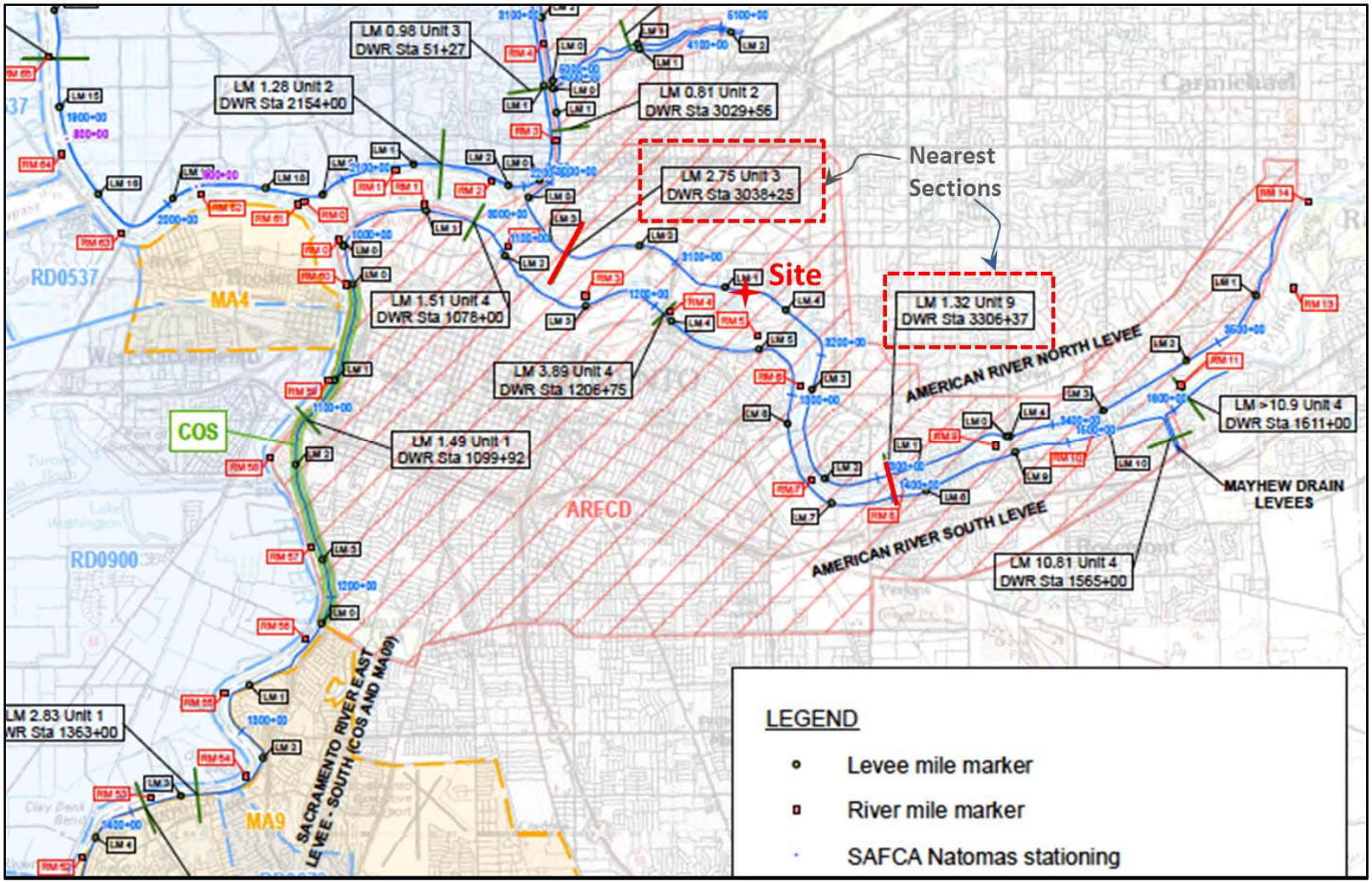

Figure C-1. Vicinity map showing the Cal Expo project site, levee mile (USACE) and river mile (CDWR) stationing, and nearest URS geologic sections to the east and west of the project site. Figure excerpted and modified from URS, 2009.

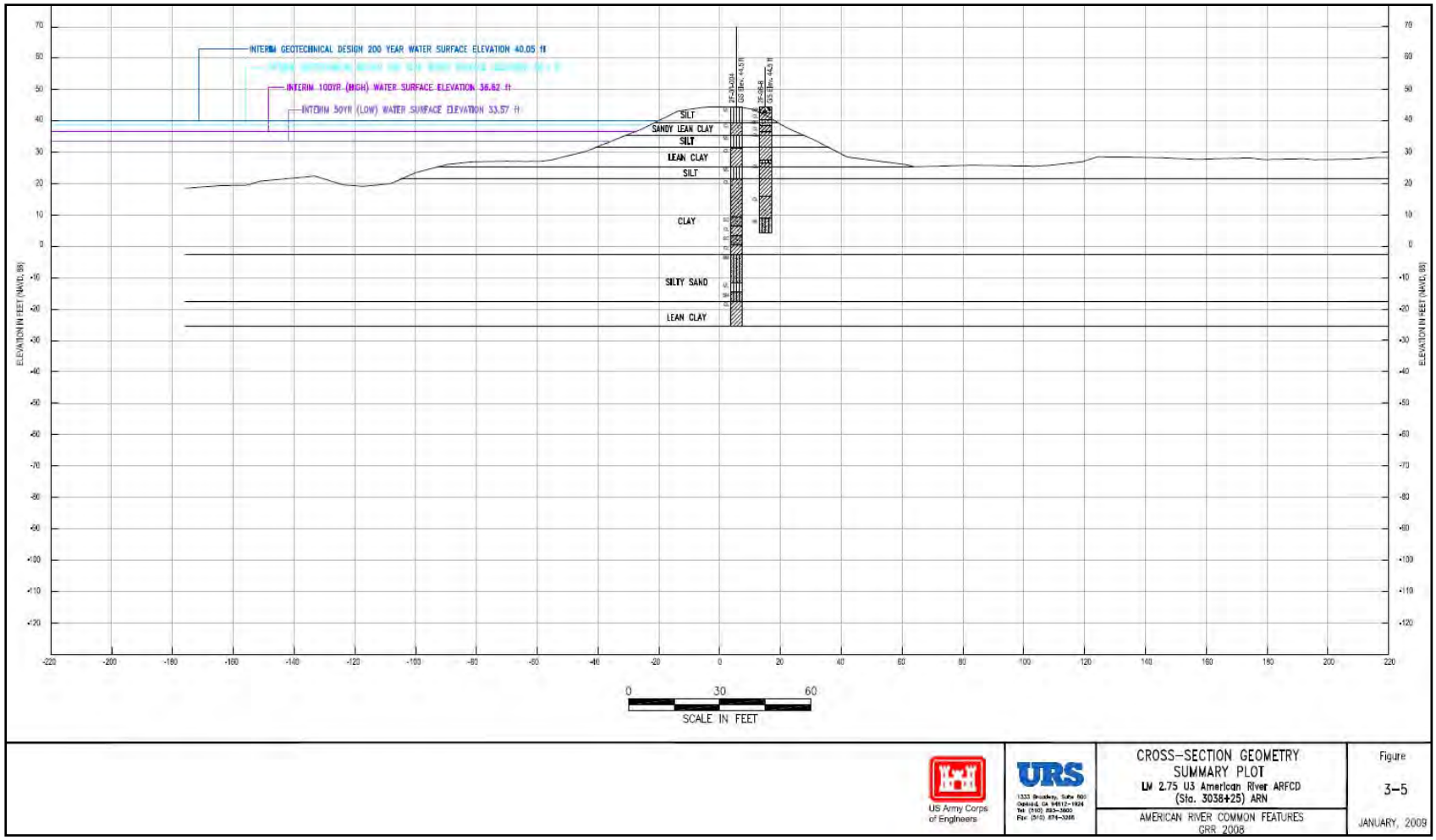

Figure C-2. Geologic Section at LM 2.75, Unit 3 (RM 3038+25 of the American River North levee) within the American River Flood Control District (ARFCD). Source: URS, 2009.

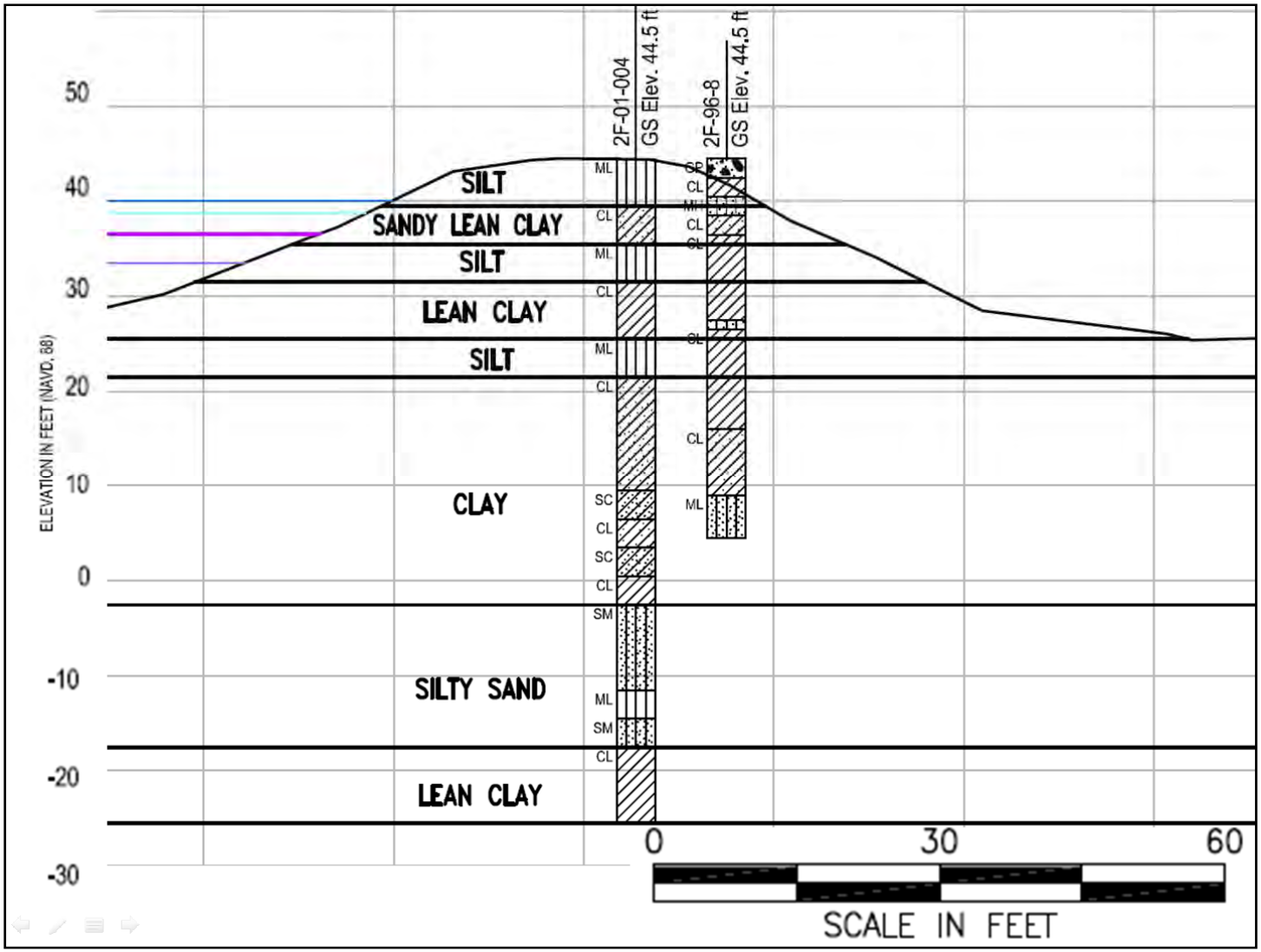

Figure C-3. Close-in view of soil borings at LM 2.75, Unit 3 (RM 3038+25 of American River North levee) within the American River Flood Control District (ARFCD) as shown on Figure C.2. Excerpted and modified from URS, 2009.

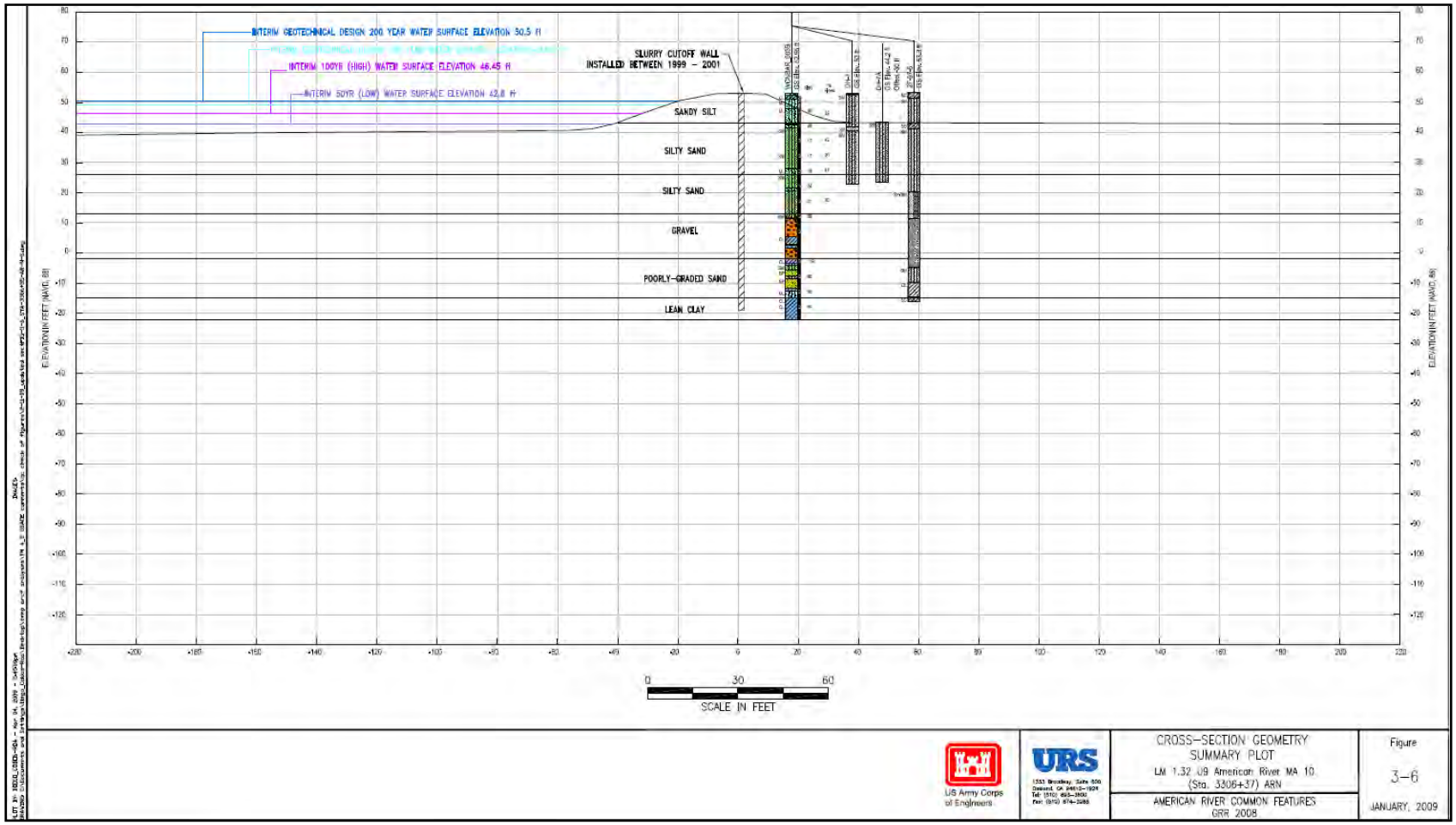

Figure C-4. Close-in view of soil borings at LM 1.32, Unit 9 (RM 3306+37 of American River North levee) within American River MA 10. Source: URS, 2009.

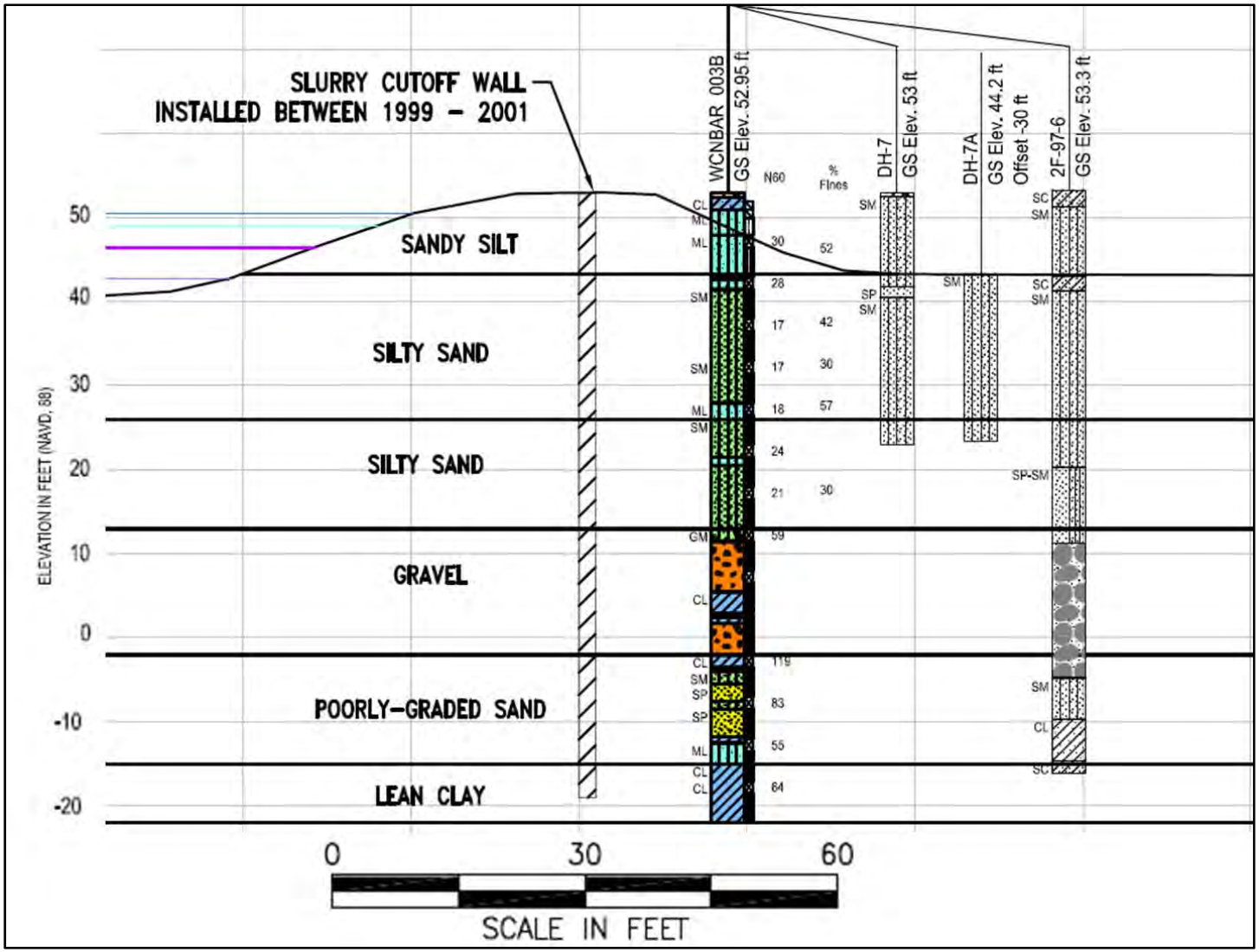

Figure C-5. Geologic Section at LM 1.32, Unit 9 (RM 3306+37) within American River MA 10. Excerpted and modified from URS, 2009.

Table C-1. Summary of strength parameters for sections at LM 1.32 U9 (DWR RM Sta. 3306+35) and LM 2.75 U3 (DWR RM Sta 3038+25) of the American River North levee.Source: URS 2009.

American River North - LM 1.32 U9 (DWR Sta. 3306+35)							
Material Description	Material Number	Strength for Partial Pool and Steady State		Strengths for Rapid Drawdown			
				Drained ($K_c = K_f$)		Undrained (K_c =1)	
		ϕ'	c'	ϕ'	c'	ψ	d
		(degrees)	(psf)	(degrees)	(psf)	(degrees)	(psf)
ML	1	35	0	35	0	14.6	480
SM	2	32	0	32	0	-	-
SM	3	33	0	33	0	-	-
GM	4	46	0	46	0	-	-
SP	5	40	0	40	0	-	-
CL	6	35	0	35	0	16.9	5078

American River North - LM 2.75 U3 (DWR Sta. 3038+25)							
Material Description	Material Number	Strength for Partial Pool and Steady State		Strengths for Rapid Drawdown			
				Drained ($K_c = K_f$)		Undrained (K_c =1)	
		ϕ'	c'	ϕ'	c'	ψ	d
		(degrees)	(psf)	(degrees)	(psf)	(degrees)	(psf)
ML	1	35	0	35	0		
CL	2	35	0	35	0	11.5	551
ML	3	33	0	33	0		
CL	4	35	0	35	0	11.5	1185
ML	5	33	0	33	0	11.8	1522
CL	6	33	0	33	0	10.2	1753
SM	7	40	0	40	0	-	-
CL	8	31	0	31	0	-	-

Table C-2. Index testing and blowcount summary for boring 2F-96-8 at American River North 3038+25. Source: URS 2009.

PROJECT NAME:	American River Common Features GRR
PROJECT NUMBER:	26816760.45300
Reach ID:	American River North 3038+25 2F-01-004

Analysis By:	Michael Kynett	Date:	9/30/2008
Check By:		Date:	

Highlight in green any assumed value

Inputs are highlighted in grey

INPUT DATA																
Boring ID	Ground Surface Elevation	Ground Water Elevation	Energy Ratio	Depth to Top of Sample	USCS Group Name and Symbol	Sampler Type	γ_m	Blows foot, N	% finer than No200	Liquid limit, LL	Plastic Index, PI	Moisture content	UU - s_u	ICU		Consol. σ'_{max}
														Confining stress	s_u	
(-)	(ft)	(ft)	(%)	(ft)	(-)	(-)	(pcf)	(-)	(%)	(%)	(%)	(%)	(psf)	(psf)	(psf)	(psf)
2F-96-8	42	22	80	0.5	GP	SPT	135	18	5							
2F-96-8	42	22	80	1	CL	SPT	110	24	90							
2F-96-8	42	22	80	2.5	MH	SPT	120	19	70							
2F-96-8	42	22	80	4.5	CL	SPT	110	15	85	28	8					
2F-96-8	42	22	80	8.5	CL	SPT	110	7	85							
2F-96-8	42	22	80	10.5	CL	SPT	110	5	85							
2F-96-8	42	22	80	12.5	CL	SPT	110	6	90							
2F-96-8	42	22	80	14.5	CL	SPT	110	6	90							
2F-96-8	42	22	80	16.5	CL	SPT	110	9	90							
2F-96-8	42	22	80	18.5	ML	SPT	120	9	57							
2F-96-8	42	22	80	22	CL	SPT	110	9	90							
2F-96-8	42	22	80	25.5	CL	SPT	110	8	90							
2F-96-8	42	22	80	29	CL	SPT	110	8	80							
2F-96-8	42	22	80	32.5	CL	SPT	110	34	58	29	15					
2F-96-8	42	22	80	36	SM	SPT	130	44	30							
2F-96-8	42	22	80	39	SM	SPT	130	71	30							

Assumed GW = 20 ft bgs and Energy Ratio =80%

Table C-3. Rational for strength parameter selection for cross section at American River North 3038+25. Source: URS 2009.

< X > signifies discarded data point suspected to be unreliable

A	B	C	D	E	F	G	H	I		J	L	M	N
Material Description	Material Number	Strength Type	Parameter	SPT	Boring Description	PI	CPT	Vane Shear Peak	Vane Shear Res.	Other	Selection	Unit Weight	Rationale
ML (1)	1	Drained	c' (psf) =								0	120	
			φ' (°) =	42							35		Friction angle reduced for conservatism
			σ'_p (psf) =										
		Undrained	s_u/σ'_{vc} =										
			s_u (psf) =										
CL (2)	2	Drained	c' (psf) =								0	110	
			φ' (°) =			35					35		
			σ'_p (psf) =	4,920							4,920		OCR = 6 based on correlations with N60
		Undrained	s_u/σ'_{vc} =	1.20							1.20		
			s_u (psf) =	1,000							1,000		
ML (3)	3	Drained	c' (psf) =								0	120	
			φ' (°) =	33							33		
			σ'_p (psf) =										
		Undrained	s_u/σ'_{vc} =										
			s_u (psf) =										
CL (4)	4	Drained	c' (psf) =								0	110	
			φ' (°) =			35					35		
			σ'_p (psf) =	11,400							11,400		OCR = 6 based on correlations with N60
		Undrained	s_u/σ'_{vc} =	1.20							1.20		
			s_u (psf) =	1,000							1,000		
ML (5)	5	Drained	c' (psf) =								0	120	
			φ' (°) =	33							33		
			σ'_p (psf) =	14,400							14,400		OCR = 6 based on correlations with N60
		Undrained	s_u/σ'_{vc} =										
			s_u (psf) =	1,600							1,600		
CL (6)	6	Drained	c' (psf) =								0	110	
			φ' (°) =			33					33		
			σ'_p (psf) =	16,000							16,000		OCR = 5 based on correlations with N60
		Undrained	s_u/σ'_{vc} =	2.00							0.83		su/σ'vc =0.23*5^0.8=0.83
			s_u (psf) =	1,500							1,500		
SM (7)	7	Drained	c' (psf) =								0	130	
			φ' (°) =	46							40		Friction angle reduced for conservatism
			σ'_p (psf) =										
		Undrained	s_u/σ'_{vc} =										
			s_u (psf) =										
CL (8)	8	Drained	c' (psf) =								0	110	
			φ' (°) =							31	31		
			σ'_p (psf) =										
		Undrained	s_u/σ'_{vc} =										
			s_u (psf) =										

Table C-4. Index testing and blowcount summary for boring WCNBAR_001B at American River North 3306+35. Source: URS 2009.

PROJECT NAME:	American River Common Features GRR
PROJECT NUMBER:	26816760.45300
Reach ID:	American River North 3306+35 WCNBAR_001B

Analysis By:	Michael Kynett	Date:	9/30/2008
Check By:		Date:	

Highlight in green any assumed value

Inputs are highlighted in grey

INPUT DATA

Boring ID	Ground Surface Elevation	Ground Water Elevation	Energy Ratio	Depth to Top of Sample	USCS Group Name and Symbol	Sampler Type	γ_m	Blows foot, N	% finer than No200	Liquid limit, LL	Plastic Index, PI	Moisture content	UU - s_u	ICU		Consol. σ'_{max}
														Confining stress	s_u	
(-)	(ft)	(ft)	(%)	(ft)	(-)	(-)	(pcf)	(-)	(%)	(%)	(%)	(%)	(psf)	(psf)	(psf)	(psf)
WCNBAR_001B	52.95	41.5	83	5	ML	SPT	120	22	35							
WCNBAR_001B	52.95	41.5	83	10	SM	SPT	130	20	15							
WCNBAR_001B	52.95	41.5	83	15	SM	SPT	130	12	35							
WCNBAR_001B	52.95	41.5	83	20	SM	SPT	130	12	30							
WCNBAR_001B	52.95	41.5	83	25	ML	SPT	120	13	35							
WCNBAR_001B	52.95	41.5	83	30	SM	SPT	130	17	20							
WCNBAR_001B	52.95	41.5	83	35	SM	SPT	130	15	30							
WCNBAR_001B	52.95	41.5	83	40	GM	SPT	135	43	15							
WCNBAR_001B	52.95	41.5	83	55	CL	SPT	110	86	35							
WCNBAR_001B	52.95	41.5	83	60	SM	SPT	130	60	35							
WCNBAR_001B	52.95	41.5	83	65	ML	SPT	120	40	35							
WCNBAR_001B	52.95	41.5	83	70	CL	SPT	110	46	35	25	8					

Table C-5. Rational for strength parameter selection for cross section at American River North 3306+35. Source: URS 2009.

Study Section: American River North Levee LM 1.32 U9 (DWR Sta. 3306+35). Data From borings WCNBAR_003B

< X > signifies discarded data point suspected to be unreliable

A	B	C	D	E	F	G	H	I		J	L	M	N
Material Description	Material Number	Strength Type	Parameter	SPT	Boring Description	PI	CPT	Vane Shear Peak	Vane Shear Res.	Other	Selection	Unit Weight	Rationale
ML (1)	1	Drained	c' (psf) =								0	120	
			φ' (°) =	45							35		Friction angle reduced for conservatism
			σ'_p (psf) =	5,700							5,700		OCR > 10 based on correlations with N60
		Undrained	s_u/σ'_{vc} =	6.40							1.45		Assume OCR = 10 for max. past pressure calc.
			s_u (psf) =	3,800							3,800		su/σ'vc =0.23*10^0.8=1.45
SM (2)	2	Drained	c' (psf) =								0	130	
			φ' (°) =	32							32		
			σ'_p (psf) =										
		Undrained	s_u/σ'_{vc} =										
			s_u (psf) =										
SM (3)	3	Drained	c' (psf) =								0	130	
			φ' (°) =	33							33		
			σ'_p (psf) =										
		Undrained	s_u/σ'_{vc} =										
			s_u (psf) =										
GM (4)	4	Drained	c' (psf) =								0	135	
			φ' (°) =	45							45		
			σ'_p (psf) =										
		Undrained	s_u/σ'_{vc} =										
			s_u (psf) =										
SP (5)	5	Drained	c' (psf) =								0	130	
			φ' (°) =	49							40		Friction angle reduced for conservatism
			σ'_p (psf) =										
		Undrained	s_u/σ'_{vc} =										
			s_u (psf) =										
CL (6)	6	Drained	c' (psf) =								0	110	
			φ' (°) =			35					35		
			σ'_p (psf) =	<54,000>							54,000		OCR > 10 based on correlations with N60
		Undrained	s_u/σ'_{vc} =	2.00							2.00		Assume OCR = 10 for max. past pressure calc.
			s_u (psf) =	8,200							8,200		

US Army Corps
of Engineers
Sacramento District

AMERICAN RIVER WATERSHED PROJECT (COMMON FEATURES), CALIFORNIA RIGHT (NORTH) BANK LEVEE STRENGTHENING

AMERICAN RIVER
CALIFORNIA

FY-1999

METRIC

Approved
Chief, Engineering Division
Date: 13 Apr 99

Prepared Under the Direction of
MICHAEL J. WALSH
LTC, US Corps of Engineers, District Engineer

Approved
Chief, Central Valley Section
Date: 12 Apr 99

Prepared by
SACRAMENTO DISTRICT
CENTRAL VALLEY SECTION

Approved
Chief, Central Valley Section
Date: 12 Apr 99

Designed by
J. MOORE
D. ROBERSON

Drawn by
J. MOORE
D. ROBERSON

Sec. No.
9985

Design File No.
401-4-1933

AMERICAN RIVER
AMERICAN RIVER WATERSHED PROJECT
(COMMON FEATURES), CALIFORNIA
RIGHT (NORTH) BANK LEVEE STRENGTHENING
COVER SHEET

Sheet reference number:
G-1
SEQ 1

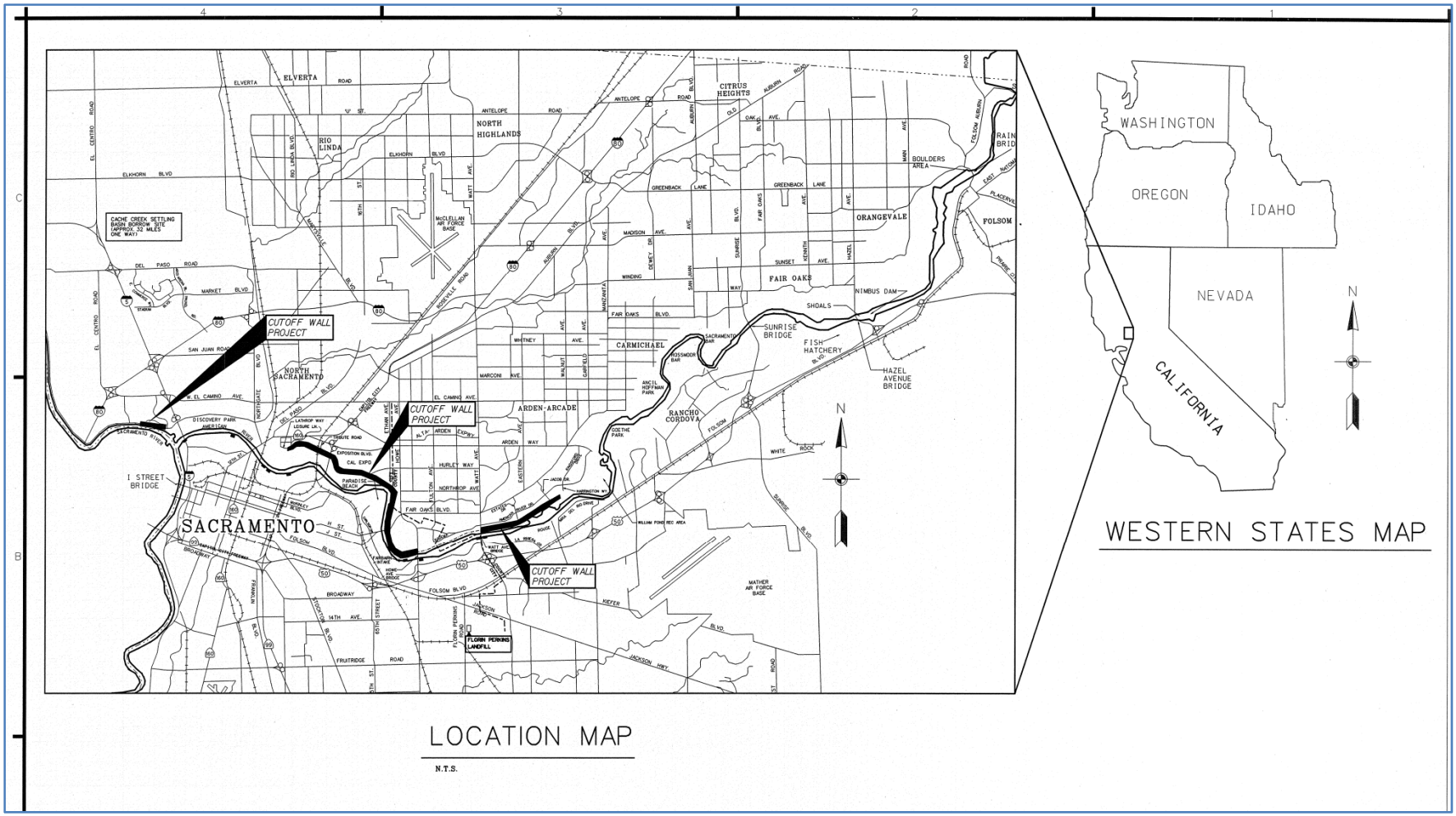

Figure C-6. Site location map showing the extent of levee improvements covered in the American River Watershed Project . Source: USACE, 1999.

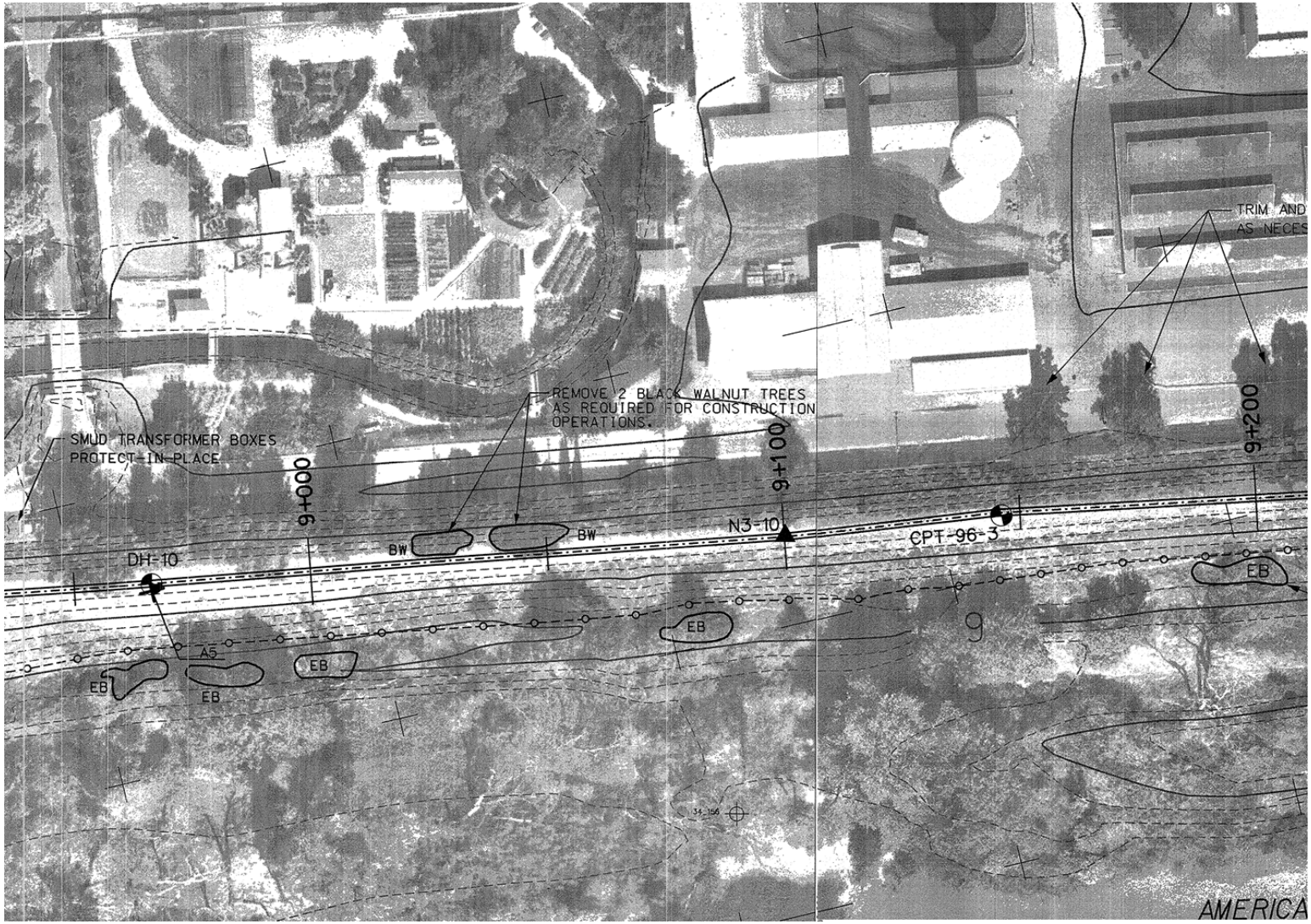

Figure C-7. Excerpt from the American River Watershed Project involving construction of a slurry wall along segments of the American River levees. Our study site is at Station 9+100 on the plan where a pipeline labeled N3-10 is shown crossing the levee. This is likely the pipeline encountered during our study. The Eucalyptus tree under study appears to be intact in the photograph. Source: USACE, 1999.

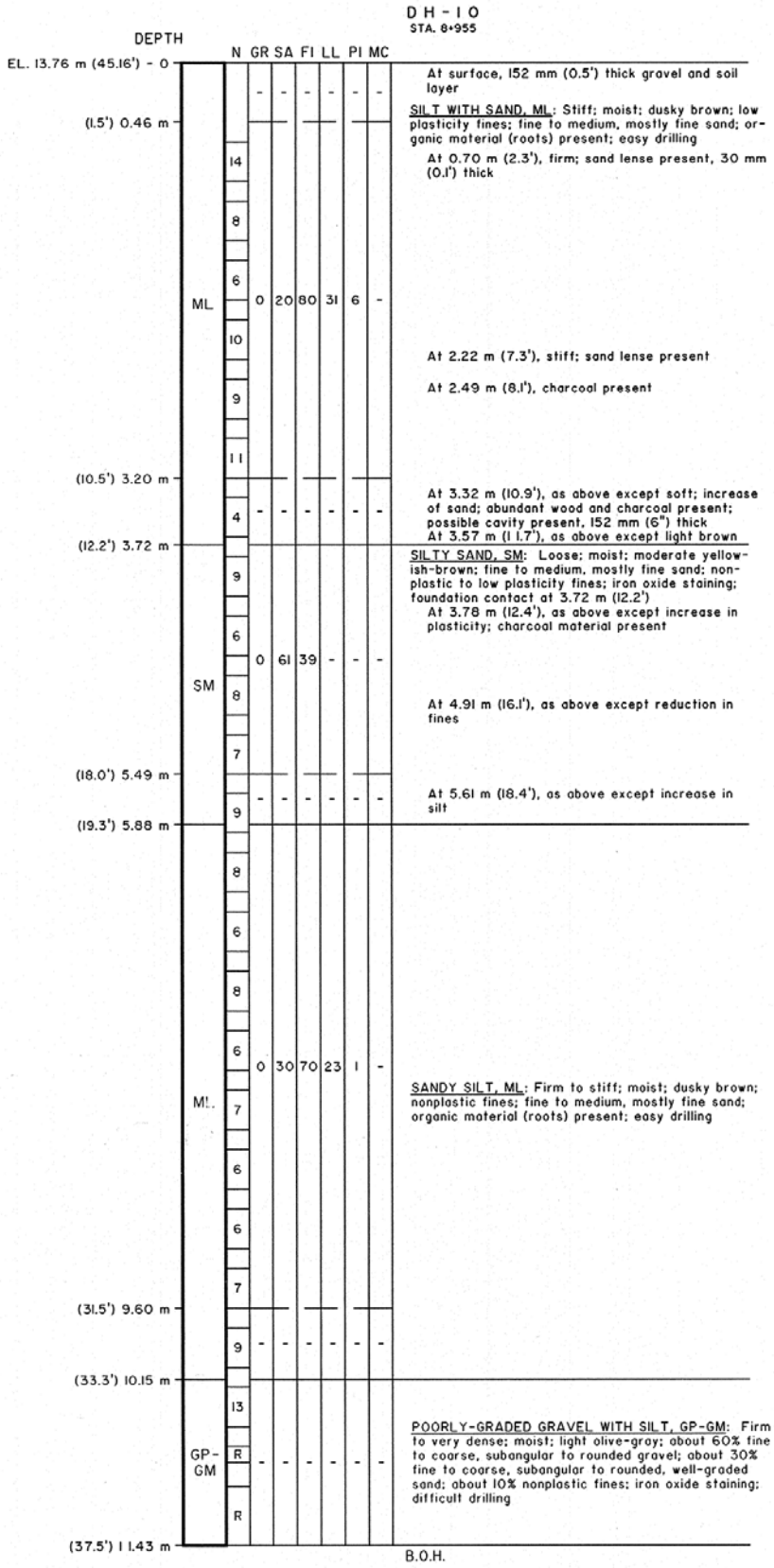

Figure C-8. Boring log DH-10 as shown on Figure C.7. Source: USACE, 1999.

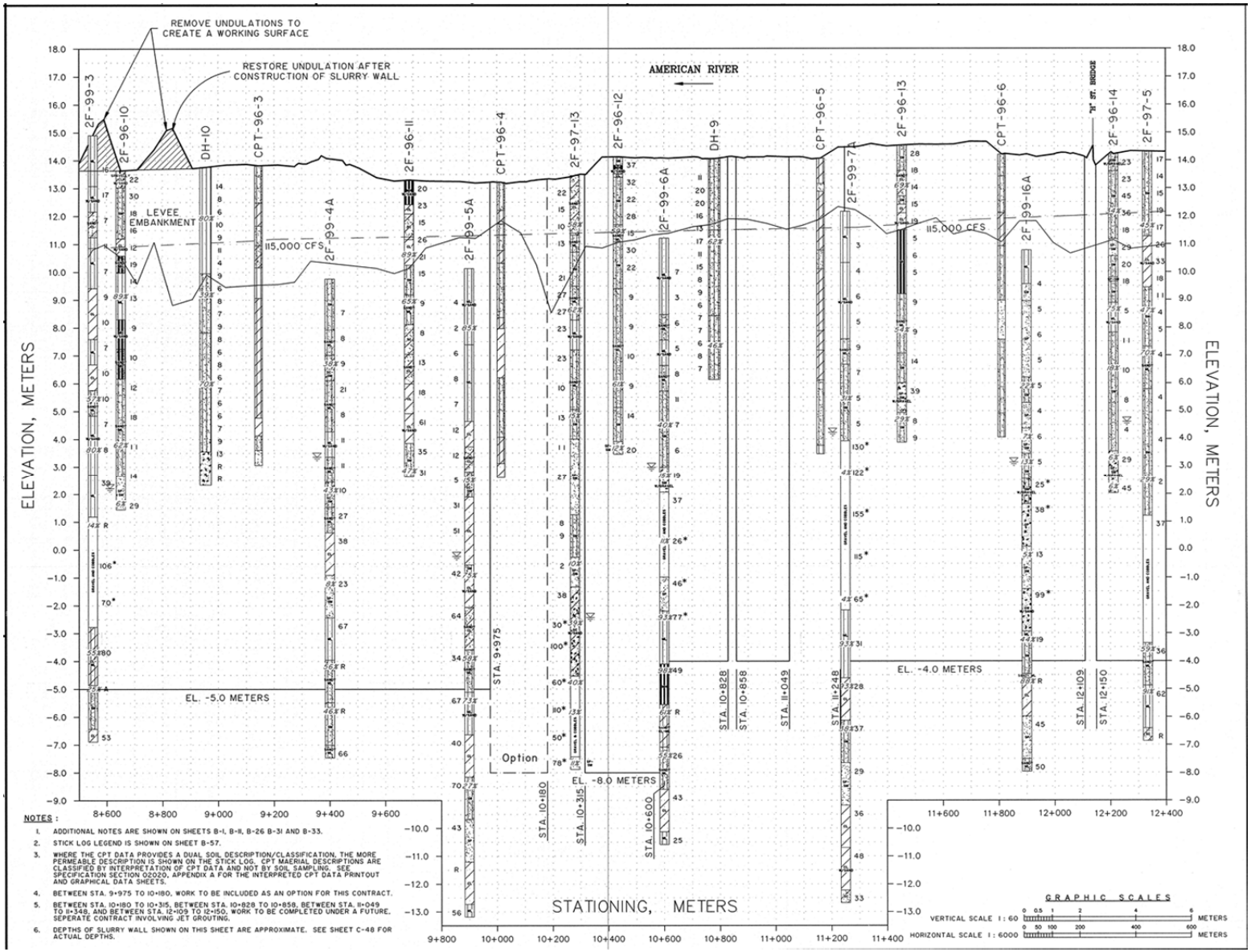

Figure C-9. Profile view along levee showing available soil data. Source: USACE, 1999.

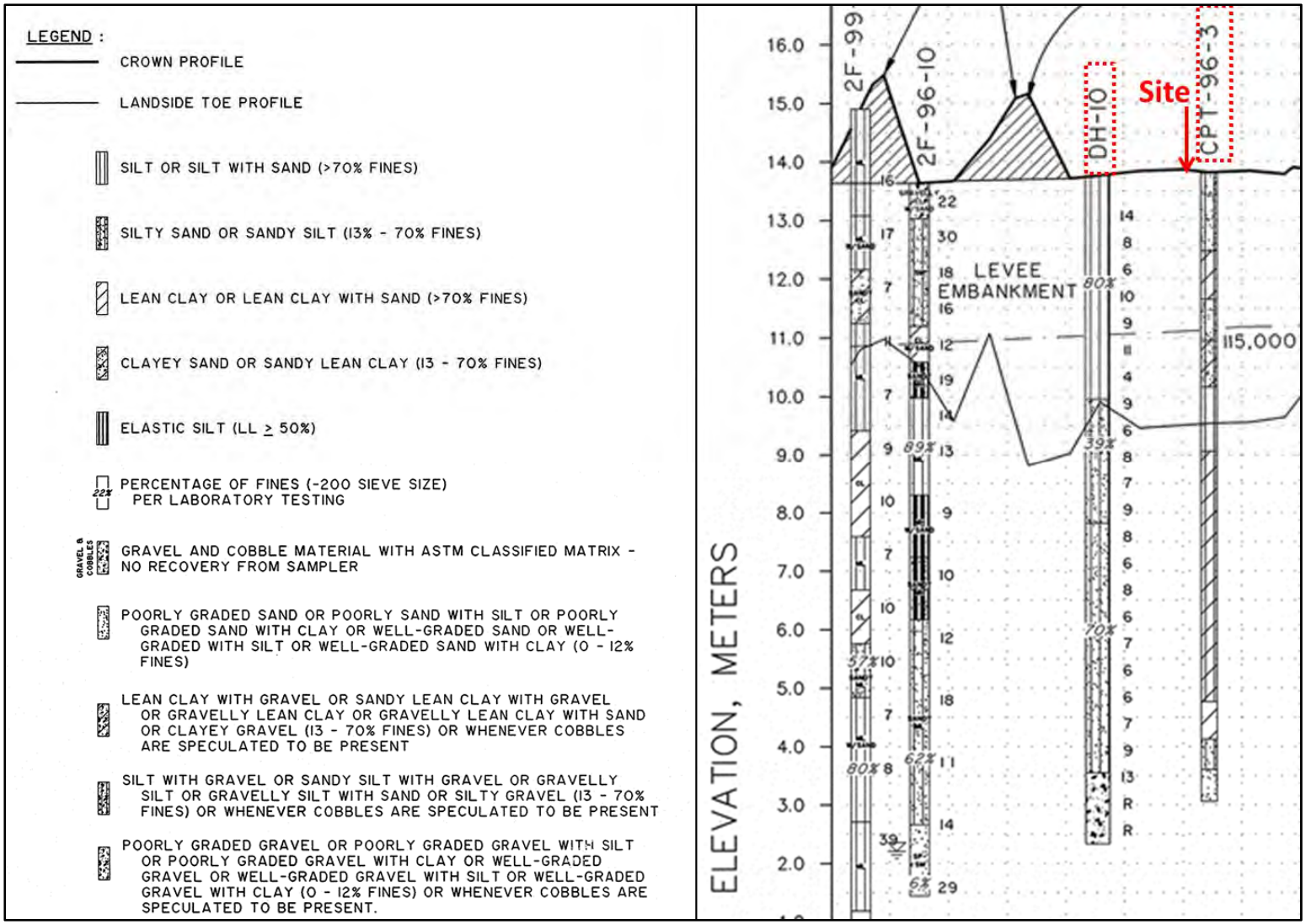

Figure C-10. Legend for Figure C.9 and close in view showing our study site in the context of the closest soil boring and cone penetration test (CPT) data. Source: USACE, 1999.

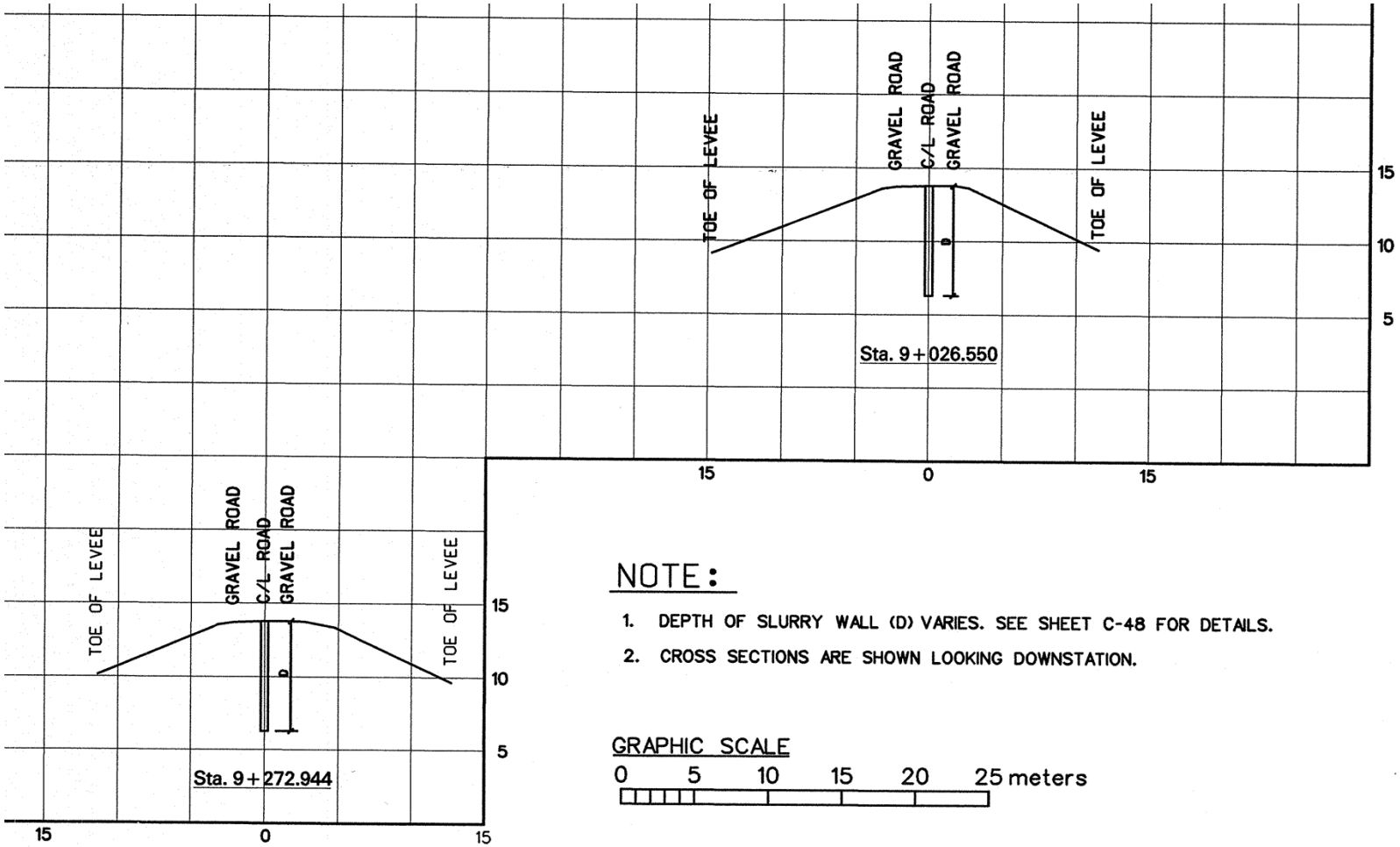

Figure C-11. Levee cross sections in the vicinity of our study site. The study site is at approximately Station 9+100. Source: USACE, 1999.

Utility Crossing Survey Point	Station (m)	Have As-Built	LS Levee Height (m)	Depth Below Crown (m)	diameter (in)	number of pipes/ distance apart (m)	Pipe Material	Utility Type
N3–10	09+100.889		4.3	5.5	1.	1	Galvanized	Water

Agency of ownership and jurisdiction	Reference to other sheets	bypass diameter if service pipe is tapped (inches)	flow rate minimum if separate hose and pump used (GPM)
Cal Expo SEE NOTES 4 SHT U-6	U-6 U-4 U-11 spec 01500-1.6.2	1"	N/A

Accommodation	Confirmation Method
COMPLETE REMOVAL OR REMOVE SEGMENTS & PLUG PIPE – RELOCATE PIPE CLOSER TO CREST	STANDARD POTHOLE PROCEDURE FROM WATER SIDE TOE

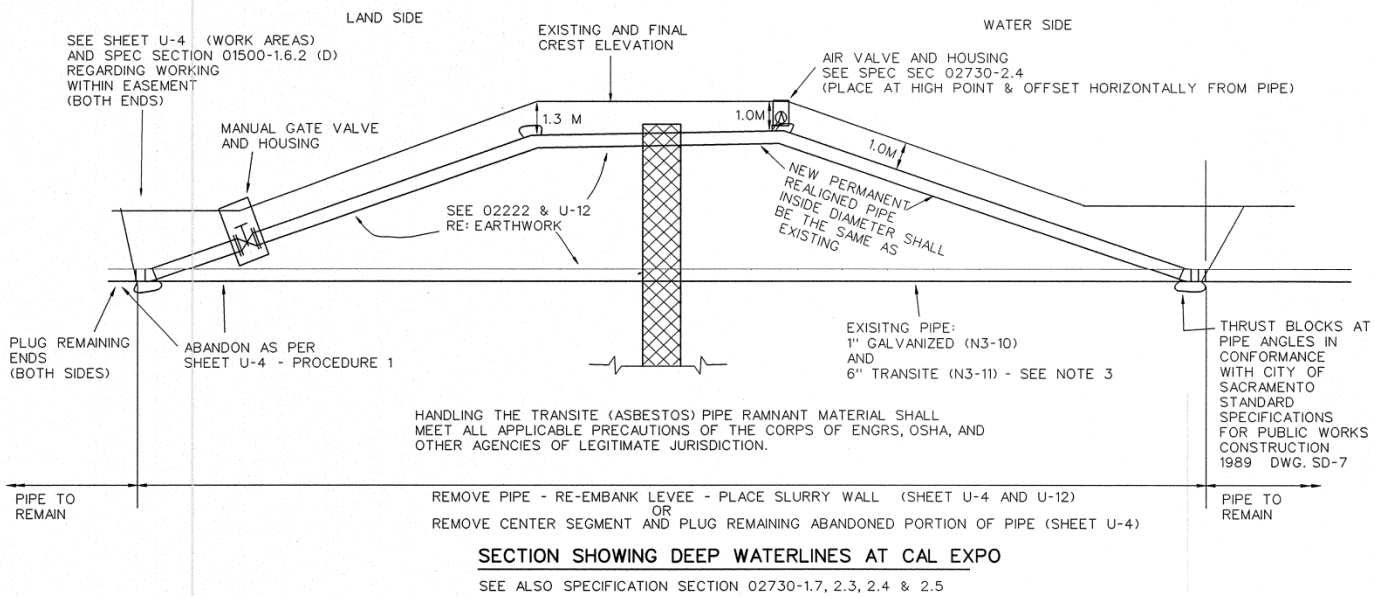

Figure C-12. Notes regarding the pipe N3-10 intersecting the study site. The pipe is shown to be a 1 inch galvanized water line that was re-routed as shown as part of the American River Watershed Project in 1999. Source: USACE, 1999.

DESIGN MEMORANDUM NO. 1

AMERICAN RIVER PROJECT, CALIFORNIA

AMERICAN RIVER LEVEE GENERAL DESIGN

25 JUNE 1956

9

SACRAMENTO DISTRICT

CORPS OF ENGINEERS

U. S. ARMY

SACRAMENTO, CALIFORNIA

Paragraphs 9 and 10 were excerpted from the American River Levee General Design (USACE, 1956) and provide an understanding of what is known of the levee history at the project site. The was constructed to USACE project standards in 1955 as summarized in paragraphs 9 and 10 below:

9. Existing Left Bank Project Levee: The existing left bank levee which protects portions of the city of Sacramento was constructed by the Sacramento District as a part of the Sacramento River Flood Control Project and completed to project standards in 1948. It extends from high ground at Mayhews downstream 10.8 miles to the mouth of the American River where it meets the left bank levee of the Sacramento River. The levee was designed and constructed to pass the Sacramento River Flood Control Project design flow (before Folsom Dam) on the American River of 180,000 c.f.s. with a freeboard of 3.0 feet and without reclamation of the north bank flood plain upstream from North Sacramento. The levee has a crown width of 20 feet, 1 on 3 riverside and 1 on 2 landside slopes and has a gravel surfacing for patrol purposes. At three locations the riverbank and levee were provided with a total of 3,000 lineal feet of bank protection as an emergency measure during and following the floods of November 1950. Intercepted interior drainage is collected by a system of ditches and is pumped over and/or through the levee at several locations. The levee and pumping plants are maintained and operated by local interests.

10. Existing Right Bank Project Levee: The existing right bank levee, which protects the city of North Sacramento, was constructed by the Sacramento District as a part of the Sacramento River Flood Control Project and completed to project standards in 1955. It extends from high ground near the junction of Howe Avenue and Arden Way downstream 3.0 miles to a junction with the left bank levee of the Natomas Canal (about 2 miles above the mouth of the American River). This levee was designed and constructed for the same flow conditions as the south levee (see paragraph 9). The levee has a crown width of 20 feet, a variable riverside slope (below the flood plane of 1 on 3 and above the flood plane of 1 on 2) and a landside slope of 1 on 2. It is gravel surfaced for patrol purposes. Intercepted interior drainage is collected by a system of ditches and is pumped over and/or through the levee at several locations. The levee and pumping plants are maintained and operated by local interests.

Figures C-13 and C.-14 show a site plan and section view, respectively, of the existing and proposed site elevations at the time of the American River Levee General Design report in June of 1956.

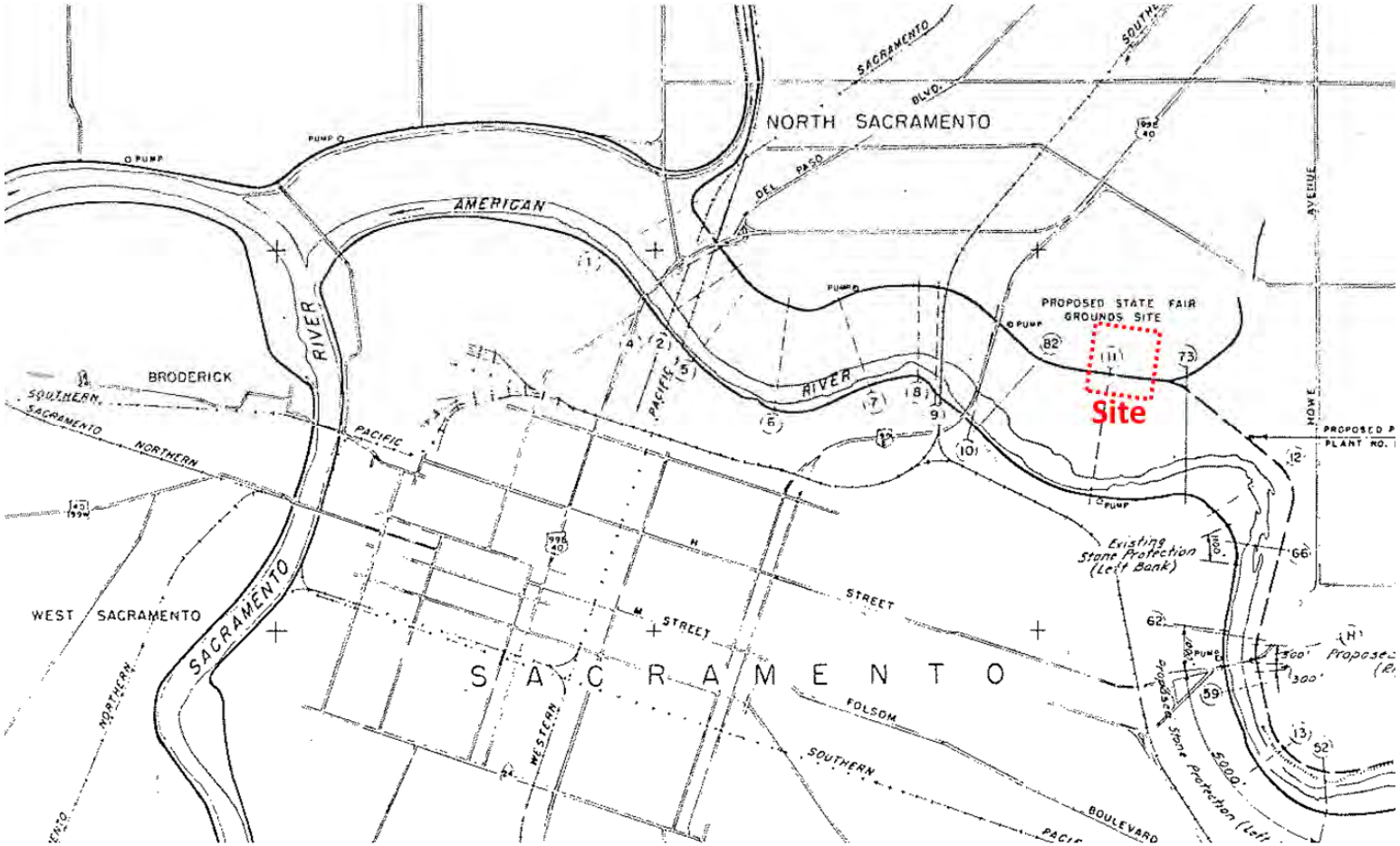

Figure C-13. Plan view showing site location. The site is shown located at section 11. Source: USACE, 1956.

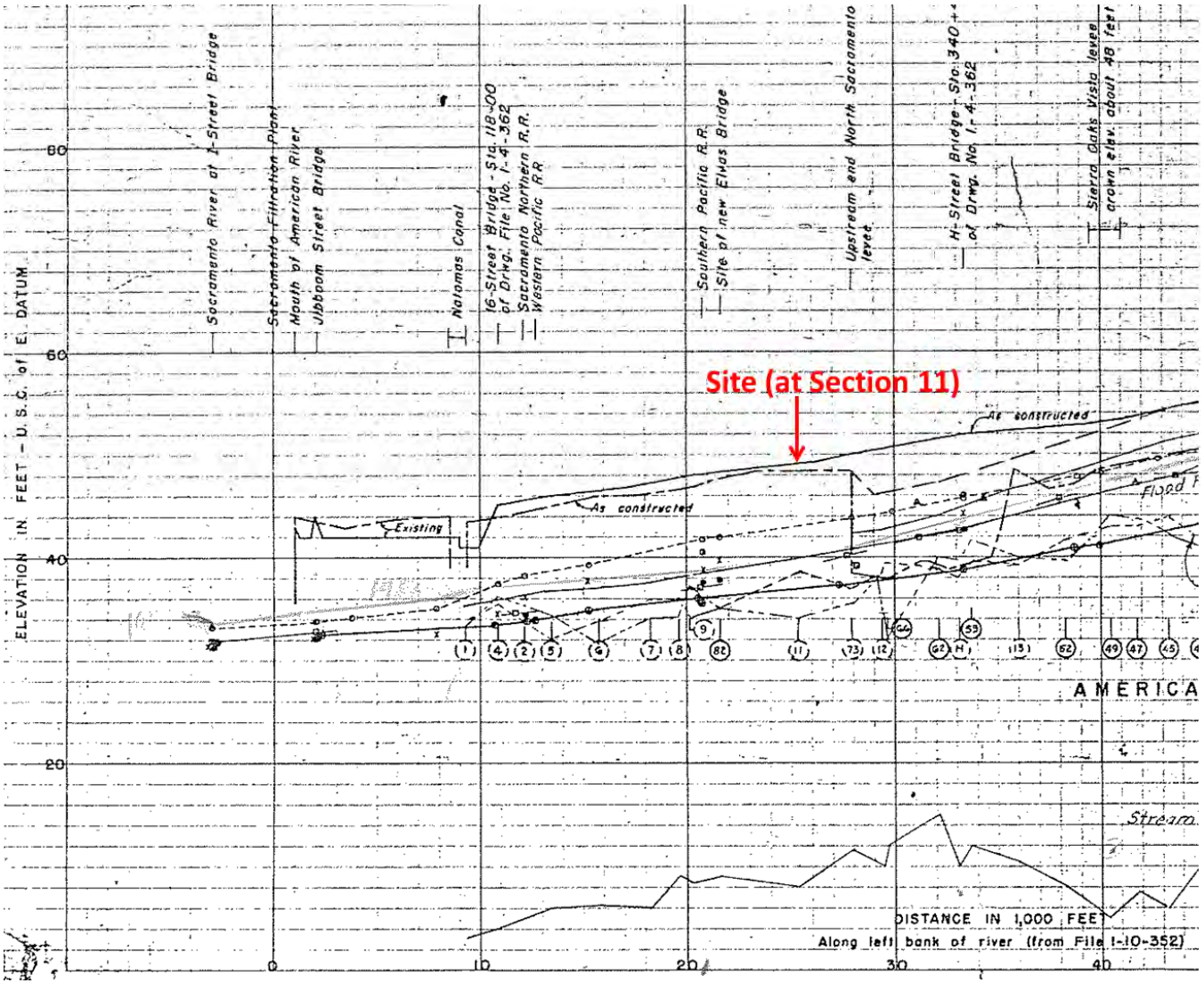

Figure C-14. Cross section view along the levee showing the crest elevation of existing and proposed levees at the time of the American River Levee General Design report dated June of 1956. It appears that the site, shown at section 11, was not proposed to be raised from an elevation of approximately 48.5 feet (NGVD29, or 51 feet NAVD88) at the time of the report in 1956. Source USACE, 1956.

APPENDIX D: TRENCH LOGS

Appendix D

Geologic sections as well as plan view and wall view trench logs are presented herein. Geologic sections are based on a set of 10 primary materials found at our study site (Figure D-1). Onsite materials consisted primarily of silts with varying amounts of clay and sand, silty sands, and lean clays. These findings are generally consistent with the findings of our soil borings (Appendix A) as well as soil information available through others (Appendix C). Subsurface stratigraphy for the segments between the trenches is shown for the control trench (Figure D-2) and the stump trench (Figure D-3).

Wall and plan view field logs typically used symbols to distinguish live and decomposing roots, pipes and other findings. A legend of symbols used is provided as Figure D-4. Plan view logs of the root system encountered in the trenches is shown on Figures D-5 and D-6. Wall logs of the uphill wall of the lower trench and the downhill wall of the upper trench are presented on Figures D-7 through D-10. Figures D-11 through D-20 break down the plan view logs into small segments and show corresponding photographs spliced together for each segment. Wall logs with corresponding spliced photographs are presented on Figures D-21 through D-31.

SOIL TYPES:

1. Sandy silt with clay (ML), brown, moist, occasional rounded to sub-rounded gravels; sand is fine-grained and uniform. Fine roots.
1a. Sandy silt with clay (ML), brown, moist, occasional rounded to sub-rounded gravels; sand is fine-grained and uniform.
2. Sandy silt/silty sand (ML/SM), brown, moist, occasional sub-rounded gravels, sand very fine grained and uniform, trace clay.
3. Clayey silt (ML) with sand, mottled dark brown and brown, moist, light cementation, trace sand
3a. Clayey silt (ML), dark brown, light cementation and soils structure
3b. Sandy silt (ML) with clay, brown
4. Silty clay/clayey silt (ML/CL), olive brown with reddish oxidation stains
5. Sandy silt (ML) with silty sand (SM) pockets, brown, moist, trace clay, sand is fine to medium grained
6. Silty sand (SM), olive brown, fine uniform sand, lightly cemented
7. Sandy silt to silty sand (ML/SM), light brown, very fine grained sand
8. Sandy silt (ML), brown, moist, weakly cemented
9. Heterogeneous blend of Materials 2 and 3b
10. Silty sand (SM) with clay, brown, moist

Figure D-1. Key to soil material types. Materials listed as ML/SM or ML/CL are materials of borderline classification where the material varies in classification somewhat across the layer.

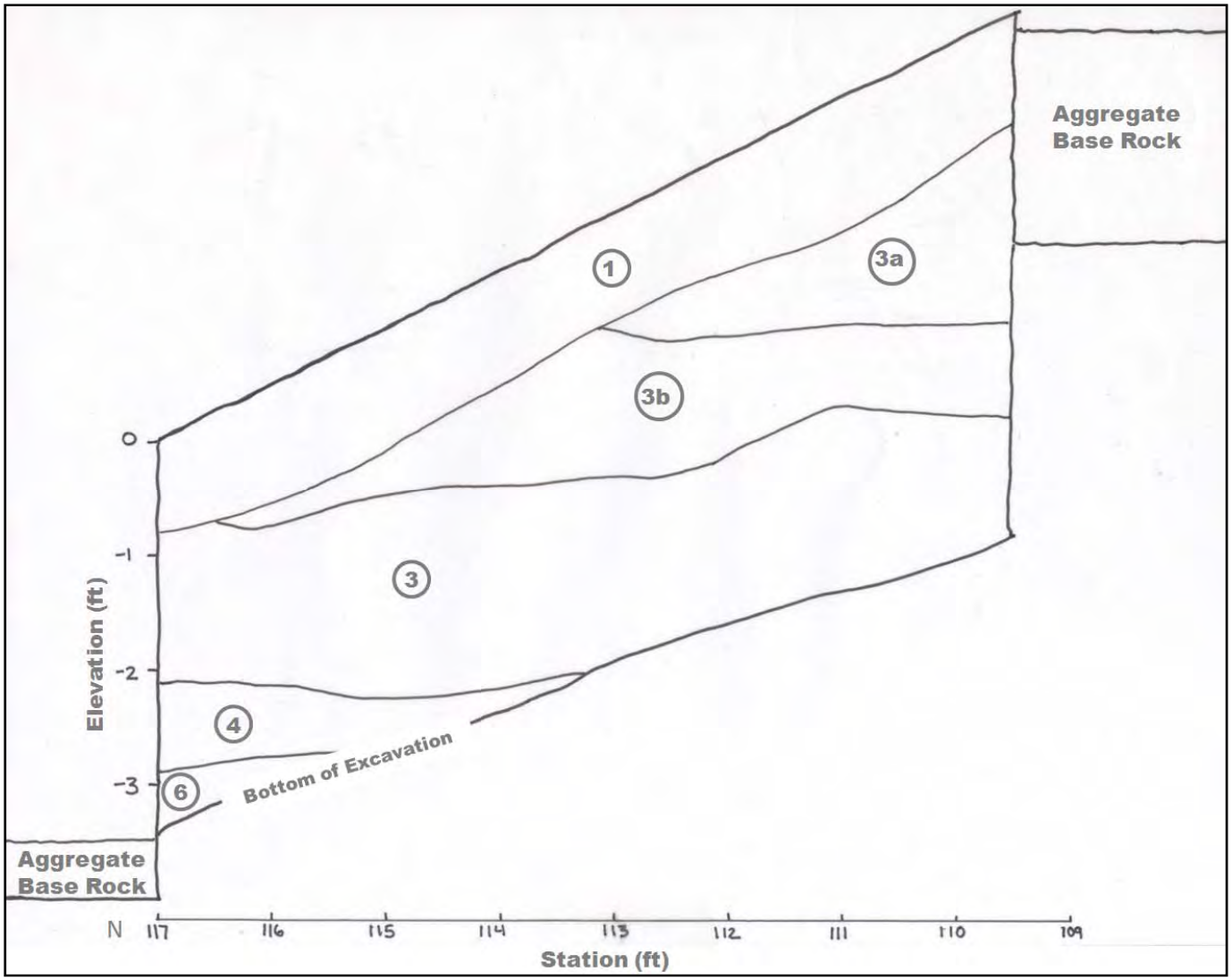

Figure D-2. Trench log at Station 125 east along control trench spanning from the upper to lower trenches (Station 109.5 to 117 north). Geologic key provided on Figure D-1.

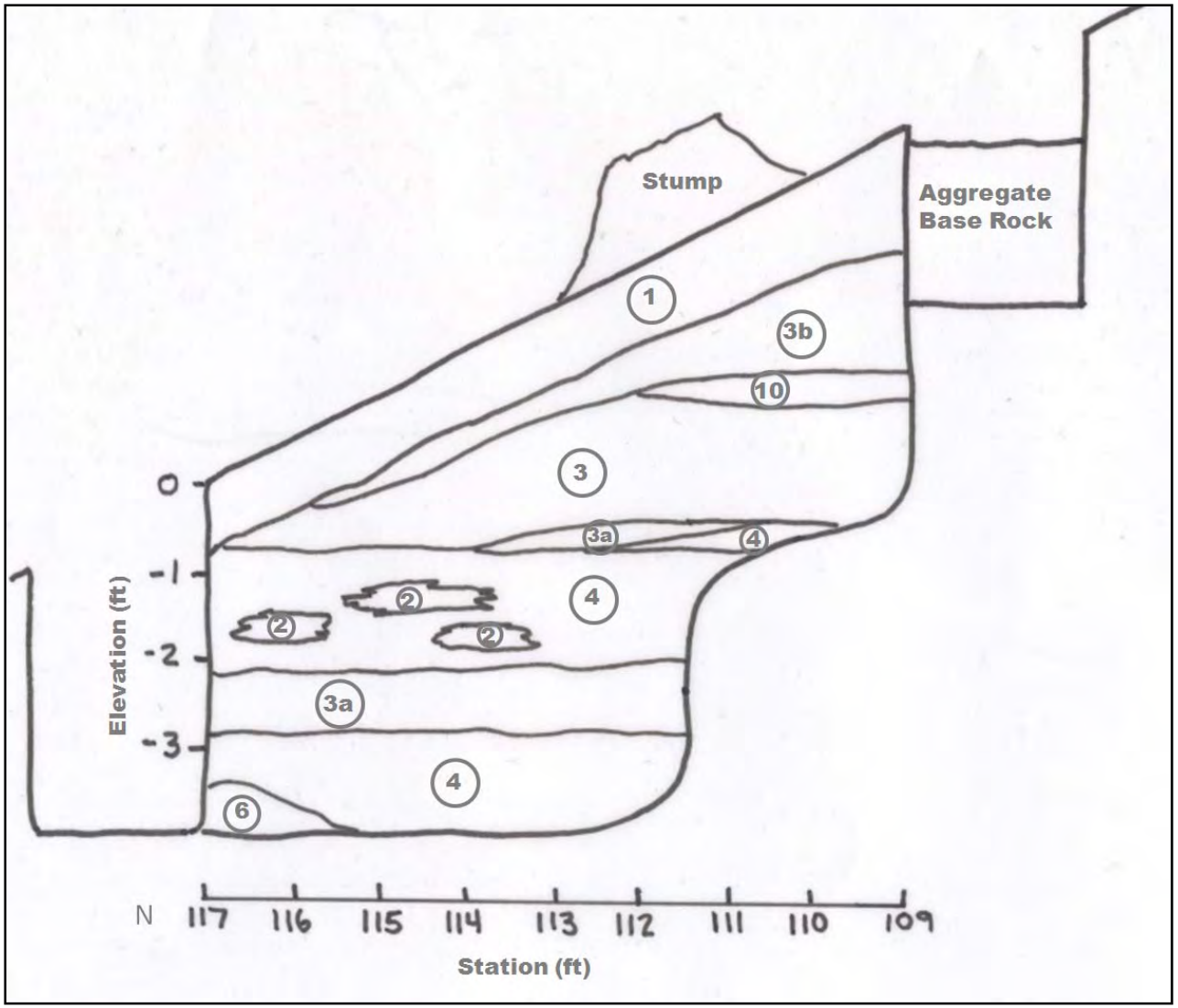

Figure D-3. Trench log at Station 148 east at the eucalyptus stump and spanning between the upper to lower trenches (Station 109.5 to 117 north). Geologic key provided on Figure D-1.

LEGEND

Wall Logs:

Animal Burrow

Pipe

Live Root

Soil layer transition

Zone of biological activity (ants burrowing)

Decomposing Root

10 Soil type (see list of soil types for material descriptions)

Plan View Logs:

Decomposing Root

Live Root

Pipe

Figure D-4. Key to plan view and wall view trench logs.

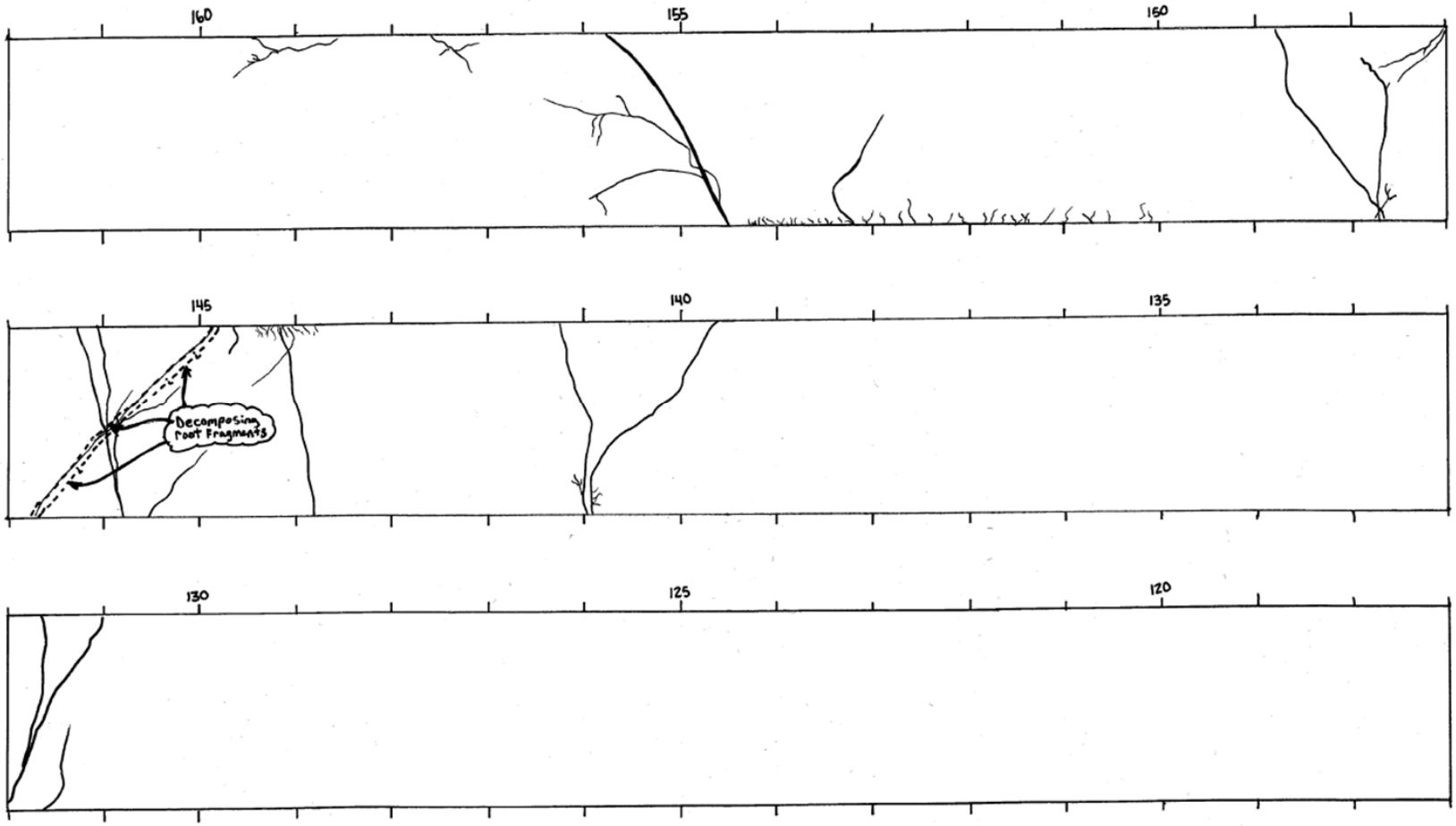

Figure D-5. Upper stump and control trench plan view logs (Stations 117-162).

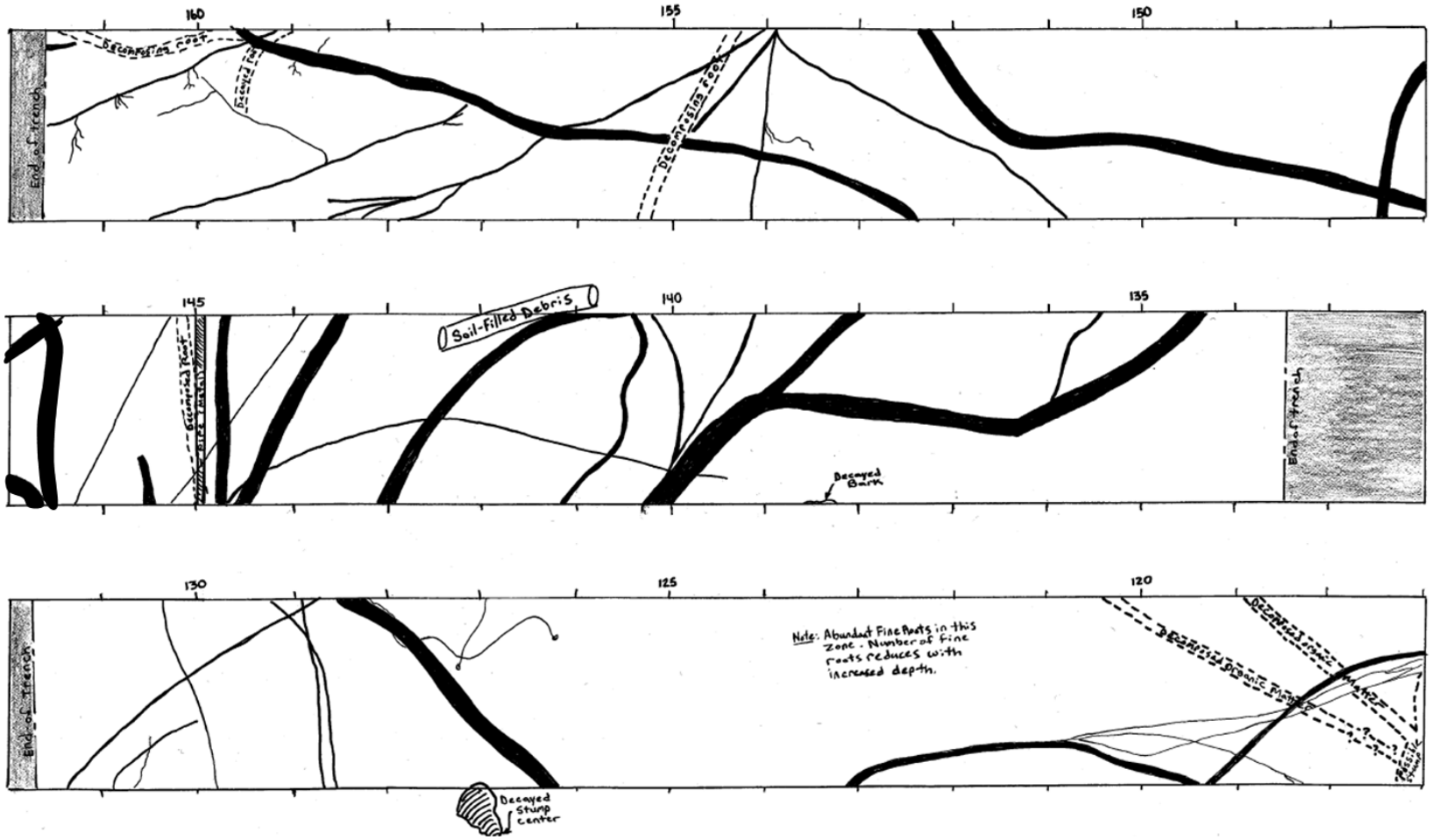

Figure D-6. Lower stump and control trench plan view logs (Stations 117-161.5).

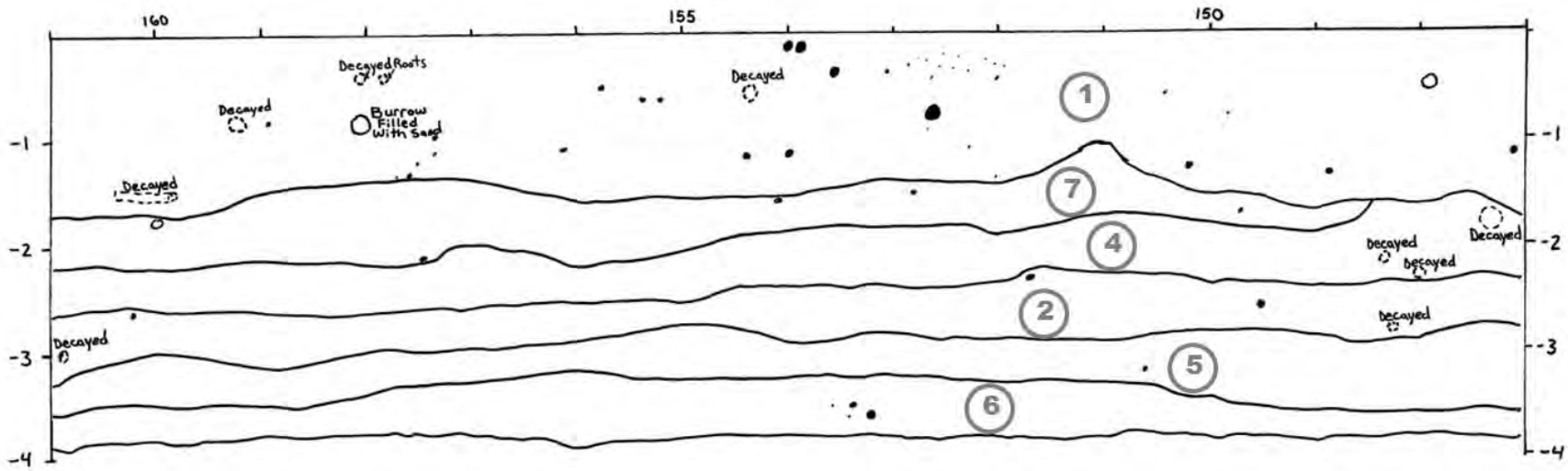

Figure D-7. Log of uphill wall of the lower stump trench, Stations 147 to 161.

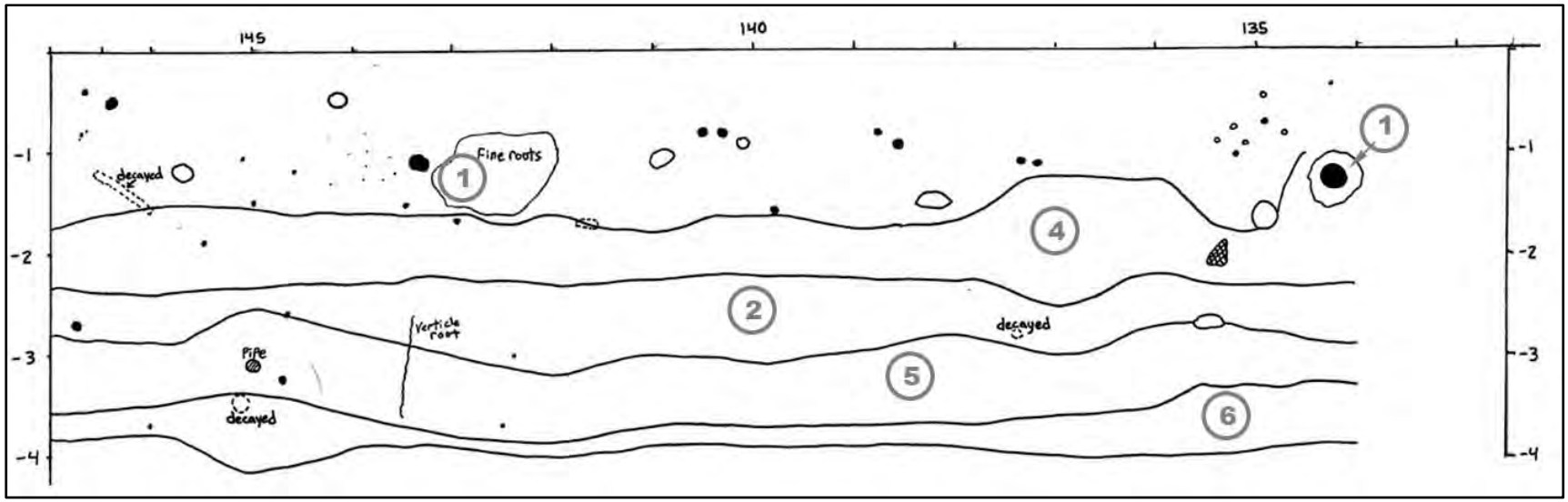

Figure D-8. Log of uphill wall of the lower stump trench, Stations 133 to 147.

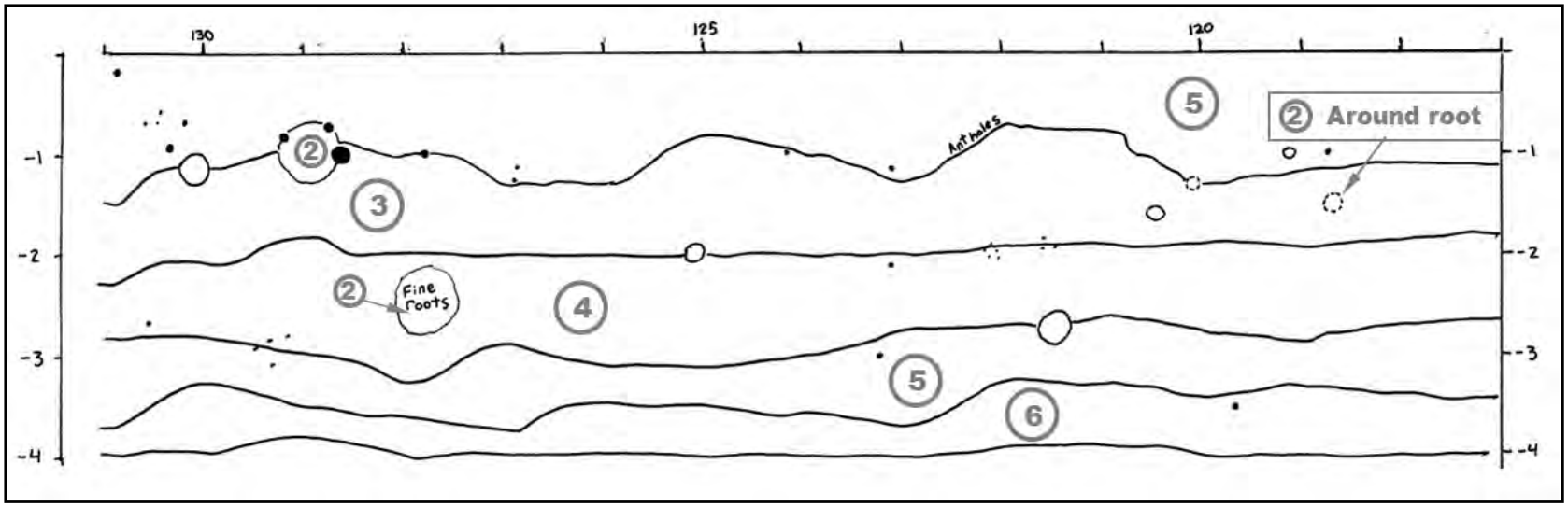

Figure D-9. Log of uphill wall of the lower control trench, Stations 117 to 131.

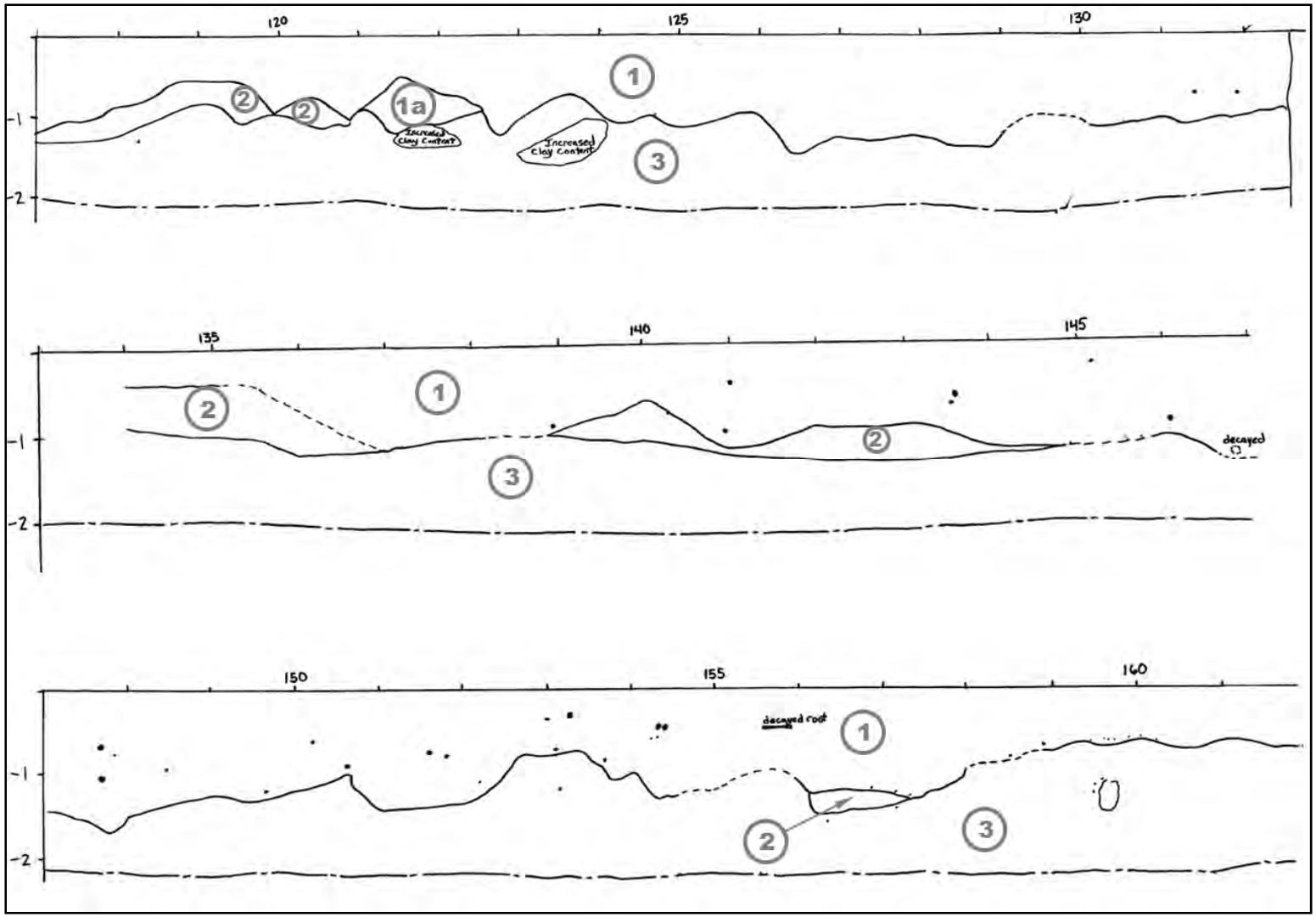

Figure D-10. Log of downhill wall of the upper trenches, Stations 117 to 162.

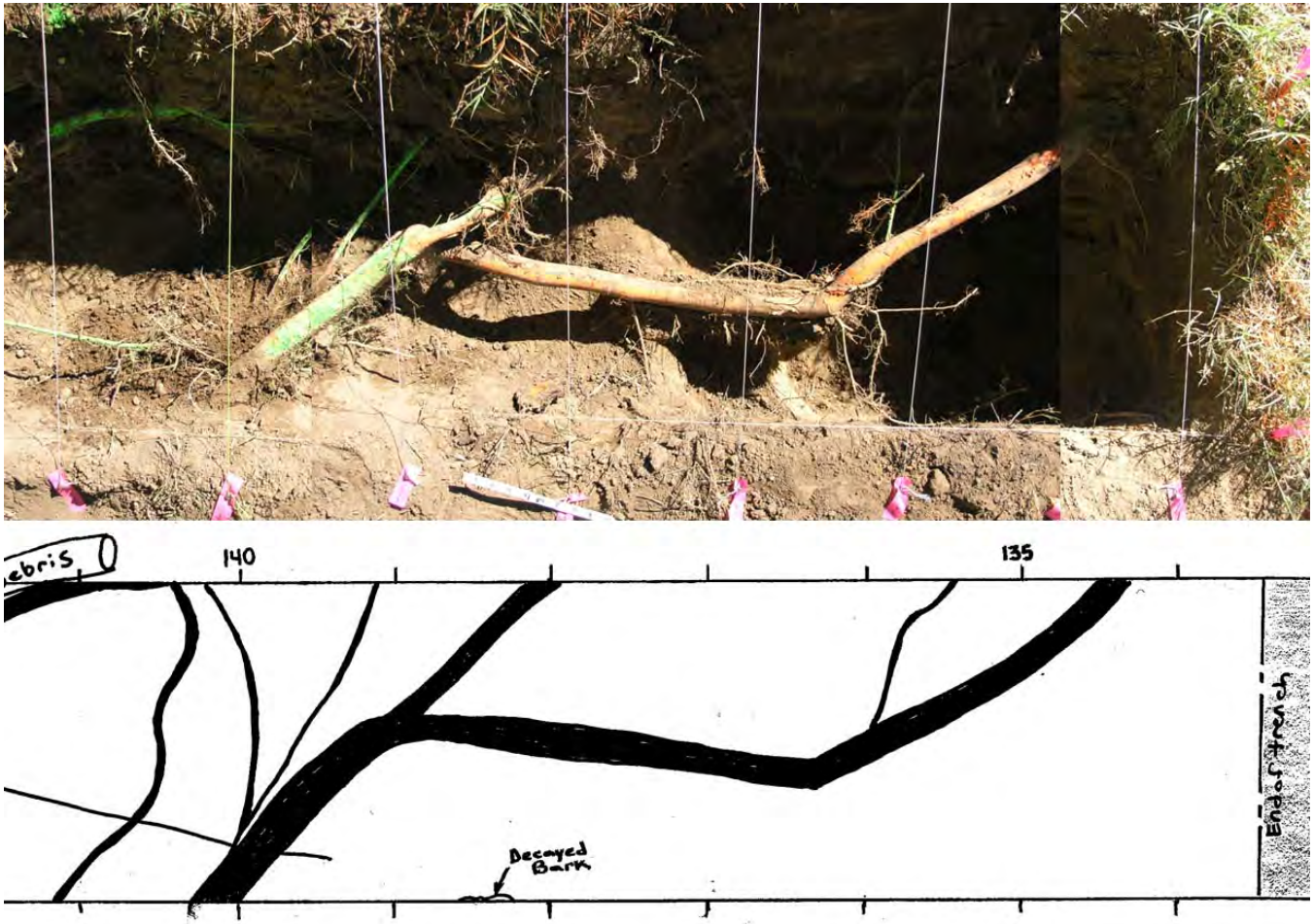

Figure D-11. Lower stump trench Stations 133-141.5. Spliced plan view photos (top) during excavation of lower stump trench. Plan view log of analogous segment is below. Not all roots in the log are visible in the photograph. Additional roots may have been revealed at deeper levels.

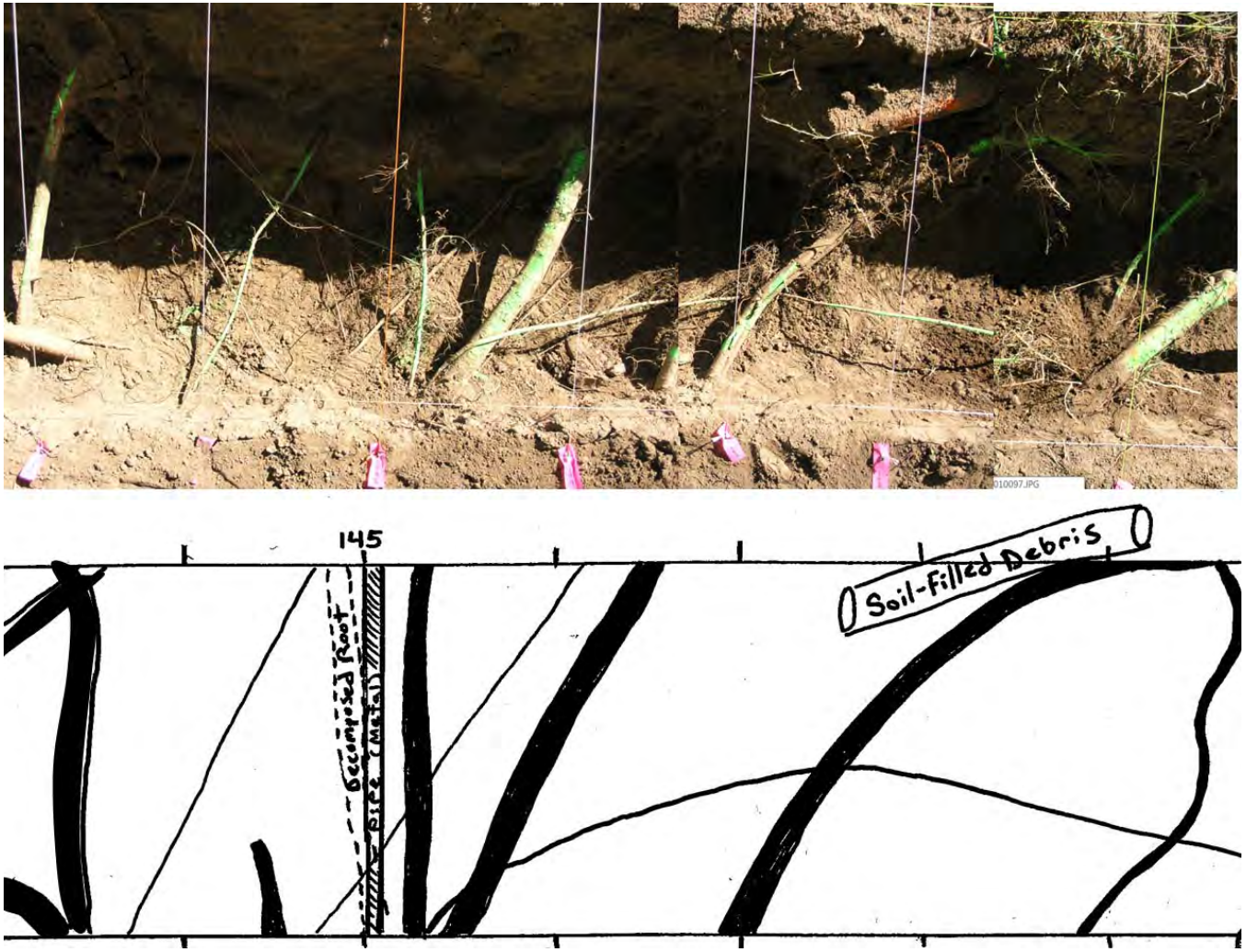

Figure D-12. Lower stump trench Stations 140.5-146 (increasing to left). Spliced plan view photos (top) during excavation of lower stump trench. Plan view log of analogous segment is below. Not all roots in the log are visible in the photograph. Additional roots may have been revealed at deeper levels.

Figure D-13. Stations 143 to 147 excavated to full depth and showing a cluster of decomposing and live roots as well as a 1-inch water pipe.

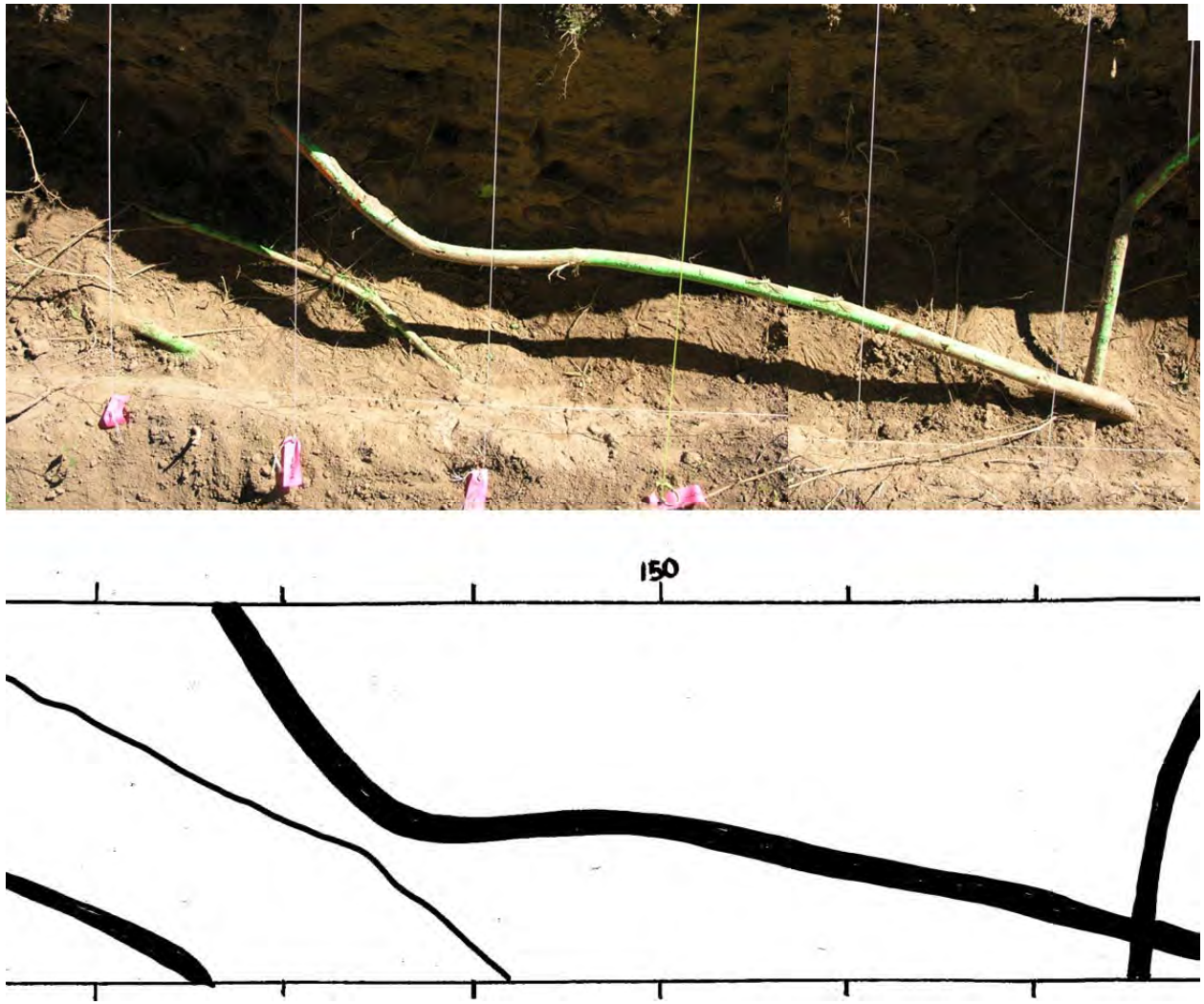

Figure D-14. Lower stump trench Stations 147.5-153.5 (increasing to left). Spliced plan view photos (top) during excavation of lower stump trench. Plan view log of analogous segment is below. Not all roots in the log are visible in the photograph. Additional roots may have been present at deeper levels.

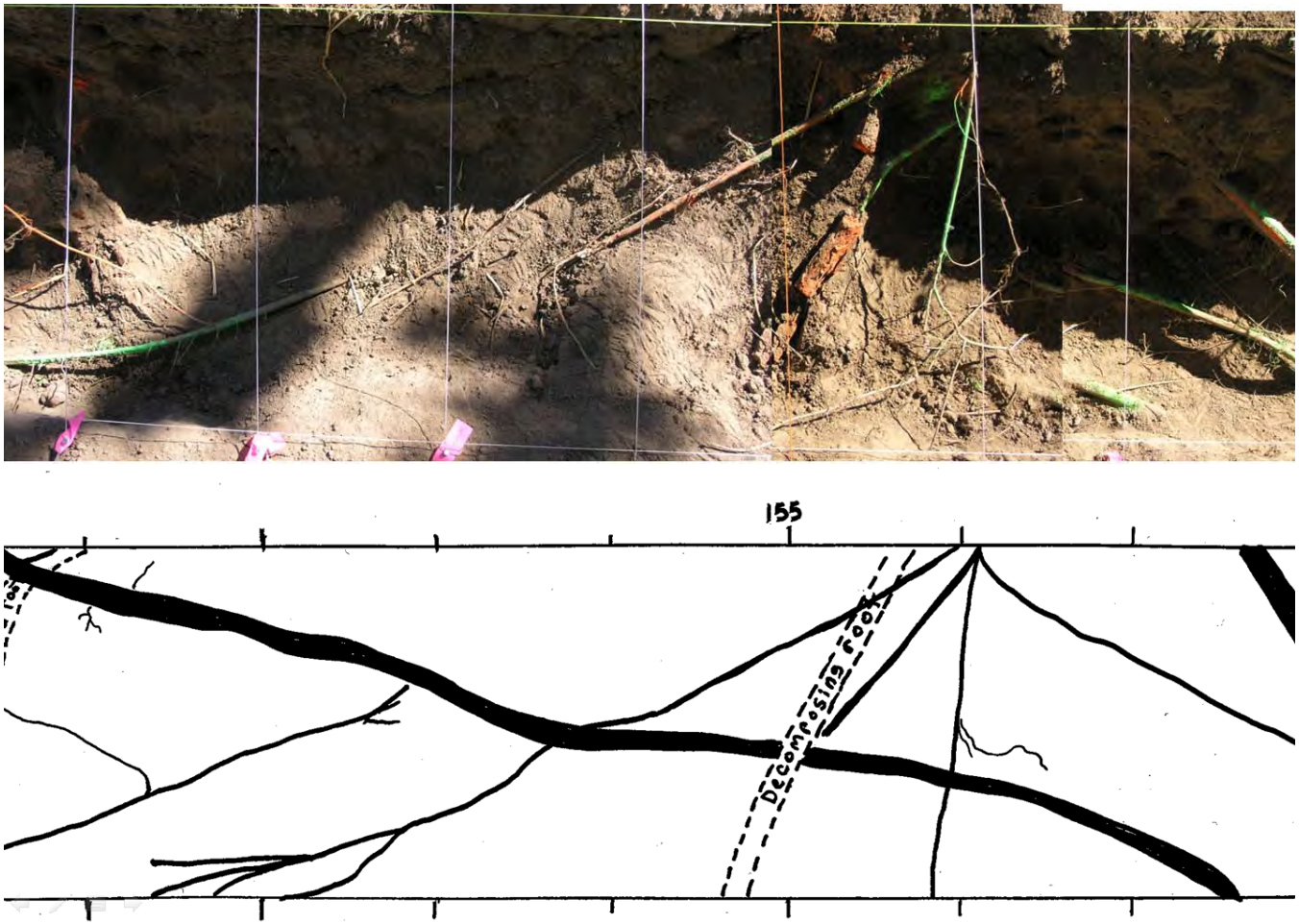

Figure D-15. Lower stump trench Stations 153-159. Spliced plan view photos (top) during excavation of lower stump trench. Plan view log of analogous segment is below. Not all roots in the log are visible in the photograph. Additional roots may have been present at deeper levels.

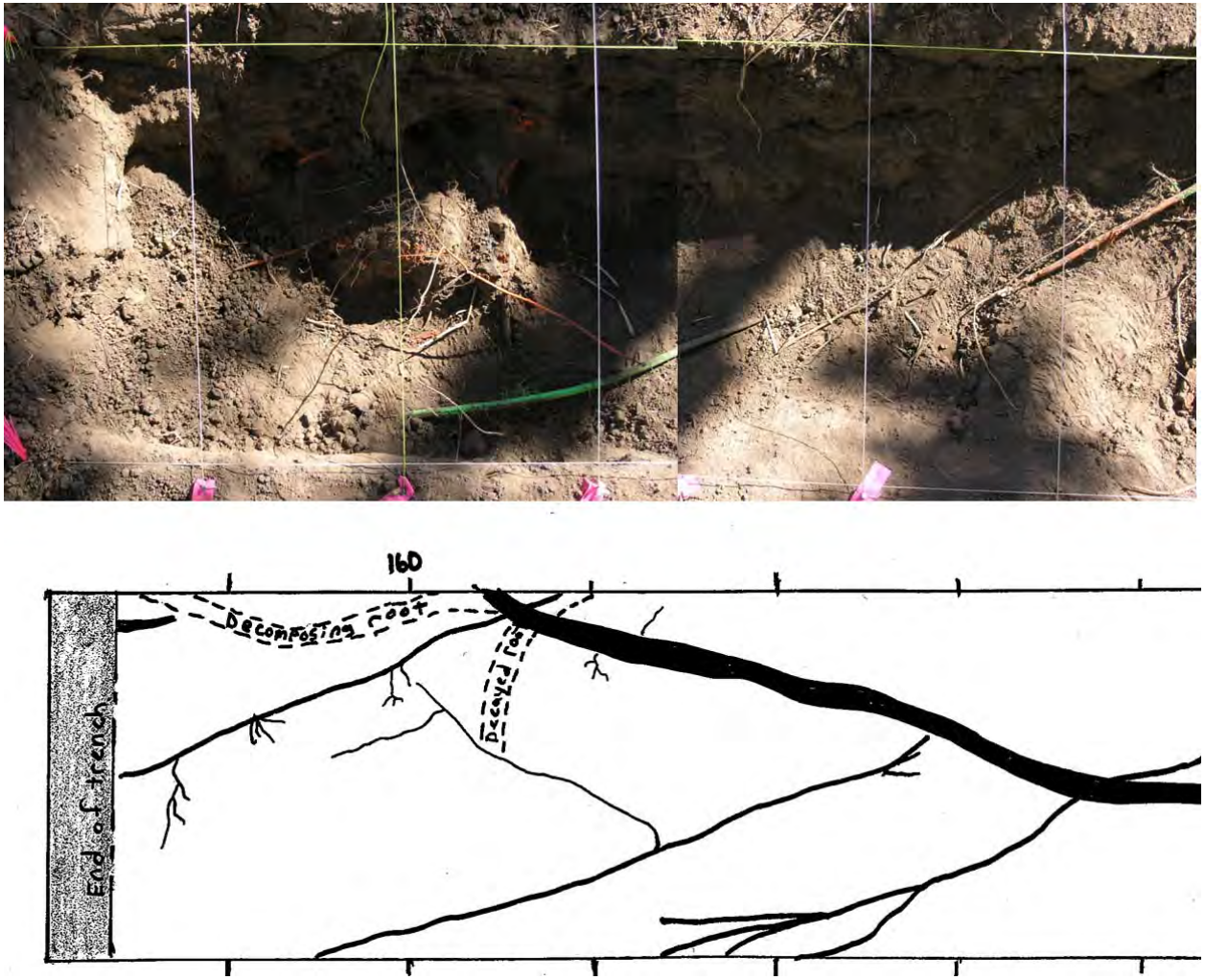

Figure D-16. Lower stump trench Stations 156-161.5 (increasing right to left). Spliced plan view photos (top) during excavation of lower stump trench. Plan view log of analogous segment is below. Not all roots in the log are visible in the photograph. Additional roots may have been present at deeper levels.

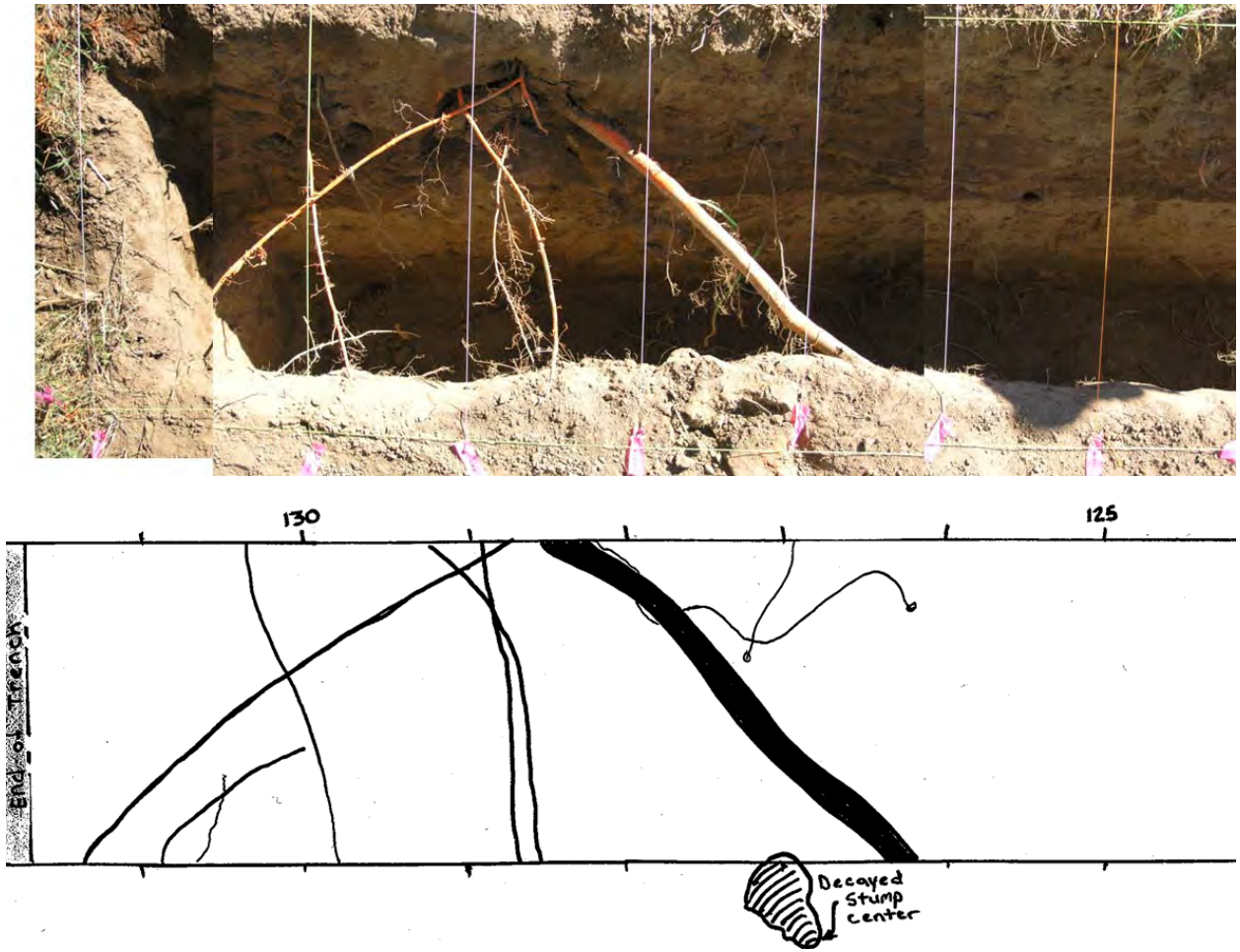

Figure D-17. Lower control trench Stations 124-132. Spliced plan view photos (top) during excavation of lower control trench. Plan view log of analogous segment is below. Not all roots in the log are visible in the photograph. Shallow roots were removed as needed to achieve depth.

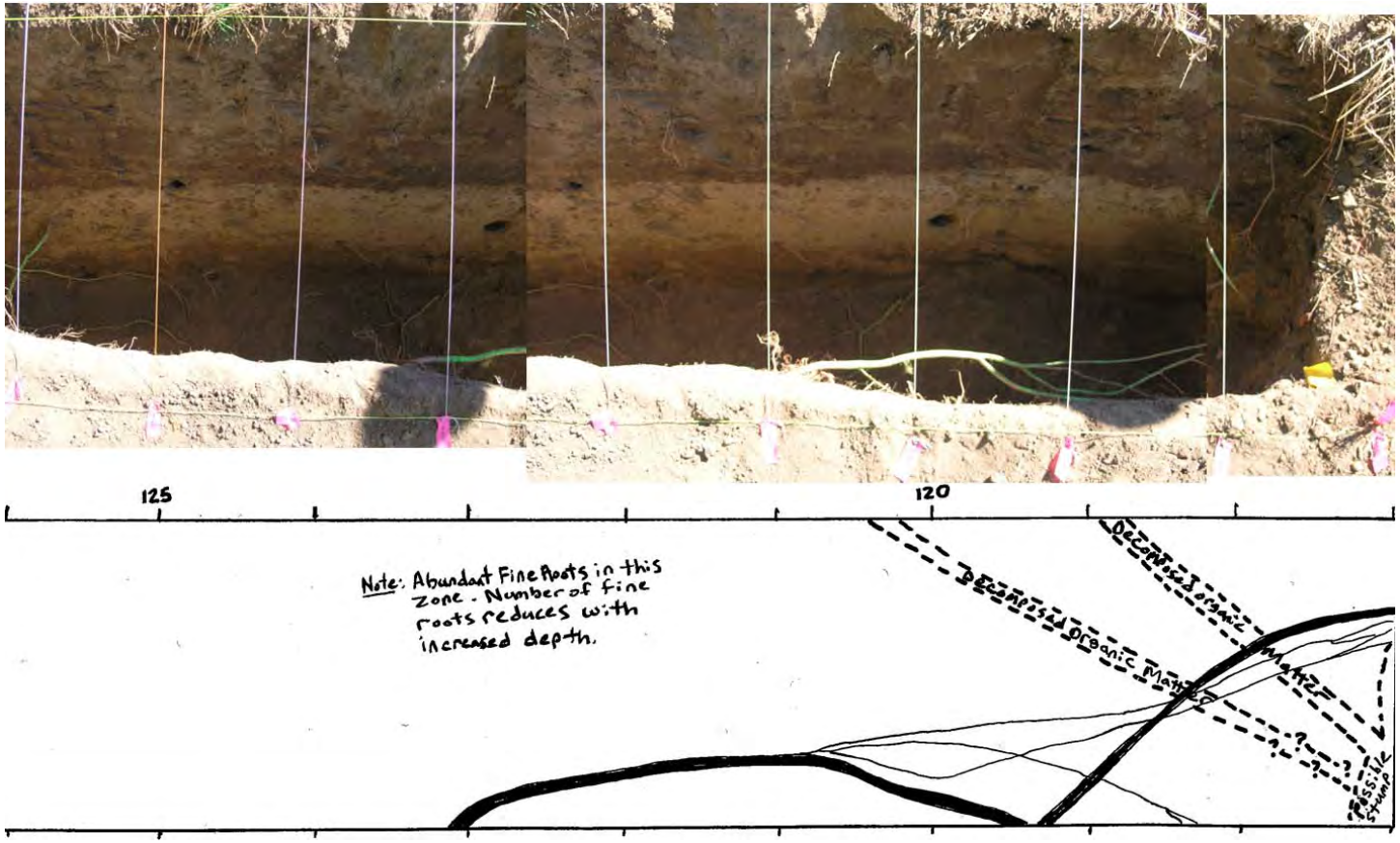

Figure D-18. Lower control trench Stations 117-126. Spliced plan view photos (top) during excavation of lower control trench. Plan view log of analogous segment is below. Not all roots in the log are visible in the photograph. Shallow roots were removed as needed to achieve depth.

Figure D-19. Photo looking east toward Station 132 from Station 118 (right) and plan view root logs (left) of upper control trench.

Figure D-20. Photo looking west (left) and plan view logs of roots (right) of upper stump trench.

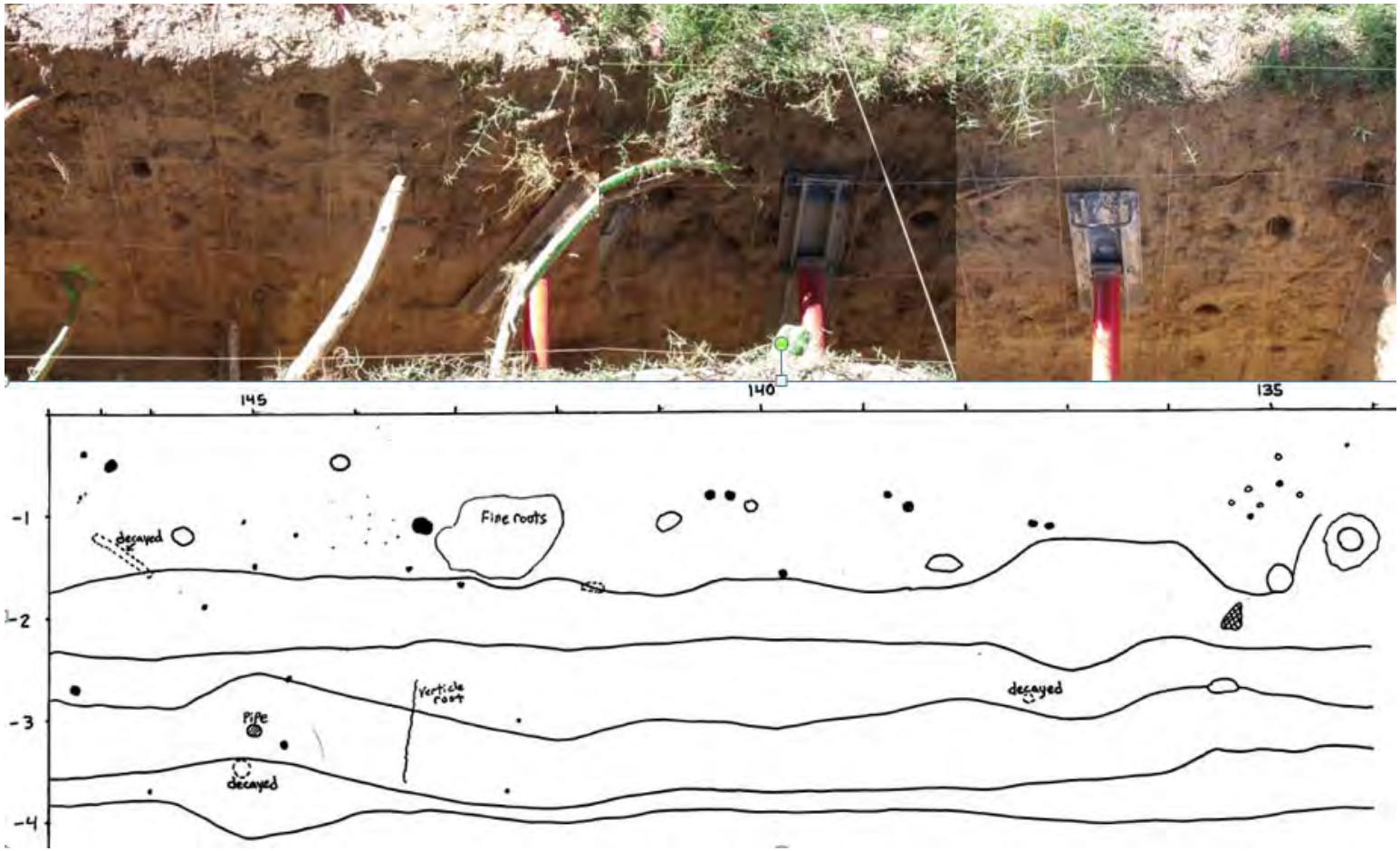

Figure D-21. Spliced photos looking south (top) and analogous uphill wall log (bottom) of lower stump trench Stations 134-147.

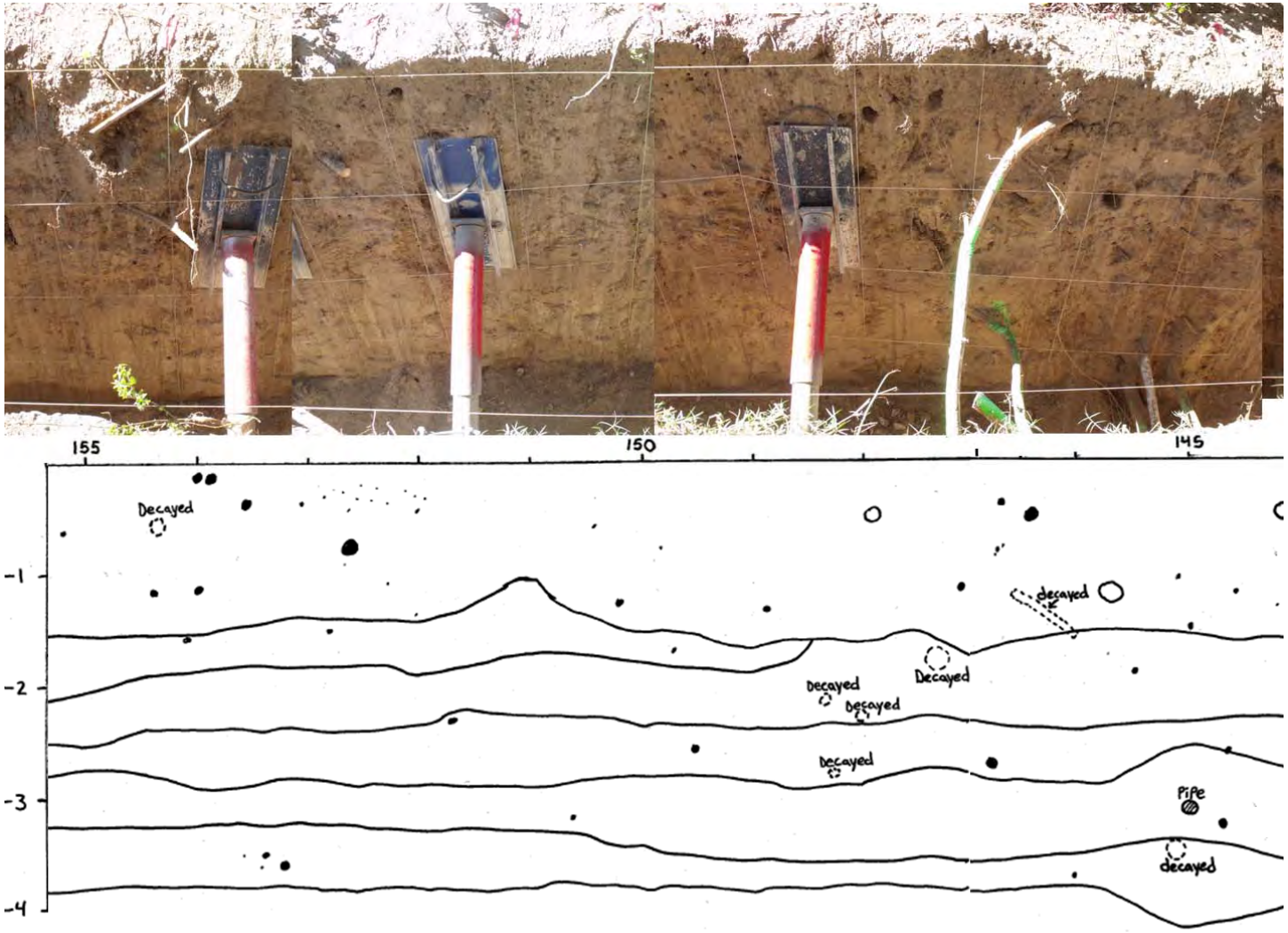

Figure D-22. Spliced photos looking south (top) and analogous uphill wall log (bottom) of lower stump trench Stations 144-155.

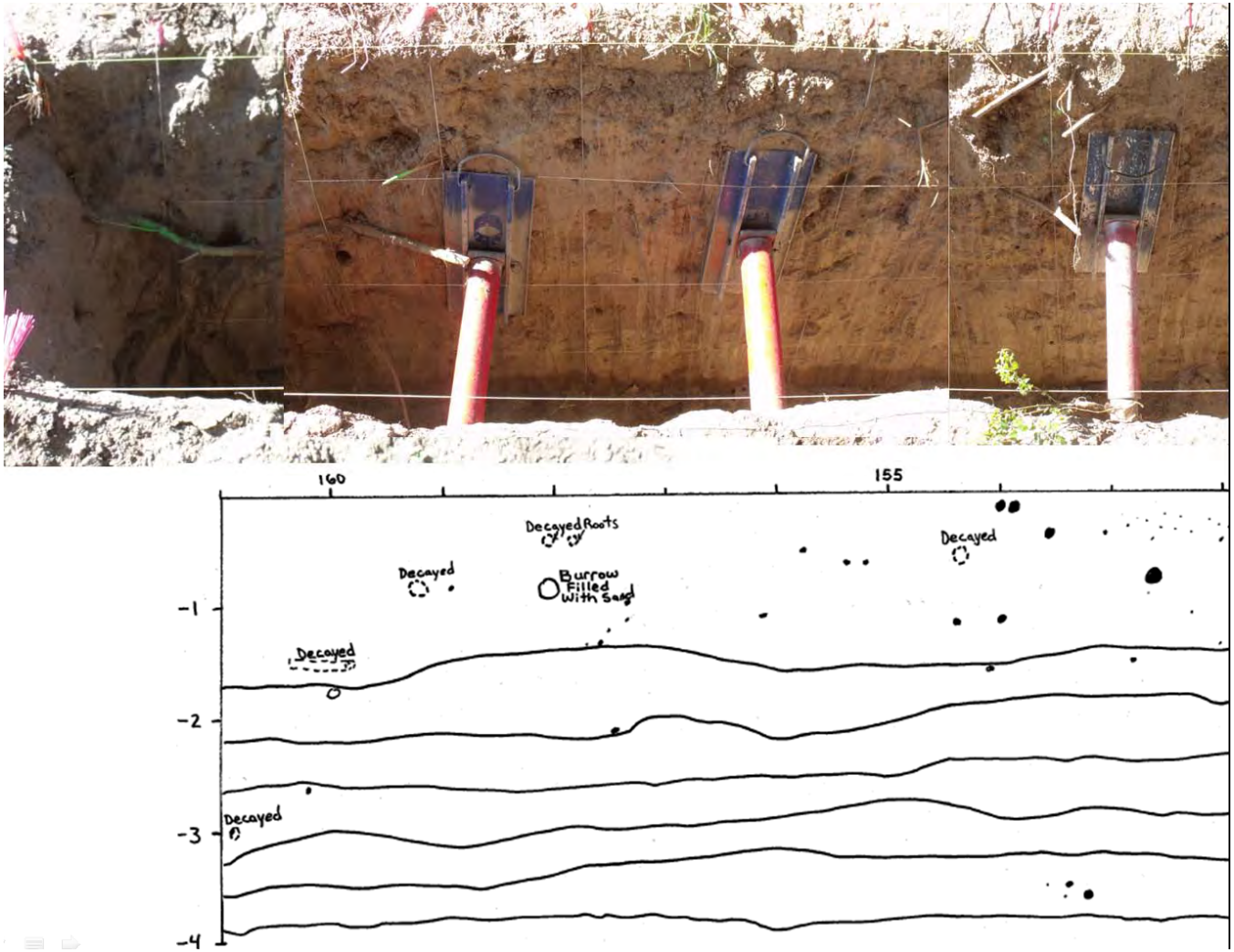

Figure D-23. Spliced photos looking south (top) and analogous uphill wall log (bottom) of lower stump trench Stations 152-161.

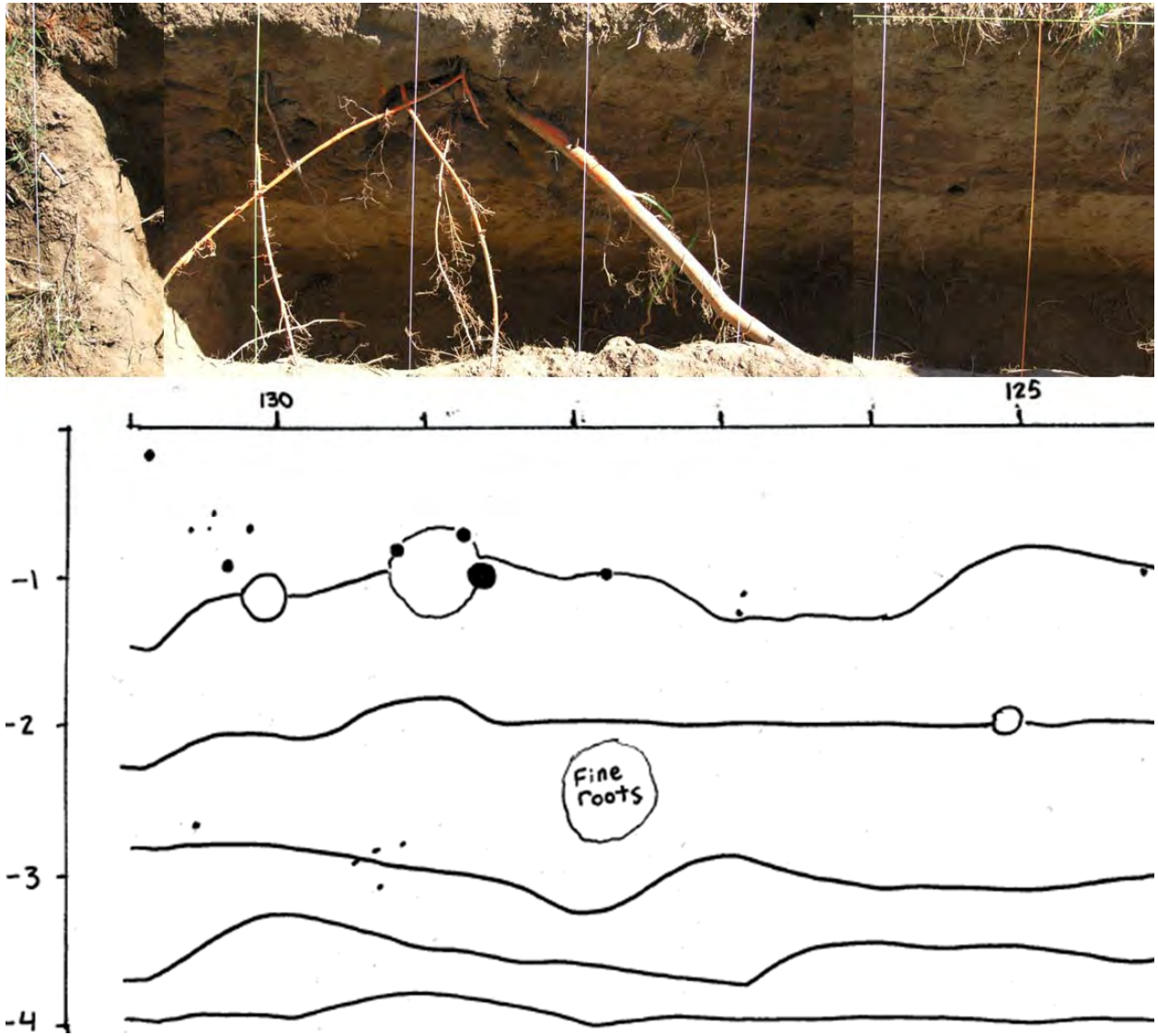

Figure D-24. Spliced photos looking south (above) and uphill wall log (below) of lower control trench Stations 124-131.

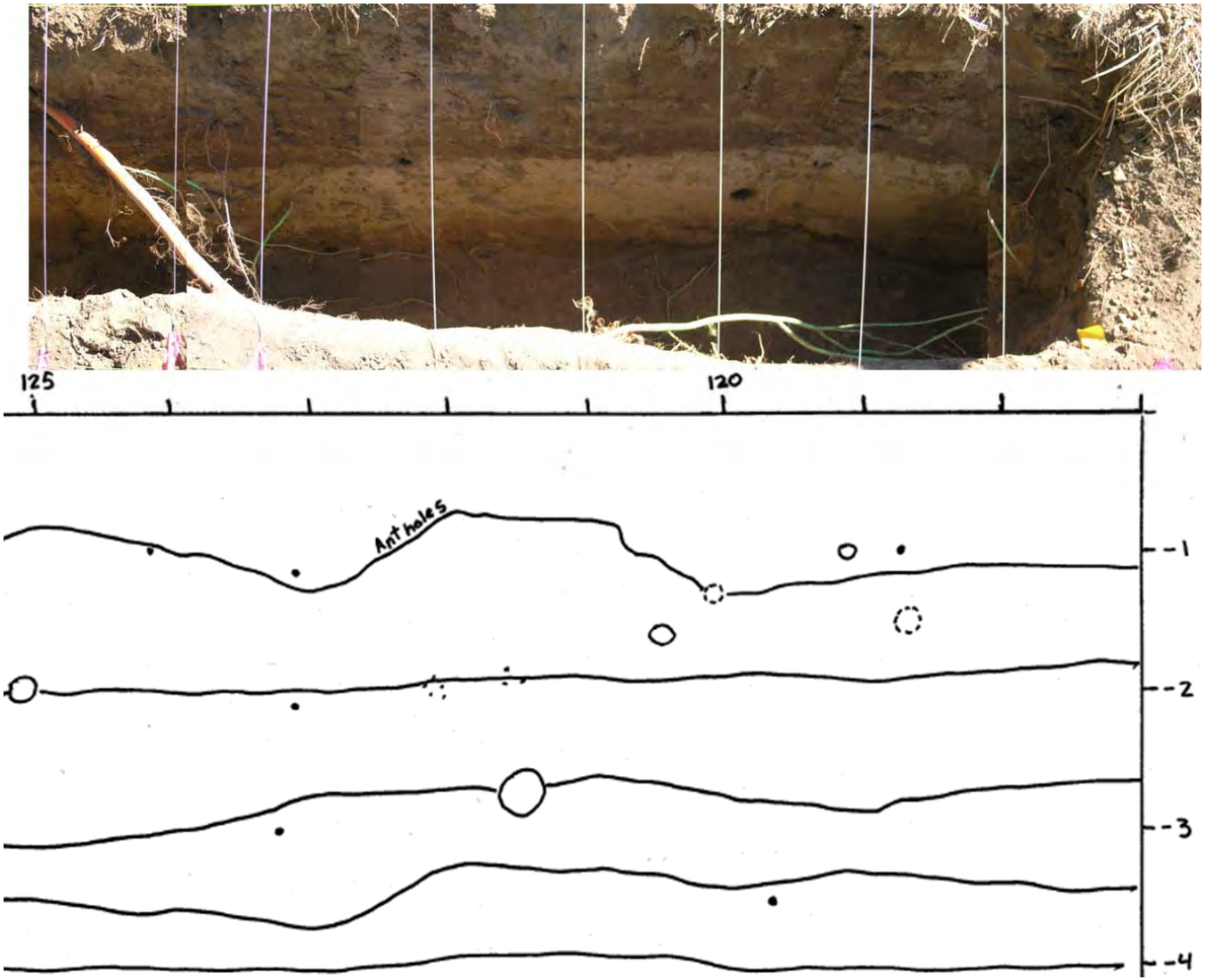

Figure D-25. Spliced photos looking south (top) and analogous uphill wall log (bottom) of lower control trench Stations 117-125.

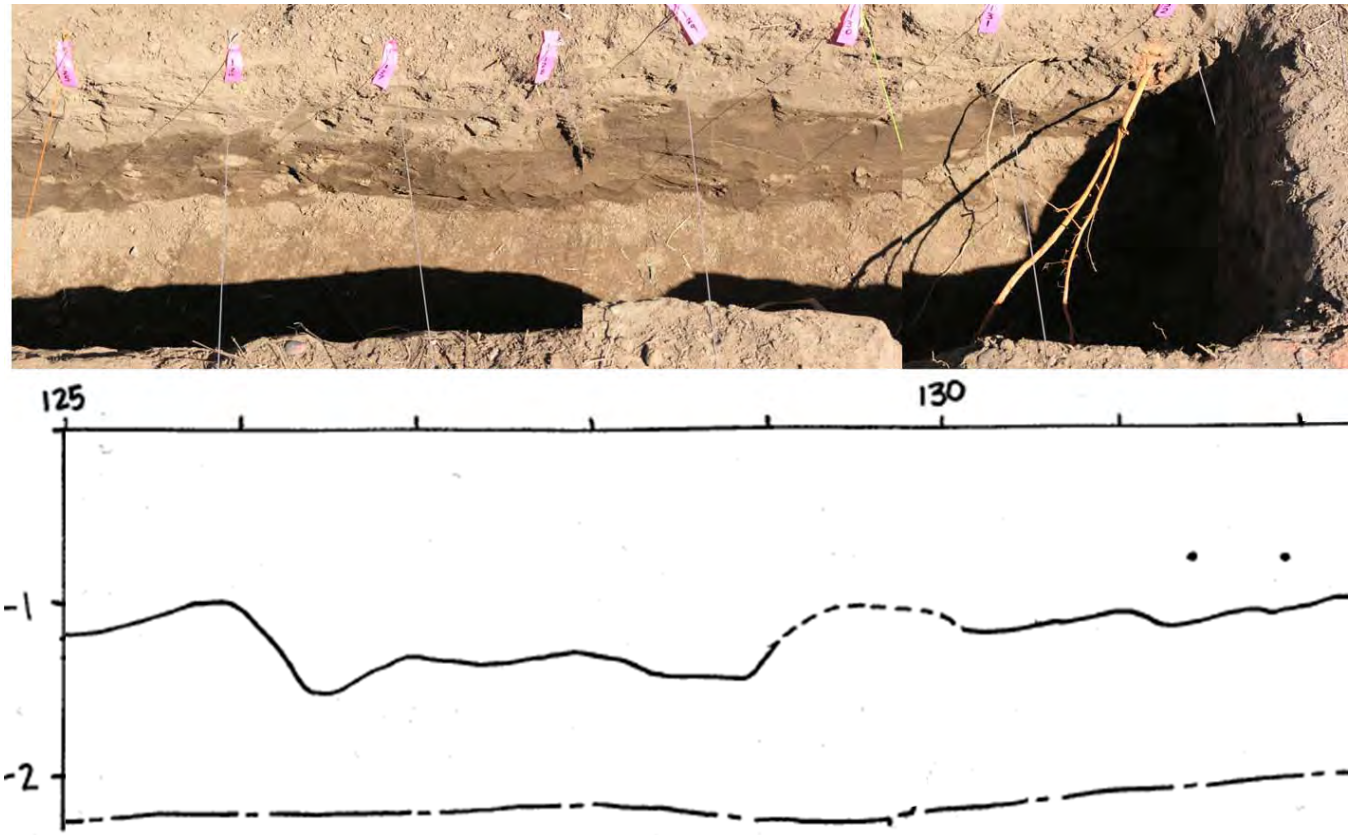

Figure D-26. Spliced photos looking north (top) and analogous downhill wall log (bottom) of upper control trench Stations 125 to 132. Photos were taken prior to excavation completion.

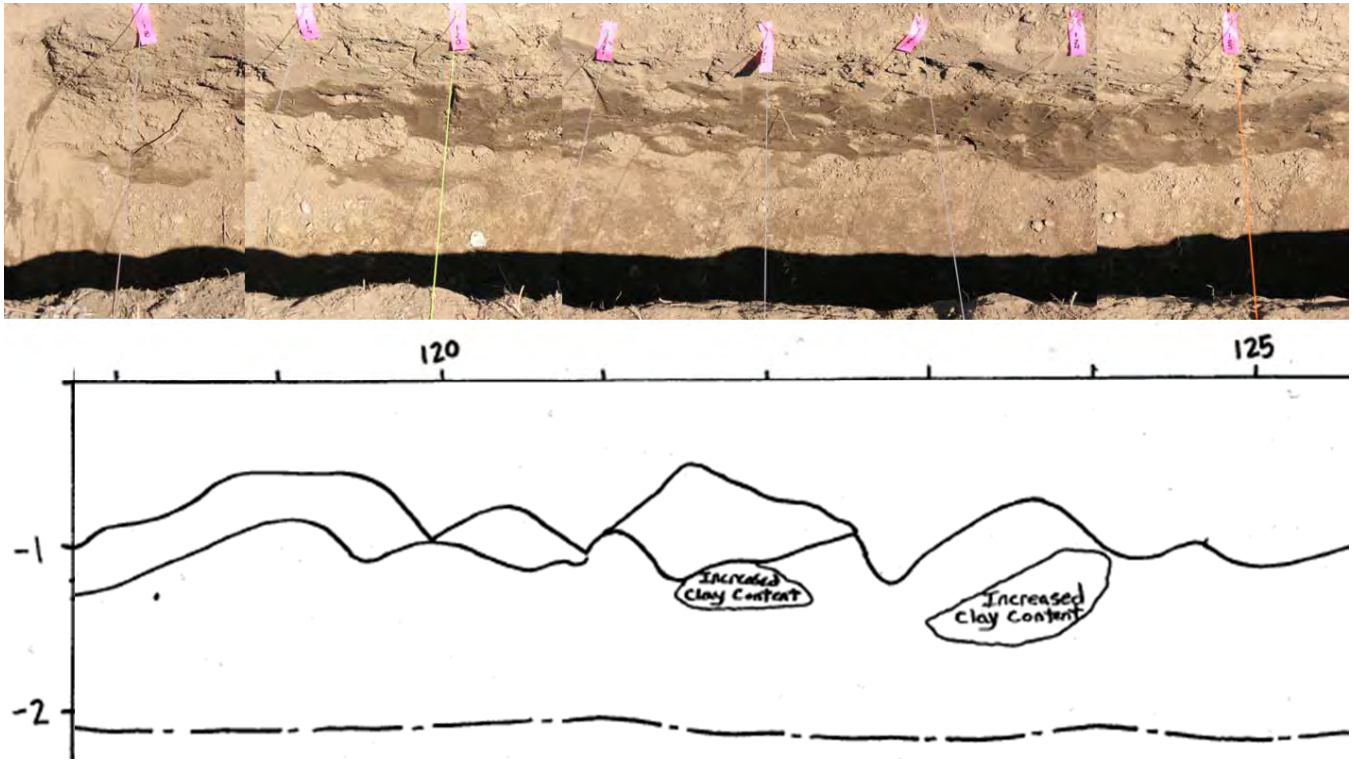

Figure D-27. Spliced photos looking north (top) and analogous downhill wall log (bottom) of upper control trench Stations 118 to 125. Photos were taken prior to excavation completion.

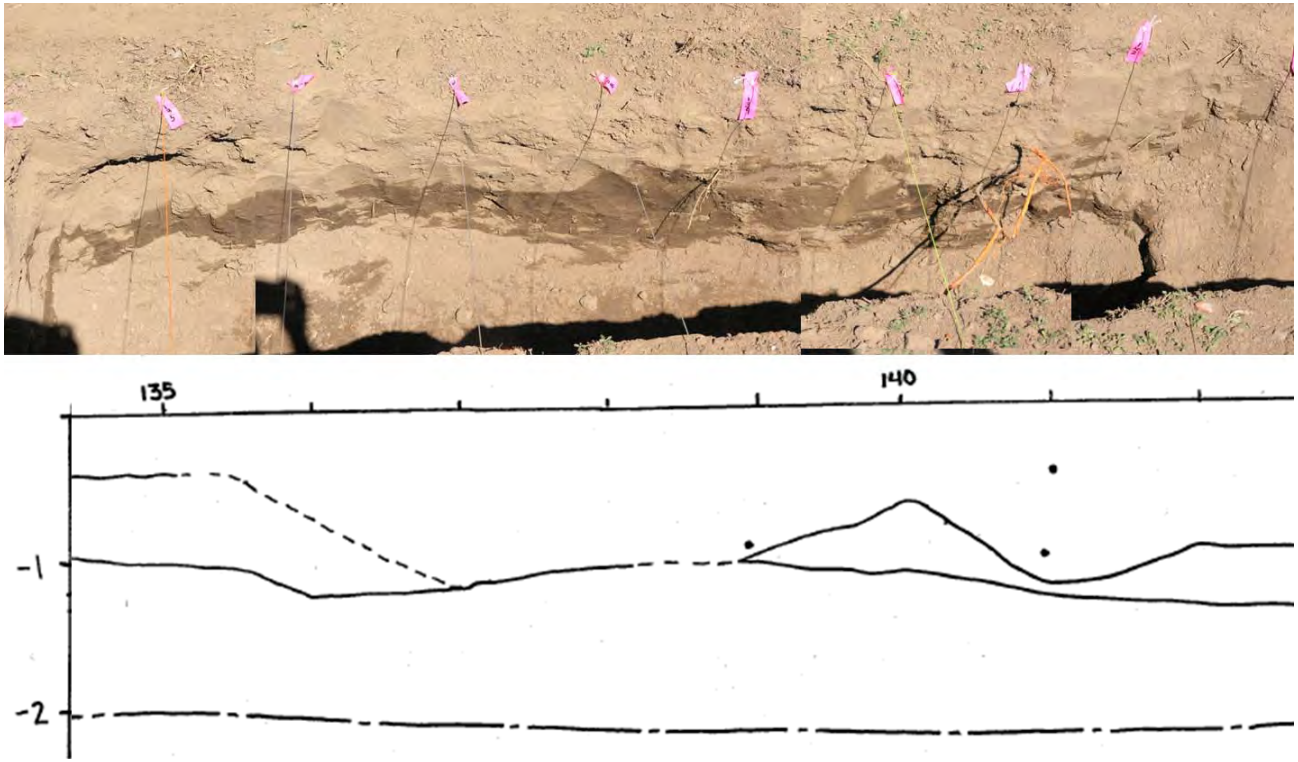

Figure D-28. Spliced photos looking north (top) and analogous downhill wall log (bottom) of upper stump trench Stations 134 to 142. Photos were taken prior to excavation completion.

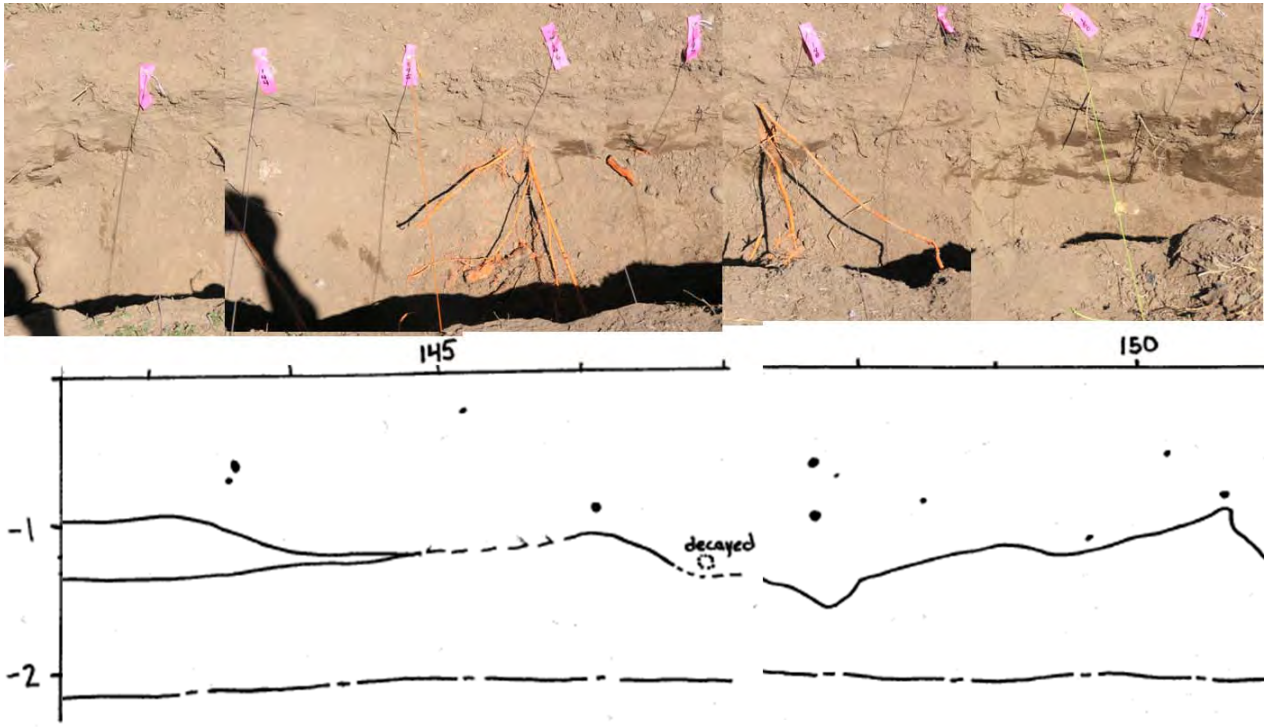

Figure D-29. Spliced photos looking north (top) and analogous downhill wall log (bottom) of upper stump trench Stations 142.5 to 151. Photos were taken prior to excavation completion.

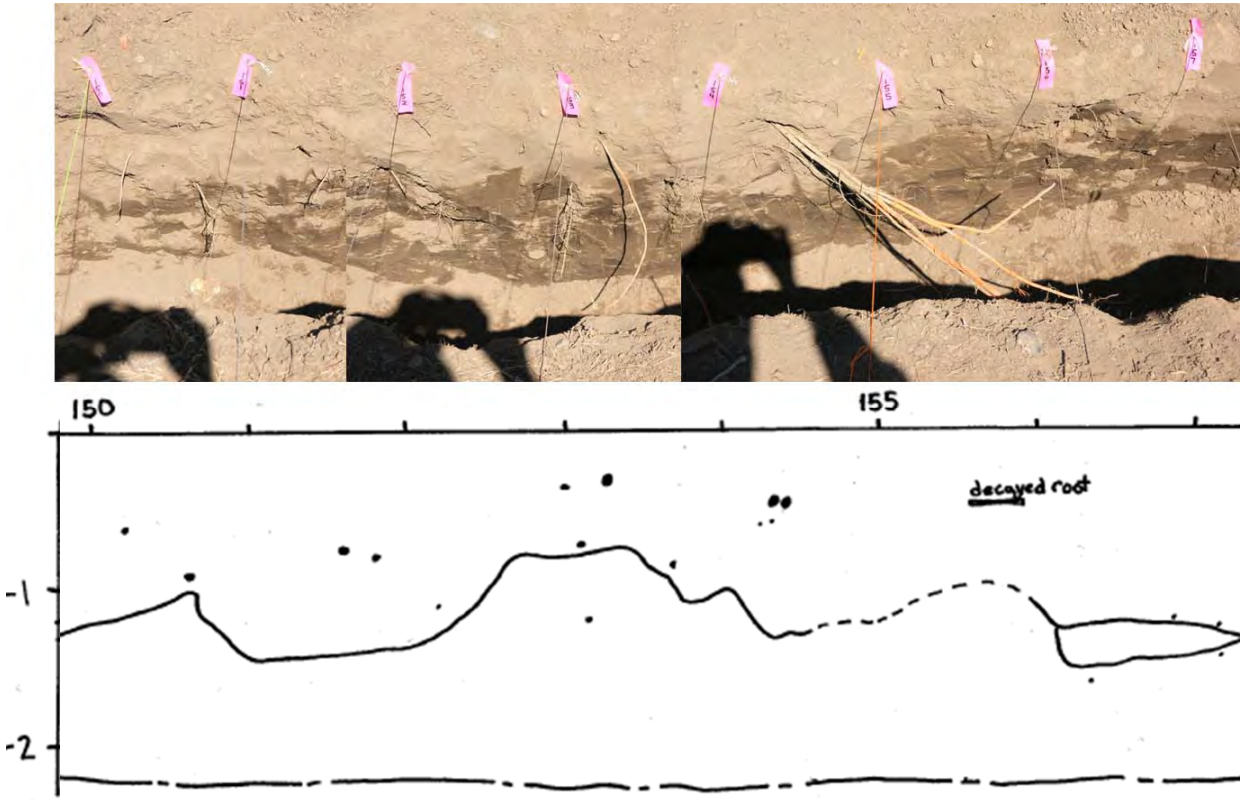

Figure D-30. Spliced photos looking north (top) and analogous downhill wall log (bottom) of upper stump trench Stations 150 to 157. Photos were taken prior to excavation completion.

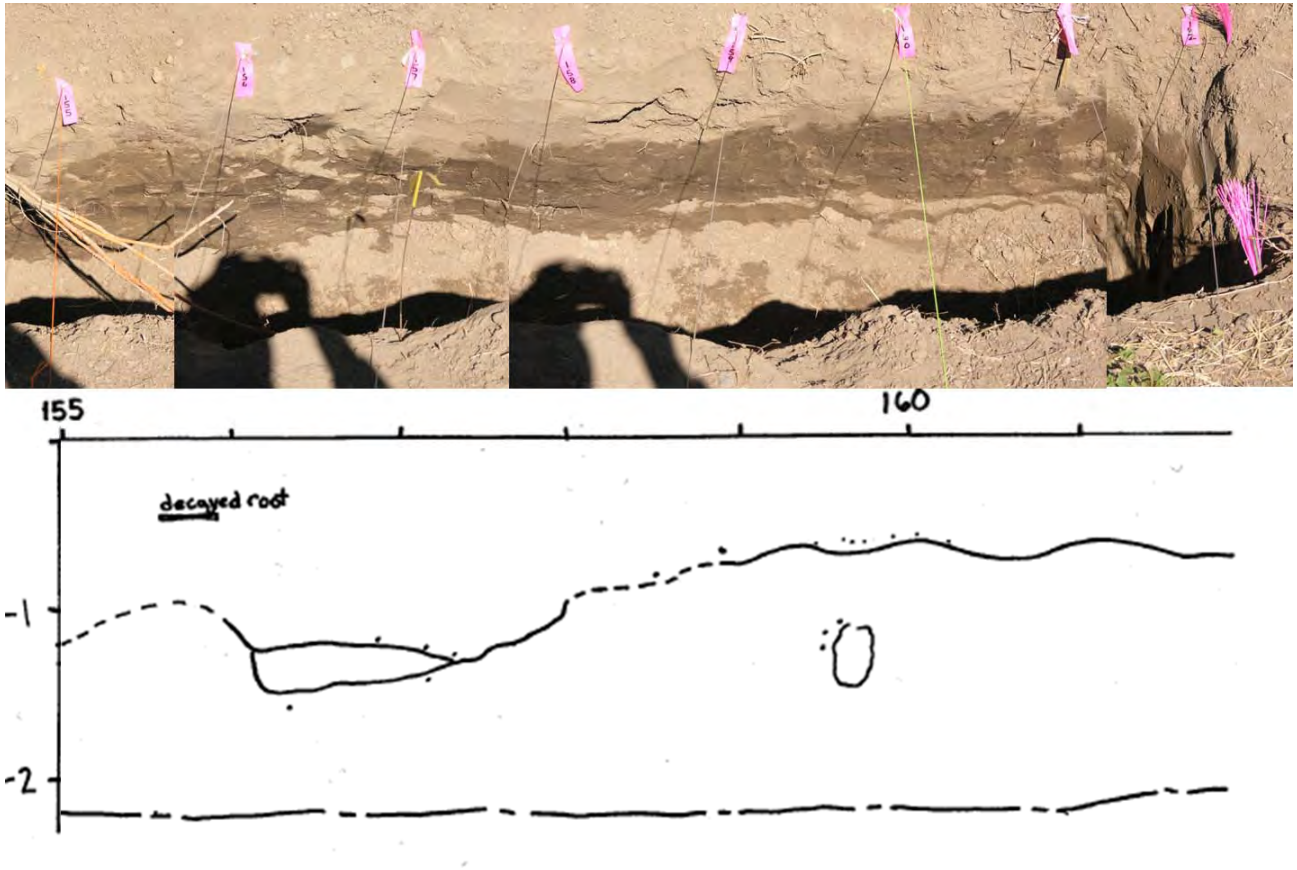

Figure D-31. Spliced photos looking north (top) and analogous downhill wall log (bottom) of upper stump trench Stations 155 to 162. Photos were taken prior to excavation completion.

APPENDIX E: INSTRUMENT DATA

Appendix E

Tensiometer data is presented first, followed by piezometer data. Tensiometer data collection began with a dry run equilibration phase. During the dry run equilibration phase, tensiometers were assembled, leak checked, installed in the ground. Soil Moisture tensiometers of 24, 48, and 60 inches in length were assembled with brass 'T' adaptors to allow for connection of both a mechanical gauge and a Model 5301 current transducer by Soil Moisture. The current transducer was wired to a Campbell Scientific CR3000 datalogger in order to continuously read the instruments. The current output from each transducer was converted to voltage using a 249 ohm resister with a resistor error of 1 percent. Based on manufacturer's specifications, currents of 4 and 20 mA correspond to soil suction values of 0 and 100 kpa, respectively. The values can be scaled linearly between these values. With a resistance of 249 ohms, using Ohms Law (which states that voltage is equal to current multiplied by resistance) voltages of 996 ohms and 4980 ohms correspond to soil suction values of 0 and 100 kpa, respectively, sharing the same linear relationship.

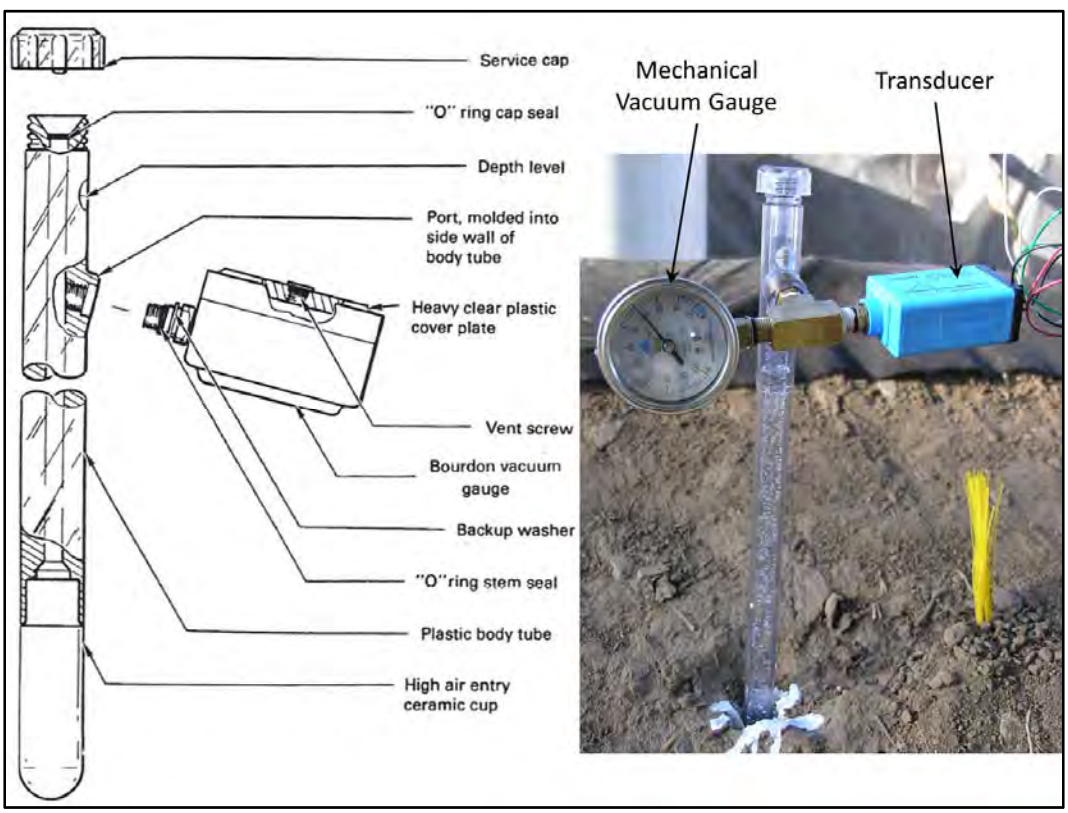

Figure E- 1. Components of a tensiometer broken down by Fredlund and Rahardjo, 2005 (left) as compared with our tensiometer equipped with both vacuum gauge and transducer (right).

Figure E- 2 shows the locations of instruments installed at the site. Tensiometers T4B-18, and T3C-36 and piezometer P2B-84 were not functional. Tensiometers were connected to the datalogger during the days leading up to the flow test to check functionality. Tensiometer T1A-36 was selected for a calibration test. The instrument was installed in the ground, and allowed to develop tensions that seemed relatively constant based on readings of the mechanical gauge. The datalogger was observed in real time while the mechanical gauge was read periodically. Mechanical gauge suction values were compared with corresponding readings from the transducer. The results are shown on Figure E- 3. At high suction values, the mechanical gauge yielded higher values of soil suction than the transducer. The instrument was opened during the test, water added, and the instrument re-sealed. After 40 minutes, tension had not increased to the level prior to opening the instrument. The mechanical gauge and the transducer were generally in good agreement for much of the test. Error of the resistor is shown on the plot and does not explain the discrepancy between the gauge and the transducer at high suction values.

Regular maintenance of the tensiometers is required in the form of water additions. Water can run low in the instrument and may need to be added periodically, dropping the tension of the instrument to zero while the cap is open. In processing the data, corrections are made to subtract the weight of the water column from the reading as the weight of the water in the instrument adds to the tension. When this correction is made to all data points, data can show falsely as negative suction, or pressure, during times when this correction is made and the tensions have not yet been re-established in the instrument following a filling event. The correction is made to account for the entire instrument length, though 24 inch instruments were installed to depths of 18 inches and 48 inch instruments were installed to depths of 36 inches. The 60 inch instruments were installed to the full instrument depth of 60 inches.

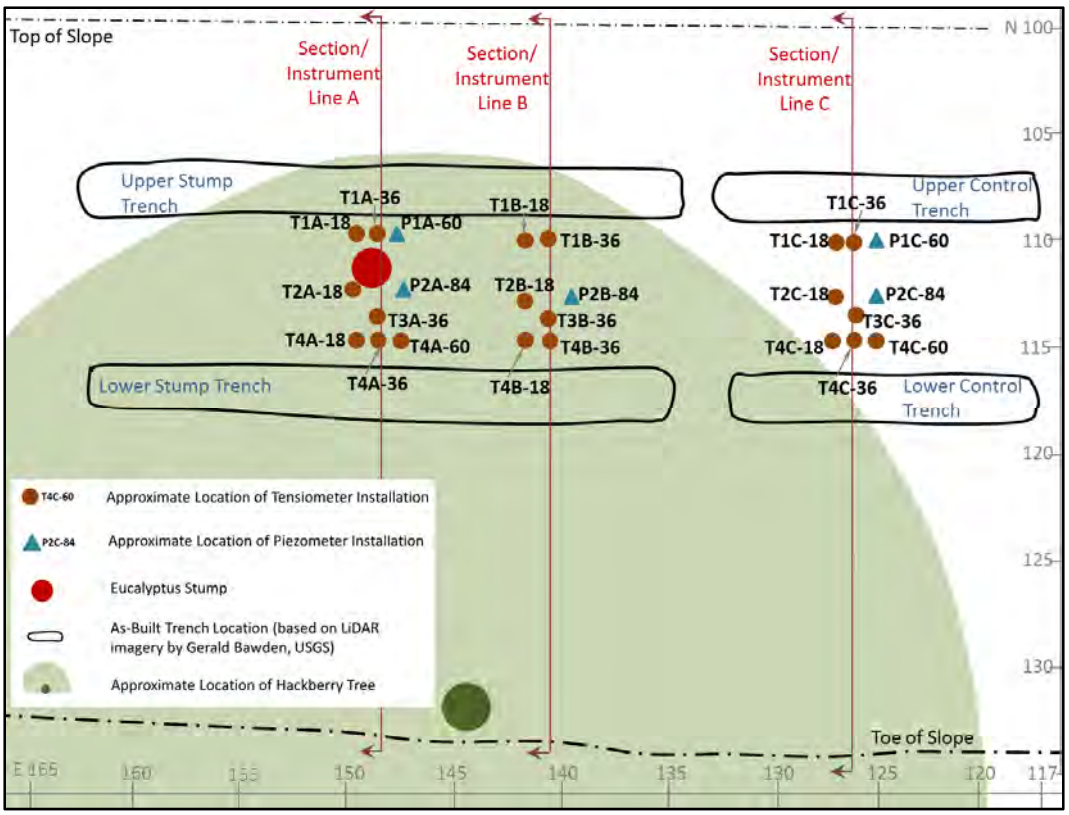

Figure E- 2. Location of instrument Lines A, B, and C, tensiometers, and piezometers.

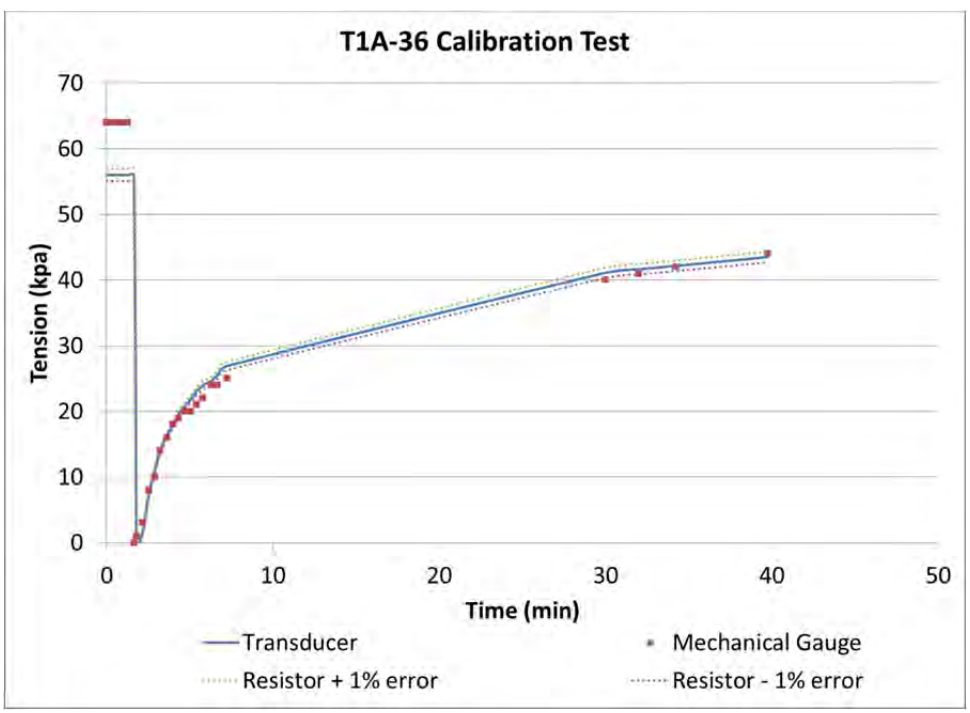

Figure E- 3. Calibration test correlating readings from mechanical vacuum gauge with transducer readings for tensiometer T1A-36.

Figure E- 4 compares mechanical gauge readings with those measured by current transducers. All instruments are shown for two time intervals on the two days just before the flow test. The flow test began on September 7, 2010 at 11:57am and comparisons between mechanical gauges and transducers were performed on September 5th and 6th. Mechanical gauge readings predicted higher values of suction than transducers in 14 of 18 tensiometers on September 5th and in 12 of 18 tensiometers on September 6th. The mean percent difference between gauge readings and transducers was 14.9 percent with a standard deviation of 11.5 percent on September 5th whereas it dropped to 13.1 percent with a 9.14 percent standard deviation the next day. Air bubbles can become trapped in the gauges and at high suction values can enter through the high air entry value ceramic cups at the base. Air content in the fill water, though minimized by boiling water in the field or bringing de-aired water from the lab prior to filling the instruments, can introduce higher errors at high suction values (approaching cavitation) as air bubbles are formed inside the instrument. Soilmoisture Equipment Corporation ceramic cups have an air entry value of about -100 kPa, however increasing this value would not improve accuracy of the instruments as the water in the tube will cavitate when the water pressure reaches -90 kPa (Fredlund and Rahardjo, 1993). Given that the height of the water column adds to the suction, the maximum value of matric suction that can be achieved with this system is 84 kPa, 78 kPa, and 75 kPa for 24 inch, 48 inch, and 60 inch instruments, respectively. Longer instruments are therefore less capable of measuring high values of matric suction.

Two days prior to the flow test, the datalogger was connected and a continuous record of soil suction was recorded for instrument Lines A (Figure E- 5), B (Figure E- 6), and C (Figure E- 7). Water was added frequently prior to the flow test as soils were unsaturated. If air bubbles are allowed to accumulate inside the instrument, matric suctions read on the instruments can falsely trend toward zero, or atmospheric pressure (Fredlund and Rahardjo, 2005). Tensiometers T3A-36, T4A-36, T1B-18, T1B-36, T2B-18, T3B-36, T4B-36, and T4C-36 generally required more water than other instruments. These instruments show matric suction values that tend to have the lowest peak values of suction as compared to other nearby instruments or comparable depth instruments in other instrument lines. Further, curve shapes tend to be irregular, always dropping, while instruments that did not require addition of water as often developed regular curves with relatively constant values of matric suction prior to the arrival of the wetting front. It is possible that air was slowly entering the system in these instruments, either through a poor seal at the ceramic cup or through air entering through the porous ceramic cup. The results from these instruments was removed from the falling head test results as the test was conducted over a period of time when no one was onsite daily to maintain water in the instruments. Peak values of suction for these instruments are unlikely to be accurate, however a distinct drop in suction was achieved in each of the instruments indicating the arrival of the wetting front. We believe that the data is accurate only for the purpose of understanding the timing of the wetting front arrival.

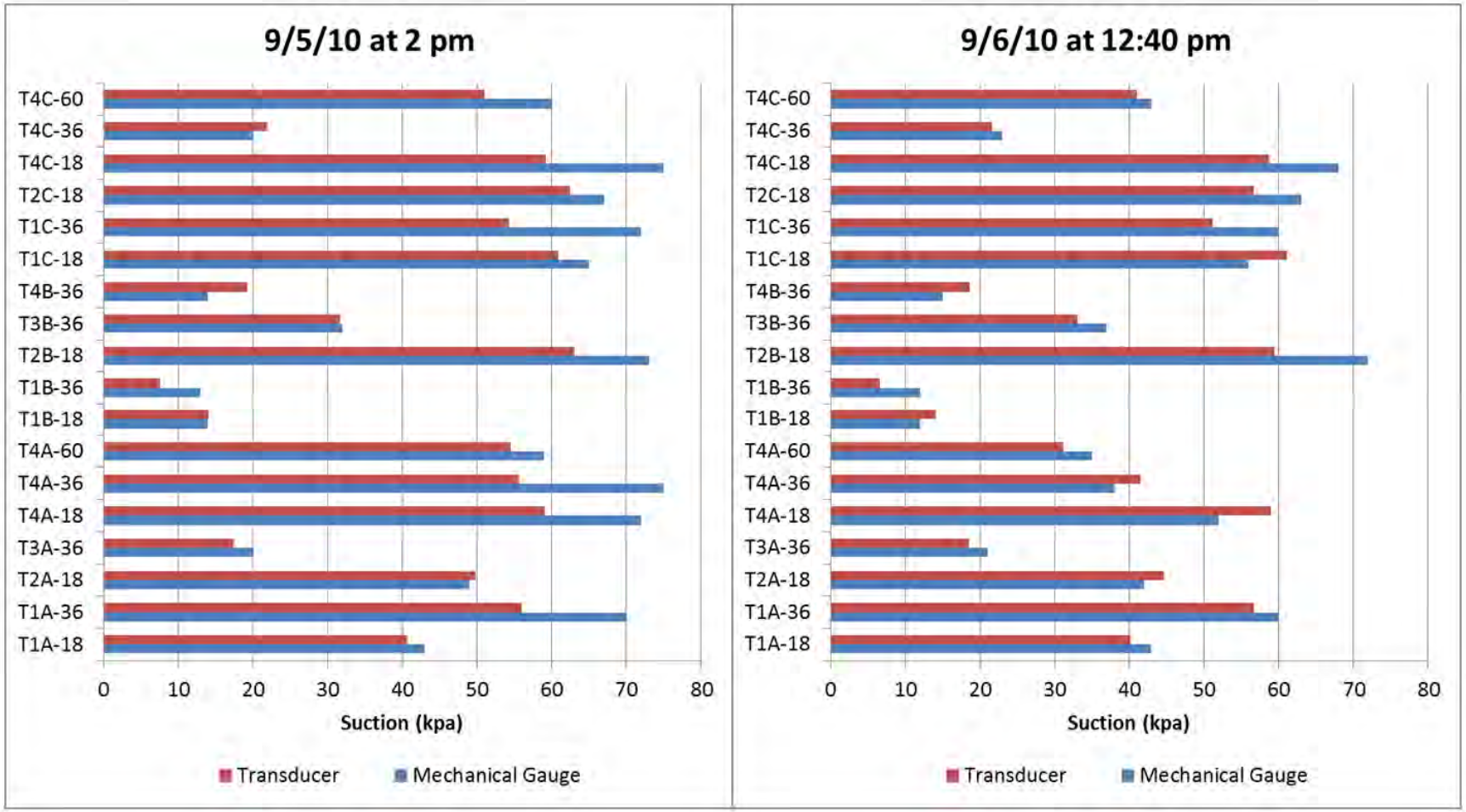

Figure E- 4. Comparison of mechanical vacuum gauge readings with transducer results for all instruments.

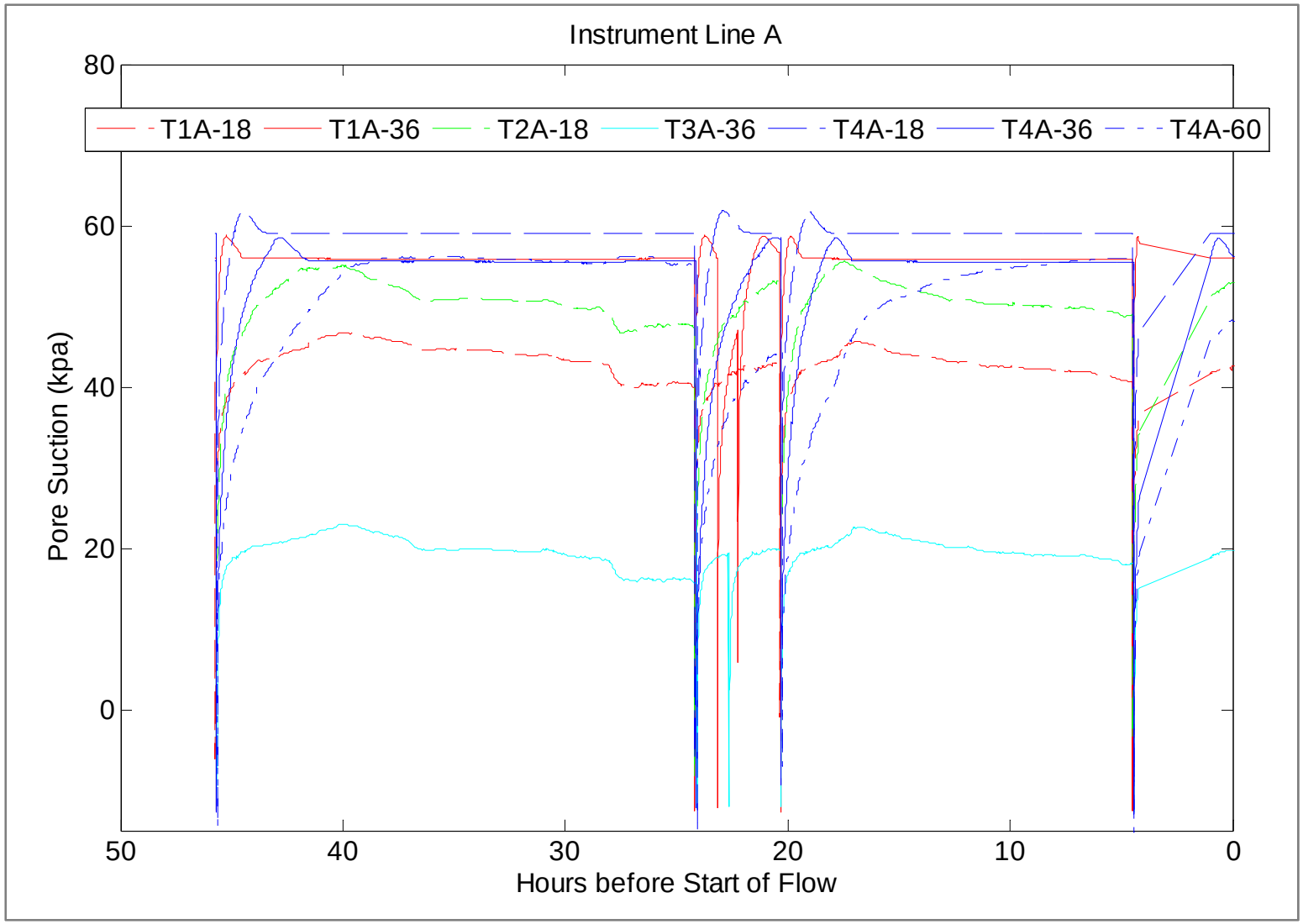

Figure E- 5. Matric suction values read from transducers at Line A tensiometers prior to the flow test.

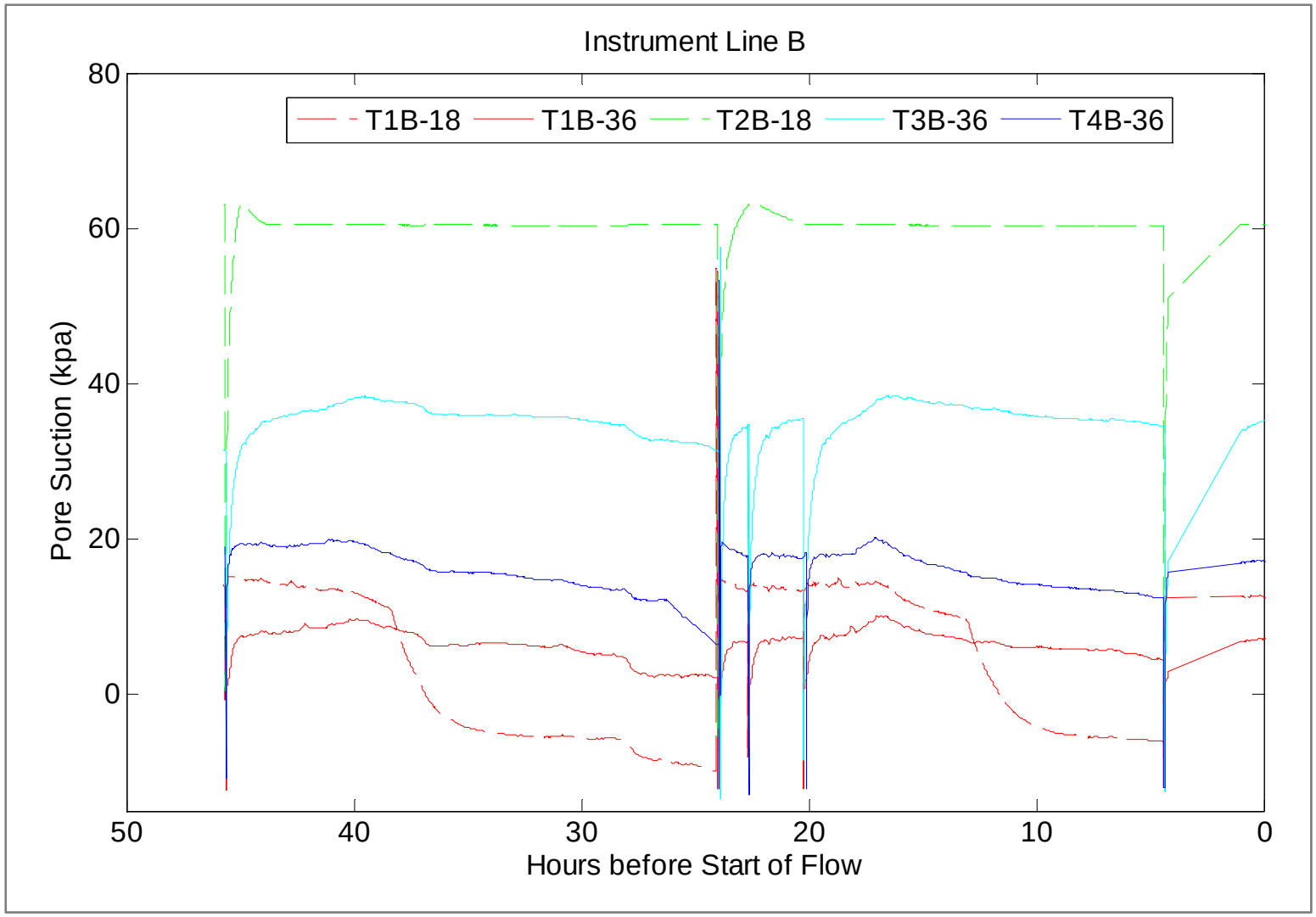

Figure E- 6. Matric suction values read from transducers at Line B tensiometers prior to the flow test.

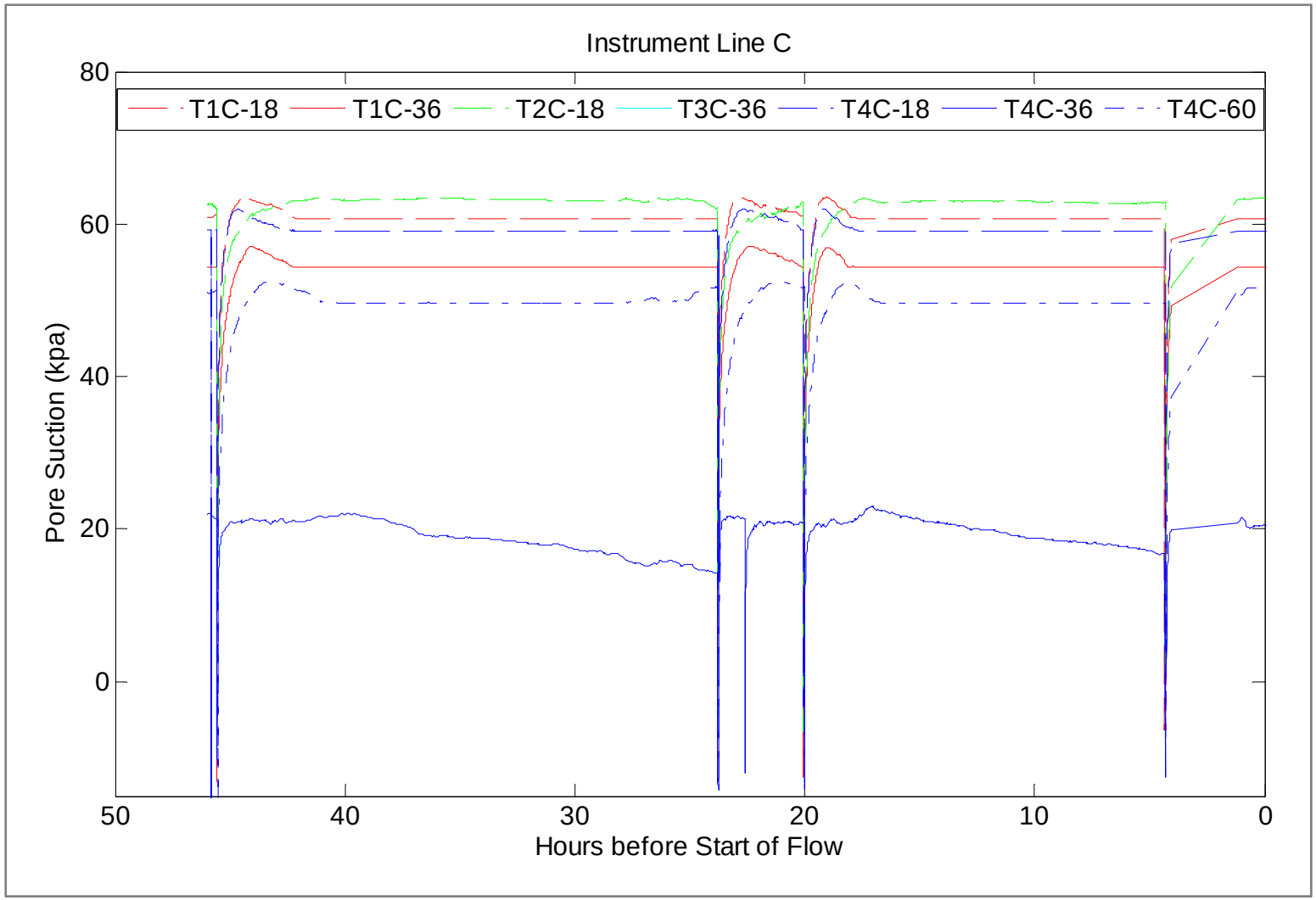

Figure E- 7. Matric suction values read from transducers at Line A tensiometers prior to the flow test.

Figure E- 8 shows a typical profile of suction with time during the flow test and the days following the test as the soil began to dry out. The plot shows the drop in tension that is expected when the instrument is opened and filled, the drop in tension associated with the arrival of the wetting front, the slight rise in soil suction when water ran low in the trenches, and the re-establishment of matric suction in the soils as drying began following the flow test.

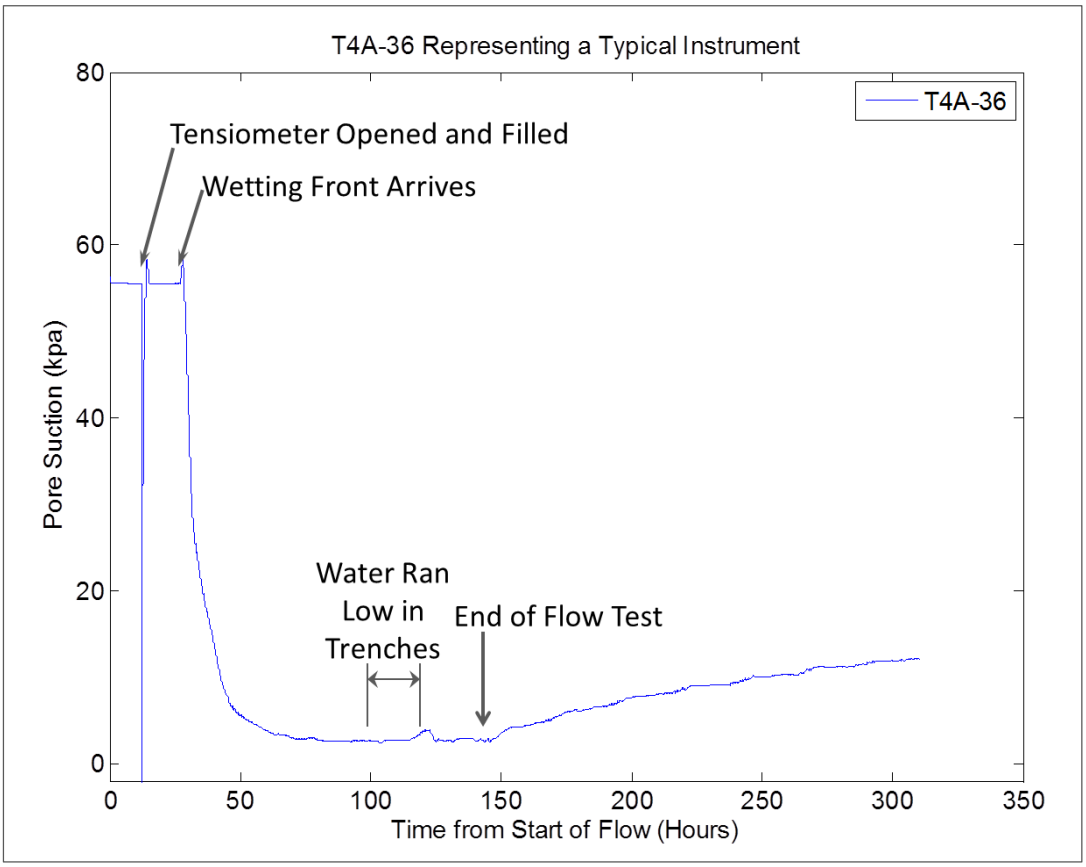

Figure E- 8. A typical tensiometer result for the flow test the drying period that followed.

Figure E- 9 provides a summary of all instrument data gathered during the flow test. Similar patterns to those of Figure E- 8 are seen with each instrument, however the arrival of the wetting front and the rate of decrease in suction values varies from almost immediately arriving to arriving after a period of nearly 3 days. Table E-1 provides a summary of wetting front and saturation front arrivals as well as steady state suction values for tensiometers. Table E-2 provides a summary of the saturation front arrival and buildup of pore pressures for piezometers. A discussion of instrument results in the context of the flow test observations is provided in Section 3.6.4.

Tensiometer data during the first 4 days of the flow test are provided by instrument line as Figure E- 10 through Figure E- 12. Tensiometer data are then displaced for like instruments across all three instrument lines with results presented on Figure E- 13 through Figure E- 19.

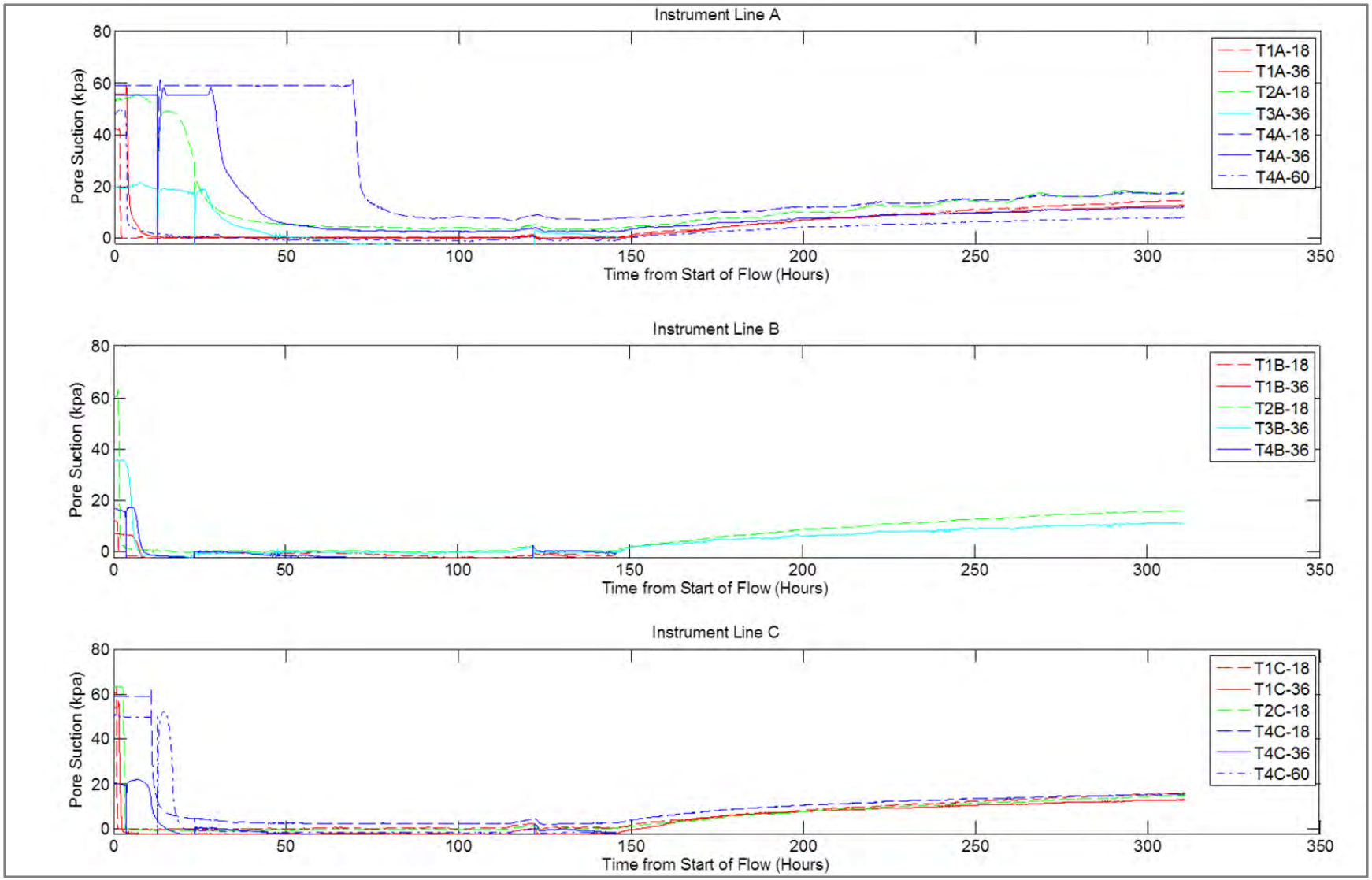

Figure E- 9. Tensiometer data for instrument Lines A, B, and C for the duration of the flow test (146.25 hours or 6 days) and the falling head and drying phase that followed.

Table E-1. Tensiometer wetting and saturation fronts.

Instrument Name	Wetting Front Arrival (hrs)	Time to Steady State (hrs)	Steady State Suction for Unsaturated Instruments (kpa)*	Saturation Achieved? (y/n)	Time of Saturation (hrs)
T1A-18	1.5	2.5	0 to 0.6	near saturation	2.5
T1A-36	3.5	13.4	0.62	n	-
T2A-18	15.6	45.5	5.7	n	-
T3A-36	26.3	92.0	Pressure	y	57
T4A-18	69.3	88.4	8.08	n	-
T4A-36	28.5	69.2	3.08	n	-
T4A-60	3.0	21.5	0	y	21.5
T1B-18	1.1	2.1	Pressure	y	1.8
T1B-36	6.2	10.2	Pressure	y	7.9
T2B-18	1.6	7.7	0.7	n	-
T3B-36	3.7	13.7	Pressure	y	9.1
T4B-36	6.2	21.1	Pressure	y	9.1
T1C-18	0.9	1.5	1.24	n	-
T1C-36	1.5	2.8	Pressure	y	2.5
T2C-18	2.7	3.5	0	y	3.5
T4C-18	10.9	43.5	2.61	n	-
T4C-36	9.6	23.6	Pressure	y	15.6
T4C-60	15.7	44.9	Pressure	y	20.9

*Instruments indicated pressures on the order of 0 to 5 kpa. Pressures not reported as instrument calibrations do not support pressures

Table E-2. Piezometer saturation fronts.

Instrument Name	Wetting Front Arrival (hrs)	Time to Steady State (hrs)	Steady State Pressure (kpa)
P1A-60	11.17	67.8	2.11
P2A-84	-	-	not reliable
P1C-60	1.55	69.5	6.7
P2C-84	13.5	67.8	8.6

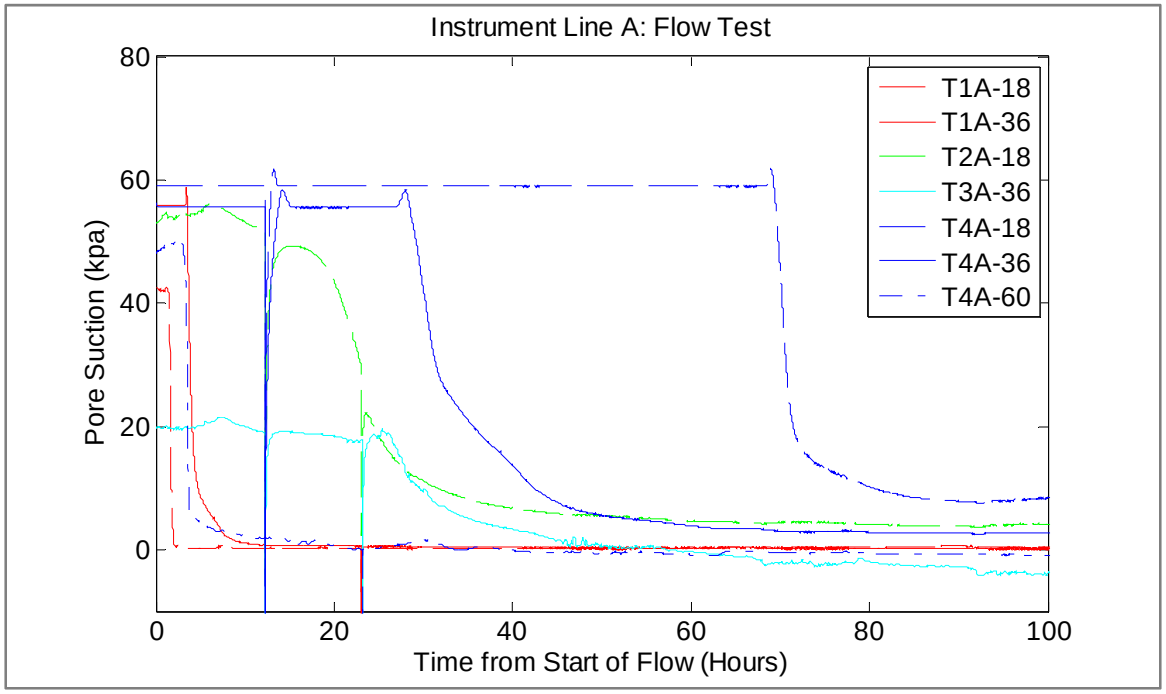

Figure E- 10. Summary of Tensiometer Data for Instrument Line A.

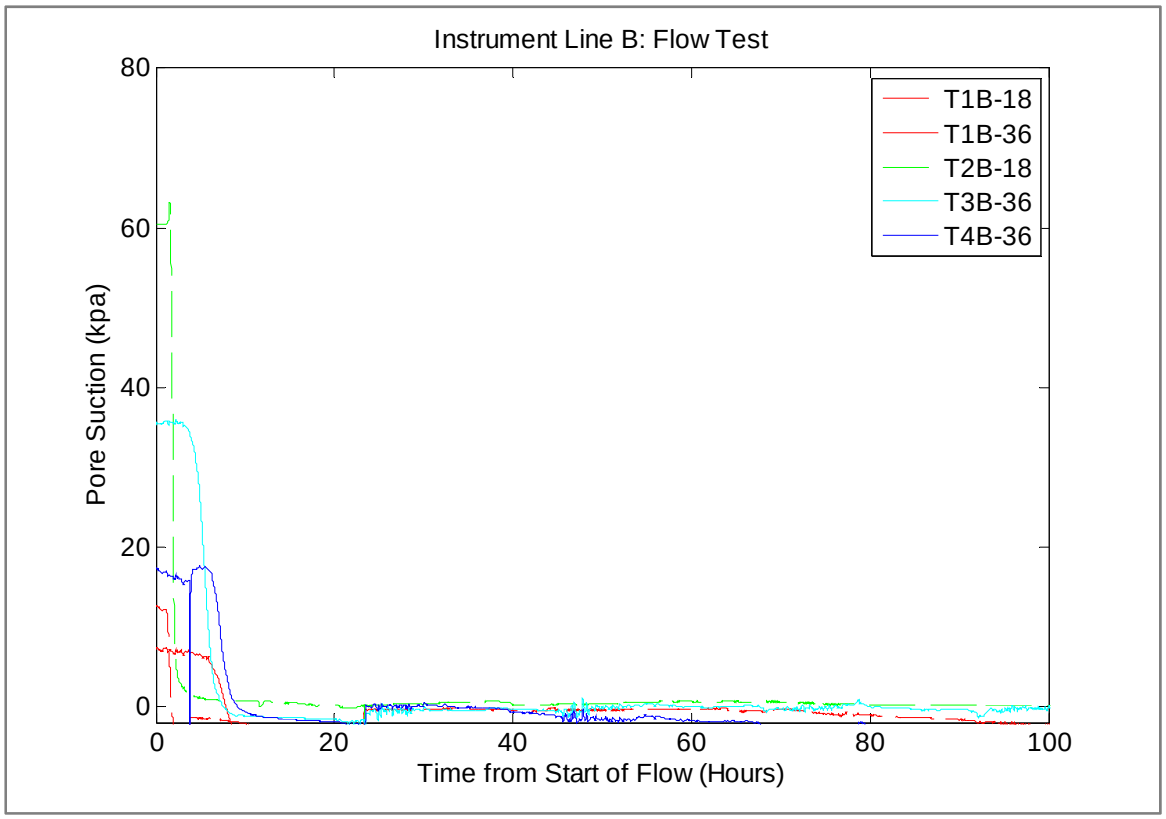

Figure E- 11. Summary of Tensiometer Data for Instrument Line B.

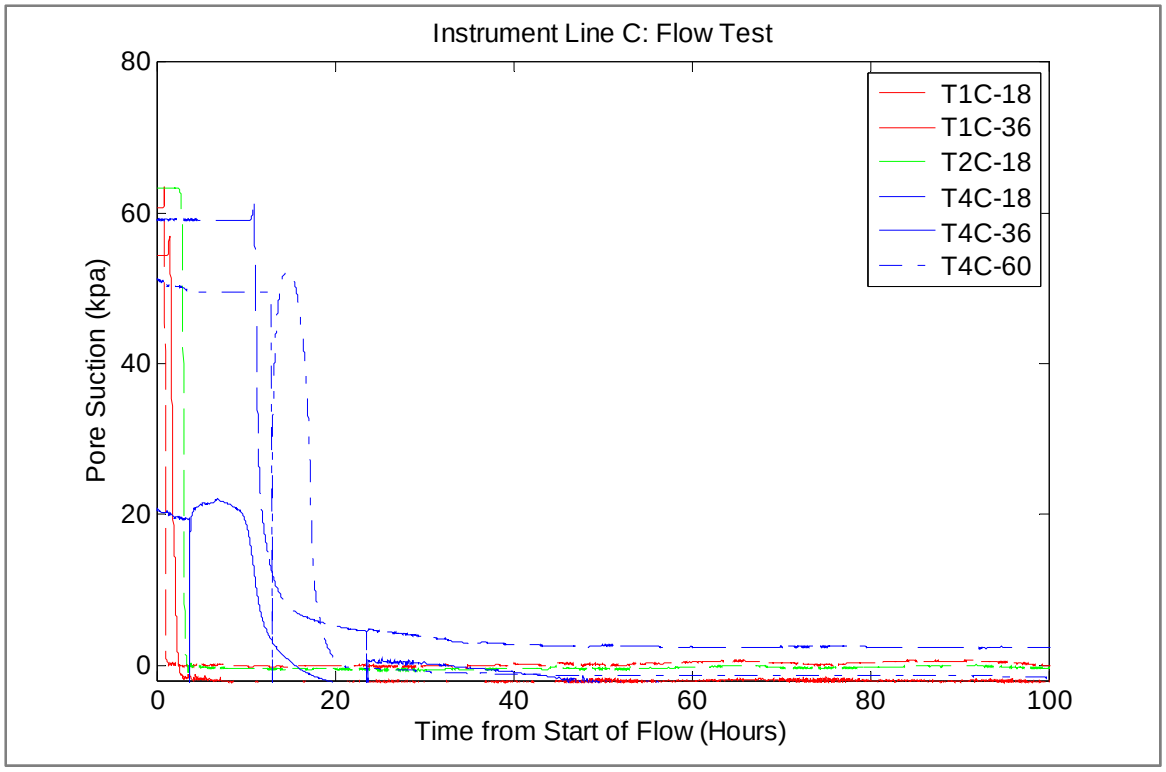

Figure E- 12. Summary of Tensiometer Data for Instrument Line C.

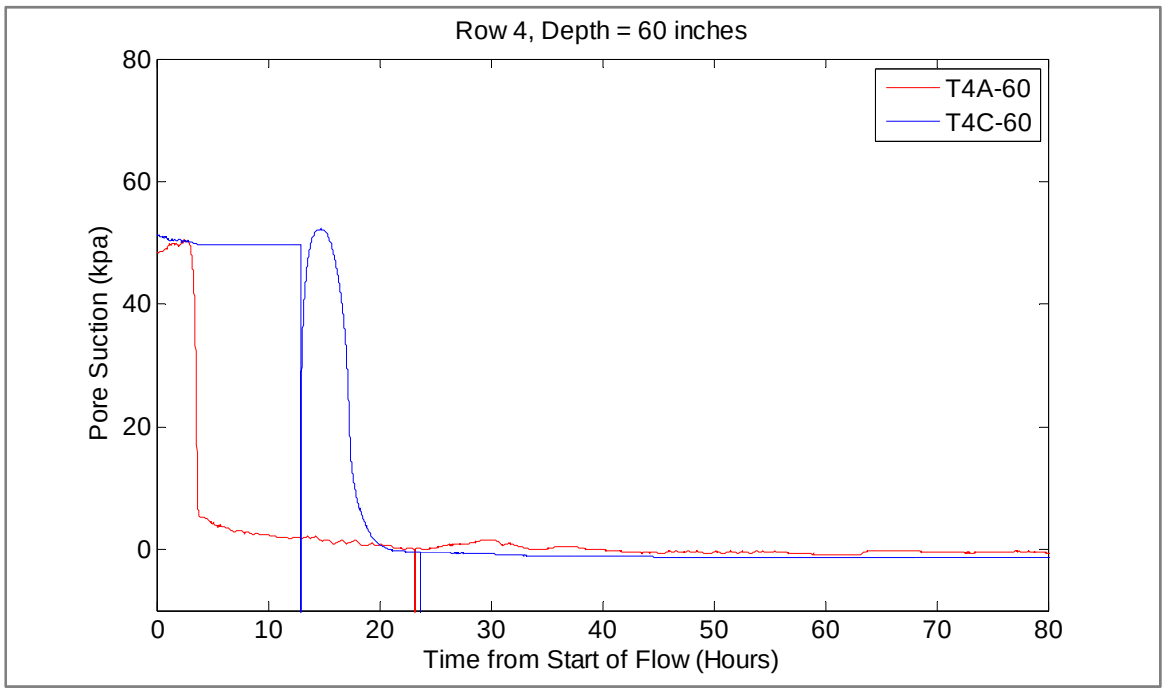

Figure E- 13. Comparison of Row 4 (below the stump) Lines A and C at 60 inch depth. Note the early saturation of the 60 inch tensiometer at Line A likely due to saturation flowing down from lower trench which was filling with water from the gopher burrow at Line B.

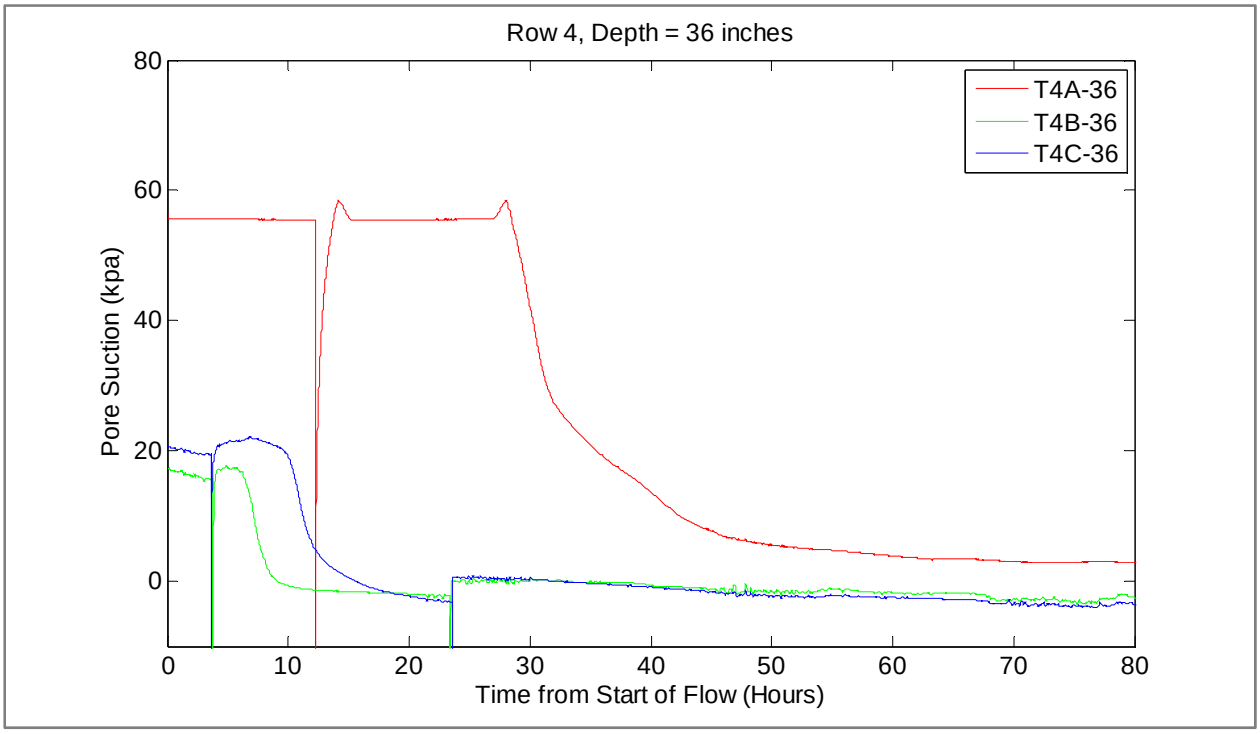

Figure E- 14. Comparison of Row 4 (below the stump) Lines A, B and C at 36 inch depth. Note that tensiometer T4A-36, below the stump, is the last to saturate.

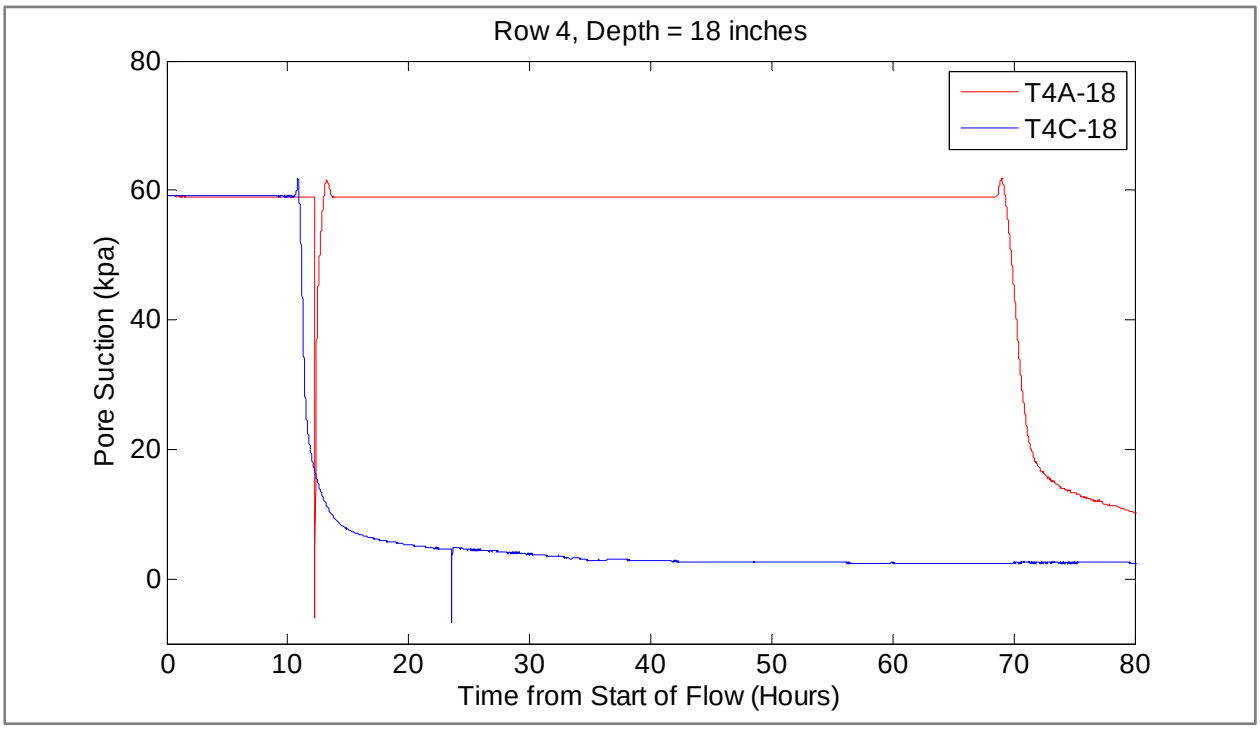

Figure E- 15. Comparison of Row 4 (below the stump) Lines A, B and C at 18 inch depth. Note that tensiometer T4A-18, below the stump, is the last to saturate.

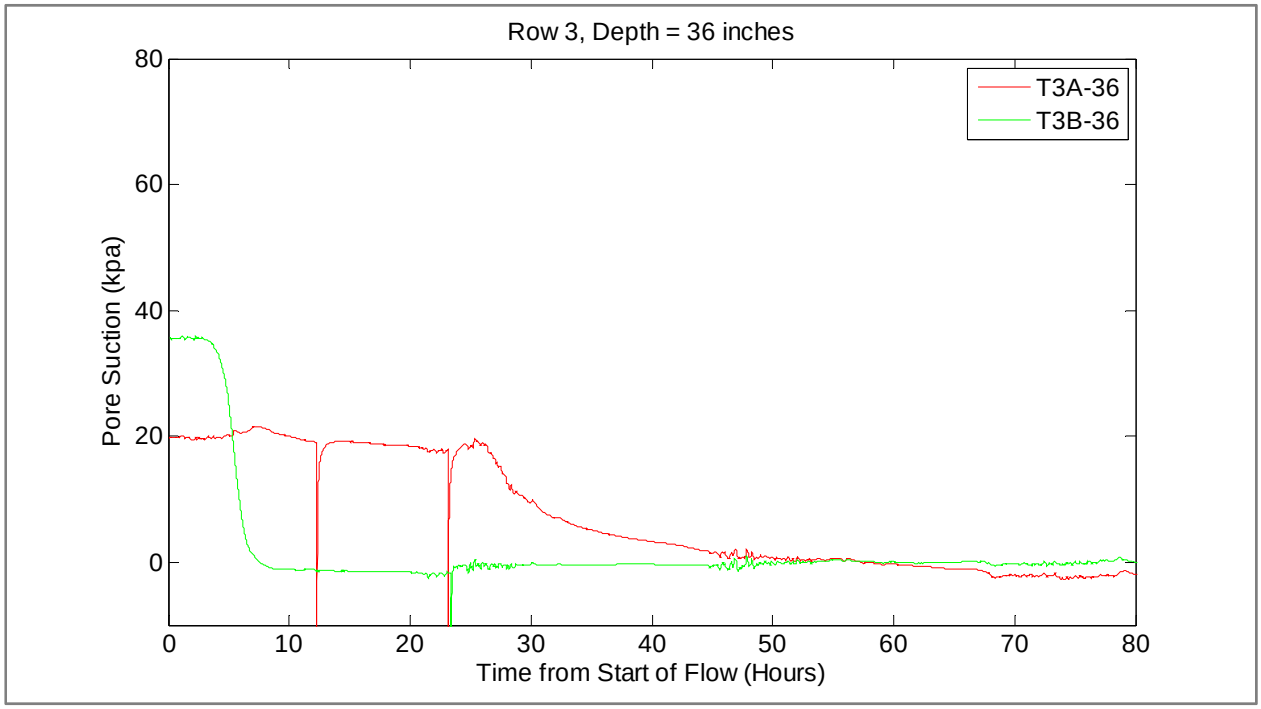

Figure E- 16. Comparison of Row 3 at Instrument Lines A and B at a depth of 36 inches. The analagous instrument at Line C was found to be non-functional during the test.

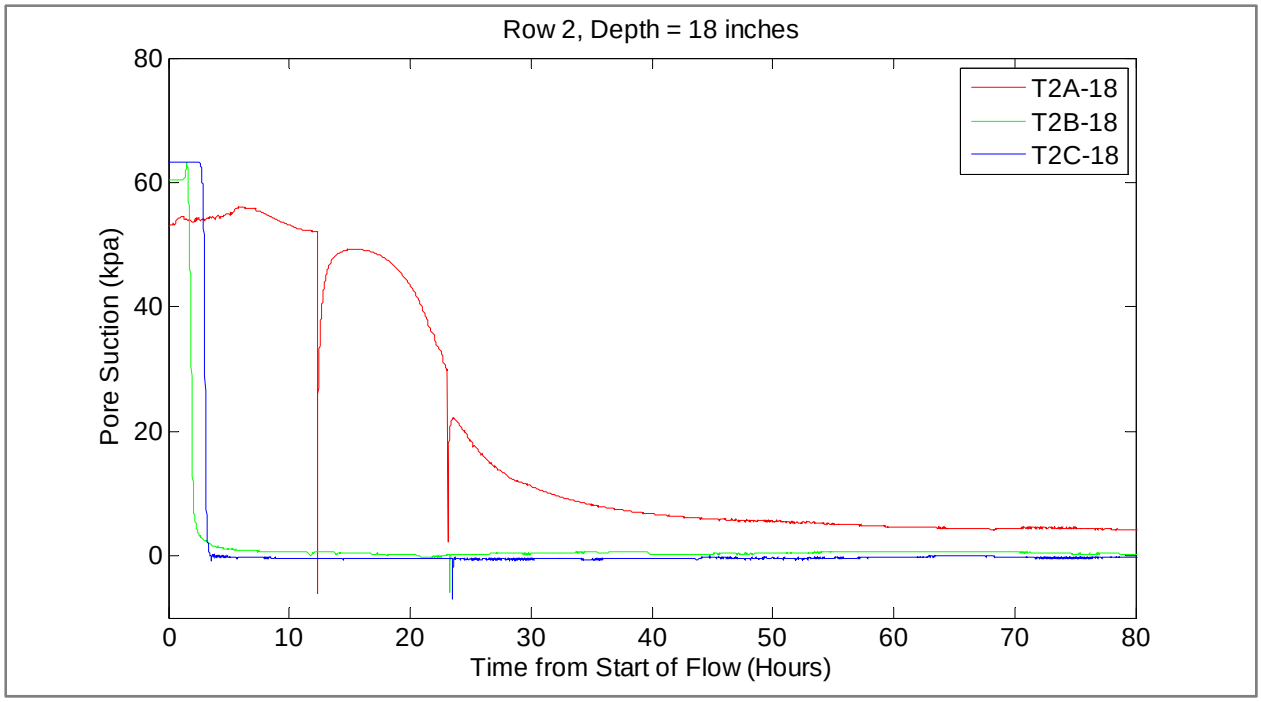

Figure E- 17. Comparison of Row 2 at Instrument Lines A, B and C at a depth of 18 inches. Note that instrument Lines B and C saturate before Line A at the stump.

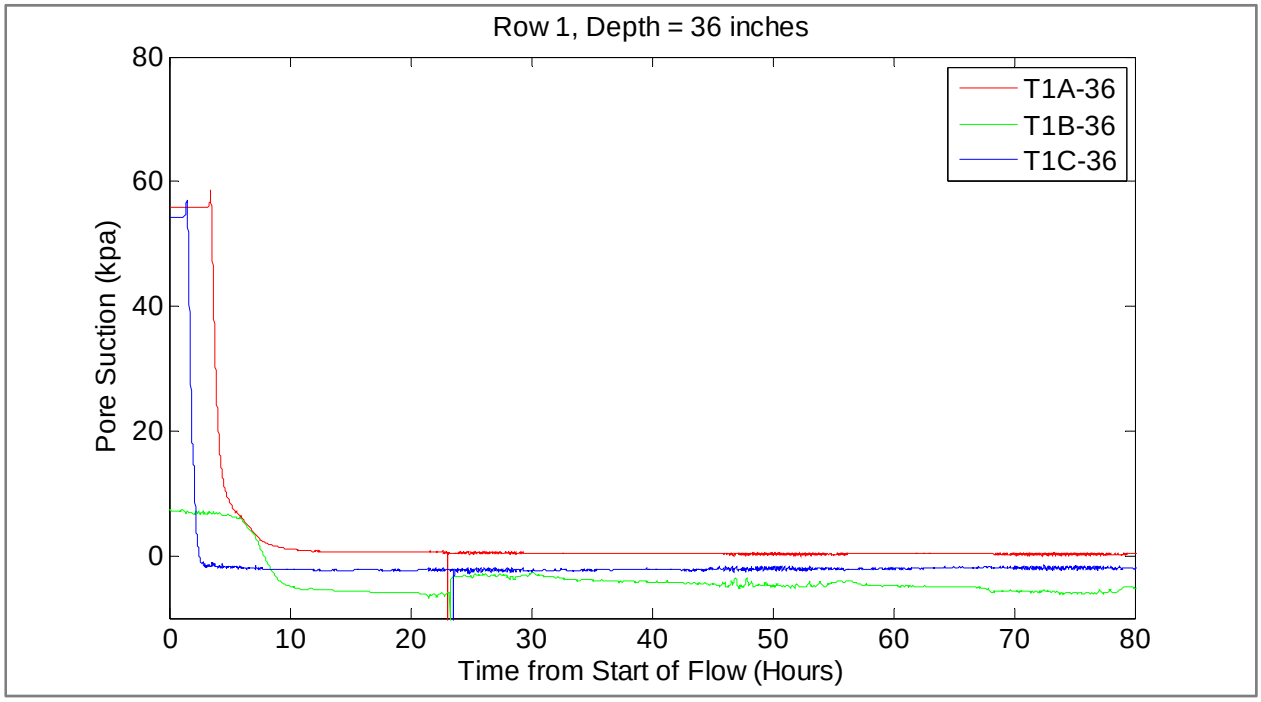

Figure E- 18. Comparison of Row 1 at Instrument Lines A, B and C at a depth of 36 inches.

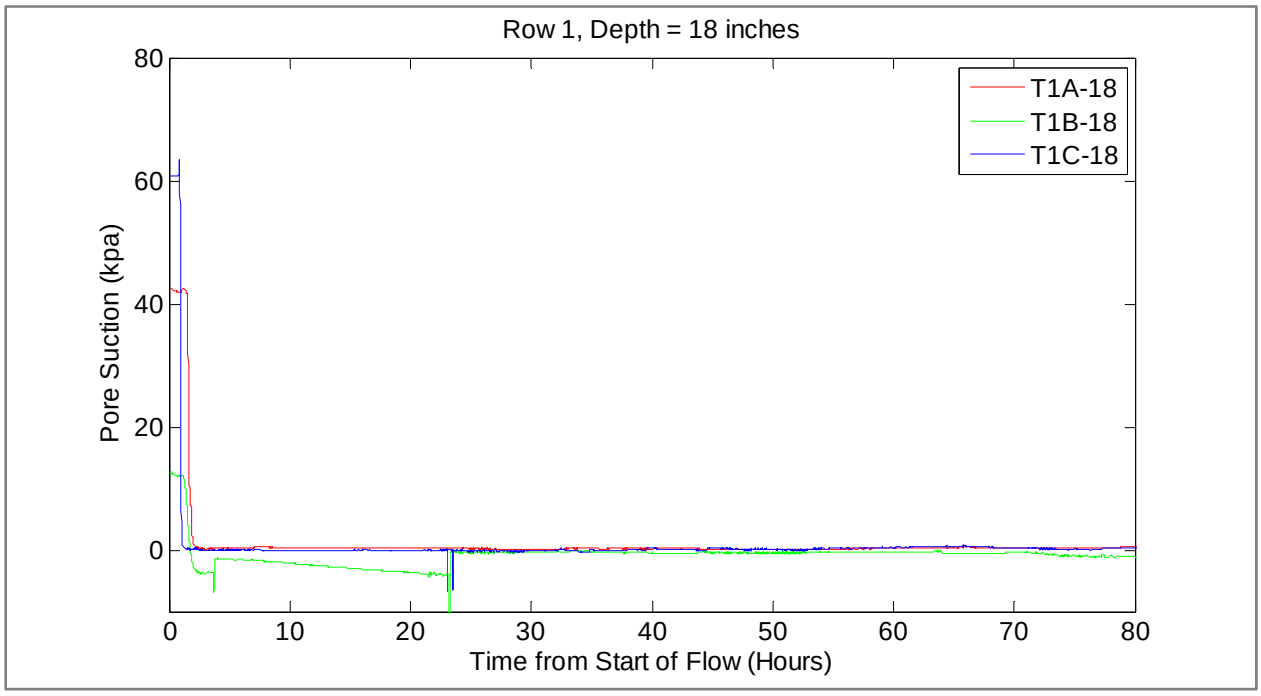

Figure E- 19. Comparison of Row 1 at Instrument Lines A, B, and C at a depth of 18 inches.

Vibrating wire piezometers were pre-saturated and were grouted into place upside down to prevent desaturation of the porous stone in accordance with the recommendations of the manufacturer, onsite consultation with Eric Mikkelson, and available literature (Mikkelsen 2002; Mikkelsen and Green, 2003; McKenna, 1995; Vaughan, 1969; Contreras et al. 2008). Piezometers were not read continuously, but at regular intervals with a Model GK-403 vibrating wire piezometer readout box. Frequency of readings was determined based on the observed rates of change in recorded pore pressures. Figure E-11 provides a summary of recorded piezometer data at instrument Lines A and C. Data results are discussed in Section 3.6.4 of the report and instrument installation is detailed in Section 3.5.3.

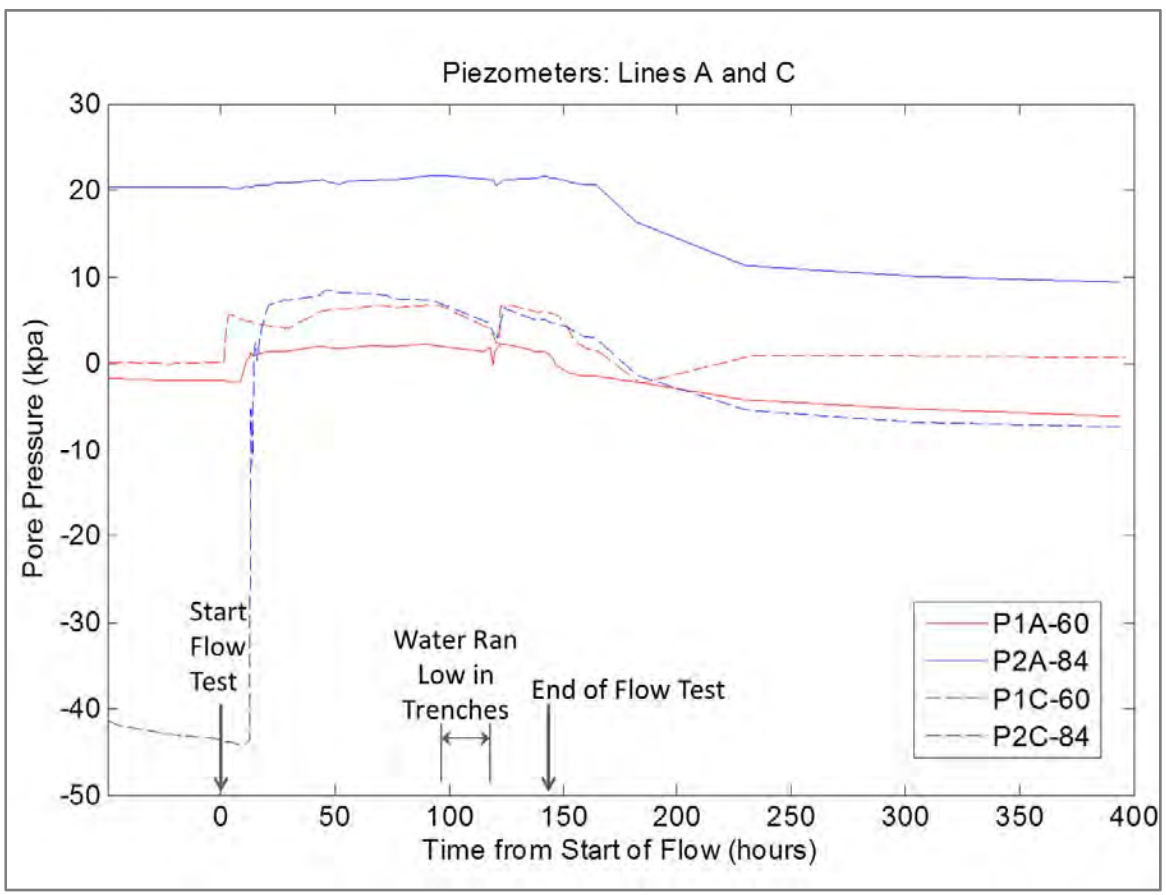

Figure E- 20. Pore pressures as measured during flow test through Instrument Lines A and C.

APPENDIX F: FIELD CHARACTERIZATION TEST LOGS

Appendix F

Root logs were created through a collaborative effort between John Lichter of Tree Associates, Dr. Richard Evans of UC Davis, and the UC Berkeley research team. Figures F-1 through F-4 provide original root logs for the uphill wall of the lower trench (Station N117), the 'Slice' 1 wall face (Station N115), the 'Slice' 2 wall face (Station N113), and the 'Slice' 3 wall face (Station N111.5). The area around the stump was logged from Station E138 to 153. 'Slice' 2 extended from E140 to 153, while 'Slice' 3 extended from E 143 to 153 due to the presence of the grouted animal burrow that we exposed and did not undermine. The excavation seemed to be an appropriate size to capture the decomposing root system with sufficient detail.

Abbreviations 'DR', 'LR', and 'H' were used to designate decomposed roots, live roots, and holes (or burrows) in the attached figures.

October 1st

Name	Root Dia (in)	Root Area	Northing	Easting	Depth	Notes
DR5	0.5	0.2	117	148.3	-2.2	Intact, vertical orientation
DR6	0.6	0.3	117	148.3	-2.7	Intact, nearly vertical
DR7	0.7	0.3	117	148	-2.3	Intact, silica flour external
DR8	0.4	0.1	117	148	-2.6	Intact
DR3	0.4	0.1	117	146.6	-1.2	Hollow
DR2	2.0	3.1	117	145.2	-3.7	
DR4	3.2	8.0	117	147.5	-1.6	As of Oct 1 log, believe silica from T4A-36
DR1	0.6	0.3	117	141.7	-1.5	
H1	2.3	4.0	117	139	-1.3	
H2	1.0	0.7	117	140	-0.9	
H3	0.9	0.6	117	140.6	-1.2	
H4	1.0	0.8	117	140.9	-1.1	
H5	2.6	5.3	117	144.3	-0.4	Ave dia; actual is 1.7x3.5
H6	1.9	2.8	117	145.7	-1.2	
H7	1.4	1.5	117	147.3	-0.35	Ave dia; actual 1.5x1.25
H8	1.5	1.8	117	147.8	-0.5	

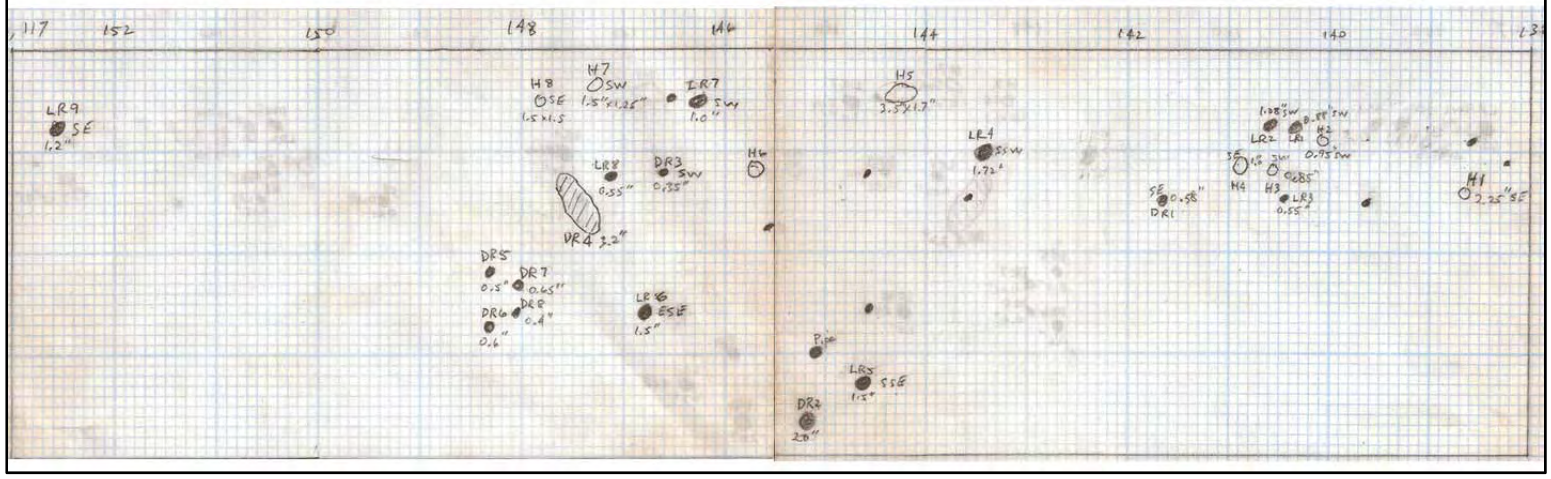

Figure F- 1. Log of original face of the uphill wall of the lower trench. Logged by John Lichter of Tree Associates and Dr. Richard Evans of UC Davis.

October 5, 2010

Name	Root Dia (in)	Root Area	Northing	Easting	Depth	Notes
DR1	0.5	0.2	114.9	139.5	-0.65	solid, no gap
DR2	2.5	4.7	114.8	143.8	-0.4	came apart in pieces, gap in places (0.25") but intermittant
DR3	1.3	1.2	114.6	147.9	-0.9	Highly decomposed with obvious gap
DR4	4.5	15.9	114.6	148.2	-0.4	intact and gapped; this is the 'nose'
DR5	1.9	2.8	114.6	148.7	-0.9	Live roots growing; root highly decomposed but no gap
DR6	1.7	2.3	114.6	148.2	-1.5	
DR7	1.0	0.7	114.6	148.4	-3	small path of silica near top of root
DR8	0.6	0.3	114.6	148.7	-2.3	
DR9	3.2	8.0	114.6	148.2	-1	intact; gapping bark; some silica; decaying bark; loose behind; 9C silica found inside and outside bark
DR10	1.0	0.8	114.6	148.7	-0.4	
DR11	0.3	0.1	114.6	148.5	-2.2	
DR12	1.2	1.1	114.6	148.6	-4.2	
DR13	1.9	2.7	114.6	148.8	-3	small gap behind filled with 'loam'
DR14	4.0	12.6	114.6	149.2	-0.2	silica flow from T4A-18; live roots growing in bark; bark mostly fully decomposed, mixed w/sand except in places
DR15	3.8	11.3	114.5	150.5	-0.1	
DR16	1.0	0.8	114.6	148.6	-1.25	
DR17	0.7	0.4	114.6	148.7	-2.1	hollow
DR18	2.0	3.1	114.7	146.7	-1.2	largely decayed; gopher hole behind
DR19	0.6	0.3	114.7	146	-1.8	
DR20	1.3	1.3	114.7	146.2	-0.4	hollow, dry
DR21	0.2	0.0	114.7	146.5	-1.5	
H1	2.5	4.9	114.9	139.2	-2.7	Actual 3x2; outlet for main burrow that flowed during test
H2	1.0	0.8	114.8	144.7	-0.9	
H3	1.5	1.8	114.7	146.8	-1	
H4	2.0	3.1	114.6	149.1	-0.6	behind DR14
H5	1.0	0.7	114.6	150.2	-0.95	May be linked to H4

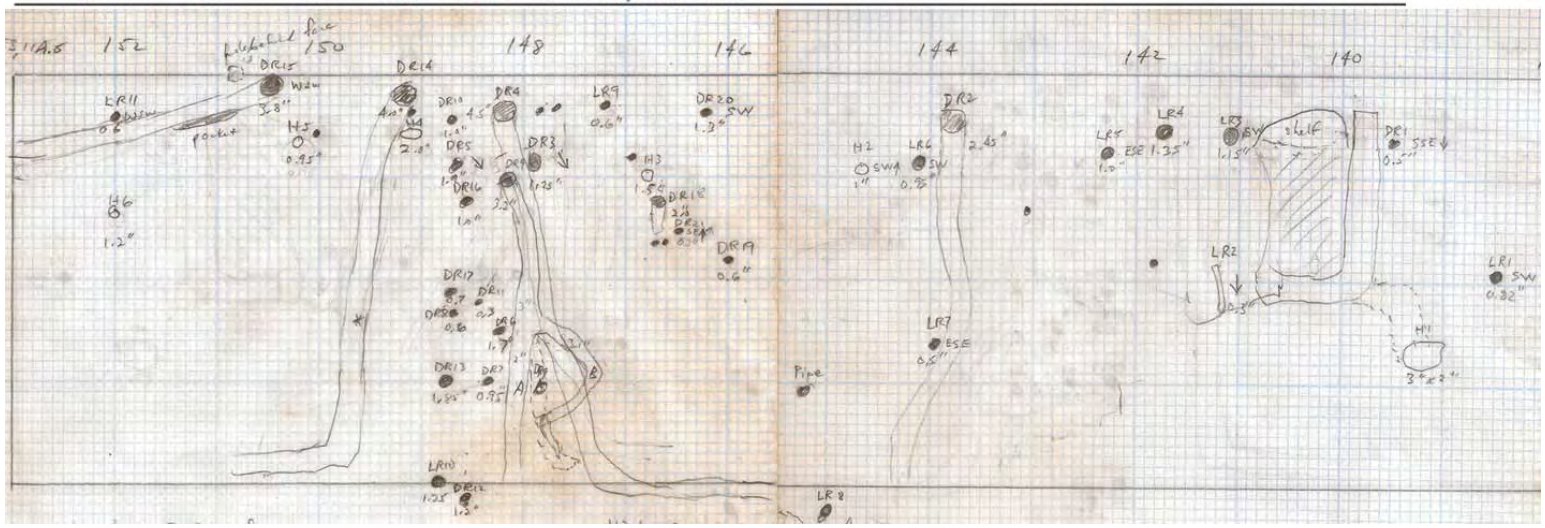

Figure F- 2. Log of wall face of 'Slice' 1 (see Section 3.7.1). Logged by John Lichter of Tree Associates and Dr. Richard Evans of UC Davis.

October 7, 2010

Name	Root Dia (in)	Root Area	Northing	Easting	Depth	Notes
DR1	1.0	0.8	113	142	-0.8	no gap
DR2	0.7	0.4	113	144.9	-0.5	
DR3	0.4	0.1	113	145.4	-2.4	no gap
DR4	1.1	1.0	113	150.6	-1	gap at bottom
DR5	1.1	1.0	113	147.6	-5.3	gap at uphill side; no gap on part of root
DR6	1.1	1.0	113	147.8	-5	no gap; crack in soil above root
DR8	6.0	28.3	113	145.7	-1	Gap between wood and bark; bark in contact with soil
DR9	4.6	16.6	113	146.2	-0.7	
DR11	4.0	12.6	113	146.3	-2	
DR12	5.4	22.9	113	147.2	-0.5	
DR14	2.3	4.2	113	152	-1.4	
DR15	1.3	1.3	113	149.3	-2.1	No gap; small live roots (<0.1") grow at base
DR16	0.8	0.4	113	145.2	-1.3	
H1	1.0	0.8	113	145.7	-0.9	no size; assume 1" based on size drawn for analysis
H2	1.3	1.2	113	148.7	-0.4	
H3	1.0	0.8	113	148.9	-0.9	
H4	1.2	1.1	113	149.8	-1.8	
H5	1.2	1.1	113	150.3	-0.6	
H6	0.9	0.6	113	150.9	-1.8	

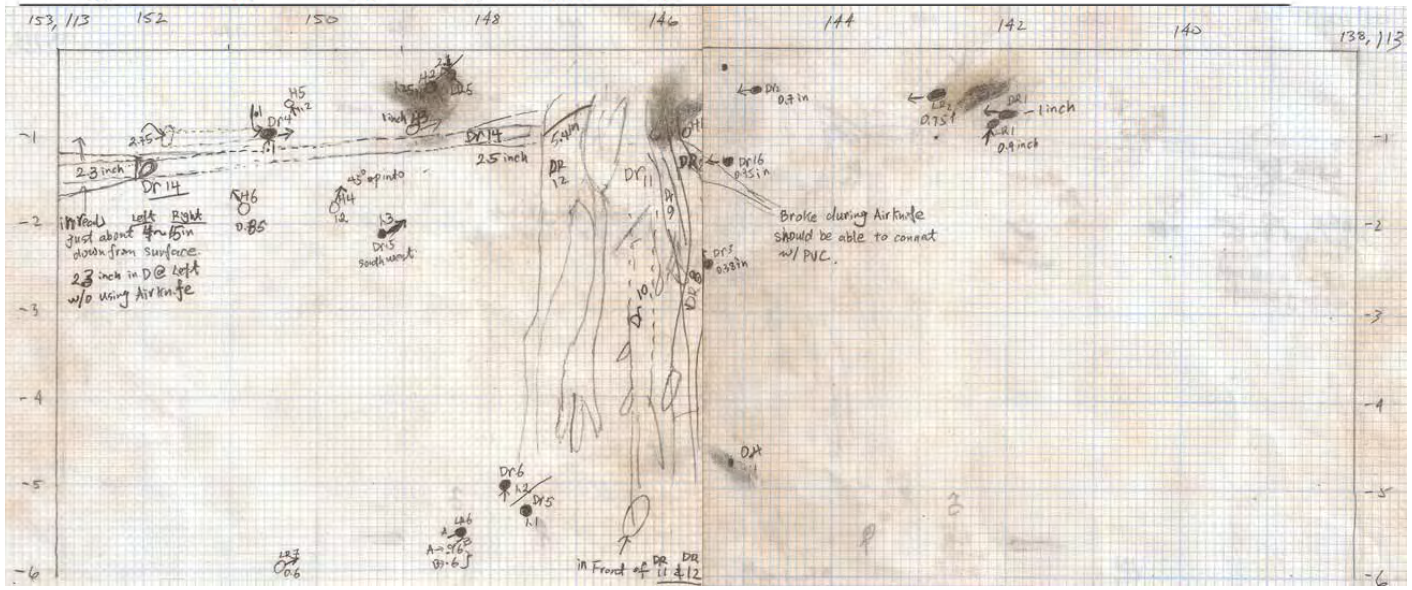

Figure F- 3. Log of wall face of 'Slice' 2 (see Section 3.7.1). Logged by John Lichter of Tree Associates and Dr. Richard Evans of UC Davis.

October 11, 2010

Name	Root Dia (in)	Root Area	Northing	Easting	Depth	Notes
DR1	2	3.141592654	111.5	146.5	-2.5	crumbly, ext. of DR8 from Oct7, appears to have been cut by trenches when pipe went in
DR2	1.15	1.038689071	111.5	146	-3.7	Powder
DR3	0.45	0.159043128	111.5	145	-5.6	decomposed, powdery
DR4	0.45	0.159043128	111.5	146.4	-4.3	breaks easily
DR5	1.3	1.327322896	111.5	146.7	-4.3	Firm
DR6	0.75	0.441786467	111.5	147	-4.7	very soft
DR7	0.78	0.477836243	111.5	147.5	-4.2	very soft
DR15	0.6	0.282743339	111.5	148	-4.2	
DR16	0.8	0.502654825	111.5	146.8	-5.2	
DR17	1.8	2.544690049	111.5	147	-5	2.5x1.1
DR18	0.25	0.049087385	111.5	146.5	-1.7	firm but crushable
DR19	0.21	0.034636059	111.5	148.4	-4.6	soft
DR20	0.83	0.541060795	111.5	148.85	-5.8	powder bark, wood is soft
DR21	1.4	1.5393804	111.5	149	-5.3	soft, bark is missing, some powder from bark
DR22	2	3.141592654	111.5	149	-5.7	spongy at cut face
DR23	0.88	0.608212338	111.5	149.5	-5.9	Powdery bark, very soft
DR24	0.34	0.090792028	111.5	150	-4.1	
DR26	6	28.27433388	111.5	147.2	-1	Bark increasingly decomposed or missing with depth
DR27	0.54	0.229022104	111.5	151.5	-4	soft, growing in face
H1	1.2	1.130973355	111.5	150.2	-1.9	
H2	1	0.785398163	111.5	151.2	-1.8	
H3	1.3	1.327322896	111.5	152	-1.15	

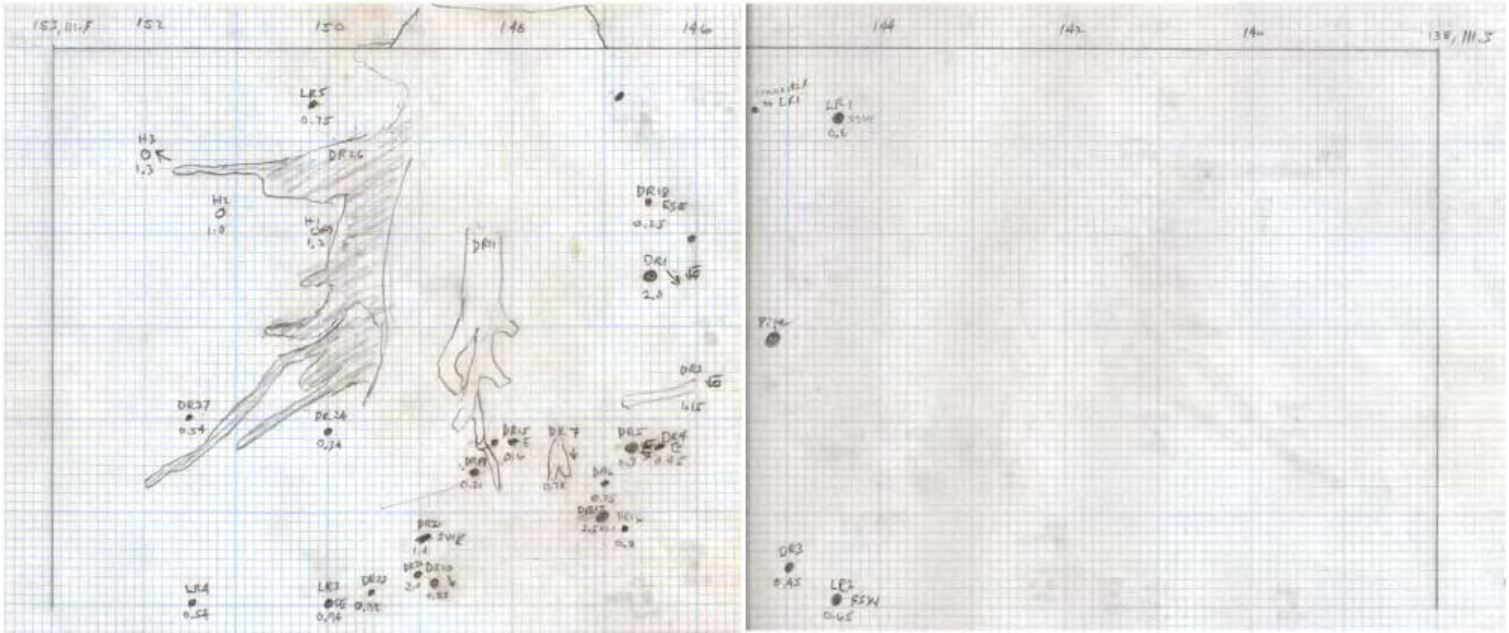

Figure F- 4. Log of wall face of 'Slice' 3 (see Section 3.7.1). Logged by John Lichter of Tree Associates and Dr. Richard Evans of UC Davis.